

Anatomy of the
Transmastoid Endolymphatic Sac Decompression
in the Management of Ménière's Disease

Richard Robert Locke

Submitted for the degree of Doctor of Philosophy

The University of Glasgow
Faculty of Biomedical and Life Sciences

April 2008

ABSTRACT

Ménière's disease affects 1 in 1000 people and produces vertigo and hearing loss (Morrison, 1981). Endolymphatic sac decompression has been advocated on the basis that endolymphatic hydrops is the underlying pathology. The endolymphatic sac is said to be the terminal dilatation of the membranous labyrinth. It has been proposed that endolymph flows from the semicircular canals and cochlea to the endolymphatic sac. Portman (1927) devised a procedure for 'decompressing' the endolymphatic sac by removal of the bone from the posterior cranial fossa to relieve the symptoms of Ménière's disease. Surgery on the endolymphatic sac remains controversial.

Shea (1979) and Bagger-Sjöbäck et al (1990, 1993) have studied the endolymphatic sac using different techniques. There are discrepancies in the results between the two studies.

The hypothesis that the endolymphatic sac can be safely approached and decompressed by a transmastoid route was tested. A total of thirteen cadaver heads and ten isolated temporal bones were used. A series of dissections were performed to examine the endolymphatic sac, perform measurements and analyse surgical approaches to the sac. Histological and electron microscopic study were performed.

The lumen of the endolymphatic sac was not always identifiable in the dura of the posterior cranial fossa or it frequently lay over the sigmoid sinus. In the dura of the posterior cranial fossa where the endolymphatic sac is located was a thickening of the dura. This thickening was present even in the absence of the endolymphatic sac. The endolymphatic sac can be safely approached by a transmastoid approach, if there is an extraosseous component to the endolymphatic sac. The proximal endolymphatic sac can be approached by posterior cranial fossa route.

ACKNOWLEDGEMENT

I wish to thank all the staff of the Laboratory of Human Anatomy at the University of Glasgow for their help and support in producing this thesis. In particular I am very grateful for the assistance of Andrew Lockhart with the processing of histology specimens, David Russell for assistance with the electron microscopy and Antony Patton with gross specimens. I would especially like to thank my supervisors, Dr John Shaw-Dunn and Mr Brian O'Reilly.

I am very grateful to the staff at the Massachusetts Eye and Ear Infirmary especially Dr Saumil Merchant for their help and advice in the processing of human temporal bones. I would also like to thank them for allowing me to examine specimens from the Temporal Bone collection and allowing photographs of specimens to be included in this thesis.

I would like to thank Dr Robin Reid and Mr Peter Kerr from the department of pathology at the Western Infirmary, Glasgow, for advice and their help in the processing of temporal bones for analysis.

Finally I would like to thank my family and friends for their support and patience whilst I worked on this thesis, especially my Father, Robert, and my friends, Sara and Mark for proof reading the thesis. Finally a thank you to Paul Rea for his friendship and support, my colleague and my friend.

DEDICATION

As I come to the end of producing this thesis I have the opportunity to think back on the work I have done and the places that it has taken me. I am grateful for the opportunity given to me to study at the University of Glasgow and in part at Harvard University Massachusetts. Whilst writing this thesis I have worked as an associate lecturer at the University of Glasgow and completed my Basic Surgical Training. This study of the temporal bone has taken more time than I and my colleagues first anticipated, however I am reminded of a quote from the New York Times: An unhurried sense of time is itself a form of wealth. Time is the simplest thing as Clifford Donald Simak said.

To my gran, Helen Brown, whom I dearly miss.

FOREWORD

Since I was a second year medical student studying anatomy at the University of Glasgow I have always had an interest in head and neck anatomy. As my career progressed I developed a keen interest in Ear, Nose and Throat surgery. After graduating and completing my house officer year I had the unique opportunity to return to the University and demonstrate in Anatomy. It was here that I was able to embark on a course of study. Initially I began with a project studying the temporal bone. This quickly flourished into a formal research project and then into this PhD thesis. With a particular interest in the temporal bone I met with Mr O'Reilly, consultant neuro-otologist. We felt that looking at the endolymphatic sac could provide further scientific evidence in the debate over the role of surgery on the sac and Ménière's disease.

My research led me to the Massachusetts Eye and Ear Infirmary in Boston where I had the privilege of examining the temporal bone collection founded by Harold Schuknecht. I was given the opportunity of presenting some of my work at the British Association of Clinical Anatomists meeting where I was awarded the Conrad Lewin Prize. This thesis which was begun whilst I was demonstrating in anatomy was completed when I was working as a senior house officer in ENT, having passed my Intercollegiate Membership of the Royal College of Surgeons and completed my Basic Surgical Training.

I hope to demonstrate the reasons why surgery on the sac may or may not be of benefit in the management of Ménière's disease. Ultimately I want to show that careful analysis of the sac and patient selection may theoretically improve outcomes in endolymphatic sac decompression surgery.

This work has been presented in part at the Scottish Otolaryngological Society and the British Association of Clinical Anatomists and won the Conrad Lewin Prize. It has been published as an abstract in *Clinical Anatomy*: LOCKE, Richard R., SHAW-DUNN, John, O'REILLY, Brian. *Clinical Anatomy* 17; 5, 444 **Anatomy of surgical access to the endolymphatic sac for the management of Ménière's Disease**

PREFACE

Ménière's disease was first described in 1861 by Prosper Ménière and consists of tinnitus, progressive sensorineural hearing loss and intermittent vertigo. Ménière was the first to propose the ear as a source of these symptoms as opposed to the central nervous system.

It is commonly believed that patients with Ménière's disease have endolymphatic hydrops, a dilatation of the membranous labyrinth. It is thought that increased volume within the endolymph compartment results in tinnitus and sensorineural hearing loss, with typical resolution when an area of the membranous labyrinth ruptures allowing the endolymph to mix with surrounding perilymph. The normal membranous labyrinth has a dilated blind ending projection that extends out of the petrous temporal bone into the dura of the posterior cranial fossa called the endolymphatic sac (Hall-Craggs, 1993).

Surgical treatment of Ménière's disease can include decompression of the endolymphatic sac in cases unresponsive to medical management. There is great debate as to the structure and function of the endolymphatic sac and the surgery of decompression (Thomsen et al, 1981). Surgery of the endolymphatic sac is designed to relieve the symptoms of hydrops by decompressing the endolymphatic sac and thereby decompress the endolymphatic compartment. Portmann (1927) described the first procedure to decompress the endolymphatic sac via a transmastoid approach; this remains the standard approach to decompress the endolymphatic sac to this day.

I hope to test the following hypotheses:

1. The endolymphatic sac is a simple sac like structure with a readily identifiable lumen
2. The endolymphatic sac is constant in size and is always identifiable in the dura of the posterior cranial fossa
3. The transmastoid approach is without hazard to surrounding structures
4. The endolymphatic sac can be satisfactorily decompressed via a transmastoid approach.

CONTENTS

Abstract	2
Acknowledgent	3
Dedication	4
Foreward	5
Preface	6
List of Tables	10
List of Figures	11
Section 1: Introduction	16
The ear	17
Temporal bone	18
The middle ear	19
The inner ear	19
The labyrinth	20
The bony labyrinth	20
The membranous labyrinth	20
Anatomy of the endolymphatic sac and duct	22
Paravestibular canaliculi	25
Histology and ultrastructure of the endolymphatic sac	25
Blood supply to the labyrinth	26
Venous drainage of the labyrinth	27
Function of the membranous labyrinth	27
Endolymph production and circulation	29
Function of the endolymphatic sac	31
Evolution of the ear	32
Development of the ear	35
Postnatal development of the ear	36
Ménière's disease first described	37
Epidemiology of Ménière's disease	39
Signs and symptoms	39
Aetiology	40
Ultrastructural changes of the endolymphatic sac in Ménière's disease	42
Diagnosis	42
Investigations	42
Imaging of the endolymphatic sac	43
Variants	44
Medical management	44
Surgical management	45
Endolymphatic sac surgery	47
Temporal bone surgery	49
Facial nerve monitoring	51
Section 2: Materials and methods	53
Material	53

Method	55
Normal osteology	56
Normal temporal bone anatomy	56
Normal gross anatomy	56
Preparation of specimens for histological analysis	57
Temporal bone histology	57
Isolated endolymphatic sac histology	58
Electron microscopy of endolymphatic sac	60
Embryology	60
Measurements of the endolymphatic sac	60
Examination of temporal bone sections from the collection at the Massachusetts eye and ear infirmary	65
Simulated surgical dissections	65
Transmastoid endolymphatic sac decompression,	65
Posterior cranial fossa retrosigmoid endolymphatic sac decompression	66
Combined transmastoid and retrosigmoid endolymphatic sac decompression	66
Middle cranial fossa endolymphatic sac decompression	66
Clinical Cases	66
Glomus jugulare resection by lateral approach	66
Retrosigmoid / suboccipital acoustic neuroma resection	68
 Section 3: Results	 69
Anatomy of the temporal bone	72
Cranial cavity	75
The ear	76
The external ear	77
The middle ear	78
Facial nerve	80
Medial dissection of the temporal bone	80
The inner ear	81
The bony labyrinth	82
The membranous labyrinth	84
The endolymphatic duct and sac	85
Histology of the membranous labyrinth	86
Histology of the endolymphatic sac	87
Scanning electron microscopy	88
Embryology of the endolymphatic sac	89
Measurements	90
Pathology in Ménière's disease	93
Endolymphatic sac decompression by Neuro-Otologist	94
Simulated endolymphatic sac decompression	96
Alternative procedures	98
Suboccipital posterior cranial fossa approach	98

Combined retrosigmoid, suboccipital and transmastoid Approach	102
Middle cranial fossa approach	105
Clinical procedures	109
Retrosigmoid / Suboccipital acoustic neuroma resection	109
Glomus jugulare resection by lateral approach	109
Section 4: Discussion	267
Statement of findings	268
Strengths and weaknesses	268
Summary of findings	269
Embryology	269
Structure	270
Dura	272
Vascular	273
Histology / Scanning electron microscopy	274
Function	275
Pathology	277
Identification of the endolymphatic sac	279
Surgery on the temporal bone	282
Transmastoid approach to decompress the endolymphatic sac	282
Identification of the endolymphatic sac by transmastoid approach	286
Alternative approaches	286
Middle cranial fossa approach	286
Posterior Cranial Fossa Approach	287
Combined Transmastoid and Suboccipital Approach	287
Section 5: Conclusion	289
Section 6: Appendices	292
Embalming protocol	293
Arterial latex injection	294
Tissue processing and embedding for paraffin wax sectioning	295
Paraffin sectioning cutting	296
Haematoxylin and eosin staining	297
Decalcification with nitric acid protocol	298
Decalcification with EDTA Protocol	299
Processing of tissue for scanning electron microscopy	300
Patient A	301
Patient B	306
Age, sex and cause of death of cadavers	310
Endolymphatic Sac Decompression	311
Dissections	312
Section 7: References	344

LIST OF TABLES

Table 1	Endolymphatic sac measurement results
Table 2	Endolymphatic sac measurement results 2
Table 3	Age, sex and cause of death of cadavers

LIST OF FIGURES

- Fig 1 Diagram of the external, middle and inner ear
- Fig 2 Diagram of the membranous labyrinth
- Fig 3 Diagram of the membranous labyrinth with the endolymphatic sac
- Fig 4 Graphical representation of extracellular fluid salt concentrations
- Fig 5 Portrait of Prosper Ménière
- Fig 6 Diagram of endolymphatic sac decompression
- Fig 7 Diagram showing operculum width
- Fig 8 Diagram showing distance from operculum to internal acoustic meatus
- Fig 9 Diagram showing distance from operculum to superior petrosal sinus
- Fig 10 Diagram showing width of endolymphatic sac
- Fig 11 Diagram showing length of endolymphatic sac
- Fig 12 Diagram showing distance from operculum to sigmoid sinus
- Fig 13 Photograph of right posterolateral view of head and neck of skeleton
- Fig 14 Diagram of right posterolateral view of head and neck of skeleton
- Fig 15 Photograph of lateral view of a right temporal bone
- Fig 16 Diagram of lateral view of a right temporal bone
- Fig 17 Photograph of inferior view of a right temporal bone
- Fig 18 Diagram of inferior view of a right temporal bone
- Fig 19 Photograph of superior view of a right temporal bone
- Fig 20 Diagram of superior view of a right temporal bone
- Fig 21 Photograph of posterior view of a right temporal bone
- Fig 22 Diagram of posterior view of a right temporal bone
- Fig 23 Photograph of posterior view of left anterior, middle and posterior cranial fossae
- Fig 24 Diagram of posterior view of left anterior, middle and posterior cranial fossae
- Fig 25 Photograph of floor of cranial cavity showing the anterior, middle and posterior cranial fossae
- Fig 26 Diagram of floor of cranial cavity showing the anterior, middle and posterior cranial fossae
- Fig 27 Photograph of posterior aspect of left temporal bone with internal acoustic meatus and jugular foramen
- Fig 28 Diagram of posterior aspect of left temporal bone with internal acoustic meatus and jugular foramen
- Fig 29 Photograph of left superficial temporal region
- Fig 30 Diagram of left superficial temporal region
- Fig 31 Photograph of left pinna dissection
- Fig 32 Diagram of left pinna dissection
- Fig 33 Photograph of anterior view of left temporal bone with tympanic cavity de-roofed and Eustachian tube exposed
- Fig 34 Diagram of anterior view of left temporal bone with tympanic cavity de-roofed and Eustachian tube exposed

- Fig 35 Photograph of lateral view of left temporal bone with glossopharyngeal, hypoglossal, vagus and accessory nerves and the internal jugular vein and internal carotid artery
- Fig 36 Diagram of lateral view of left temporal bone with glossopharyngeal, hypoglossal, vagus and accessory nerves and the internal jugular vein and internal carotid artery
- Fig 37 Photograph of inferior view of the jugular fossa and the parts of the ear
- Fig 38 Diagram of inferior view of the jugular fossa and the parts of the ear
- Fig 39 Photograph of inferior view of nerves within the jugular fossa
- Fig 40 Diagram of inferior view of nerves within the jugular fossa
- Fig 41 Photograph of lateral view of tympanic membrane, tympanic cavity and superior semicircular canal
- Fig 42 Diagram of lateral view of tympanic membrane, tympanic cavity and superior semicircular canal
- Fig 43 Photograph of medial view of the course of the internal carotid artery
- Fig 44 Diagram of medial view of the course of the internal carotid artery
- Fig 45 Photograph of cochlea after removal of the bony wall of the promontory
- Fig 46 Diagram of cochlea after removal of the bony wall of the promontory
- Fig 47 Photograph of superior view of left temporal bone with tympanic cavity de-roofed and genicular ganglion exposed
- Fig 48 Diagram of superior view of left temporal bone with tympanic cavity de-roofed and genicular ganglion exposed
- Fig 49 Photograph of vertical segment of facial nerve visualised through mastoid
- Fig 50 Diagram of vertical segment of facial nerve visualised through mastoid
- Fig 51 Photograph of medial view of nasopharynx
- Fig 52 Diagram of medial view of nasopharynx
- Fig 53 Photograph of medial view of intraosseous course of the internal carotid artery
- Fig 54 Diagram of medial view of intraosseous course of the internal carotid artery
- Fig 55 Photograph of medial view of the course of the internal carotid artery
- Fig 56 Diagram of medial view of the course of the internal carotid artery
- Fig 57 Photograph of right temporal bone showing opened internal acoustic meatus, cochlea and semicircular canals
- Fig 58 Diagram of right temporal bone showing opened internal acoustic meatus, cochlea and semicircular canals
- Fig 59 Photograph of left superior, lateral and posterior semicircular canals opened
- Fig 60 Diagram of left superior, lateral and posterior semicircular canals opened
- Fig 61 Photograph of membranous labyrinth within the bony labyrinth
- Fig 62 Diagram of membranous labyrinth within the bony labyrinth
- Fig 63 Photograph cochlea and cochlear nerve
- Fig 64 Diagram cochlea and cochlear nerve
- Fig 65 Photograph of histological specimen of saccule, utricle and endolymphatic duct stained with haematoxylin and eosin

- Fig 66 Photograph of posterior aspect of right temporal bone with dura mater partly removed
- Fig 67 Diagram of posterior aspect of right temporal bone with dura mater partly removed
- Fig 68 Photograph of posterior aspect of right temporal bone showing intra and extra osseous parts of the endolymphatic sac
- Fig 69 Diagram of posterior aspect of right temporal bone showing intra and extra osseous parts of the endolymphatic sac
- Fig 70 Photograph of the intraosseous part of the endolymphatic sac
- Fig 71 Diagram of the intraosseous part of the endolymphatic sac
- Fig 72 Photograph of posterior view of right temporal bone revealing labyrinth
- Fig 73 Diagram of posterior view of right temporal bone revealing labyrinth
- Fig 74 Photograph of superior view of drilled left temporal bone
- Fig 75 Diagram of superior view of drilled left temporal bone
- Fig 76 Photograph of section of cochlea stained with haematoxylin and eosin
- Fig 77 Photograph of section of cochlea duct stained with haematoxylin and eosin
- Fig 78 Photograph of section of cochlea stained with masons trichrome
- Fig 79 Photograph of section of intermediate endolymphatic sac stained with haematoxylin and eosin
- Fig 80 Photograph of section of distal endolymphatic sac stained with haematoxylin and eosin
- Fig 81 Photograph of section of distal endolymphatic sac stained with haematoxylin and eosin
- Fig 82 Electron micrograph of transverse section of endolymphatic sac
- Fig 83 Electron micrograph of the internal surface of the endolymphatic sac
- Fig 84 Electron micrograph of the basement membrane of the endolymphatic sac
- Fig 85 Photograph of a section of a 27mm human embryo head stained with haematoxylin and eosin
- Fig 86 Photograph of a section of a 55mm human embryo head stained with haematoxylin and eosin
- Fig 87 Photograph of a section of a 55mm human embryo head stained with haematoxylin and eosin
- Fig 88 Photograph of the operculum and endolymphatic sac
- Fig 89 Diagram of the operculum and endolymphatic sac
- Fig 90 Photograph of the endolymphatic sac with the lumen opened
- Fig 91 Diagram of the endolymphatic sac with the lumen opened
- Fig 92 Photograph of a section of the affected cochlea, right, from a patient with unilateral Ménière's disease stained with haematoxylin and eosin
- Fig 93 Photograph of a section of the left temporal bone showing the endolymphatic sac from a patient with long standing Ménière's disease, stained with haematoxylin and eosin
- Fig 94 Photograph of a section of the right temporal bone from a patient with previous endolymphatic sac decompression and stent insertion stained with haematoxylin and eosin
- Fig 95 Photograph of a right mastoid process

- Fig 96 Photograph of a right cortical mastoidectomy and endolymphatic sac decompression
- Fig 97 Photograph of a right cortical mastoidectomy and endolymphatic sac decompression
- Fig 98 Photograph of a right superficial head dissection
- Fig 99 Diagram of a right superficial head dissection
- Fig 100 Photograph of the superficial structures behind the pinna
- Fig 101 Diagram of the superficial structures behind the pinna
- Fig 102 Photograph of superficial left head and neck dissection
- Fig 103 Diagram of superficial left head and neck dissection
- Fig 104 Photograph of posterior view of left pinna dissection
- Fig 105 Diagram of posterior view of left pinna dissection
- Fig 106 Photograph of left bony external acoustic meatus
- Fig 107 Diagram of left bony external acoustic meatus
- Fig 108 Photograph of left mastoid process with periosteum removed
- Fig 109 Diagram of left mastoid process with periosteum removed
- Fig 110 Photograph of left mastoid process with cortex removed
- Fig 111 Diagram of left mastoid process with cortex removed
- Fig 112 Photograph of left cortical mastoidectomy and endolymphatic sac decompression
- Fig 113 Diagram of left cortical mastoidectomy and endolymphatic sac decompression
- Fig 114 Photograph of left mastoid post endolymphatic sac decompression
- Fig 115 Diagram of left mastoid post endolymphatic sac decompression
- Fig 116 Photograph of superficial back of head and neck dissection
- Fig 117 Diagram of superficial back of head and neck dissection
- Fig 118 Photograph of neck dissection following removal of trapezius
- Fig 119 Diagram of neck dissection following removal of trapezius
- Fig 120 Photograph of lateral view of neck dissection
- Fig 121 Diagram of lateral view of neck dissection
- Fig 122 Photograph of longissimus capitis
- Fig 123 Diagram of longissimus capitis
- Fig 124 Photograph of posterior view of right suboccipital triangle
- Fig 125 Diagram of posterior view of right suboccipital triangle
- Fig 126 Photograph of posterior view of left suboccipital triangle
- Fig 127 Diagram of posterior view of left suboccipital triangle
- Fig 128 Photograph of posterior view of deep neck dissection
- Fig 129 Diagram of posterior view of deep neck dissection
- Fig 130 Photograph of lateral view of posterior cranial fossa opened
- Fig 131 Diagram of lateral view of posterior cranial fossa opened
- Fig 132 Photograph of superior aspect of space between hind brain and clivus
- Fig 133 Diagram of superior aspect of space between hind brain and clivus
- Fig 134 Photograph of space between hindbrain and anterior wall of the posterior cranial fossa
- Fig 135 Diagram of space between hindbrain and anterior wall of the posterior cranial fossa

- Fig 136 Photograph of left and right suboccipital triangles
- Fig 137 Diagram of left and right suboccipital triangles
- Fig 138 Photograph of right deep suboccipital dissection
- Fig 139 Diagram of right deep suboccipital dissection
- Fig 140 Photograph of posterior view of right posterior cranial fossa opened
- Fig 141 Diagram of posterior view of right posterior cranial fossa opened
- Fig 142 Photograph of posterior view of hindbrain with cerebellum removed
- Fig 143 Diagram of posterior view of hindbrain with cerebellum removed
- Fig 144 Photograph of posterior view of anterior wall of left posterior cranial fossa
- Fig 145 Diagram of posterior view of anterior wall of left posterior cranial fossa
- Fig 146 Photograph of posterior view of deep back of head and neck dissection
- Fig 147 Diagram of posterior view of deep back of head and neck dissection
- Fig 148 Photograph of left parotid gland
- Fig 149 Diagram of left parotid gland
- Fig 150 Photograph of left parotid gland with main trunk of facial nerve
- Fig 151 Diagram of left parotid gland with main trunk of facial nerve
- Fig 152 Photograph of left vertical segment of the facial nerve
- Fig 153 Diagram of left vertical segment of the facial nerve
- Fig 154 Photograph of left temporal bone and suboccipital dissection
- Fig 155 Diagram of left temporal bone and suboccipital dissection
- Fig 156 Photograph of left view of head and neck dissection
- Fig 157 Diagram of left view of head and neck dissection
- Fig 158 Photograph of dura mater being elevated from the floor of the cranial cavity
- Fig 159 Diagram of dura mater being elevated from the floor of the cranial cavity
- Fig 160 Photograph of lateral view of left middle cranial fossa
- Fig 161 Diagram of lateral view of left middle cranial fossa
- Fig 162 Photograph of left internal acoustic meatus de-roofed and facial nerve retracted
- Fig 163 Diagram of left internal acoustic meatus de-roofed and facial nerve retracted
- Fig 164 Photograph of superior view of dissected left middle cranial fossa floor
- Fig 165 Diagram of superior view of dissected left middle cranial fossa floor
- Fig 166 Intraoperative photograph of acoustic neuroma resection showing cerebellum being retracted through an occipital craniotomy
- Fig 167 Intraoperative photograph of glomus jugulare resection showing skin flap being retracted to reveal mastoid process
- Fig 168 Intraoperative photograph of glomus jugulare resection following superficial parotidectomy and transposition of the vertical segment of the facial nerve

Section 1

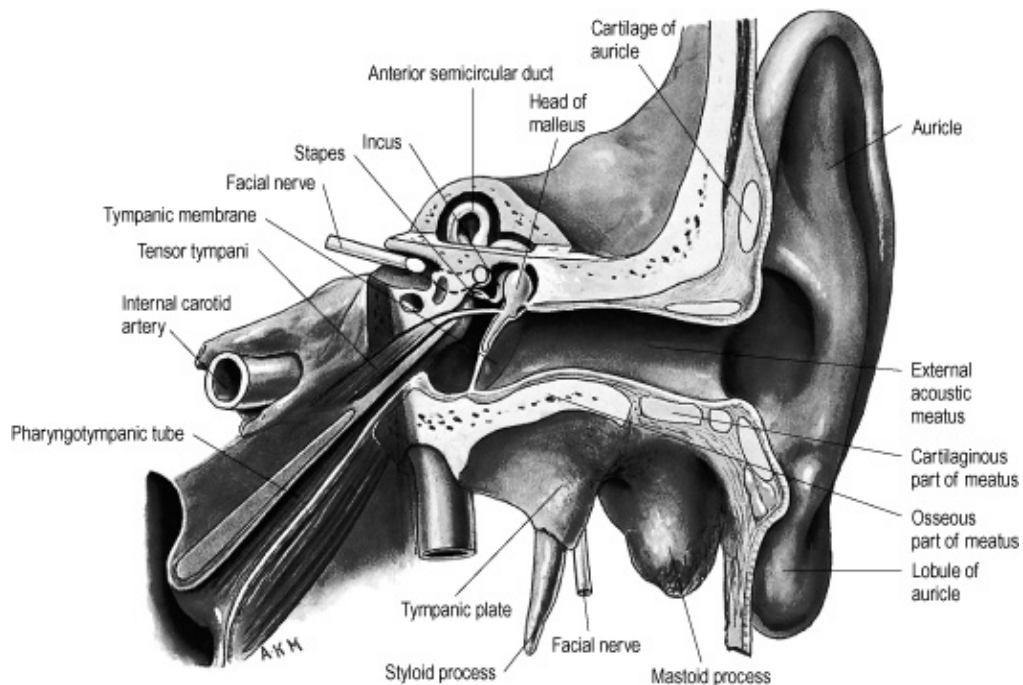
Introduction

The one thing that is clear about the inner ear is that there is a lot which is unclear. Debate about the structure of the ear dates back to the very first anatomists and their descriptions. Bartholomeas Eustachio (1520-1574) vehemently criticised Vesalius' description of the organ of hearing, going so far as to say that Vesalius' entire work "failed to contain a shred of truth" (Lustis et al, 1998).

There has also been much debate on the aetiology and management of diseases of the ear. In 1837, Joseph Toynbee after hearing one of the best known "aurists" of the time, John Harrison Curtis, speak to the Medical Society in London vowed to "rescue aural surgery from the hands of quacks." He believed that adequate dissection of temporal bones from patients with known inner ear disease would be required to create a strategy for the management of ear disease (Baloh, 2000).

THE EAR

The ear contains the peripheral auditory and vestibular apparatus. The ear can be divided into three parts, the external ear, the middle ear and the inner ear.



© Elsevier Ltd 2005. Standing: Gray's Anatomy 39e

Figure 1: Diagram of the external, middle and inner ear

In figure 1, the external ear can be seen separated from the middle ear by the tympanic membrane. The middle ear in turn is separated from the inner ear by a bony partition, which has two windows, with the oval window being covered by the stapes. The external ear is formed by the auricle and external auditory meatus which has cartilaginous and bony components. Each ear acts as a distance receptor for the collection, conduction, modification, amplification and analysis of complex waves of sound reaching them.

The external ear is concerned with directing sound towards the middle ear. The middle ear contains the auditory ossicles: malleus, incus and stapes. The middle ear communicates with the pharynx by the Eustachian, pharyngotympanic, tube. The internal carotid artery passes through the temporal bone in proximity to the inner ear structures.

Due to the structure, human ears are extremely sensitive to alterations in frequency, intensity and phase of sound and can locate the source if both ears are used. The normal adult ear is capable of hearing sound frequencies in the range of 20 to 20000 Hertz (cycles per second) and is most sensitive to sounds in the range of 1500 to 3000 Hertz (Fletcher et al, 1933). The middle and inner ear lie within the petrous part of the temporal bone.

TEMPORAL BONE

Temporal is derived from the Latin *temporalis*, originating from *tempus*, *tempor*, meaning time (Oxford dictionary of English, 1995). The hair on the temporal region is the first to turn white, and therefore the underlying bone was named the temporal bone, to mark the passage of time (Oxford English Dictionary).

The following description can be obtained from a standard anatomical text such as Gray's Anatomy (Standring et al, 2004). The temporal bone consists of four fused parts, squamous part, petrous part, tympanic plate and styloid process, and it forms part of the lateral wall and base of the skull. Anteriorly the squamous part articulates with the parietal bone and greater wing of the sphenoid to form part of the pterion. The zygomatic

process of the temporal bone articulates with the zygomatic bone anteriorly. Posteriorly and medially the temporal bone articulates with the occipital bone. The apex of the petrous part marks the boundary from the middle to the posterior cranial fossa and the tentorium cerebelli attaches to the superior border of the petrous border running medially until the posterior clinoid process.

The 'Petrous' part of the temporal bone is derived from the Greek, *petra* meaning rock and pertaining to the density of the bone surrounding the inner ear. The petrous bone lies in the skull base; it is pyramidal in shape and is limited posteriorly by the occipital bone and anteriorly by the sphenoid bone. The apex is directed anteromedially, pointing towards the posterior clinoid processes. The anterior surface lies posterolateral to the apex and forms the posterior wall of the middle cranial fossa, the posterior wall forms part of the anterior wall of the posterior cranial fossa. The petrous temporal bone contains the tympanic cavity and the inner ear.

THE MIDDLE EAR

The middle ear is formed by two connecting cavities, the mastoid cavity and the tympanic cavity. The tympanic cavity contains the ossicles and two muscles attached to them, tensor tympani and stapedius. The middle ear facilitates the amplification of sound waves and acts as an impedance match between the air of the outside and middle ear cavity and the fluid cavities of the inner ear. Due to the small size of the inner tympanic membrane, the oval window compared to the size of the outer tympanic membrane, there is an increase in the pressure by fifteen to twenty times. Sound wave vibrations may also be suppressed within the middle ear by the contraction of stapedius or tensor tympani, to protect the delicate inner ear structures. The middle ear is connected to the nasopharynx by the Eustachian tube. The basal turn of the cochlea, part of the inner ear, protrudes into the middle ear forming the promontory.

THE INNER EAR

The inner ear contains the sense organs of hearing and balance. Within the inner ear the cochlea is concerned with the conversion of sound wave vibrations into electrical

impulses which are then conducted along the cochlear division of the vestibulocochlear nerve. The semicircular canals are concerned with the conversion of angular acceleration into electrical impulses which are carried along the vestibular component of the vestibulocochlear nerve along with the impulses from the saccule and utricle which are concerned with the detection of linear acceleration and gravity.

THE LABYRINTH

Due to the complexity of the structure the inner ear is referred to as the labyrinth, the bony labyrinth and the membranous labyrinth. Labyrinth is derived from the Greek laburinthos meaning a complicated irregular network of passages or paths (Oxford Dictionary of English, 2005)

THE BONY LABYRINTH

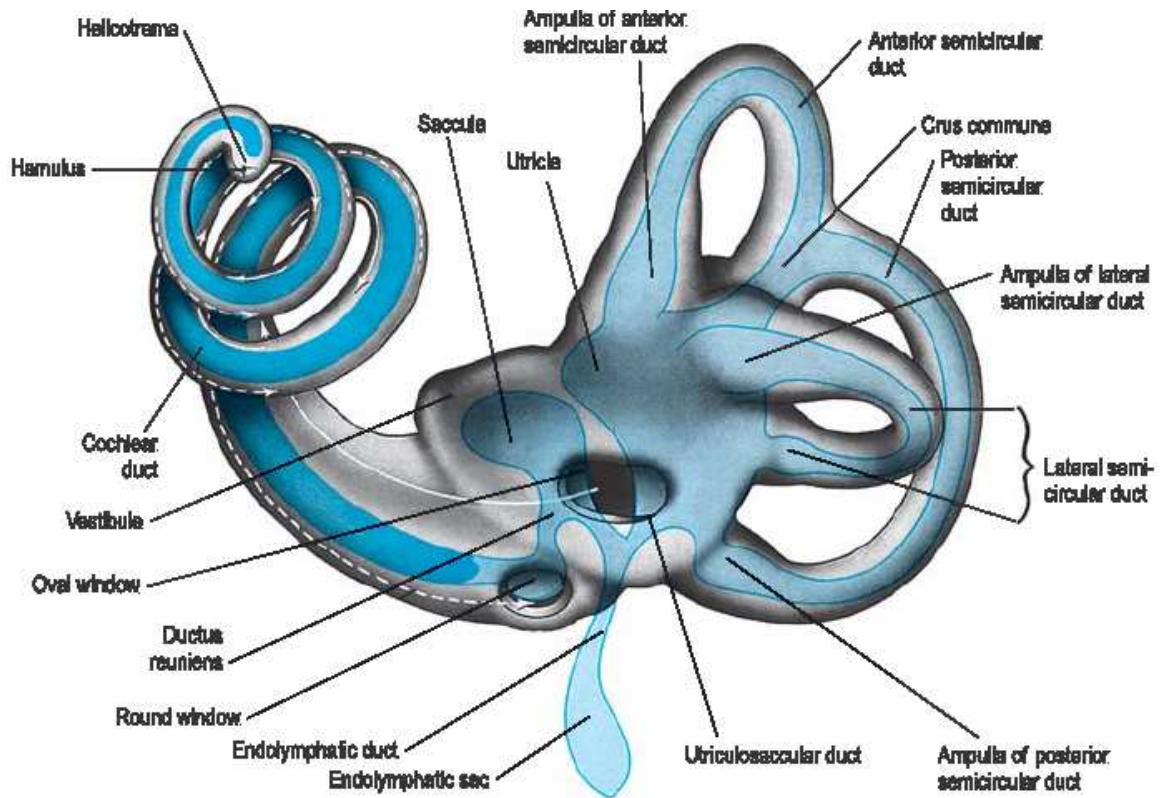
The description of both the bony and membranous labyrinths are taken from a standard anatomical text, Grays Anatomy (Standring et al, 2005) and a specialised text on temporal bone anatomy, Anatomy of the Temporal Bone with Surgical Implications (Schuknecht et al, 1986). The bony labyrinth is a series of cavities found within the petrous part of the temporal bone and the membranous labyrinth is a series of ducts and sacs found within the bony labyrinth. The three parts of the bony labyrinth are the vestibule, the semicircular canals and the cochlea. The vestibule is situated medial to the tympanic cavity with the semicircular canals anteriorly and the cochlea posteriorly. There are three semicircular canals, lateral posterior and superior.

The bony labyrinth is lined by periosteum and a very thin serous membrane which secretes a fluid called perilymph. This membrane continues along with the cochlear vein along the cochlear duct to communicate with the subarachnoid space.

THE MEMBRANOUS LABYRINTH

Within the bony labyrinth is the membranous labyrinth which follows the same general arrangement as the bony labyrinth, with the exception of the vestibule where the utricle and saccule are present. The membranous labyrinth is filled with a fluid called

endolymph which does not communicate with the perilymph. The membranous labyrinth is held in place by membranous bands which span the perilymph from the bony wall.



© Elsevier Ltd 2005. Standing: Gray's Anatomy 39e

Figure 5, Diagram of the membranous labyrinth

Figure 5 shows the saccule, which lies in the spherical recess of the vestibule. It receives innervation from the vestibular nerve, and communicates with the cochlear duct by the ductus reuniens of Hensen. The endolymphatic duct is also given off which is joined by the utriculosaccular duct from the utricle. The endolymphatic duct then continues in the vestibular aqueduct to end in a blind sac called the endolymphatic sac on the posterior wall of the petrous bone.

The utricle is larger than the saccule and lies posteriorly in the vestibule. It is oblong in shape; the part which lies in the elliptical recess of the vestibule has a thicker lining and receives nerve fibres from the vestibular nerve. The utricle communicates with the semicircular ducts by five openings.

The semicircular ducts are on average about one quarter of the diameter of the semicircular canals and are eccentrically placed within the bony canal. In the ampulla of the semicircular canals lies the transverse septum in which the final divisions of the vestibular nerve innervating the canals end.

Within the cochlea the membranous labyrinth forms the cochlear duct which lies upon the spiral osseous lamina and basal membrane and is roofed by the vestibular membrane which spans from the periosteum of the spiral lamina to the bony wall. The cochlear duct, scala media, is eccentrically located and resembles a triangle with the outer wall formed by a thickened layer of periosteum. This thickened periosteum is called the spiral ligament and superiorly it contains vascular loops and is called the stria vascularis. The cochlear duct is closed at the apex and communicates with the saccule proximally.

ANATOMY OF THE ENDOLYMPHATIC DUCT AND SAC

Within the bony vestibule, on the anteroinferior wall of the utricle, part of the membranous labyrinth, is a structure referred to by some as the utriculoendolymphatic valve. This valve separates the embryological pars inferior, (saccule and cochlea) from the pars superior, utricle and semicircular canals. The valve is formed by an inward projection of the wall of the utricle, thickened to form a rigid lip which is resistant to movement and presses against the junction of the inferior wall and the utricular duct. It has been theorised that when endolymph pressure is high the flexible wall is pushed away from this more resistant lip and the valve opens allowing endolymph to flow from the utricle into the utricular duct. When pressure is low the wall presses against the lip and the valve is closed. The utricular duct joins with the endolymphatic duct, which arises from the saccule, the endolymphatic sinus, a dilatation in the wall occurs distal to this union (Schuknecht et al, 1975).

The sinus is located in a depression on the posterior wall of the vestibule. The sinus narrows and forms the endolymphatic duct as it enters into the vestibular aqueduct of the petrous bone. Within 1mm of the vestibular orifice the duct narrows to form the isthmus of the endolymphatic duct which at 0.3mm in diameter is the narrowest part. The

endolymphatic duct continues in a posterior direction then it bends to pursue a lateral and inferior course within the bony vestibular aqueduct. The arterial supply of the vestibular aqueduct and its contents is from a branch of the posterior meningeal artery and a branch of the internal auditory artery. The venous drainage is through the vestibular aqueduct vein. Within the petrous bone the vestibular aqueduct enlarges to house the part of the endolymphatic sac (Schuknecht et al, 1986).

The endolymphatic sac is said to be located partly within the petrous bone covered by a scale of bone called the operculum and partly within the layers of dura in the posterior cranial fossa. The sac lies on the posterior surface of the petrous bone in a depression on the surface called the foveate impression. This is located about 10mm lateral to the internal auditory meatus and 10mm inferior to the superior petrosal sulcus. The sac can be divided up several ways, e.g. into subosteal and intradural sections. The length of the intradural portion is variable and depends on the degree of pneumatization of the petrous bone. A short intradural and long subosteal section would be associated with rich pneumatization. A diagram of the endolymphatic duct and sac in relation to the other parts of the membranous labyrinth can be seen in figure 6.

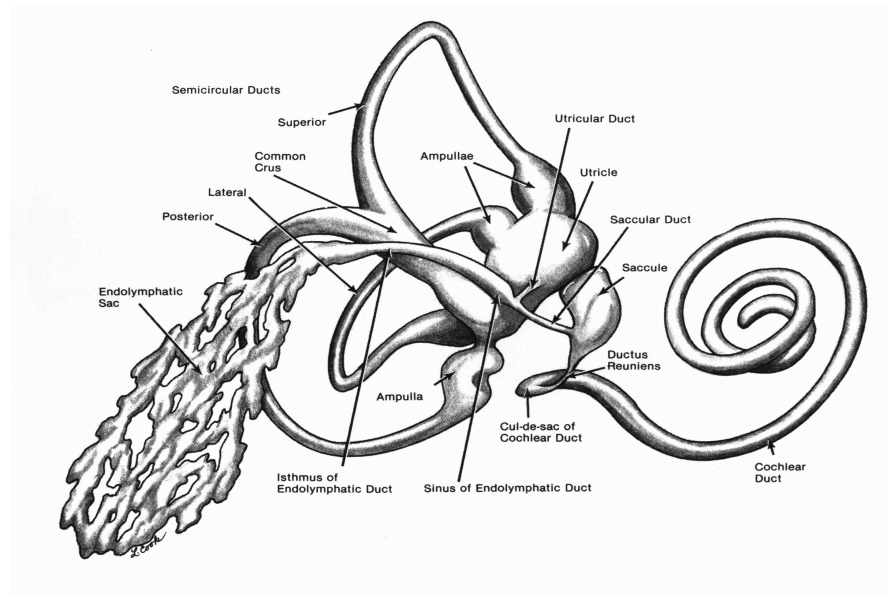


Fig 6: Diagram of the membranous labyrinth with endolymphatic sac
From Anatomy of the Temporal Bone with Surgical Implications, Schuknecht, 1986

The anatomical structure and variability of the adult endolymphatic sac has been studied by Shea et al (1979) and Bagger-Sjöbäck et al (1990). Shea used a method of injecting the endolymphatic compartment with dye and then performing a decompression procedure, Bagger-Sjöbäck et al used 3D reconstruction of specimens processed histologically. The results from the two methods do not correlate. It also revealed that the distal portion is separated into tubules running longitudinally and which do not reunite at the termination of the sac. The sac was fusiform and the extraosseous portion was three times the volume of the intraosseous portion.

Studies have shown that there is great variability in the size of the whole endolymphatic sac. This is not random, because there is a correlation between the size of the vestibular aqueduct and the size of the sac, for example a small diameter aqueduct was associated with a smaller sac (Danckwardt-Lillieström, 2000).

As surgery on the endolymphatic sac is normally performed on the extraosseous portion, it is also worth noting the great variability in the size of this particular portion. In some there may be no extraosseous portion or that part may consist of multiple microscopic tubules which would not be identifiable at surgery (Bagger-Sjöbäck, 1993). It has also been shown that, the distal portion of the endolymphatic sac, although it may be large in size may not have any discernable confluent area within it and that it may also overlap the sigmoid sinus (Friberg et al, 1988).

From a mastoidectomy approach it has been suggested that the endolymphatic sac lies on a line which is projected from the lateral semicircular canal and bisects the posterior semicircular canal (Shambaugh, 1966). The endolymphatic sac can be visualised in Trautmann's triangle using the dome of the horizontal semicircular canal, the medial edge of the sigmoid sinus and the short process of the incus as identifiable landmarks, without the need to 'blue line' the posterior semicircular canal which would increase the risk of postoperative hearing loss (Shea et al, 1979).

PARAVESTIBULAR CANALICULI

There are normally two paravestibular canaliculi which accompany the vestibular aqueduct and the endolymphatic duct. The course and number are variable with many studies giving varied results. The larger of the two originates at the vestibule, superomedial to the aperture of the vestibular aqueduct. It follows a path terminating at the surface of the petrous bone inferior the vestibular aqueduct. It contains a small artery and the vein of the vestibular aqueduct, and it may join with the vestibular aqueduct (Ogura, 1971, Stahle et al, 1974).

HISTOLOGY AND ULTRASTRUCTURE OF THE ENDOLYMPHATIC SAC

The endolymphatic sac can be divided into three morphologically distinct regions in mammals, the proximal portion (pars proximalis) leading on to the rugose region (pars intermedius) and then expanding into the distal sac (pars distalis). In humans the pars proximalis and pars intermedius are contained within the temporal bone and the pars distalis is the intradural portion. The pars proximalis is the section between the isthmus of the endolymphatic duct and the rugose part of the sac (Bagger-Sjöbäck, 1993).

The epithelium is simple in nature, ranging from squamous, through cuboidal to low columnar. The epithelium is thrown into folds with polypoid projections and tubular formations. There are mitochondria rich cells with light cytoplasm, and microvilli on the cell surface. Schindler (1980) describes two major epithelial cell types. Type I cells have an ovoid nucleus which is pale. Cytoplasm varies from pale to dark. There is an ordered arrangement of microfilaments which appear to arise from the basal region of the nuclear envelope and extend into the basilar infoldings of the cell membrane. There is both smooth and rough endoplasmic reticulum, most prominent in the apex near the Golgi apparatus. These cells contain many membrane-bound inclusions and mitochondria are seen in the region of the golgi apparatus and along the plasma membrane between adjacent cells. This suggests an active role for these cells, perhaps secretory. Type II cells have smaller irregular edged nuclei, without nucleolus. The cells have fewer microvilli extensions into the sac lumen and there is no well developed

microfilament network. The cytoplasm is often darker. Type I cells make up 80% of the epithelium of the rugose portion and Type II cells make up 20% of the epithelium.

Beneath the basement membrane lies a loose-areolar type connective tissue containing macrophages, fibroblasts and occasional smooth muscle cells. It also contains a rich capillary network which extends into the rugose infoldings. In the distal section the connective tissue is denser with prominent collagen filaments and less extensive capillary network. (Schindler, 1980)

BLOOD SUPPLY TO THE LABYRINTH

The petrous temporal bone encases the internal carotid artery as it passes through the carotid canal to gain access to the cranial cavity. The **internal carotid artery** arises from the common carotid artery and passes up the neck lateral to the pharynx to enter the carotid canal in the temporal bone. The carotid canal is lined by an extremely thin layer of bone and it is possible for aneurysms of the artery to invade the middle ear resulting in a pulsatile mass in the middle ear with possible pulsatile tinnitus (Rhoton, 2000, Dhillon et al, 1999).

The arterial supply is important in considering disease in the ear but also extremely important when considering otological surgery. The large arteries which provide branches for the temporal bone and its contained structures are the maxillary artery and the anterior inferior cerebellar artery which is a branch of the **basilar artery** (Schuknecht et al, 1986).

The anterior inferior cerebellar artery gives off a branch which forms a loop adjacent to the internal auditory meatus. Occasionally this loop is formed from a branch of the accessory anterior inferior cerebellar artery or posterior inferior cerebellar artery. Occasionally the middle meningeal artery or accessory meningeal arteries enter the temporal bone (Rhoton, 2000).

The main vessel supplying the membranous labyrinth is the **labyrinthine artery**, a branch of the anterior inferior cerebellar artery which arises from the basilar artery. The labyrinthine artery arises within the cranial cavity and provides a supply to the dura lining the internal auditory canal and the bone surrounding the canal. It divides to form the common cochlear artery and the anterior vestibular artery. The common cochlear artery then divides to form the main cochlear artery, which supplies the upper three quarters of the modiolus and cochlea, and the vestibulocochlear artery. The vestibulocochlear artery in turn divides to form the posterior vestibular artery and the cochlear ramus, which supplies the remainder of the cochlea and modiolus. The posterior vestibular artery, along with the anterior vestibular artery, supplies the utricle, the saccule and the three semicircular canals (Axlesson, 1968).

VENOUS DRAINAGE OF THE LABYRINTH

The anterior vestibular vein drains the ampullae of the superior and lateral semicircular canals and the utricle. The posterior vestibular vein drains the ampulla of the posterior canal, the saccule and the inferior end of the cochlea. The anterior and posterior vestibular veins join with the vein of the round window forming the vestibulocochlear vein. The cochlea is drained by the anterior and posterior spiral veins, which unite to form the common modiolar vein. There are shunts between the anterior and posterior spiral veins. The common modiolar vein and the vestibulocochlear vein join to form the inferior cochlear vein which drains into the inferior petrosal sinus (Standring et al, 2004).

The veins of the membranous semicircular canals flow towards the non-ampulated end, and join to form the vein of the vestibular aqueduct. The vestibular aqueduct vein drains into the lateral venous sinus. It reaches this by passing along the vestibular aqueduct or one of the paravestibular canaliculi (Orgura, 1971).

FUNCTION OF THE MEMBRANOUS LABYRINTH

Sound waves crossing the cochlear duct cause the basement membrane to vibrate, and vibrations occur at different points on the membrane depending on the frequency. As the basement membrane is displaced the hair cells detect this as they are also fixed by the

tectorial membrane. The result is electrical impulses produced at specific areas within the cochlea depending on specific frequencies of sound. Sound can be distinguished by the brain as noise, without repeating pattern, or musical, with repeating pattern (Fletcher, 1938).

The organ of Corti within the cochlea contains the hair cells, arranged into a row of inner hair cells and three rows of outer hair cells. Each inner hair cell has between 20 and 50 stereocilia projecting into the tectorial membrane. Movement of the stereocilia opens transduction ion channels allowing entry of potassium and calcium ions and generating a transduction current. This then causes the release of neurotransmitters from the base of the hair cell which stimulates the cochlear nerve. The transduction channels are partially open in the resting position, generating spontaneous activity in the auditory nerve. The frequency of movement of the stereocilia is matched by the frequency of the initial sound stimulus (Raphael, 2003).

Also contained within the inner ear are the three semi-circular canals and two otoliths, concerned with balance and the detection of angular and linear acceleration. The organs of balance are responsible for the conversion of movement into electrical impulses which are conducted along the vestibular component of the vestibulocochlear nerve. Input from the semicircular canals is required for balance.

The semicircular canals function by moving with the head as they are fixed in bone. The fluid contained within the canals will move relative to the fixed canal. Due to the inertia of the fluid, this movement of the fluid relative to the bone is measurable and interpreted by the brain as acceleration or deceleration. Hair cells on the ampullary crest have stereocilia which project into the cupula. Movement of the endolymph deflects the cupula therefore stimulating the hair cells which in turn send impulses along the vestibular nerve. Depending on the direction of the hair cell movement, the cells are either stimulated or inhibited (Pasha, 1993).

The three main functions of the vestibular apparatus are to maintain the direction of eye gaze during movements of the head, to help maintain upright posture, and to provide awareness of position and acceleration of the body. Abnormal input from the vestibular apparatus can result in nystagmus, vertigo and be accompanied with nausea (Pasha, 1993).

ENDOLYMPH PRODUCTION AND CIRCULATION

The endolymph which fills the membranous labyrinth is produced by the marginal cells of the stria vascularis in the cochlea. The dark cells of the cristae and maculae share many similarities to the marginal cells of the stria vascularis. Endolymph is reabsorbed within the endolymphatic sac, the nonsensory component of the membranous inner ear. Endolymph is a unique extracellular fluid due to its ionic composition. Endolymph has low sodium content and high potassium content. In this respect endolymph resembles intracellular fluid in ionic composition. Recent observations have shown multiple possible control mechanisms for endolymph production; strial marginal cells may be stimulated by beta 1 adrenergic receptors and inhibited by M3 and / or M4 muscarinic receptors (Wangemann, 2002).

Endolymph is maintained within the cochlea and the labyrinth at a resting potential by the cycling of potassium ions, creating an ionic gradient. This charge is essential for sensory cell transduction. There is a cycle in which the potassium ions are transported across the cells in the stria vascularis of the cochlea, thus maintaining endolymphatic potential and creating endolymph. Potassium ions enter into hair cells by an apical transduction channel, opened when the stereocilia on the hair cell move. The potassium ions are then released into the perilymph by basolateral channels. Potassium ions are released from intermediate cells into the interstitial space via a channel and thus generating the endocochlear potential. Potassium ions are then taken up by the strial marginal cells and then finally secreted by apical transporters into the endolymph completing the cycle. A similar cycle exists in the vestibular labyrinth. Mutations of the potassium ion transporter genes can result in deafness in humans. (Wangemann, 2001)

It has been shown in studies that normally there is no measurable flow of endolymph within the membranous labyrinth and that a small (70nL) increase in volume results in no overall flow. This would suggest that in the normal state, endolymph is maintained without significant volume flow. However a larger increase in volume has been shown to result in longitudinal flow of endolymph towards the endolymphatic duct and sac (Salt, 1995, 1997). It has also been shown that if the cochlear fluid volume is reduced, there is flow of endolymph from the endolymphatic sac along the endolymphatic duct towards the cochlea. Salt (1995) therefore postulated that the endolymphatic sac may have a role in endolymph production as well as resorption. Both studies show (however) small volume changes in endolymph are compensated for locally.

It is generally believed that endolymph flows, when the volume is increased, towards the endolymphatic duct and sac where it is reabsorbed as part of inner ear homeostasis (Guild, 1927). Studies have shown that obstruction of the absorptive ability of the endolymphatic duct and sac, for example by obstruction of the endolymphatic duct, results in endolymphatic hydrops (Lohuis et al, 1999).

Further support to the possible secretory role of the endolymphatic sac comes from animal studies which have shown that endolymphatic volume changes results in morphological changes. Increasing the volume of fluid in the endolymphatic sac results in a decrease in the stainable homogenous substance that can be seen within the lumen of the sac. Decreasing the endolymphatic fluid volume results in an increase in the homogenous substance. Macrophages and the epithelium of the sac have been implicated in the process of removal of homogenous substance. These results show that the endolymph volume may be regulated by active secretion and resorption of a lumen expanding substance within the sac (Rask-Andersen et al, 1999).

It has also been shown in animal studies that in normal ears the endolymph and endocochlear potential are insensitive to volume increases in the scala tympani but are sensitive to volume increases in the scala vestibuli. The authors concluded that as a result endolymphatic pressure or movements would not be affected by cerebrospinal fluid

pressure, which would be transmitted to the scala tympani along the cochlear aqueduct (Salt 1998). However Konradsson et al using tympanic membrane displacement showed that conduction of pressure from cerebrospinal fluid to perilymph was more marked in diseased ears of patients with Ménière's disease. They speculated that this may be part of the pathogenesis of Ménière's disease and that cerebrospinal fluid pressure and perilymphatic pressure affect endolymphatic pressure and movement (Konradsson et al, 2000).

FUNCTION OF THE ENDOLYMPHATIC SAC

The endolymphatic sac is thought to have a role in endolymphatic volume control and (possible) pressure regulation. There are structural and physiological mechanisms described along with theories for endolymph production and absorption by the sac. Wackym et al (1987) postulated possible mechanisms of pressure regulation by the endolymphatic sac. These theories were derived from electron microscopy of the epithelium and structure of the endolymphatic sac.

First was pressure regulation by endolymph resorption, a passive transcellular movement of water across the epithelium, and an active transcellular ion exchange and an active transcellular vacuolar bulk endolymph outflow. These mechanisms may regulate endolymphatic pressure by resorbing endolymph and lowering the volume in the endolymphatic compartment.

Secondly pressure regulation by mechanical factors, the sharp angle between the endolymphatic duct and the endolymphatic sac may prevent sudden backflow of endolymph, produced for example by an increase intracranial pressure. The elasticity of the sac may be to accommodate transient increases in endolymphatic volume and thus prevent the pressure becoming too high. Schuknecht also described the utriculoendolymphatic valve which is thought to maintain endolymphatic volume within the cochlear and semicircular ducts and allow endolymph to flow into the endolymphatic duct and sac when the pressure rises (Schuknecht et al, 1975).

Third, it may regulate pressure by secretory mechanisms, within the smaller tubules a homogenous substance was found and identified as proteoglycans with a high affinity for water. Secretion of this homogenous material into the lumen of the endolymphatic sac would attract water and thus increase endolymphatic volume. By the same principle, absorption of this material would reduce the water content and thus volume of the endolymphatic compartment (Wackym et al, 1987).

There is evidence for possible local control mechanisms for endolymph haemostasis. Specific atrial natriuretic peptide receptors have been identified within the endolymphatic sac, with a predominance of the ANP-B receptor subclass. It has been postulated that inner ear fluid homeostasis could be regulated by a locally effective paracrine system involving the ANP system, analogous to other organ systems of the body. It would involve either endolymph production in the stria vascularis or endolymph absorption by the endolymphatic sac. (Dornhoffer et al, 2002). Extracts of endolymphatic sacs when infused intravenously into live rats has been shown to produce a natriuretic response. The active substance has been named saccin (Qvortrup, 1999).

Along with the function of inner ear fluid homeostasis, there is also evidence to suggest an immunological role of the endolymphatic sac. Bui et al (1989) found lymphocytes, mainly T suppressor / cytotoxic cells, lymphocytes and plasma cells within the endolymphatic sacs of patients with acoustic tumours by immunohistochemical means. It has been shown that after exposure of the nasopharynx to infection, specific antigen-sensitised memory cells can be located within the endolymphatic sac. The route by which they get to the endolymphatic sac is not known; no antigen could be detected in the Eustachian tube or middle ear. It is speculated that after exposure to antigens or infection in the nasopharynx, systemic memory cells from the cervical lymph nodes circulate to the endolymphatic sac via the bloodstream or lymphatics (Gloddek et al, 1998).

EVOLUTION OF THE EAR

The ear is essentially a mechano-electric transducer, to convert movement into electrical stimuli that can be conducted along nerve tissue, for example converting the vibrations of

sound into electrical impulses in the cochlea nerve and conversion of movement of the head into electrical impulses in the vestibular nerve. The rest of the ear and its development are concerned with conveying the movement of the head (angular and linear acceleration) towards the transducing hair cells. The energy of movement is transferred from movements of the head through the fixed temporal bone, and sound vibrations are conveyed from the outer, through the middle, and into the inner ear. The evolution of the ear can be looked at in many ways. For example, the evolution of the anatomy of the ear, and how the movement detectors or semicircular canals in fish have evolved into the semicircular canals in man. Another example is the hair cell structure and how it compares between simple invertebrates and mammals. Thirdly at the molecular level, examining the genes that form the ear, and look for similarities and how and when new genes have been added and where they may have originated from.

A study of the development of the ear in different species, vertebrates and invertebrates may give an understanding of how it has evolved over the past 600 million years. Fritsch and Beisel (2001) presented the three major aspects of inner ear evolution as: development and evolution of vertebrate hair cells, development and evolution of the innervation of ear and development and evolution of the inner ear morphology.

Paramecium putrinum, a slipper shaped ciliate which is found in oxygenated aquatic environments feeding near vegetative matter, is able to balance within water by the use of hairs immersed in liquid. The first ear may have developed in the coelenterates, some 900 million years ago, and is manifest today as the statocyst in the jellyfish. The statocyst is a cystic organ at the base of the tentacles, containing a statolith, small stone (Taylor, 1969).

The human ear is likely to have originated from that of the fish with increasing complexity and the transition from water to land and air. Along the sides of fish are the lateral line organs, a series of pits called neuromasts formed by pits, cups and ampullae and innervated by the seventh, ninth and tenth cranial nerves. The semicircular canals

developed from the head section of the lateral line organs. The cochlear duct is thought to have developed from the lagena on the floor of the saccule (Taylor, 1969).

As the lateral line organ is bathed in sea water and the movement of the water is detected and correlates to the movement of the fish, the hair cells of the inner ear are fixed by the surrounding bony structure and bathed in endolymph which moves relative to the rest of the body allowing detection of motion.

The composition of endolymph is a unique extracellular fluid. Figure 7 allows comparison the perilymphatic fluid within the scala vestibule and the scala tympani with endolymph and cerebrospinal fluid.

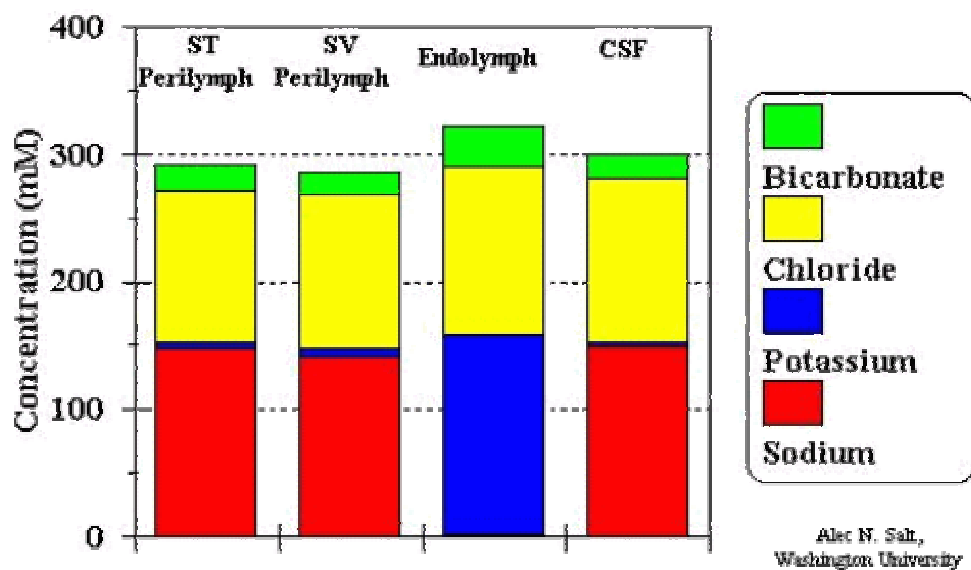


Figure 7: Graphical representation of extracellular fluid salt concentrations
From Washington University, Cochlea Fluid Lab

When sea water is examined the percentage weight of sodium is 30.8%, chloride is 55.3% and potassium is 1.1%. This is similar in composition to that of endolymph.

There are similarities at the cellular and molecular level between invertebrate mechanosensory systems and the vertebrate inner ear hair cell system. To create the receptor potential of hair cells, they are bathed in potassium rich endolymph. A discontinuous potassium ion gradient is maintained by the presence of tight junctions in the auditory and vestibular organs in *Drosophila*.

The increasing complexity of the vertebrate inner ear through species is apparent. The formation of the horizontal canal in ratfish correlates with the expression the *Otx* gene which is absent in the more primitive lamprey which has only two semicircular canals. Conservation of developmental regulatory genes suggests homology between a subset of invertebrate mechanosensory neurones with vertebrate hair cells. Constraints are imposed by certain genes, impairing further evolutionary divergence; one example may be the common bilateral mechano-electric transducing system.

Webster (1966) describes greater morphological diversity in the external ear than in the middle ear and the least in the inner ear, reflecting developmental stresses. He noted that the semicircular canal system with the utricle and saccule are found in all vertebrates. The middle ear with the tympanic membrane and ossicles are only found in tetrapods and the pinna is found only in mammals.

DEVELOPMENT OF THE EAR

The human inner ear is a complex structure, with many identifiable stages in its development. The general principles are outlined in standard textbooks (Larsen 2001, Strandring et al, 2004)

The external and middle ear develop from structures of the first and second pharyngeal arches and the first pharyngeal cleft and pouch. The first pharyngeal pouch gives rise to tubotympanic recess which then differentiates into the tympanic cavity and the Eustachian tube. The three ossicles are formed from the cartilage of the first and second pharyngeal arches. The pinna forms from six auricular hillocks on the opposing edges of

the first and second pharyngeal arches. The first pharyngeal cleft lengthens to form the beginning of the external auditory canal. The tympanic membrane develops from the pharyngeal membrane separating the first pharyngeal pouch and cleft and as such it contains a surface ectoderm layer, fibrous, mesoderm layer and an inner endodermal layer. The membranous labyrinth develops from the otic placode which forms from the epidermis. The bony labyrinth develops from calcification of the mesenchymal condensation around the membranous labyrinth which forms the otic capsule.

POSTNATAL DEVELOPMENT OF THE EAR

Postnatal development of the temporal bone is concerned in part with pneumatisation of the mastoid and temporal bone, i.e. with the appearance of air cell tracts, which are communicating air filled spaces within the temporal bone. The mastoid communicates with the tympanic cavity which is aerated by means of the Eustachian tube.

Conditions that affect aeration of the mastoid, also affect the growth of the temporal bone. Failure of aeration results in altered growth of the bone. This is an important surgical point, in that when operating on ears with pathology there may be abnormal anatomical arrangements as a result of reduced or altered pneumatisation. As well as allowing air flow, these communications may allow the spread of infection through the temporal bone. Sometimes accessory regions become pneumatised, via accessory tracts, these regions are not normally pneumatised. These tracts can involve parts of the temporal bone or adjacent bones, forming zygomatic, squamous occipital or styloid air cells (Schuknecht et al, 1986)

The tracts mark out a path through the temporal bone around most of the important structures. A description of these tracts can be found in 'Anatomy of the temporal bone with surgical implications' by Schuknecht (1986). The **posterosuperior cell tract** extends from the mastoid anteriorly and laterally to lie in the angle of bone between the posterior and middle cranial fossa. The **posteromedial cell tract** extends anteriorly and medially from the mastoid to lie under the posterior surface of the petrous bone. The **perilabyrinthine tracts** extend from epitympanic area of the middle ear to the

supralabyrinthine area and from the hypotympanic area to the infralabyrinthine area. The **peritubal tract** extends from the Eustachian tube towards the apex anterior to the internal carotid artery. The **subarcuate cell tract** extends from the mastoid anteriorly and medially towards the apex, passing inferior to the arc of the superior semicircular canal.

Studies have shown that the maturation of the endolymphatic sac into its definitive adult form can occur well after birth in some cases, but most specimens had an adult form by one year. It was shown that development to adult form and growth to adult size are not correlated (Matthew, 2000).

MÉNIÈRE'S DISEASE FIRST DESCRIBED

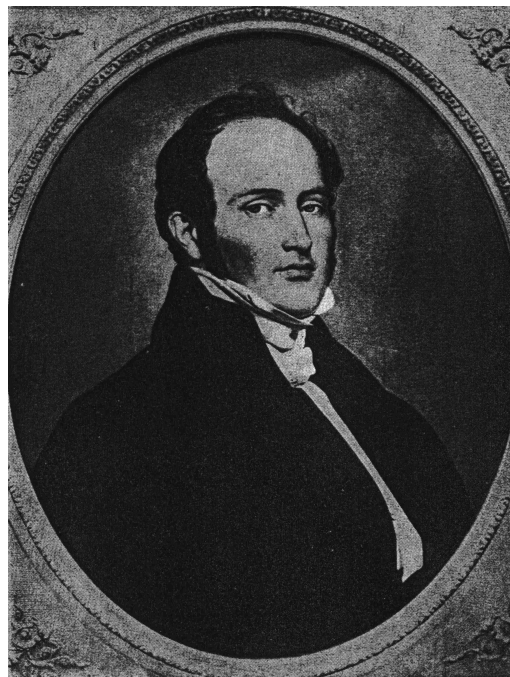


Figure 9: Portrait of Prosper Ménière
(Atkinson, 1961)

Prosper Ménière was born in the Loire Valley on 18th June 1799, 10 years after the French Revolution. He became a medical student at the Hotel Dieu in Angers and moved to the sister hospital in Paris. He was awarded the Gold Medal in 1826 and his Doctorate in 1828. Ménière worked as a clinical assistant to Dupuytren. In 1848 Ménière

published his French translation of Kramer's "Treatise on Diseases of the Ear". He presented his own four papers to the Paris Academy of Medicine. Ménière died on 6th January 1862 at the age of 62 from pneumonia (Morrison, 1997).

In his first paper, presented on January 8, 1861, 'A Report on Lesions of the Inner Ear giving rise to Symptoms of Cerebral Congestion of Apoplectic Type', Ménière describes the autopsy findings of a young woman who presented completely and suddenly deaf with severe vertigo. She had travelled by night in winter, on the box seat of a stagecoach. At autopsy the semicircular canals of the inner ear were found to be filled with a red, plastic matter, a sort of bloody exudate, a few traces of which were found in the vestibule but did not exist at all in the cochlea. This has resulted in the incorrect belief that haemorrhage into the labyrinth is linked to Ménière's disease (Atkinson, 1961, Baloh, 2001). It is here for the first time that some of the symptoms previously thought to be only cerebral in origin have been linked to the inner ear, although in the case of the young patient the diagnosis was more likely to be acute labyrinthitis or possibly leukaemia which can cause haemorrhage into the labyrinth in the late stage. Ménière postulated that the symptoms of vertigo may originate from the inner ear, and with the evidence of this woman who had vertigo and pathological findings in the inner ear, he was able to make the link.

In the first paper Ménière also presents a series of patients who have a group of symptoms 'which are always the same, apparently serious, giving the impression of an organic lesion of the most distressing kind, recurring from time to time over weeks, months, years, then disappearing suddenly and presenting as a result common to them all the abolition of a special sense.' It is here that Prosper Ménière initially presented the symptoms of hearing loss, episodic vertigo and non-pulsatile tinnitus (Atkinson, 1961). This paper suggested for the first time that damage or disease in the inner ear or more precisely the semi-circular canals and not cerebral congestion may result in these symptoms (Baloh, 2001)

Further evidence that Ménière's disease is principally a disease of the inner ear, the labyrinth, and not a disease of the central nervous system lies in the fact that it is cured by labyrinthectomy or vestibular nerve section. That is to say in unilateral disease, surgical destruction of the labyrinth or surgical transection of the vestibular nerve controls the vertigo. In a study of 126 patients with vertigo, Gacek (1996) found that labyrinthectomy relieved vertigo in 98.8% of cases and vestibular neurectomy in 97.8% of cases.

EPIDEMIOLOGY OF MÉNIÈRE'S DISEASE

Ménière's disease affects 1 in 1000 in the United Kingdom, both sexes equally. The peak onset of age is between 20 and 50 years. The disease predominantly affects white people. (Saeed, 1998) Incidence of disease subsequently affecting both ears after initial presentation in one ear is 40% (Morrison, 1981). The disease can occur in children, with up to 3% of Ménière's patients being children (Meyerhoff et al, 1978).

SIGNS AND SYMPTOMS

Ménière's disease is an idiopathic presentation of Ménière's syndrome, characterised by episodic vertigo lasting from (between) minutes to hours, progressive sensorineural hearing loss, tinnitus and fullness in the ear (Pasha, 1993).

The progression of the disease can be categorised into three generally recognised stages. In the **first stage** the main symptom is vertigo (the sensation of movement when the body is stationary), rotatory or rocking and may be associated with nausea or vomiting. There is no loss of consciousness and attacks which may be accompanied by fullness in the ear last between 20 minutes and several hours. Hearing is normal in remission. The **second stage** features sensorineural hearing loss which is progressive with incomplete recovery between attacks. The hearing loss is initially at lower frequencies. The **third stage** is characterised by progressive hearing loss without fluctuation. Deafness occurs and the vertigo often lessens, alternatively it may continue. The patient has difficulty balancing (Saeed, 1998).

Prognosis is poor with continuing loss of hearing resulting in disability. Within a few years, 10% sufferers are crippled in terms of their normal everyday life. The outlook is especially bad if the disease is diagnosed in childhood (Morrison, 1989).

AETIOLOGY

Many theories for the causes of Ménière's disease have been proposed, but the cause remains obscure. Ménière's disease may be the common final pathway for different types of inner ear disease or trauma.

Hallpike and Cairns (1938) described endolymphatic hydrops in temporal bone specimens from patients with Ménière's disease. Prominent distension of the entire membranous labyrinth was seen, but it was most pronounced in the saccule with loss of the perilymphatic space. Hallpike and Cairns presumed that as the saccule had a thinner wall than the utricle, approximately one third of the thickness, it would be more prone to damage from volume changes. The inner ear was like a balloon containing fluid placed inside another container with fluid and a fixed wall. As the pressure rose within the endolymph the membranous wall would dilate to a point. Beyond this point, small increases in fluid content would result in large pressure changes. They believed that the tinnitus and vertigo were due to ischaemia of the end organs as a result of the pressure effects of hydrops within the inner ear.

Endolymphatic hydrops could be the result of excess endolymph production, decreased resorption or altered flow. It can be secondary to viral infection, syphilis, autoimmune disease, trauma, congenital abnormalities, and transient ischaemic attacks. Altered glycoprotein metabolism may result in dysregulation of inner ear fluid volume causing abnormal osmotic pressure and quantitative volume differences between perilymph and endolymph resulting in hydrops. Fibrosis of endolymphatic duct and sac impairs endolymph absorption and may result in hydrops (Morrison, 1981).

A further suggestion is that when endolymphatic hydrops causes symptoms of Ménière's disease it is because of damage to and tears of the membranous labyrinth. Membranous labyrinth distension may cause micro tears which allow the endolymph and perilymph to mix resulting in instant vertigo and some permanent damage to hair cells. The tear then seems to seal spontaneously after 2-3 hours. The inner ear fluid re-equilibrates with resolution of vertigo. Repeated ruptures may then result in progressive sensorineural hearing loss, this being characteristic of Ménière's disease (Baloh, 2001).

Auto antibodies to the endolymphatic sac in cases of Ménière's disease have been demonstrated. These are associated with a group of older patients and with more severe disease (Alleman et al, 1997). COCH5B2 which is a protein expressed in the vestibular system and the cochlea has been shown to be a target antigen in some cases of sensorineural hearing loss and Ménière's disease (Boulassel et al, 2001).

Calenoff et al (1995) demonstrated IgE specific for HSV-1, HSV-2, Epstein Barr virus and/ or cytomegalovirus in the serum of 9 out of 10 Ménière's patients and only 4 out of 10 in the control group. They postulated that immune complex formation between latent virus in the inner ear and circulating IgE would result in chemotactic and vasoactive substances being released. Vasoactive substances could result in excessive intralabyrinthine fluid formation and inflammatory cells recruited would result in gradual but permanent damage to the inner ear structures.

Some cells of the endolymphatic sac have been shown to have possible endocrine function, secreting a peptide called, "saccin". It has been postulated that abnormalities of this role may affect fluid balance within the inner ear resulting in Ménière's disease (Qvortrup, 1996).

Anatomical variants have been shown to be associated with Ménière's disease. It has been shown that the length of external aperture of the vestibular aqueduct is significantly shorter in patients with Ménière's disease. The shorter the aperture, the more often hydrops was present (Shea et al, 2000). Hosseinzadeh et al (1998) reported a case of a

patient with mechanical obstruction of the endolymphatic duct by an anomalous vein of the vestibular aqueduct; the vein was approximately four to five times the normal diameter. This obstruction resulted in endolymphatic hydrops and the symptoms of Ménière's disease. This shows how anatomical variations can result in endolymphatic hydrops.

ULTRASTRUCTURAL CHANGES OF THE ENDOLYMPHATIC SAC IN MÉNIÈRE'S DISEASE

In a study by Schindler (1980) in which biopsies were taken from the endolymphatic sac of patients undergoing drainage procedures, all biopsies were abnormal. There was sloughing of the luminal epithelium with thickening of the basilar lamina and fibrosis of the perisaccular connective tissue. The endoplasmic reticulum appears less extensive than commonly seen in normal epithelial cells. There are gaps between adjacent surface cells and collagen fibrils lie on the luminal surface of the sac (Schindler, 1980). Studies have shown that a dense product can be seen in the lumen of the sac along with evidence of merocrine secretion. A deposition of fibrous material below the epithelium can also be seen, and appears to be produced by the epithelium. Perisaccular fibrosis is believed to be a feature of Ménière's disease and it is possible that it is produced by the epithelium itself (Birgitta et al, 2001).

DIAGNOSIS

Diagnosis is based primarily on clinical history, examination and audiological findings, to exclude other causes of hearing loss and vertigo. The clinical features as discussed are recurring attacks of vertigo, tinnitus and ipsilateral hearing loss. The tinnitus is non-pulsatile with improvement following attacks (Morrison, 1981). On pure tone audiometry, low frequency fluctuating loss is seen with a combination of fluctuating low frequency and non-changing high frequency loss (Mateijsen et al, 2001).

INVESTIGATIONS

Electrocochleography is a way of measuring electrical impulses within the cochlear or auditory nerve induced by stimuli. Within 5 milliseconds of stimulation an action

potential (AP) is produced within the auditory nerve and the summing potential (SP), direct endocochlear potential is measured. Endolymphatic hydrops is indicated by an abnormal SP/AP ratio (Odabasi et al, 2000). Electrocochleography has been proposed as an important prognostic test for Ménière's syndrome (endolymphatic hydrops) and is also of use in determining likely benefit for endolymphatic sac surgery (Camilleri et al, 2001). Glycerol acts as an osmotic diuretic which may improve symptoms temporarily in the presence of hydrops, within 30 – 60 minutes (Morrión, 1981).

IMAGING OF THE ENDOLYMPHATIC SAC

An important part of the management of inner ear disease is imaging. **Computerised tomography** and **magnetic resonance imaging** along with three-dimensional reconstructive techniques allow clinicians to view the middle and inner ear in very high detail (Louryan, 1999). Malformations can be detected as well as pathology such as pontine angle tumours which may give rise to symptoms similar to those of Ménière's disease. In cases of Ménière's disease, imaging can be useful in planning surgery and assessing the results of surgery. There are correlations between Ménière's disease and imaging and surgical findings of the endolymphatic sac. Kobayashi et al showed that there was a significant correlation between magnetic resonance imaging (T2 weighted) of the endolymphatic sac and that seen in surgery. Therefore MRI could detect normal sized, atrophic or absent endolymphatic sacs (Kobayashi et al, 2000).

It is also possible that MRI can be used in diagnosis of Ménière's disease. Research by Dimitriy et al showed that MRI scanning (T1 weighting) with gadodiamide contrast enhancement could distinguish the perilymph and endolymph and for the first time, endolymphatic hydrops could be detected by MRI in vivo (Niyazov et al, 2001).

Imaging also allows the analysis of possible aetiologies of Ménière's disease. Submillimeter MRI scanning of the endolymphatic duct in patients with and without Ménière's disease revealed that the endolymphatic duct was significantly less frequently visualised on the affected sides of patients with Ménière's disease (Bradley et al, 1996).

VARIANTS

Cochlear hydrops can occur in isolation without vertigo, and vestibular hydrops can occur without loss of hearing or tinnitus. Delayed endolymphatic hydrops can occur with loss of hearing followed by the typical symptoms of Ménière's disease (Schuknecht, Tsun-Sheng, 2001). 'Drop attacks' or 'otolithic crisis of Tumarkin' are sudden falls due to otological causes without loss of consciousness, characterised by the feeling of being picked up and then thrown to the ground. These are important to diagnose as this condition, potentially serious especially in the elderly, can be cured by ablative vestibular surgery (Ishiyama et al, 2001).

MEDICAL MANAGEMENT

The majority of treatments for Ménière's disease, with the exception of ablative surgical procedures, do not have a high level of effectiveness and add to the controversy and debate around this disease (Merchant, 1995).

Medical management can be divided into those two groups; those for symptom control during acute 'attacks' and those for prevention of vertigo.

In prevention of attacks, dietary recommendations are given. These are aimed at attempting to regulate the fluid balance within the inner ear by, for example avoiding alcohol and caffeine which may produce fluid shifts across the membranous labyrinth by their presence in the fluids of the inner ear (Pfaltz, 1986). Early medical management with a low sodium diet and thiazide diuretic may be important (Devaiah et al, 2000). Storper et al concluded that in combination with a low sodium diet and a diuretic, glycopyrrolate could reduce symptoms of vertigo (Storper et al, 1998). The use of diuretics remains controversial (Merchant, 1995). The glycerol dehydration test results in a transient improvement in symptoms and is believed by some to be extremely useful in the diagnosis of Ménière's disease (Pfaltz, 1986).

Among vasodilators, histamine agonists may be used; but paradoxically histamine antagonists are also used to treat acute attacks of vertigo. This apparent paradox is

because histamine agonists improve function of damaged inner ear cells reducing ischaemia of the stria vascularis. Histamine antagonists also act centrally to reduce vertigo. Cinnarizine, a calcium channel blocker, and clonazepam, a benzodiazepine, may also be used as vestibular suppressants. Prochlorperazine, a phenothiazine antipsychotic is commonly used to control vertigo (Brookes, 1996). An analysis of randomised controlled trials of betahistine (histamine agonist) showed no overall benefit and insufficient evidence is available to show any effectiveness for Ménière's diseases (James et al, 2000).

Aminoglycosides, gentamycin and streptomycin can be used for vestibular ablation with hearing preservation. These agents are most effective when given by intratympanic injection (Blakley, 2000). Intratympanic gentamycin injection does have a higher incidence of sensorineural hearing loss than endolymphatic sac decompression (Nadol et al, 2005).

SURGICAL MANAGEMENT

In patients with significant disease that does not respond adequately to medical therapy, surgical options may be considered, along with intratympanic gentamycin injection.

The surgical procedures can be divided into ablative or non ablative procedures or hearing preserving and hearing destructive procedures. Ablative procedures involve arresting the vestibular input from one ear by the use of surgical labyrinthectomy or chemical labyrinthectomy, intratympanic gentamycin. Surgical labyrinthectomy results in complete sensorineural hearing loss whereas chemical labyrinthectomy is more likely to leave serviceable hearing. Non ablative procedures include vestibular neurectomy, internal shunt procedures such as sacculotomy or cochleosacculotomy and endolymphatic sac procedures such as decompression and stenting. Endolymphatic sac decompression and stenting, vestibular nerve section and to a degree gentamycin injection are hearing preserving.

Ablative procedures are contraindicated in bilateral disease and in ears with good serviceable hearing or in the only hearing ear. Vestibular nerve section or labyrinthectomy would be contraindicated if the contralateral side has reduced vestibular function. Labyrinthectomy and endolymphatic sac decompression are contraindicated in chronic otitis media (Schuknecht 1978).

Sacculotomy involves introducing a pick through the oval window via the tympanic cavity which is reached by retracting the tympanic membrane. The pick is thought to produce a fistula between the endolymph in the saccule and the perilymph around it. This technique fails to take into account that the saccule is often adherent to the footplate of the stapes.

Cochleosacculotomy can be performed under a local anaesthetic, making it a more suitable choice in patients unsuitable for a general anaesthetic. The surgical procedure involves retracting the tympanic membrane to gain access to the middle ear and then introducing a right angled pick through the round window and advancing it in the direction of the oval window for 3mm. The aim is to create a fracture and disrupt the osseous spiral lamina of the cochlea and the cochlear duct, so as to create an endolymphatic – perilymphatic fistula and reduce endolymphatic hydrops (Schuknecht, 1982).

Labyrinthectomy is the ablation of the vestibular labyrinth on one side and is effective because the central nervous system can compensate for unilateral input. It is conducted via a mastoid approach under general anaesthesia and results in complete loss of hearing on the operative side. Vestibular neurectomy is selective division of the vestibular component of the vestibulocochlear nerve. The degree of CNS compensation to unilateral vestibular input is less. Vestibular neurectomy should only be considered if the hearing loss is mild (Gacek, 1996). It can be carried out by several techniques, trans-mastoid (retrolabyrinthine) and retrosigmoid being the most common (Megerian, 2002). It has been shown that hearing continues to deteriorate following vestibular neurectomy and continuing medical management is required (Quaranta, 1997). Following vestibular

ablative surgery is important that the patient is not exposed to vestibular suppressant drugs for an excessive period of time as this reduces the compensatory mechanisms (Smith, 2000).

ENDOLYMPHATIC SAC SURGERY

Surgery on the endolymphatic duct or sac is aimed at decreasing the pressure in the endolymphatic space whilst preserving hearing and vestibular function. Portmann (1927) presented his paper on an operation to drain the endolymphatic sac for the relief of vertigo. He suggested that pressure in the endolymphatic sac was affected by changes in intracranial pressure, because of the position of the sac and also changes in intralabyrinthine volume changes. His operation aimed to decompress the sac by removing the lateral bony wall and making a small incision to allow free drainage of endolymph. Animal experiments had shown that such drainage resulted in reduced tone on the ipsilateral side suggesting a vestibular effect.

Endolymphatic sac surgery can be carried out by a transmastoid approach. Both are conducted under general anaesthesia. The more common approach is the mastoid approach. Access to the mastoid for initial cortical mastoidectomy is by a postauricular incision. The following are the surgical steps devised by Professor Georges Portmann (1927) for the relief of vertigo. These steps have since been modified to form the transmastoid approach to endolymphatic sac decompression and stenting.

From Portmann's original work:

Step 1: The incision is made down to the bone along the retro-auricular groove and the surface of the mastoid is exposed. The spine of Henlé and the external petrosquamous suture are identified.

Step 2: Trepanning of the mastoid is carried out on a plane lower than for the classical trepanning for mastoiditis.

Step 3: The bony wall of the sinus groove having been exposed and its medial part removed, the dura is detached from the posterior surface of the petrous bone, passing medially and slightly superiorly for 3 to 4mm. A protector is put in place and the bony area which represents the most external part of the endolymphatic fossa is removed. Care is taken not to damage the facial nerve which lies in the aqueductus Fallopiian canal.

Step 4: The petrous wall of the endolymphatic sac is freed by removing the greater part of the endolymphatic fossa. Using a very fine needle mounted on a luer syringe, one makes an exploratory puncture of the sac in contact with the zone of adhesion. The operator, who can feel the sensation of penetrating the little cavity of the saccus, then makes, with a paracentesis knife, an incision from 2 to 3mm long in the saccus. One or two drops of clear fluid should flow from the opening of the wound.

The retro-auricular wound is now sutured. Slight drainage is possible by the insertion of a piece of gauze, in the event of any considerable bleeding.

(Portmann, 1927)

Among the possible surgical complications are: formation of fistula with the posterior semicircular canal with possible loss of hearing and vestibular dysfunction, cerebrospinal fluid leak, laceration of the sigmoid sinus with resultant haemorrhage, postoperative fixation of the ossicles by bone dust, otitis media and meningitis. There may also be resultant hearing defects (possibly total) and increased vertigo.

The advent of surgical microscopes and high speed drills has led to refinement of Portmann's original procedure, figure 10. This surgical technique was then modified and the medial wall of the sac was opened, exposing the lumen to the subarachnoid space. The insertion of stents or valves then allowed for an endolymphatic mastoid shunt, and an endolymphatic subarachnoid shunt. Pulec (1995) concludes that the endolymphatic subarachnoid shunt provides a high success rate. It can reduce the risk of permanent hearing loss, especially if carried out early in the disease, and if it fails then there remains the possibility of further surgery.

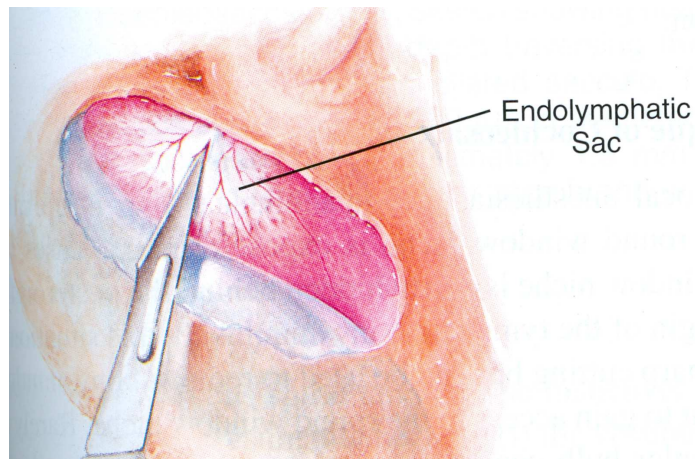


Fig 10 Diagram of endolymphatic sac decompression
(Nadol, 1993)

Endolymphatic sac surgery remains controversial. Thomsen et al (1981) conducted a double blind, placebo controlled study in which patients received an endolymphatic mastoid shunt or placebo procedure. They concluded that the efficacy of surgery was not related to the surgical technique used but placebo effect. This study did show however there was a difference in the objective assessment of sensorineural hearing loss, favouring the endolymphatic sac decompression group. Sodermann et al (1996) believe that endolymphatic sac surgery has a low rate of complications and remains a good first choice surgical therapy. Endolymphatic surgery remains the most commonly used operation for Ménière's disease when there is still functional hearing (Saeed, 1998).

As otology, neurosurgery and neurotology surgery have developed, methods and the specialised equipment to perform them have been developed. These allow surgery on parts of the cranial base including the temporal bone which have previously been inaccessible or impossible to perform due to the associated morbidity and mortality.

TEMPORAL BONE SURGERY

There are recognised standard approaches to the petrous part of the temporal bone which can be used surgically (Rhoton 2000, Rhoton 2002). These approaches can be modified or combined with others to improve access depending on the aims of the surgery. The approach used would depend on the condition and the part of the temporal bone affected.

These are extensively discussed in the literature. Of the approaches, a **middle cranial fossa**, a **posterior cranial fossa (retro-sigmoid)**, a **transmastoid** (with translabyrinthine, transcochlear, infralabyrinthine and retrolabyrinthine or translabyrinthine presigmoid variants) and a **preauricular subtemporal-infratemporal fossa** approach are recognised.

A **middle cranial fossa approach**, involves a temporal craniotomy superior to the zygoma and external acoustic meatus. The temporal lobe of the brain is retracted along with the overlying dura, and this allows identification of the superior surface of the petrous temporal bone. The approach can be employed in removing small tumours within the internal acoustic meatus. The arcuate eminence and the greater superficial petrosal nerve are identified first when elevating the dura of the floor of the middle cranial fossa. In a study of 100 temporal bones, the bone overlying the geniculate ganglion and the genu of the facial nerve was absent in part or completely in 15 bones, and in a further 15 cases no bone covered the greater petrosal nerve. It was also noted that the bone covering the petrous carotid, separating it from the greater petrosal nerve, may be absent (Rhoton, 2000).

A **posterior cranial fossa, retrosigmoid, approach** reaches the posterior surface of the petrous temporal bone through an occipital craniotomy extending laterally as far as the sigmoid sinus. The suboccipital region is approached taking care not to disturb the vertebral artery. The posterior cranial fossa is opened by dividing the dura. The cerebellum is carefully retracted medially so as not to disturb the cerebellar veins. The posterior surface of the petrous temporal bone is identified.

A **transmastoid approach** provides access to the petrous part of the temporal bone through the mastoid process. A posterior auricular incision is used to expose the mastoid cortex which is then drilled to gain access to the petrous part. A translabyrinthine approach involves drilling through the semicircular canals and the vestibule to open the full length of the internal acoustic meatus. A transcochlear modification allows drilling through the cochlea to provide wider access to the petrous apex. An infralabyrinthine

approach involves an initial cortical mastoidectomy and then drilling inferior to the posterior canal, superior to the digastric apex and between the vertical segment of the facial nerve and the sigmoid sinus. The petrous apex is reached by a small window between the jugular bulb and the posterior semicircular canal, making this approach difficult or inappropriate if there is a high jugular bulb.

The **infratentorial presigmoid variant of the transmastoid approach** involves a cortical mastoidectomy and a temporooccipital craniotomy to expose the posterior edge of the sigmoid sinus posteriorly. The dura of the posterior cranial fossa medial to the sigmoid sinus forming Trautmann's triangle is then excised to expose the cerebellopontine angle with the tentorium cerebelli visualised superiorly. This access can be gained by drilling the bone posterior to the labyrinth whilst keeping the labyrinth intact (retrolabyrinthine presigmoid) or by drilling through the labyrinth thus increasing the exposure (translabyrinthine presigmoid). The presigmoid approach can also be extended superiorly, above the level of the tentorium cerebelli as a supratentorial and infratentorial presigmoid transmastoid approach by increasing the size of the temporal craniotomy.

FACIAL NERVE MONITORING

The facial nerve is particularly at risk in temporal bone surgery. The aim of temporal bone surgery is also to remove diseased tissue or to alleviate symptoms of disease whilst preserving facial nerve function. Surgeons will take great care to avoid wounding the facial nerve. Trauma and irritation of the facial nerve may cause conduction abnormalities and result in varying degrees of traumatic facial palsy on the operated sided. Facial palsy can cause significant morbidity including drying and scarring of the cornea with impairment of vision.

It has been shown that intraoperative monitoring of the facial nerve reduces iatrogenic intraoperative facial nerve injury. In some procedures, facial nerve stimulators are employed, where electrical stimulation of the facial nerve induces contraction of the

muscles of facial expression on that side. This requires that the face is visible during the procedure. There were reports of injury to the facial nerve with some of the early stimulators. Facial nerve stimulators allow early identification of the facial nerve and mapping of the facial nerve in soft tissues, tumour and bone and assessment of facial nerve function and prognosis at the end of surgery (Silverstein et al, 1991).

The detection of muscle electrical activity by electromyographic recording uses electrodes placed in orbicularis oculi and orbicularis oris, because they are innervated by the facial nerve. A ground electrode is situated on the forehead. This system can use surface electrodes, bipolar hook wire electrodes or subdermal needle electrodes.

A modernised intraoperative video monitoring system has been advocated by some. In this method the patient wears a custom made mask covering half the face which has video cameras centred on the external side of the eye and on the labial commissure. The images are analysed using a digital videoanalysis system. The videomonitoring system was reported as giving fewer false positive responses than the electromyographic recording (Filipo et al, 2000).

Section 2

Materials and Methods

MATERIAL

63 gross dissections were performed. All dissections were performed on embalmed human cadavers at the University of Glasgow. 6 complete cadavers, 12 half heads and 5 isolated temporal bones were used for dissection. These were selected from the standard stock of bodies and temporal bones at the University of Glasgow. Cadavers were preserved using the arterial injection method via the right common carotid artery (appendix 1). All the cadavers used for head and neck dissections had the arterial system injected using coloured latex (appendix 2). Six cadavers for detailed dissection were selected from the standard stock that had been used for a Plastic surgery flap course at the University of Glasgow. Many of the half heads that were used for measurements of the endolymphatic sac had previously been dissected by the dental class; however the dura covering the petrous temporal bone was intact.

For **dissections performed on half heads**, the head and neck was removed from the rest of the body in the standard manner with the structures anterior to the vertebral column divided at the level of the manubrium and the vertebral column divided between C6 and C7. The soft tissues of the head and neck were initially bisected with a scalpel and then the head was bisected using a band saw.

To **demonstrate the osteology** of the head and neck and temporal bone, a dried skeleton, skull and temporal bone of Asian origin were used.

To demonstrate the normal anatomy, detailed dissections were performed on a series of isolated temporal bone blocks, one complete head and neck and four half heads.

Isolated decalcified temporal bone dissections were performed by first removing the temporal bone in a tissue block by bisecting the head with a band saw and then removing the occipital bone posteriorly with a sagittal cut. A sagittal cut anteriorly through the middle of the greater wing of the sphenoid and then horizontal cuts through the squamous

part of the temporal bone superior to the petrous part and through the neck at the level of the first or second cervical vertebrae completed the removal of the block. The amount of tissue removed with the petrous part of the temporal bone was variable, but a block would not be used if the petrous part were damaged. The blocks of tissue with the temporal bones were kept in a 10% embalming fluid, 90% water solution until required. The blocks selected for the following dissections were then decalcified using the nitric acid protocol (appendix 9).

Fourteen half heads were dissected so that **measurements** relating to the endolymphatic sac could be made. The transmastoid approach to decompress the endolymphatic sac was studied by performing the dissection on three separate temporal bones.

A series of dissections was used to demonstrate the **surgical approaches** to the endolymphatic sac. Histological analysis and electron microscopy of the endolymphatic sac was performed on material obtained from cadaver specimens.

METHOD

A Swann Morton size 24 blade on a number 4 handle and a size 4 blade on a number 3 scalpel handle were used along with fine and coarse dissecting forceps for the dissections. When required a Carl Zeiss operating microscope was used, the microscope was centralised halfway along the focusing depth and then set at the lowest magnification to begin with. The eyepieces were adjusted to correct the focusing. A Xomed micro-craft power system and straight handled drill with a range of burr sizes was used when required. The drill speed was set at 2000 revolutions per minute and the flow of irrigation solution was set at the highest level. An Aerosol Products suction pump was used as required and the bottle was emptied prior to use.

The dissections were adapted from dissections described in Cunningham's Manual of Practical Anatomy, Volume three, Head and Neck and Brain (Romanes, 1985) and A

New System of Dissection (Zuckerman et al 1981). Essential Anatomy for Trainee Surgeons, a Temporal Bone Surgery Manual produced by Mr. Brian O'Reilly (2002), Consultant Otolologist and Neuro-Otolologist was also used.

The dissections along with the histology, embryology and osteology were photographed using a Nikon Coolpix 4500 digital camera. All photographs were taken at a resolution of 2272 * 1704 pixels and edited using GST Photoshop Pro 7.

NORMAL OSTEOLOGY

A full dried skeleton of Indian origin was used for the normal osteology.

NORMAL TEMPORAL BONE ANATOMY

Temporal bones from dried Indian skulls were used and photographed to demonstrate the lateral, inferior, superior and posterior views.

NORMAL GROSS ANATOMY

To demonstrate the normal anatomy in relation to the petrous temporal bone and the endolymphatic sac 21 dissections were performed.

The following dissections were performed:

1. Floor of cranial cavity
2. Eustachian tube
3. Temporal bone with jugular nerves
4. Deep neck and temporal and infratemporal fossa
5. External auditory canal and tympanic membrane
6. Jugular fossa
7. Neck and temporal and infratemporal fossa and sphenoid
8. Tympanic ring and cavity
9. Jugular fossa

10. Tympanic cavity
11. Left decalcified petrous temporal bone
12. Right decalcified petrous temporal bone
13. Left petrous temporal bone
14. Right petrous temporal bone
15. Posterior surface of petrous temporal bone
16. Genicular ganglion
17. Left cortical mastoidectomy
18. Lateral wall of pharynx
19. Carotid canal and siphon
20. Endolymphatic sac and petrous temporal bone
21. Otic capsule

PREPARATION OF SPECIMENS FOR HISTOLOGICAL ANALYSIS

Otic capsule (Cadavers 9 and 10)

Four drilled otic capsules were decalcified according to the EDTA protocol in appendix 7. Two of the bones were then processed for histology, (appendix 3). One in every 10 slices was then retained (appendix 4) and stained with either hematoxylin and eosin or masson's (appendix 5).

Temporal bone histology

Temporal bone blocks were removed from the standard stock of cadaver heads. For histological analysis, smaller temporal bone blocks were required than the blocks taken for temporal bone dissections. The heads had previously been bisected and then dissected by students. The temporal bones however were not dissected. The temporal bone blocks were removed with care so as not to damage the middle or inner ear structures. Once the brain had been removed the tentorium cerebelli was removed. Using a band saw the head was bisected, then a cut was made 25mm anterior and parallel to the superior petrosal sinus. A cut was then made perpendicular to the sinus 10mm medial to the internal acoustic meatus. Another cut was then made perpendicular to the sinus, medial to the squamous part of the temporal bone which went through the external

auditory meatus and separated the squamous part from the petrous part. A final cut was then made horizontally through the block 10mm inferior to the internal acoustic meatus. The block was then decalcified according to the EDTA protocol in appendix 7.

The decalcified temporal bone block was then processed according to the protocol in appendix 4. The block was then sectioned at 9 micrometers and every 10th section was stained with hematoxylin and eosin according to the protocol in appendix 5.

Isolated endolymphatic sac histology

The intradural component of an endolymphatic sac was removed from a standard head. The vault and the brain had previously been removed and the head had been bisected. To increase access to the posterior cranial fossa a wedge of soft tissue from the occipital and suboccipital region and part of the underlying occipital bone was removed.

A 20mm incision was made in the dura superior and medial and parallel to the operculum. The dura was then carefully peeled inferiorly and laterally to the operculum. At this point the endolymphatic sac was visualised entering the posterior cranial fossa from under the operculum. Incisions were then made from the previous incision down to the sigmoid sinus. However so as not to damage the sac the incision medially deviated medially and the incision laterally deviated laterally. These two incisions were then joined by one along the medial and superior wall of the sigmoid sinus. A further incision was made in the opposing wall of the sigmoid sinus. The block of tissue comprising dura mater, endolymphatic sac and part of the sigmoid sinus was then carefully stripped from the underlying bone. The endolymphatic sac was divided as it enters the posterior cranial fossa. Care was taken not to damage the sac. The sac was then processed for histological analysis according to appendix 4. The sac was sectioned perpendicular to the long axis and stained with hematoxylin and eosin (appendix 5)

ELECTRON MICROSCOPY OF ENDOLYMPHATIC SAC

To confirm that indeed the endolymphatic sac had been successfully dissected, the medial wall was removed and prepared for scanning electron microscopy according to the

schedule in appendix 8. One sac was cut into sections perpendicular to the long axis of the sac to allow visualisation of the sac lumen. The sections were then processed for scanning electron microscopy according to the schedule in appendix 8

EMBRYOLOGY

To examine the development of the endolymphatic sac and the association with development of the temporal bone, specimens from the prepared human embryo sets at the University of Glasgow (27mm, 45mm and 55mm human embryos) were studied and photographed

MEASUREMENTS OF THE ENDOLYMPHATIC SAC

(Cadavers 4, 5, 6, 7, 8, 9, 10, 11 and 12)

This dissection was performed on 14 half heads (from 9 cadavers), which had been dissected by the second year dental students. The vault had been removed along with the brain in every case. The tentorium cerebelli had been either completely removed or cut along the edge of the petrous apex where the superior petrosal sinus is located. The sigmoid sinus had been opened in the majority of cases, but had not been removed. The cut ends of the trigeminal nerve, the abducens nerve and the vestibulocochlear and facial nerves were visible. The heads had been bisected along the midline with a band saw. In most cases the dura on the posterior surface of the petrous part of the temporal bone was intact.

The dissection began by using the band saw to make a coronal cut that removed the majority of the occipital bone, to allow easier visualisation of the posterior surface of the petrous temporal bone. The cut was made about 4 cm posterior to the external auditory meatus, so that the all of the petrous part of the temporal bone and the sigmoid sinus were left behind. The superior petrosal sinus was opened by removing the remaining part of the tentorium cerebelli with a longitudinal incision parallel to the long axis of the petrous temporal bone and immediately posterior to it. The operculum was located as a ridge on the posterior surface, which is visible through the dura mater. A semi-circular curved

incision was made through the full thickness of the dura mater superior and medial to the operculum, with the operculum forming the base of the semi-circle. The curve started five millimeters lateral to the operculum and ended five millimeters medial to the operculum, on the same axis as the operculum, and the apex was five millimeters superior and medial to the centre of the operculum.

Using forceps the dura was slowly elevated and pulled in the direction of the operculum and then stripped of the operculum. As the dura continued to be elevated, pulled inferiorly and medially, it was freed from its attachments medial and lateral to the operculum and the endolymphatic fossa. The endolymphatic sac was noted emerging from under the operculum, through the opening of the vestibular aqueduct onto the posterior surface of the temporal bone, and lying in the endolymphatic fossa. The dura mater was elevated and stripped from the endolymphatic sac until the sigmoid sinus was reached. A hole was made in the endolymphatic sac using a scalpel and the lumen was identified. A blunt probe was introduced into the lumen to identify the inferior, medial and lateral limits of the endolymphatic sac.

The following measurements were then taken:

Opérculum width (fig 11)

Lateral limit of vestibular aqueduct to internal acoustic meatus (fig 12)

Medial limit of vestibular aqueduct to internal acoustic meatus (fig 12)

Medial limit of vestibular aqueduct to superior petrosal sinus (fig 13)

Lateral limit of vestibular aqueduct to superior petrosal sinus (fig 13)

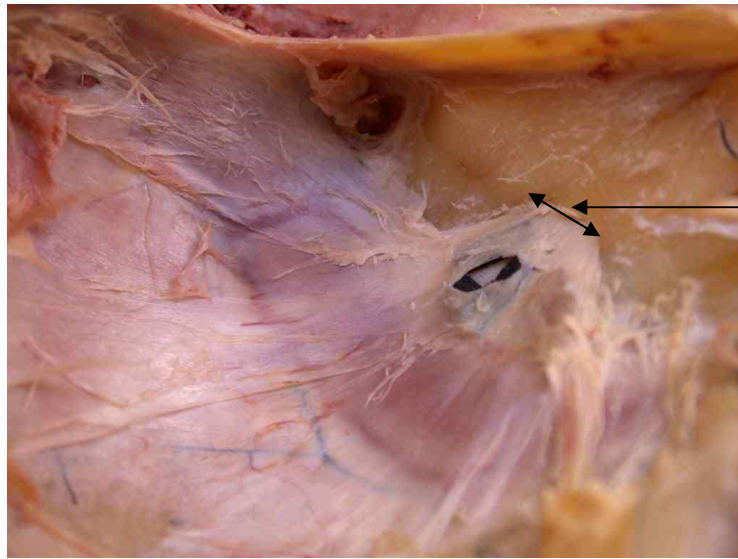
Maximum width of the endolymphatic sac (fig 14)

Endolymphatic sac length (fig 15)

Medial limit of vestibular aqueduct from sigmoid sinus (fig 16)

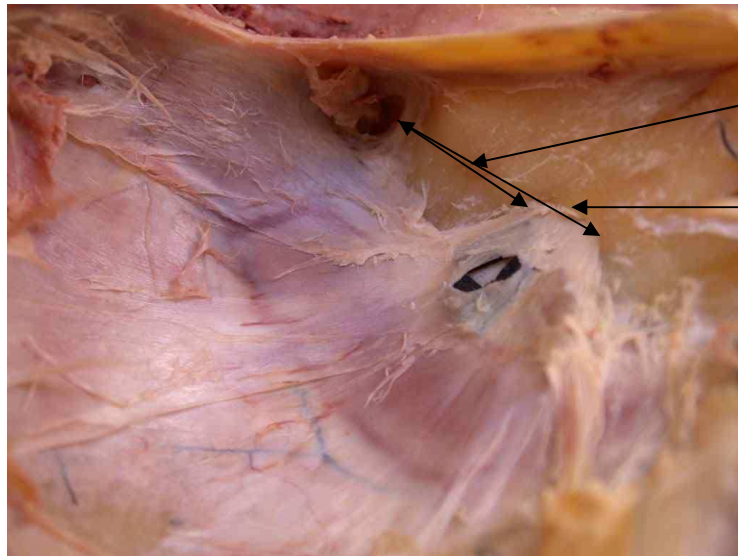
Lateral limit of vestibular aqueduct from sigmoid sinus (fig 16)

(along axis perpendicular to the operculum)



Operculum width

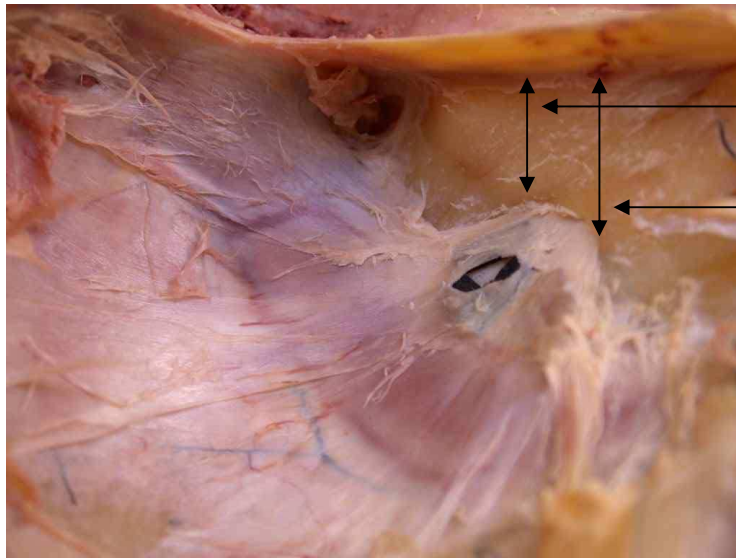
Figure 7 Diagram showing operculum width



Distance from operculum to internal acoustic meatus (lateral)

Distance from operculum to internal acoustic meatus (medial)

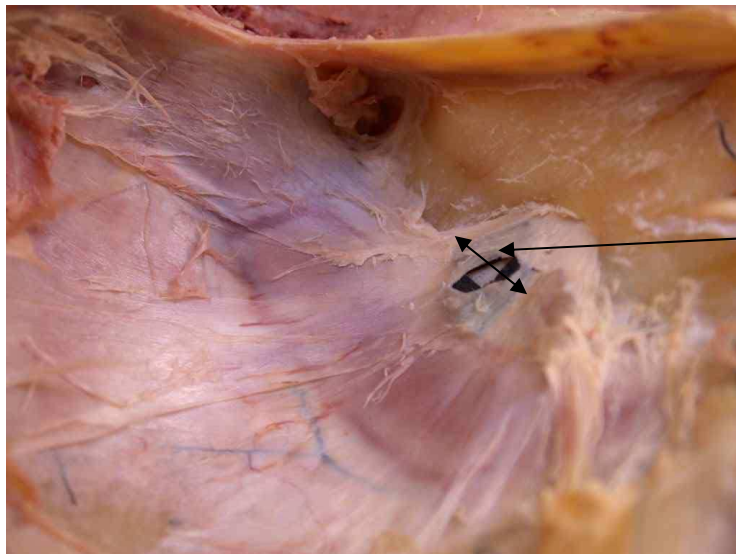
Figure 8 Diagram showing distance from operculum to internal acoustic



Distance from operculum to superior petrosal sinus (lateral)

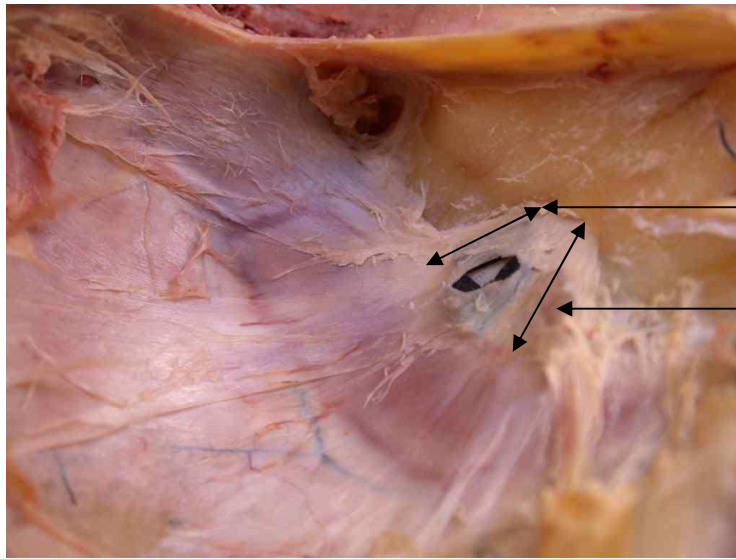
Distance from operculum to superior petrosal sinus (medial)

Figure 9 Diagram showing distance from operculum to superior petrosal sinus



Width of endolymphatic sac

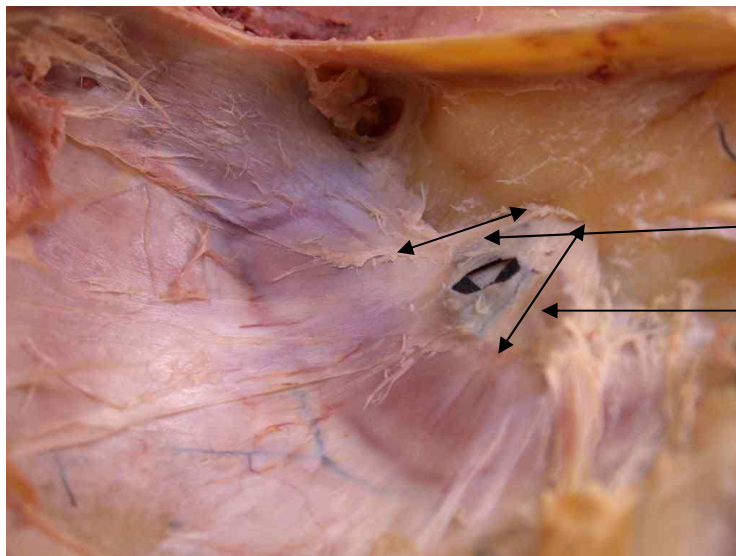
Figure 10 Diagram showing width of endolymphatic sac



Length of endolymphatic
sac (Lateral)

Length of endolymphatic
Sac (medial)

Figure 11 Diagram showing length of endolymphatic sac



Distance from
operculum to sigmoid
sinus (lateral)

Distance from
operculum to sigmoid
sinus (medial)

Figure 12 Diagram showing distance from operculum to
sigmoid sinus

EXAMINATION OF TEMPORAL BONE SECTIONS FROM THE COLLECTION AT THE MASSACHUSETTES EYE AND EAR INFIRMARY

To examine a case of endolymphatic sac stenting and a case of endolymphatic hydrops, two specimens from the register of temporal bones at the Massachusetts Eye and Ear Infirmary were studied. The bank contains harvested temporal bones from patients with known pre-existing ear disease. The bones are decalcified in EDTA and processed in celloidin and cut at 15 micrometers according to the schedule in appendix 4. They are stained with hematoxylin and eosin. The histological specimens are then stored along with the patients' notes and a summary of their otological history and otopathology reports.

The first case was a 12 year old girl with diagnosed unilateral Ménière's disease. Her full otological history and temporal bone pathology is in appendix 9. A mid modiolar section from both ears was photographed for comparison.

The second case is an 81 year old man with long standing severe bilateral Ménière's disease. The left ear had an endolymphatic sac decompression and stent insertion prior to death. The full otological history and temporal bone pathology is in appendix 10.

SIMULATED SURGICAL DISSECTIONS

Transmastoid endolymphatic sac decompression (cadavers 3 and 13)

The initial dissection was carried out by Mr O'Reilly (as in appendix 12) and then repeated by myself to study the procedure.

The following 5 dissections were used to examine the transmastoid endolymphatic sac decompression.

22. Superficial head and neck
23. Back of head and neck
24. Face
25. Pinna
26. Mastoidectomy

Posterior cranial fossa retrosigmoid endolymphatic sac decompression and combined transmastoid and retrosigmoid endolymphatic sac decompression

The following 9 dissections as detailed were used to dissect the proximal endolymphatic sac and to examine a means by which both the proximal and distal, intra and extraosseous portions, of the endolymphatic sac could be decompressed.

27. Back of neck
28. Suboccipital
29. Deep suboccipital and neck
30. Posterior and middle cranial fossa
31. Suboccipital and brainstem
32. Deep back of neck
33. Deep back of head
34. Extratemporal portion of facial nerve
35. Cortical mastoidectomy and endolymphatic sac

Middle Cranial fossa endolymphatic sac decompression

This potential means of decompressing the sac was examined with dissection 38.

36. Middle cranial fossa petrous temporal bone dissection
37. Petrous temporal bone dissection

Clinical Cases

Glomus jugulare resection by lateral approach

Performed at the Southern General Hospital, Glasgow, 2002 by Mr. B. O'Reilly. For excision of a jugular bulb glomus jugulare tumour.

Carotid arteriography with embolisation of the small vessels was carried out 24 hours prior to surgery. Electrical monitoring was performed on the facial nerve during this procedure. The skin of the head and the neck on the left side was shaved. The patient was positioned, lying on his back with his head pointing to the right. The mastoid tip and

the angle of the mandible were marked. Haemostasis was maintained by cauterizing small vessels with diathermy and tying the larger vessels.

A large reversed C shaped incision was made in the skin of the left side with the upper limb being about 2cm above the external acoustic meatus and the inferior limb passing down onto the neck about 2cm below the angle of the mandible. The posterior limb of the C lay about 5cm behind the pinna.

The skin was retracted anteriorly. The external auditory meatus was divided all the way through and then lateral part was sewn shut using a fascial flap. The skin flap was then taken further forward, dissecting it from the superficial musculaponeurotic layer covering the parotid gland. The great auricular nerve was identified passing over the surface of sternocleidomastoid.

The posterior fibres of temporalis were retracted superiorly and the periosteum over the mastoid process and lower part of the squamous part of the temporal bone was removed.

The mastoid was drilled to reveal the sigmoid sinus posteriorly, the middle cranial fossa dura superiorly, the mastoid tip with the digastric apex inferiorly and the posterior wall of the external auditory canal in front. The vertical segment of the facial nerve was uncovered in the Fallopian canal from the stylomastoid foramen inferiorly to the junction of the lateral and posterior canal superiorly. The lateral and posterior semicircular canals were identified.

Inferior to the posterior belly of digastric the internal carotid artery, the external carotid artery and the internal jugular vein were identified. Loose slings were place around the internal carotid artery and the internal jugular vein.

The posterior external auditory canal wall was removed down to the level of the facial nerve. The main trunk of the facial nerve was identified entering the parotid gland. The

facial nerve was separated from the surrounding parotid tissue as a superficial parotidectomy was performed.

A groove was drilled in the wall of the attic and the facial nerve was then freed from the fallopian canal and transposed into the new groove. Sutures were used to hold the facial nerve in a flap of the remaining parotid tissue.

The posterior belly of digastric was divided and the styloid process was fractured. The bone posterior to the sigmoid sinus was drilled to reveal the dura posterior to it. A small hole was made in the dura posterior to the sigmoid sinus. The sigmoid sinus was then clamped and sewn shut superior to the jugular bulb. The remaining bone around the anterior, posterior and lateral aspect of the jugular bulb was removed.

In the neck the glossopharyngeal nerve was identified along with the vagus nerve, accessory nerve and the hypoglossal nerve. The internal jugular vein was sewn shut. The jugular bulb was opened and the tumour removed. The inferior petrosal sinus was then plugged.

The hole in the dura mater was then sewn shut. The bone defect was repaired by cranioplasty, using a hydroxyapatite paste, which was allowed to cure before the overlying tissues were closed and then the skin closed.

Retrosigmoid / suboccipital acoustic neuroma resection

Performed at the Southern General Hospital, Glasgow, 2002 by Mr. B. O'Reilly. For excision of an acoustic neuroma; extending from the internal acoustic meatus into the posterior cranial fossa.

During this procedure electrical facial nerve monitoring was employed. The patient was positioned in the sitting position and the right side of the head and neck was shaved. A line was drawn from the inion to the upper border of the external auditory meatus. A vertical incision approximately 8cm long was made from just above the supramastoid

crest down about 1.5cm posterior to the mastoid process. The subcutaneous tissues were divided down to the depth of the occipital bone. Haemostasis was maintained by cauterizing small vessels with diathermy and tying the larger vessels. Any veins encountered on the back of the head, neck or sub-occipital region were cauterized. The emissary veins were dissected and cauterized. The superficial tissues and divided muscle were retracted and the periosteum over the occipital bone was exposed.

A craniotomy was performed, beginning with a burr-hole at the transverse-sigmoid sinus junction. A rounded craniotomy was performed about 4cm in diameter with the anterior border being the posterior border of the sigmoid sinus.

The dura was incised and retracted with sutures. The arachnoid was opened to expose the cerebellopontine angle. The right lobe of the cerebellum was retracted to increase the exposure. The part of the acoustic neuroma which extended into the cerebellopontine angle was debulked. The operculum and foveate impression on the posterior surface of the petrous temporal bone were identified.

The dura lateral to the internal acoustic meatus was resected. The bone lateral to the internal acoustic meatus was drilled in a U shape, with the superior limb of the U being the superior border of the internal auditory meatus and the inferior limb being the inferior border of the internal acoustic meatus. The fundus of the internal auditory canal was then opened and the bone was removed from the level of the sub-arcuate artery superiorly to the jugular fossa inferiorly. The dura forming the lateral wall of the canal was removed and the tumour resected from the canal along with the superior and inferior vestibular nerves. The facial nerve was left intact.

The remainder of the tumour was then removed from the cerebellopontine angle. The dural opening on the posterior surface of the temporal bone was sewn shut and then the dural opening under the occipital area was repaired. The bone defect was repaired by cranioplasty, using a hydroxyapatite paste, which was allowed to cure before the overlying tissues were closed and then the skin closed.

Section 3

Results

The skull is positioned at the top of the cervical vertebral column and makes up part of the axial skeleton. The skull is formed by flat bones and irregular bones which, with the exception of the mandible are joined by fibrous sutures. The skull consists of two parts, the cranium and the facial skeleton. The skull is formed by 22 bones, 8 bones in the cranium and 14 bones in the facial skeleton (Figures 13 + 14).

The facial skeleton is that part which makes no contribution to the formation of the cranial cavity. There are two pairs of openings in the facial skeleton, the nasal fossae either side of the midline in the upper part of the face, which open anteriorly and posteriorly. Lateral to the nasal fossae is the orbit, which is occupied by the eye. The inferior border of the orbit is formed by the maxilla medially and the zygomatic bone laterally. The zygomatic bone has a process that joins with the zygomatic process of the temporal bone to form the zygomatic arch, a bar of bone that can be seen projecting from the inferior margin of the orbit anteriorly to the anterior aspect of the external acoustic meatus posteriorly (Figures 13 + 14).

The cranium is formed by two parts, the roof, posterior and side walls are referred to as the calvaria and the floor is referred to as the cranial base. The calvaria is formed by a series of flattened bones, anteriorly by part of the frontal bone, posteriorly by part of the occipital bone, in-between by the parietal bones and laterally by the squamous part of the temporal bone (Figures 13 + 14).

The base of the skull consists of a large block of bone in the midline extending from the ethmoid anteriorly to and encircling the foramen magnum posteriorly and consisting of the body of the sphenoid and the body of the occipital bone (clivus). These two bones also have lateral projections forming part of the floor of the cranial cavity. The floor also contains blocks of bone that have formed around the sense organs, the ethmoid anteriorly and the otic capsule of the ear in the petrous temporal bone laterally.

The sphenoid has a cuboid shaped body in the midline, which contains the sphenoidal air sinuses. It has two sets of lateral projections on either side called the greater and lesser pterygoid plates on either side.

The basilar part of the occipital bone continues posteriorly and laterally as the lateral portions forming the foramen magnum is continuous with the squamous part, posterior to the foramen magnum. The squamous part is composed of the planum occipitale inferior to the highest nuchal line and the planum nuchale superior to this line. The lateral parts have oval shaped condyles on the inferior aspect which articulate with the superior facets of the atlas. The hypoglossal canal is located at the base of each condyle and they point forwards and laterally. The squamous part is found to curve both from side to side and downwards. The external surface has a projection which is midway between the top of the squamous part and the foramen magnum called the external occipital protuberance (Figures 13 + 14).

The mandible which forms part of the skull and it articulates with the temporal bone. The mandible consists of two rounded bodies which fuse anteriorly in the midline at the symphysis menti. On the upper aspect of the body is the alveolar ridge which contains sockets for the roots of the lower dentition. Adjacent to the second premolar tooth on the outer aspect of the body is the mental foramen. The body is continuous with a flattened process called the ramus which has two projections superiorly, the coronoid process anteriorly and the condyloid process posteriorly which bears the head of the mandible. The body is continuous with the posterior margin of the ramus at the angle of the mandible (Figures 13 + 14).

The skull articulates with the spinal column via the occipital condyles. There are seven cervical vertebrae. Four cervical vertebrae are typical and three are atypical. A typical cervical vertebrae consists of a body and a neural arch which encloses the vertebral foramen. The neural arch is formed by two pedicles and two laminae. Where the laminae meet in the midline a spinous process is found which for typical cervical vertebrae is bifid. Where the pedicle and lamina meet are the transverse process and

superior and inferior articular facets. In cervical vertebrae the transverse processes have a foramen transversarium (Figures 13 + 14).

ANATOMY OF THE TEMPORAL BONE

The hair on the head over the squamous portion of the temporal bone is the first to turn grey on many people, signifying the passage of time and ageing. It is for this reason that the underlying bone has been named the way it has. The temporal bone consists of four fused parts, squamous part, petrous part, tympanic plate and styloid process; it forms part of the lateral wall and base of the skull (Figures 15 + 16). Anteriorly the squamous part articulates with the parietal bone and greater wing of the sphenoid to form part of the pterion.

The petrous part forms by ossification of the auditory capsule cartilage, the squamous part forms by intramembranous ossification, from mesenchyme that has been induced by the developing brain, dermal bone. The tympanic plate is also dermal bone which in other mammals forms the angular which is a bone of the lower jaw. The styloid process forms by ossification of cartilage from the hyoid arch. The petrous part and the styloid process therefore represent part of the chondrocranium, developed in cartilage and the tympanic plate and petrous part represent part of the membranous neurocranium.

The squamous part forms the base of the temporal fossa, it is smooth and is covered by and provides attachment for the temporalis muscle. The supramastoid crest curves backwards and upwards on the lateral surface of the squamous part and is continuous with the root of the zygomatic process. Between the upper and posterior part of the external acoustic meatus and the supramastoid crest is the suprameatal triangle. The spine of Henle is a small projection of bone pointing forwards from the inferior part of the suprameatal triangle (Figures 15 + 16).

The tympanic plate forms the floor and part of the walls of the external acoustic meatus by fusion with the squamous, petrous and mastoid parts. The fusion of these bones forms the bony part of the ear canal (Figures 15 + 16).

There is a sulcus for the middle temporal artery on the lateral wall and the internal, medial, surface has impressions corresponding to the surface of the temporal lobe of the brain and the posterior branches of the middle meningeal artery (Figures 17 + 18). On the inferior aspect are the articular tubercle and the mandibular fossa which forms the superior part of the temporomandibular joint. The mandibular fossa is limited anteriorly by the articular tubercle and posteriorly by the tympanic plate. Laterally the posterior edge of the articular surface forms a lip of bone called the postglenoid tubercle. In the articular fossa lies the squamotympanic fissure which is divided medially into the posterior petrotympanic and anterior petrosquamous sections by the tegmen tympani which is an outgrowth of the petriotic bone (Figures 19 +20).

The styloid process is smooth curved projection from the inferior aspect and is fused with the tympanic plate. It is formed by the inferior projection, vaginal process, of the tympanosquamous fissure. It is of variable length and gives attachment to the stylohyoid, styloglossus and stylopharyngeus muscles. The stylomastoid foramen is found between the styloid and mastoid processes and transmits the main trunk of the facial nerve as it exits the skull (Figures 19 + 20).

The petriotic bone in humans is described in two parts, the petrous and the mastoid parts. The mastoid part is also partly formed by an inferior projection of the squamous part. The mastoid bone is composed of air cells and communicates with the tympanic cavity via the mastoid antrum. The projection of the mastoid part is the mastoid process which on the lateral aspect bears the attachment of the sternocleidomastoid, posterior auricular and occipital muscles. Medial to these attachments is the mastoid notch to which attaches the posterior belly of the digastric muscle. The occipital artery lies in an impression medial to the attachment of the digastric muscle, and the mastoid branch of the occipital artery pierces the lateral wall of the mastoid bone along with the mastoid emissary vein. On the internal surface posteromedially lies the impression of the sigmoid sinus (Figures 21 + 22).

The petrous part lies in the skull base; it is pyramidal in shape and is limited posteriorly by the occipital bone and anteriorly by the sphenoid bone. The apex is directed anteromedially, pointing towards the posterior clinoid processes. The anterior surface lies posterolateral to the apex and forms the posterior wall of the middle cranial fossa, the posterior wall forms part of the anterior wall of the posterior cranial fossa (Figures 21 + 22).

Anteriorly the petrous part has a protrusion, the arcuate eminence underneath which lies the superior semicircular canal. Posterolateral to the apex is the trigeminal impression on which lies the trigeminal ganglion, which is covered by a fold of dura mater forming the trigeminal cave. Posterolateral to the trigeminal impression lies the tegmen tympani. The tegmen tympani is the thin bony roof of the tympanic cavity. The anterior aspect of the tegmen tympani projects downwards between the squamous and tympanic parts of the temporal bone. The formed petrotympanic part (Glaserian fissure) of the squamotympanic fissure communicates with the tympanic cavity and at the medial end is the canaliculus conveying the chorda tympani to the exterior of the skull. There are two orifices present opening onto the anterior surface, these are the hiatus for the greater petrosal nerve and more anterolateral hiatus for the lesser petrosal nerve.

The posterior surface of the petrous part lies in a vertical plane, superiorly lies the sulcus of the superior petrosal sinus and inferiorly lies the sulcus of the inferior petrosal sinus. The internal auditory meatus lies posteriorly at the mid-point between the base and apex of the petrosal pyramid. The internal auditory meatus points laterally towards the external auditory meatus. The subarcuate fossa leads into the petromastoid canal. One centimetre below the superior petrosal sinus and 1cm lateral to the internal auditory meatus lies the orifice of the vestibular aqueduct (Figures 21 + 22).

Within the internal acoustic meatus the horizontal crest can be seen dividing the fundus of the meatus into superior and inferior parts. The superior part is then further subdivided by the vertical crest forming the facial canal medially and the superior vestibular area

laterally. The inferior part is divided into a cochlear area medially and an inferior vestibular area laterally.

CRANIAL CAVITY

The cranial cavity can be described as having three cranial fossae, anterior, middle and posterior. The anterior cranial fossa extends from the frontal bone anteriorly to the lesser wing of the sphenoid posteriorly (Figures 23 + 24). The middle cranial fossa extends from the lesser wing of the sphenoid anteriorly to the superior margin of the petrous temporal bone posteriorly and includes the hypophyseal fossa. The posterior cranial fossa extends from the superior margin of the petrous temporal bone posteriorly and includes the posterior clinoid processes in the middle which are in a line continuous with the petrous apex to the occipital bone posteriorly (figures 25 + 26).

The dura mater lining the inside of the cranial cavity consists of two layers, a periosteum and the dura mater. These layers are stuck together. The dura with periosteum is adherent to the bones forming the cranial cavity, however it is more tightly adherent at suture lines and cranial foramina where it is continuous with the periosteum on the outside of the cranial cavity.

The dura mater also forms partitions in the cranial cavity, the falx cerebri and the tentorium cerebelli. The falx cerebri lies in the mid-sagittal plane and is sickle shaped, narrow (front to back) anteriorly where it attaches to the crista galli and wide (front to back) posteriorly where it attaches to the tentorium. The free edge extends towards the corpus callosum. In the attached edge superiorly lies the superior sagittal sinus, in the free edge lies the inferior sagittal sinus and in the edge which attaches to the tentorium cerebelli lies the straight sinus. The transverse sinuses lie at the attachment of the tentorium cerebelli to the occipital bone. The superior sagittal sinus formed the right transverse sinus and the straight sinus formed the left transverse sinus at the confluence of sinuses (figures 23 + 24). The straight sinus also receives the great cerebral vein. The falx cerebri and the tentorium cerebelli meet posteriorly at the internal occipital protuberance where the confluence of sinuses is positioned (figures 25 + 26). The right

and left cavernous sinuses are joined by the right and left sphenoparietal sinuses and are connected by the intercavernous sinus. The cavernous sinuses are joined to the respective jugular bulbs by the right and left inferior petrosal sinuses. The tentorium attaches laterally to the superior border of the petrous temporal bone and contains the superior petrosal sinus on both sides. Posteriorly the tentorium attaches to the occipital bone and contains the right and left transverse sinuses at the attachment. Anteriorly the tentorium is incomplete to allow passage of the brainstem, basilar arteries and cranial nerves (figures 25 + 26).

The infratentorial segment of the posterior cranial fossa contains the cerebellum, medulla oblongata and pons along with the vertebral and basilar arteries. Above the level of the tentorium the mid brain can be seen with the superior colliculus and cerebral aqueduct posteriorly and cerebral peduncles anteriorly.

Within the posterior cranial fossa the oculomotor, trochlear, trigeminal, abducens, facial, vestibulocochlear, glossopharyngeal, vagus, accessory and hypoglossal cranial nerves leave the brainstem in the posterior cranial fossa and then exit the cranial cavity directly from the posterior cranial fossa or travel upwards and forwards into the middle cranial fossa first (Figures 27 + 28).

The trigeminal nerve can be seen entering Meckels cave in the posterior cranial fossa and then lying under the middle cranial fossa. The facial and vestibulocochlear nerves can be seen partially twisting around each other and leaving the posterior fossa by entering into the temporal bone via the internal acoustic meatus. The glossopharyngeal, Vagus and Accessory nerves can be seen exiting the posterior cranial fossa via the jugular foramen with the glossopharyngeal exiting through a separate tunnel in the foramen (Figs 27 + 28).

THE EAR

The ear was found to consist of three parts, the external ear, middle ear and inner ear.

THE EXTERNAL EAR

The two parts of the external ear are the auricle and the external acoustic meatus. The external ear extends from the pinna laterally to the tympanic membrane medially.

The auricle is oval in shape, widest at the top and narrower at the bottom. The auricle consists of a cartilage model covered in skin with the exception of the lobule at the inferior aspect of the auricle which is formed from fatty tissue covered by skin. The folds in the cartilage are called the helix and antihelix, tragus and antitragus. The concha leads to the opening of the external acoustic meatus. The auricle is attached to the skull by two ligaments and three muscles. The extrinsic muscles of the ear are auricularis anterior, superior and posterior. Auricularis superior is the largest and is fan shaped arising from the cranial aponeurosis and inserting into the superior aspect of the pinna. Auricularis posterior is smaller and flattened, inserting into the inferior aspect of the back of the pinna (figures 29 + 30). There are anterior and posterior ligaments.

The pinna is supplied by branches of the posterior auricular, superficial temporal and occipital arteries. The external acoustic meatus is supplied by branches of the maxillary, superficial temporal and the posterior auricular arteries. The nerve supply is via the greater auricular, auriculotemporal, vagus and lesser occipital nerves (figures 31 + 32).

The external acoustic meatus is composed of two parts, a cartilaginous part and a bony part and extends from the pinna to the tympanic membrane. The meatus from external to internal is first directed inward, forward and upward. It then changes to be directed inwards, and backwards and then inward, forward and downward. It is approximately 25mm in length and narrows to an isthmus about 10mm from the auricle. It is composed of an outer cartilaginous part and an inner bony part (figures 33 + 34). The proximal, cartilaginous part is formed by an incomplete ring of cartilage which is completed superiorly by a membrane. The bony part consists of a complete ring of bone formed by the fused tympanic plate and the mastoid process and the squamous part forming the roof. The suprameatal triangle is positioned at the most superior and posterior aspect of the external auditory meatus, at the root of the zygomatic process (figures 35 + 36).

The tympanic membrane is positioned obliquely so that the roof of the meatus is shorter than the floor. The styloid process of the temporal bone can be seen inferiorly projecting anteriorly, medially and inferiorly. The main trunk of the facial nerve is visible as it leaves the stylomastoid foramen which is positioned just below and behind the most inferior and posterior part of the external acoustic meatus, where the tympanic plate meets the mastoid process. The glossopharyngeal, vagus and accessory nerves are visible as they pass through the jugular foramen, inferior to the middle ear (figures 35 + 36).

THE MIDDLE EAR

The middle ear has two connecting parts, the tympanic cavity and the mastoid cavity which are linked to the nasopharynx by the Eustachian tube. The Eustachian tube can be seen passing inferior and medial to the trigeminal ganglion (figures 37 + 38). The Eustachian tube can be traced anteriorly and medially from the middle ear cavity to the nasopharynx. The tympanic cavity and the mastoid cavity connect at the aditus ad antrum which is positioned superiorly.

Inferior to the tympanic cavity is the jugular fossa which contains the jugular bulb and the glossopharyngeal, vagus and accessory nerves. Medial to the jugular fossa is the internal carotid artery as it enters the carotid canal (figures 39 + 40).

The tympanic cavity is an irregular, laterally compressed space contained within the petrous part of the temporal bone. It is an air filled space containing three bones for the conduction of tympanic membrane vibrations towards the inner ear: the malleus, incus and stapes. The cavity is divided into two spaces, the tympanic cavity proper and the attic or epitympanic recess which lies superior to the tympanic membrane and the surrounding tympanic ring (figures 41 + 42). The head of the malleus and the body of the incus are visible in the epitympanum. The cavity is lined by ciliated columnar epithelium.

The lateral wall is formed mainly by the tympanic membrane surrounded by an incomplete ring of bone. The ring is incomplete superiorly forming a notch. The medial, labyrinthic, wall is a bony partition separating the middle ear from the inner ear with two apertures, the fenestra vestibuli, on which lies the footplate of the stapes, and the fenestra cochleae (figures 43 + 44).

Medial to the tympanic membrane is found the handle of the malleus and the long process of the incus. The articulation between the incus and the stapes is visible along with the stapedius muscle. Superiorly the lateral process of the malleus is visible with the attached anterior and posterior malleolar folds. The chorda tympani passes through the middle ear cavity from posterior to anterior within the layers of the tympanic membrane (figures 43 + 44). The bulge on the medial wall, the promontory, is formed by the basal turn of the cochlea. The roof is formed by the tegmen tympani. The auditory or Eustachian tube connects the anterior wall to the nasopharynx. The floor, or jugular wall, is formed by a thin plate of bone which separates the cavity from the jugular fossa (figures 45 + 46).

It is through an aperture on the floor adjacent to the labyrinthic wall that the tympanic branch of the glossopharyngeal nerve passes. The posterior wall is wider superiorly and has the irregularly shaped mastoid antrum which allows communication between the mastoid air cells and tympanic cavity via the aditus ad antrum. The anterior or carotid wall separates the carotid artery from the tympanic cavity with a thin plate of bone perforated by the tympanic branch of the internal carotid artery and the deep petrosal nerve which conveys sympathetic fibres from the carotid plexus to the tympanic plexus.

Contained within the tympanic cavity are the ossicles, which are the three smallest bones in the human body. The handle of the malleus attaches to the internal surface of the tympanic membrane at the umbo. The head of the malleus articulates with the body of the incus. The long process of the incus articulates with the head of the stapes. The footplate of the stapes covers the fenestra vestibuli. The two smallest striated muscles in the human body, stapedius and tensor tympani are also found in the tympanic cavity.

Tensor tympani attaches to the head of the malleus and stapedius attaches to the stapes (figures 45 + 46). On the medial wall, in front of the fenestra cochleae, is the promontory, formed by the basal turn of the cochlea. On the surface of the promontory is the tympanic plexus, a network of nerve fibres from the tympanic branch of the glossopharyngeal nerve, branches from the geniculate ganglion of the facial nerve and sympathetic branches from the carotid plexus (figures 45 + 46). The promontory is formed by the basal turn of the cochlea (figures 45 + 46).

FACIAL NERVE

The facial nerve enters the petrous part of the temporal bone through the internal acoustic meatus. At the fundus of the meatus the facial nerve lies superiorly and medially. The nerve is traveling anterolaterally, but at the fundus it changes direction to pass medially and expands to form the genicular ganglion. The facial nerve makes a sharp right angle turn at the genicular ganglion and the horizontal segment of the nerve passes posteriorly and laterally, positioned anterior and lateral to the vestibule. At the genicular ganglion the greater and lesser superficial petrosal nerves are given off from the facial nerve (figures 47 + 48). These branches emerge from the temporal bone to pass into the middle cranial fossa. At the point where the lateral semicircular canal and posterior semicircular canal are close, as seen through the mastoid cavity, the facial nerve changes direction again with a sharp turn from the horizontal segment downwards to form the vertical segment. The vertical segment passes to the stylomastoid foramen where it leaves the temporal bone. Just before reaching the foramen the facial nerve gives off the chorda tympani branch which travels through a bony canal in the posterior wall (figures 49 + 50). This canal turns on to the lateral wall, and the nerve continues across the tympanic membrane between the fibrous and mucous layers heading towards the chorda tympani canaliculus.

MEDIAL DISSECTION OF THE TEMPORAL BONE

The Eustachian tube extends from the tympanic cavity to the nasopharynx. It consists of two parts, an anterior cartilaginous portion and a posterior bony portion. The opening of the cartilaginous portion into the nasopharynx is hooded by the tubal elevation of

cartilage covered by respiratory epithelium. Levator veli palatini attaches to the medial aspect of the cartilaginous portion of the Eustachian tube and the under surface of the petrous part of the temporal bone (figures 51 + 52). Tensor veli palatini is attached to the lateral aspect of the cartilaginous portion of the Eustachian tube and the adjacent scaphoid fossa of the medial pterygoid plate (figures 53 + 54).

The vidian nerve is located in a bony tunnel in the floor of the sphenoidal air sinus, extending from the foramen lacerum posteriorly to the pterygopalatine ganglion anteriorly in the pterygopalatine fossa. The pterygopalatine ganglion is attached to the maxillary nerve and to the palatine and infraorbital nerves (figures 53 + 54).

The internal carotid artery is located lateral to the wall of the pharynx with branches of the superior cervical ganglion and carotid plexus on its surface. The sympathetic chain lay posterior to the carotid sheath and the vagus nerve lay in the carotid sheath with the internal carotid artery and the internal jugular vein. The internal carotid artery bends sharply medially and anteriorly at about a 90 degree angle as it enters the carotid canal. The internal carotid then bends sharply again at about 90 degrees to leave the carotid canal. The carotid plexus winds around the artery. The internal carotid then bends sharply around the sphenoid bone to form the carotid siphon within the cavernous sinus.

The internal carotid artery can be seen travelling up from the bifurcation of the common carotid at the upper border of the thyroid cartilage towards the base of the skull, lying parallel to the vertebral column. The artery lies below the mucosa of the pharynx. The glossopharyngeal nerve also lies below the mucosa of the pharynx crossing behind the internal carotid artery. The sympathetic chain is parallel to the internal carotid along with the vagus nerve (figures 55 + 56).

THE INNER EAR

The inner ear consists of a series of cavities within the petrous temporal bone called the bony labyrinth. Inside the bony labyrinth is a smaller cavity of similar shape but formed by a thin membrane, called the membranous labyrinth.

THE BONY LABYRINTH

The three parts of the bony labyrinth are the vestibule, the semicircular canals and the cochlea. The vestibule is situated medial to the tympanic cavity with the semicircular canals anteriorly and the cochlea posteriorly (figures 57 + 58). It measures 5mm from anterior to posterior, 5mm from superior to inferior and 3mm from medial to lateral. The medial wall is perforated anteriorly for the passage of nerve filaments to the saccule in a circular recess. There is a recess inferiorly formed by the bifurcation of a ridge, the crista vestibuli, which lies posterior to the spherical depression, and which is perforated by nerve fibres supplying the vestibular end of the ductus cochlearis. Superiorly there is an oval depression adjacent to the crista vestibuli. This is perforated by holes which convey nerve fibres to the ampulla of the lateral and superior semicircular canals. Nerve fibres are conveyed to the utricle via holes in the pyramidal end of the crista vestibuli. At the posterior aspect of the medial wall is the opening of the vestibular aqueduct, which contains the vestibular vein and the endolymphatic duct, a prolongation of the membranous labyrinth. The endolymphatic duct is continuous with the endolymphatic sac which lies in the layers of the dura mater within the posterior cranial fossa. Posteriorly are the five orifices of the semicircular canals and anteriorly is the opening which communicates with the cochlea.

There are three bony semicircular canals, superior (anterior), posterior and lateral (horizontal). They measure 0.8mm in diameter and form approximate circles of unequal length. Each has a dilatation at one end which is called the ampulla which measures approximately 1.6mm in diameter. They open into the vestibule via five orifices because the posterior and superior canals join to form the crus commune at one end to enter the vestibule (Figs 59 + 60).

The lateral semicircular canal is the smallest of the canals. It is positioned horizontally within the temporal bone projecting backwards and laterally from the vestibule. It measures 12 to 15mm. Both right and left lateral canals lie in a similar plane. The

ampulated end is superior and posterior on the vestibule, superior to the fenestra vestibuli and adjacent to the ampulated end of the superior canal.

The posterior and superior canals lie at right angles to each other, with the right superior canal being in the same plane as the left posterior canal. The left superior canal is in the same plane as the right posterior canal. The superior canal lies in a vertical plane, lying perpendicular to the long axis of the petrous bone (figures 61 + 62). The superior projection forms the arcuate eminence. It is ampulated laterally and this end opens into the superior and lateral aspect of the vestibule. The other end, the crus commune, enters superiorly and medially. This canal measure 15mm to 20mm.

The posterior canal lies in a vertical plane parallel to the long axis of the petrous bone. It measures 18mm to 22mm and the ampulated end opens posteriorly and inferiorly into the vestibule.

The cochlea lies anterior to the vestibule and the semicircular canals. The cochlea is essentially a hollow blind ending tube which makes two and three quarter turns around a central axis and projects outwards from the base with decreasing radius to form a conical projection. The central axis which it spirals around is a cone formed of bone called the modiolus (figures 63 + 64). The base is at the level of the internal acoustic meatus. It could be described as like the terminal threads on a screw. The apex of the cochlea points anterolaterally and the cochlea is on a downward inclination. The dimensions of the cochlea are 9mm in diameter across the base and 5 mm from base to apex.

Within the spiral is the osseous spiral lamina which projects outwards from the central modiolus towards the periphery. This lamina is incomplete at the periphery but the basilar membrane joins it to the side wall and separates the canal into two sections, which are able to communicate at the apex. Below the lamina the scala tympani is formed and above the lamina the scala vestibuli is formed. The apical communication is formed because the osseous spiral lamina and basilar membrane do not continue to the apex, this communication is called the helicotrema. The modiolus is perforated by orifices for

passage of nerve fibres from the cochlear division of the vestibulocochlear nerve. Some of the nerve fibres follow the spiral canal of the modiolus, which houses the spiral ganglion and follow the path of the spiral lamina. The canal of the cochlea has three openings at the base: the fenestra cochleae which communicates with the tympanic cavity but is closed by the secondary tympanic membrane in life, an opening into the vestibule and the cochlear duct which communicates with the surface of the petrous bone.

The endolymphatic duct passes posteriorly towards the posterior surface of the petrous temporal bone and then inferiorly and expands deep to the operculum (figs 78 + 79).

Within the bony labyrinth is the membranous labyrinth which follows the same general arrangement, with the exception of the vestibule where the utricle and saccule are present.

THE MEMBRANOUS LABYRINTH

The saccule lies in the spherical recess of the vestibule. It receives innervation from the vestibular nerve and communicates with the cochlear duct by the canalis reuniens of Hensen.

The utricle is larger than the saccule and lies posteriorly in the vestibule. It is oblong in shape; the part which lies in the elliptical recess of the vestibule has a thicker lining and receives nerve fibres from the vestibular nerve. The utricle communicates with the semicircular ducts by five openings.

The semicircular ducts are on average about one quarter of the diameter of the semicircular canals and are eccentrically placed within the bony canal.

Within the cochlea the membranous labyrinth forms the cochlear duct which lies upon the spiral osseous lamina and basilar membrane and is roofed by the vestibular membrane which spans from the periosteum of the spiral lamina to the bony wall. The cochlear nerve can be seen entering the modiolus of the cochlea. The cochlear duct, or scala

media, is eccentrically located and in section resembles a triangle with the outer wall formed by a thickened layer of periosteum. This thickened periosteum is called the spiral ligament and superiorly it contains vascular loops and is called the stria vascularis.

The endolymphatic duct is also given off from the saccule which is joined by the utriculosaccularis duct from the utricle (figure 65). The endolymphatic duct then continues in the vestibular aqueduct to end in a blind sac called the endolymphatic sac on the posterior wall of the petrous bone.

THE ENDOLYMPHATIC DUCT AND SAC

Within the bony vestibule on the anteroinferior wall of the utricle, is a thickened inward projection, a lip which forms the inner wall of the utriculo-endolymphatic valve. The outer wall is formed by the wall of the utricle (figure 65). This separates the embryological pars inferior, saccule and cochlea from the pars superior, utricle and semicircular canals. The utricular duct joins with the endolymphatic duct, which arises from the saccule. The endolymphatic sinus is a dilatation of the endolymphatic duct proximally (figure 65).

The sinus is located in a depression on the posterior wall of the vestibule. The sinus narrows and forms the endolymphatic duct as it enters into the vestibular aqueduct of the petrous bone. Within 1mm of the vestibular orifice the duct narrows to form the isthmus of the endolymphatic duct which at 0.3mm in diameter is the narrowest part. The endolymphatic duct continues in a posterior direction then it bends to follow a lateral and inferior course within the bony vestibular aqueduct. Along side the endolymphatic duct within the vestibular aqueduct are other smaller ducts, the paravestibular canaliculi. Within the petrous bone the vestibular aqueduct enlarges to house the proximal part of the endolymphatic sac.

The endolymphatic sac is located partly within the petrous bone covered by a sliver of bone called the operculum and partly within the layers of dura in the posterior cranial fossa. The sac lies on the posterior surface of the petrous bone in a depression on the

surface called the foveate impression. This is located about 10mm lateral to the internal auditory meatus and 10mm inferior to the superior petrosal sulcus. The operculum is also inferior to the subarcuate fossa on the posterior surface of the temporal bone. The extraosseous portion of the endolymphatic sac projects within the dura mater towards the sigmoid sinus laterally and the jugular bulb medially (figures 66 + 67).

The endolymphatic sac lies posterior to the posterior semicircular canal. The extraosseous portion of the endolymphatic sac is found to lie within a fibrous thickening in the dura mater. When opened, adhesions are visible within the endolymphatic sac (figures 66 + 67). The proximal part of the endolymphatic sac can be found deep to the operculum within the vestibular aqueduct, a channel within the petrous temporal bone (figures 68 + 69). The superior border of the extraosseous portion lay in the same place as the lateral semicircular canal. The medial border of the intraosseous part of the sac is found to lie posterior to and at the medial limit of the posterior semicircular canal, where it communicates with the vestibule (figures 70 + 71). As the endolymphatic sac extends towards and emerges from under the operculum, the distance between the sac and the posterior canal increases to about 2mm of dense bone (figures 72 + 73).

HISTOLOGY OF THE MEMBRANOUS LABYRINTH

The bony labyrinth was seen as a series of connecting cavities within the petrous part of the temporal bone. Within the bony labyrinth is the membranous labyrinth. The outline of the bony labyrinth can be drilled from the petrous temporal bone. The bony labyrinth can be seen with the internal and external acoustic meati attached, pointing towards each other, and the tympanic cavity opened (figures 74 + 75).

The cochlea consists of the bony canal within which lies the smaller cochlear duct, or scala media. The scala vestibuli lies above the cochlear duct and the scala tympani lies below the cochlear duct. The roof of the cochlear duct is formed by the vestibular membrane (of Reissner) and the floor is formed by the basilar membrane. The vestibular membrane consists of flattened epithelial cells. The basilar membrane attaches to the

osseous spiral lamina around the modiolus and inserts into the spiral ligament around the periphery. The limbus of the spiral lamina lies on the osseous spiral lamina and provides attachment for Reissner's membrane and the tectorial membrane which lies within the cochlear duct. The peripheral part of the tectorial membrane lies on the spiral organ (figure 76).

The spiral organ consists of a row of inner hair cells with adjacent pillar cells followed by three rows of outer hair cells and then the cells of Hensen. The Tunnel of Corti is formed by the pillar cells between the inner and outer hair cells and the basilar membrane. The tectorial membrane lies on the stereocilia of the inner and outer hair cells (figure 77).

The stria vascularis is located on the external wall of the cochlear duct between Reissner's membrane and the spiral prominence. The stria vascularis consists of a stratified epithelium with an underlying plexus of blood vessels (figure 77).

A horizontal section through the cochlea reveals the turns of the cochlea in cross-section with the modiolus in the middle. The scala vestibuli and scala tympani are visible with the interscalar septum. The organ of Corti lying on the basilar membrane contains the inner hair cells. The inner hair cells are associated with the spiral ganglion where ganglion cells are present. These cells are in turn associated with the cochlear nerve (figure 78).

HISTOLOGY OF THE ENDOLYMPHATIC SAC

The proximal and intermediate parts of the endolymphatic sac are lined with cuboidal epithelium. The proximal part and the majority of the intermediate part of the endolymphatic sac are found within the petrous temporal bone. The proximal part consists mainly of a single tubular structure with convoluted cuboidal epithelium. Surrounding the duct and within the vestibular aqueduct are paravestibular canaliculi containing numerous small blood vessels. The first segment of the endolymphatic duct is

essentially horizontal and 'J' shaped. The intermediate part which is contained within bone is formed by multiple tubules with a cuboidal epithelium (figure 79)

The distal segment of the sac lies on a vertical plane partially within and on the surface of the petrous temporal bone. The distal endolymphatic sac is lined with a low cuboidal epithelium. In the distal endolymphatic sac two epithelial cell types were identified. One cell type has a dark nucleus positioned adjacent to the luminal edge of the cell. The other cell type appears to have slightly lighter cytoplasm and a centrally placed nucleus (figure 80).

The distal endolymphatic sac is arranged in longitudinal parallel tubules which do not communicate with the sigmoid sinus or any other visualised space or cavity. A colloid like material was visualised within the lumen of the sac (figure 80).

Large longitudinal veins run parallel with the long axis of the sac at the distal end of the endolymphatic sac, deep to the sac, within the dura mater. There is a thickening of the dura mater around the endolymphatic sac which extends to the sigmoid sinus, beyond the end of the sac itself (figure 81).

SCANNING ELECTRON MICROSCOPY

In a cross section of the distal part of the endolymphatic sac, the tubular structure of the sac can be seen adjacent to the dura mater. The fine tubular structure of the sac has been partially damaged. A blood vessel can be seen deep to the epithelium. Debris can be seen in the lumen of the sac (figure 82).

In a section of the distal endolymphatic sac which has been de-roofed the epithelial lining of the sac is arranged in flattened sheets of cells. On either side of the flattened epithelial cells the roughened fibrous tissue of the dura mater is visible (Fig 83). At higher magnification the cells of the sac appear to have an organised arrangement with central

areas protruding into the lumen, representing the nuclei of the cells, similar to the lining of the membranous labyrinth in the vestibule.

Deep to the epithelial lining there is a fibrous basement membrane on which were found large macrophages with many processes present (figure 84).

EMBRYOLOGY OF THE ENDOLYMPHATIC SAC

In a 27mm human embryo (about 54 days) the developing malleus and incus can be seen with the tubotympanic recess behind. Medial to these is the developing inner ear. On this section the upper part of the membranous labyrinth is visible, the pars superior of the labyrinth (figure 85).

In a 55mm human embryo, on coronal sectioning, again the main parts of the external, middle and inner ears can be seen. The fused auditory hillocks forming the pinna can be seen laterally and again the external auditory meatus is filled with a meatal plug. The malleus, incus and stapes are visible in the tympani cavity. The facial nerve is visible adjacent to the basal turn of the cochlea (figure 86). Extending from the vestibule of the labyrinth the endolymphatic duct is visible within the vestibular aqueduct as it makes its way to the posterior cranial fossa (figure 87). The endolymphatic duct in the vestibular aqueduct lies on the same plane as the endolymphatic sac and the vestibule at this stage. The association of the endolymphatic sac and the sigmoid sinus is seen.

The hollowed cavities of the membranous labyrinth of the inner ear are visible. Medially lie the turns of the developing cochlea which is formed from the pars inferior. Laterally are the semicircular canals formed from the pars superior. On the left the lateral semicircular canal and the crus communaee are visible. On the right the endolymphatic duct can be seen arising from the vestibule and turning sharply backwards towards the posterior cranial fossa (figure 87).

The distal endolymphatic sac is visible as the terminal dilatation of the endolymphatic duct within the dura mater of the posterior cranial fossa. The endolymphatic sac is seen

to lie on a similar plane to the endolymphatic duct and the vestibule. The sac can be seen at this stage to be a simple structure with a single lumen. Medial to the endolymphatic sac and duct which can be seen in the vestibular aqueduct is the internal auditory meatus lying between the developing semicircular canals and the cochlea. Nerve fibres can be seen entering the internal auditory meatus (figure 87).

MEASUREMENTS

From the series of fourteen dissected temporal bones from 9 bodies, measurements of the endolymphatic sac and the relationship to surrounding structures were made. Peeling the dura down from the operculum revealed the endolymphatic sac as it emerges from the temporal bone (figures 88 + 89). Removal of the dura down to the sigmoid sinus then revealed the dural thickening which contains the endolymphatic sac and the sac itself (figures 90 + 91). The measurements are detailed in the following tables.

Cadaver	Sex	Age	Operculum width	distance from IAM		Distance from SPS		Width of sac	length of sac		Distance from SS	
				M	L	M	L		M	L	M	L
4 Left 1	F	81	6.5	8.6	13.3	10.7	9.1	14.4	7.5	7.2	8.2	8.0
4 Left 2			5.6	9.6	13.9	10.9	9.9	13.8	7.6	10.6	8.6	8.2
4 Left mean			6.1	9.1	13.6	10.8	9.5	14.1	7.6	8.9	8.4	8.1
4 Right 1			4.6	11.0	13.3	8.5	5.3	15.5	9.9	10.5	9.0	5.5
4 Right 2			3.5	9.9	13.8	7.4	6.7	10.2	10.1	9.6	7.7	7.6
4 Right mean			4.1	10.5	13.6	8.0	6	12.9	10.0	10.1	8.4	6.6
5 Right 1	M	92	6.0	10.2	14.4	14.1	10.4	sac lumen not identified			11.8	10.7
5 Right 2			6.2	11.4	13.3	13.2	11.1				10.7	13
5 Right mean			6.1	10.8	13.9	13.7	10.8	not identified			11.3	11.9
6 Left 1	F	96	3.8	8.8	11.2	11.4	11.2	15.9	13.8	12.5	10.4	11.3
6 Left 2			4.0	8.7	12.2	11.9	11.3	16.0	12.9	11.9	10.1	11.8
6 Left mean			3.9	8.8	11.7	11.7	11.3	16.0	13.4	12.2	10.3	11.6
7 Right 1	F	88	4.2	9.8	12.6	11.3	10.6	11.4	12.0	12.0	11.2	10.7
7 Right 2			4.9	9.9	13.4	11.3	10.4	10.2	12.6	12.3	11.3	11.7
7 Right mean			4.6	9.9	13.0	11.3	10.5	10.8	12.3	12.2	11.3	11.2
8 Left 1	M	90	1.2	10.7	10.7	11.8	12.3	13.8	16.4	12.6	14.4	16.7
8 Left 2			2.2	10.3	11.5	11.9	12.2	15.8	16.0	14.4	15.0	16.5
8 Left mean			1.7	10.5	11.1	11.9	12.3	14.8	16.2	13.5	14.7	16.6
8 Right 1			2.3	10.2	11.5	13.0	12.9	13.4	17.2	14.9	14.1	14.8
8 Right 2			1.6	10.3	11.3	12.2	12.3	14.2	17.4	15.2	15.2	14.9
8 Right mean			2.0	10.3	11.4	12.6	12.6	13.8	17.3	15.1	14.7	14.9

Table 1: Table of measurements of endolymphatic sac

Number	Sex	Age	Operculum width	distance from IAM		Distance from SPS		Width of sac	length of sac		Distance from SS	
9 Left 1	F	83	4.2	8.5	11.2	8.7	5.7	6.8	9.9	10.4	11.3	10.3
9 Left 2			5.0	8.7	10.4	8.3	5.7	7.2	10.7	10.8	12.2	10.6
9 Left mean			4.6	8.6	10.8	8.5	5.7	7.0	10.3	10.6	11.8	10.5
9 Right 1			3.5	9.9	13.2	6.2	6.2	12.7	9.6	8.7	14.6	9.3
9 Right 2			4.3	9.7	13.3	6.1	6.4	12.5	9.7	8.6	14	8.7
9 Right mean			3.9	9.8	13.3	6.15	6.3	12.6	9.7	8.7	14.3	9.0
10 Right 1			3.7	10.2	12.5	10.4	10.2	9.8	11.1	11.9	12.2	14.5
10 Right 2			3.4	8.9	11.8	10.2	10.2	10.3	11.7	11.8	12.3	14.9
10 Right mean			3.6	9.55	12.2	10.3	10.2	10.1	11.4	11.9	12.3	14.7
11 Left 1			5.7	10.2	15.7	10.2	9.4	sac lumen not identified			8.3	8.4
11 Left 2			8.1	10.5	14.4	10.2	10.2				8.8	8.5
11 Left mean			6.9	10.4	15.1	10.2	9.8	not identified			8.55	8.5
11 Right 1	F	78	5.5	9.2	13.6	12.1	11.7	9.2	9.5	10.7	11.9	12.1
11 Right 2			5.2	8.8	12.8	11.7	11.6	9.7	9.2	11.2	12.0	12.3
11 Right mean			5.35	9.0	13.2	11.9	11.7	9.5	9.4	11.0	12.0	12.2
12 Left 1			6.5	8.9	13.3	12.3	9.3	11.7	10.7	8.8	10.5	8.1
12 Left 2			6.6	8.9	12.7	12.4	9.2	12.2	10.3	8.8	10.3	8.0
12 Left mean			6.6	8.9	13	12.4	9.3	12.0	10.5	8.8	10.4	8.1
12 Right 1	F	65	3.5	8.2	10.5	10.7	9.2	10.3	3.3	4.3	7.5	11.3
12 Right 2			4.2	8.8	11.3	10.3	9.2	9.6	3.7	4.6	8.2	12.2
12 Right mean			3.9	8.5	10.9	10.5	9.2	10.0	3.5	4.45	7.9	11.8
mean values		84	4.5	9.6	12.6	10.7	9.6	11.9	11.0	10.6	11.1	11.1

Table 2: Table of measurements of endolymphatic sac

In summary the width of the operculum was 4.5mm. The distance of the operculum from the internal acoustic meatus was 9.6mm to the medial limit and 12.6mm to the lateral limit. The distance of the operculum to the superior petrosal sinus was 10.7mm on the medial limit and 9.6mm on the lateral limit.

The endolymphatic sac itself was on average 11.9mm wide, 11.0mm in length on the medial edge and 10.6mm long on the lateral edge. On two temporal bones the extraosseous part of the endolymphatic sac could not be identified, although the thickening of the dura in which the sac would lie was still visible. The medial limit of the operculum was 11.1mm from the sigmoid sinus and the lateral limit was 11.1mm from the sigmoid sinus or jugular bulb.

The internal acoustic meatus was 5.6mm from the superior petrosal sinus medially and 7.1mm at the lateral limit of the meatus. The average height of the internal acoustic meatus was 4.4mm.

There is great variability in the size of the extraosseous portion of the endolymphatic sac, between cadavers and between each side in the one cadaver. There may be no extraosseous portion identifiable, and it may also overlap the sigmoid sinus.

PATHOLOGY IN MÉNIÈRE'S DISEASE

In two cases of known Ménière's disease, post mortem examination of the temporal bones revealed the presence of endolymphatic space distension in the affected ears.

The first case (appendix 9) is a 12 year old girl who was diagnosed with unilateral Ménière's disease affecting the right ear prior to death. Post-mortem histological examination of the left ear, conducted in 1995, was clinically normal but revealed distension of the endolymphatic space at the apex of the cochlea, close to the helicotrema. Otherwise the left ear appeared normal with only artifact changes. Examination of the right ear revealed extensive and diffuse endolymphatic space distension affecting both the vestibular and cochlear (scala media) parts of the membranous labyrinth. Reissner's

membrane was identified herniating through the helicotrema of the cochlea (figure 92). The organ of Corti essentially appears normal. There are breaks present in the wall of the utricle. The saccule is extensively dilated, touching the footplate of the stapes. The endolymphatic duct and sac appeared normal in both ears.

In the second case, an 81 year old man with long standing severe bilateral Ménière's disease, post-mortem histological examination of both ears revealed essentially normal bony labyrinths. Both membranous labyrinths show extensive dilatation of the endolymphatic compartment. Reissner's membrane is displaced into scala vestibuli. There is also herniation of Reissner's membrane through the helicotrema in both ears. Both saccules are dilated and are in contact with the footplate of the stapes. Examination of the left utricle revealed a break in the wall. The endolymphatic sacs in both ears were small (figure 93).

The patient had a left endolymphatic sac decompression and silastic stent insertion for Ménière's disease. The bone of the mastoid was absent in the area from the posterior semicircular canal medially to the sigmoid sinus laterally. The outline of the silastic stent is visible penetrating the layers of the dura mater lateral to the endolymphatic sac on the left side and surrounded by fibrous tissue. A hole is present in the dura mater where it is penetrated by the stent. The stent is not in, or in contact with, the endolymphatic sac (figure 94).

ENDOLYMPHATIC SAC DECOMPRESSION BY NEURO-OTOLOGIST

As this cadaver had previously been dissected by students, there was little to demonstrate of the structures superficial to the mastoid bone. Clearing of the mastoid however revealed the mastoid emissary foramen with the mastoid emissary vein lying in it. The spine of Henle was uncovered at the superior and posterior aspect of the external auditory meatus adjacent to the suprameatal triangle (figure 95).

The sigmoid sinus posteriorly with an overlying bony plate was found to lie posteriorly. Anteriorly is the posterior bony wall of the external auditory canal and superiorly is the dura of the middle cranial fossa.

Drilling medially from MacEwan's triangle, the suprameatal triangle, to about the depth of 10mm revealed the aditus ad antrum, the communication between the mastoid cavity and the tympanic cavity of the middle ear. The dense smooth bone around the lateral semi-circular canal was identified protruding into the mastoid antrum. Through the antrum the body and short process of the incus are visible along with the incudostapedial articulation in the tympanic cavity.

Following removal of the air cells of the mastoid the lateral aspect of the posterior semi-circular canal was identified posterior and slightly medial to the lateral semi-circular canal.

Removal of the air cells inferiorly towards the mastoid tip adjacent to the sigmoid sinus revealed the superior part of the digastric ridge. From inside the mastoid the digastric ridge appears as the digastric apex, passing inferiorly and medially and then superiorly and medially, from posterior to anterior, towards the stylomastoid foramen. The vertical segment of the facial nerve is located in the fallopian canal running from the stylomastoid foramen to the point above where the inferior aspect of the lateral semicircular canal abuts the posterior semicircular canal (figure 96).

The dura of the posterior cranial fossa is visible from the superior petrosal sinus superiorly to the jugular bulb inferiorly and from the posterior semicircular canal medially to the sigmoid sinus laterally. A trapezoid shaped thickening of the dura is visible extending from a narrow apex behind the posterior semicircular canal to a wide base adjacent to the sigmoid sinus. The superior limit of this thickening appears to be parallel to, and on the line of the axis of, the lateral aspect of the lateral semicircular canal (figure 97).

SIMULATED ENDOLYMPHATIC SAC DECOMPRESSION

The craniofacial muscles are found immediately deep to the overlying skin and often adherent to the skin. The circular muscles around the orifices are visible: orbicularis oculi around the eye with palpebral and orbital parts, and orbicularis oris around the mouth. The other muscles around the mouth are depressor anguli oris and levator anguli oris, depressor labii inferioris and levator labii superioris, and zygomaticus major. The broad musculofibrous sheet, occipitofrontalis, extends from the eyebrows anteriorly to the highest nuchal line on the occipital bone posteriorly. Frontalis is the anterior muscular part which is long and broad and is adherent to the superficial fascia of the eyebrows and the muscle fibres blend with those around the eye. Occipitalis is the posterior muscular part which is shorter than the frontal part; it originates from the highest nuchal line and the mastoid part of the temporal bone. Platysma is visible around the anterior part of the neck extending up onto the inferior part of the face and merging with the muscles around the mouth. Risorius is also visible, an extension of platysma projecting posteriorly and superiorly onto the face. Temporoparietalis lies between the auricularis superior and anterior muscles and the frontalis muscle (figures 98 + 99).

The great auricular nerve is visible emerging from behind sternocleidomastoid and extending towards the inferior part of the auricle, branching as it approaches the auricle. The lesser occipital nerve also emerges from behind sternocleidomastoid and branches as it travels up towards the back of the head, parallel to the direction of sternocleidomastoid. One large branch is seen coursing to the superior part of the auricle where a branch of the nerve appears to join with a branch of the posterior auricular nerve. The posterior auricular nerve emerges from under the deep fascia inferior to the auricle (figures 100 + 101).

Anterior to the pinna is the superficial temporal artery, a terminal branch of the external carotid artery. The superficial temporal artery can be seen dividing into an anterior and a posterior division proximally. The artery appears tortuous. The posterior auricular artery is seen on the scalp posterior to the pinna. Branches of the auriculotemporal nerve are visible running with the superficial temporal artery. The auriculotemporal nerve can be

seen as separate from the facial nerve. Posterior to the superficial temporal artery is the superficial temporal vein (figures 102 + 103).

The fan shaped auricularis superior can be seen, originating from the temporal part of the epicranial aponeurosis and inserting onto the anterior part of the helix of the pinna (Figs 102 + 103). The cartilaginous parts of the ear are visible, including the helix which extends along the posterior border from the top down to the tail of the helix posteroinferiorly. The lamina of the tragus is visible anteriorly along with the spine of the helix. The small nerves and vessels lying on the surface of the cartilage are branches of the facial nerve, great auricular nerve and the lesser occipital nerve along with the vagus and glossopharyngeal nerves. The slender auricularis posterior muscle is visible extending from the mastoid process onto the vertical ridge on the posterior aspect of the concha. The posterior auricular ligament lies superior to the posterior auricular muscle and it also extends from the mastoid process to the ridge on the back of the concha. A branch of the posterior auricular artery is also visible coursing onto the superior part of the medial surface of the pinna (figures 104 + 105).

Division of the muscles and ligaments followed by removal of the pinna shows that the posterior auricular artery passes the external acoustic meatus posteriorly, and the superficial temporal artery passes it anteriorly. There is still fascia and periosteum overlying the mastoid process (figures 106 + 107).

With the temporalis fascia removed, along with the periosteum overlying the mastoid process, the fibres of temporalis can be seen converging and passing deep to the zygomatic arch. The posterior, horizontal, fibres can be seen parallel to the superior edge of the mastoid process. With sternocleidomastoid removed, the insertion of splenius capitis onto the mastoid can be seen. The lateral fibres of occipitalis are visible at the posterior aspect of the mastoid process. The external auditory meatus and the tympanic plate are visible anterior to the mastoid. The main trunk of the facial nerve can be seen as it passes anterior and inferior to the mastoid, coursing from medial to lateral. The

posterior auricular artery winds from inferior to superior over the surface of the mastoid, superficial to it (figures 108 + 109).

With removal of the cortex of the mastoid from the supramastoid crest superiorly, to the line of the sigmoid sinus posteriorly, the mastoid tip and along the posterior aspect of the bony wall of the external acoustic meatus anteriorly, the mastoid air cells become visible. The middle cranial fossa dura is identified superiorly at the level of the supramastoid crest. With the removal of the bone between the supramastoid crest superiorly and the posterior and superior bony wall of the external acoustic meatus the bone of the lateral semicircular canal is visualised along with the aditus ad antrum into which it protrudes (figures 110 + 111).

The posterior canal is then identified posterior to the lateral canal and lying on an axis approximately at 90 degrees to the lateral canal. The facial nerve is identified lying in a canal from the stylomastoid foramen inferiorly to the junction of the posterior and lateral semicircular canals superiorly (figures 112 + 113). Removal of the bone between the posterior canal and the sigmoid sinus reveals the dura of the posterior cranial fossa from the superior petrosal sinus superiorly to the jugular bulb inferiorly. Once again a thickening of the dura is present projecting from posterior to the posterior semicircular canal and downwards toward the sigmoid sinus (figures 114 + 115).

ALTERNATIVE PROCEDURES

Suboccipital Posterior Cranial Fossa Approach

The upper fibres of trapezius are visible attached to the medial third of the superior nuchal line, the external occipital protuberance and the ligamentum nuchae. The upper part of sternocleidomastoid is attached to the tip of the mastoid. Splenius capitis is partly visible lying deep to trapezius and then passing out from under the muscle to run under sternocleidomastoid to attach to the mastoid process. In the triangle formed between trapezius, the visible part of splenius capitis and the occipital bone, the greater occipital nerve emerges to run up the back of the head where it lies next to the occipital artery.

Parallel to and immediately posterior to the upper part of sternocleidomastoid is the lesser occipital nerve (figures 116 + 117).

Removal of the upper part of trapezius and sternocleidomastoid muscles allows the visualisation of both splenius capitis muscles. They originate from the ligamentum nuchae and spinous process of C7 and the upper thoracic vertebrae and insert onto the mastoid process and the lateral third of the superior nuchal line. The greater occipital nerves can be seen emerging from between the fibres of the upper part of semispinalis capitis on both sides and then coursing superiorly and laterally onto the back of the head (figures 118 + 119). Deep to splenius capitis lies semispinalis capitis, the inferior part of which is crossed by splenius cervicis, originating from the upper thoracic spinous processes and inserting into the posterior tubercles of the transverse processes of C1, C2 and C3. The accessory nerve is visible passing into the reflected part of trapezius.

Longissimus capitis can be seen inserting onto the mastoid process; inferiorly however the muscle lies deep to serratus posterior superior which itself is deep to rhomboid major and rhomboid minor. Levator scapulae originates from the transverse processes of C1 to C4 and inserts onto the superior part of the medial border of the scapula. Superiorly this muscle is crossed by a large vein (figures 120 + 121).

Retraction of the scapula and levator scapulae, division of serratus posterior superior and removal of the inferior part of semispinalis cervicis allows the visualisation of some of the other muscles of the upper part of the back. The separation between the different muscles is not clear. Semispinalis capitis can be seen attaching to the thoracic spinous process and lateral to this, the attachment of longissimus thoracis into the transverse processes of the thoracic vertebrae is visible (figures 122 + 123).

Removal of semispinalis capitis reveals the underlying fascia, which removed in turn, reveals a very dense venous plexus around the muscles of the suboccipital triangle (figures 124 + 125).

The posterior belly of digastric can be seen originating from the digastric groove and passing superficial to the transverse process of the atlas, the first cervical vertebrae (C1). Deep to digastric, the occipital artery is visible (figures 126 + 127).

The muscles of the suboccipital triangle can now be seen. Superior oblique runs from the transverse process of C1 to the base of the occipital bone. The inferior oblique muscle runs from the transverse process of C1 to the spinous process of C2. Rectus capitis posterior major extends from the spinous process of C2 to the base of the occipital bone and rectus capitis posterior minor extends from the spinous process of C1 to the base of the occipital bone. In the floor of the suboccipital triangle the vertebral artery was identified adjacent to the posterior arch of atlas and the first cervical nerve positioned below the vertebral artery. The internal carotid artery is visible inferior and anterior to the origin of levator scapulae (figures 126 + 127).

Removal of the inferior oblique muscle, round which the greater occipital nerve winds by passing inferior to the inferior edge of the muscle and then coursing superiorly, allows visualisation of the posterior arch of the atlas and the lamina of the second cervical vertebra. The greater occipital nerve is the dorsal ramus of the second cervical nerve; the ventral ramus courses around the vertebral artery. The third cervical nerve lies inferior to the greater occipital nerve. The deep cervical vein is visible lateral to semispinalis cervicis (figures 126 + 127).

Removal of the muscles of the suboccipital triangle allows the visualisation of the atlas and the axis, the first and the second cervical vertebrae. The vertical part of the vertebral artery can be seen in part between the foramen transversarium of C1 and C2. The close proximity of the vertebral artery and the internal carotid artery in this region is apparent. The internal jugular vein can be seen lateral to the internal carotid artery (figures 128 + 129).

The dura mater overlying the cervical spinal cord is visible between the posterior arches of C1 and C2. The dorsal rami of the first, second and third cervical nerves are visible.

The ventral rami of the second cervical nerve winds laterally around the vertebral artery. The rounded dorsal spinal root ganglion of the second cervical nerve lies inferior to the posterior arch of C1. The dense posterior atlanto-occipital membrane runs between the posterior part of the base of the occipital bone and the posterior arch of C1 (figures 128 + 129).

With removal of the bone posterior and superior to the mastoid process, the dura of the posterior and middle cranial fossa can be visualised. The posterior limb of the middle meningeal artery lies superficial to the dura mater, deep to the bone and runs posteriorly and superiorly (figures 130 + 131).

The transverse venous sinus of the skull runs from the confluence of sinuses at the internal occipital protuberance laterally and anteriorly, curving upwards towards the sigmoid sinus. The sigmoid sinus curves inferiorly and medially, posterior and medial to the mastoid process (figures 130 + 131).

With retraction of the dura mater of the posterior cranial fossa, the subarachnoid space is opened and the pia mater can be seen on the surface of the cerebellum with the vessels coursing over the surface.

With the aid of an operating microscope the dura mater covering the posterior surface of the petrous temporal bone can be visualised. The glossopharyngeal nerve enters the jugular fossa through a notch in the superior aspect of the jugular foramen. A fibrous band separates this from the rest of the foramen where the vagus and the cranial and spinal components of the accessory nerve leave the cranial cavity. The vertebral artery can be seen inferior to the cranial roots of the accessory nerve.

The trigeminal nerve along with the anterior inferior cerebellar artery can be seen entering the trigeminal cave, or Meckels cave, with the dura of the tentorium cerebelli superiorly, and the cerebellum posteriorly. The facial and vestibulocochlear nerves pass into the internal acoustic meatus (figures 132 + 133).

The superior petrosal sinus lies in the attached edge of the tentorium cerebelli to the petrous temporal bone. The internal acoustic meatus is positioned inferior to the superior petrosal sinus. Along with the facial and the vestibulocochlear nerve the nervus intermedius enters the internal acoustic meatus. With the microscope focused on the dura of the posterior surface of the temporal bone immediately lateral to the internal acoustic meatus, the foveate impression is visible. The superior and medial border of the foveate impression is formed by the operculum. The operculum forms a ridge with the overlying dura. The foveate impression is visible as the hollowed area inferior to the ridge formed by the operculum (figures 134 + 135).

Combined retrosigmoid, suboccipital and transmastoid approach

The posterior triangle of the neck is bounded anteriorly by the posterior border of sternocleidomastoid, posteriorly by the lateral border of trapezius and inferiorly the base is formed by the clavicle. The floor of the triangle is formed by fascia covering the underlying muscles: semispinalis capitis and splenius capitis superiorly, levator scapulae in the middle and the scalene muscles inferiorly. The occipital artery is visible overlying semispinalis capitis at the apex of the posterior triangle. The great auricular and transverse cervical nerves are seen to perforate the deep fascia at Erb's point and wind around the posterior edge of sternocleidomastoid. The spinal accessory nerve perforates the fascia about 1cm above Erb's point as it emerges from under sternocleidomastoid to cross the posterior triangle superficially and enter the superior border of trapezius. The lesser occipital nerve courses up the posterior triangle behind and parallel to the posterior border of sternocleidomastoid.

With splenius capitis and semispinalis capitis removed on both sides the suboccipital triangle is visible. The greater occipital nerve can be seen winding around the inferior margin of the inferior oblique before passing superiorly onto the back of the head. Semispinalis cervicis inserts onto the spinous process of C2 (figures 136 + 137).

Rectus capitis posterior minor attaches to the posterior tubercle of the atlas. Removal of the muscles of the suboccipital triangle and the atlanto-occipital membrane reveals the base of the occipital bone and the posterior aspect of the foramen magnum (figures 138 + 139).

Removal of the posterior aspect of the basilar part of the occipital bone and the underlying dura reveals the posterior and inferior surface of the cerebellum. The pia mater can be seen on the surface of the cerebellum along with the cerebellar vessels (figures 140 + 141).

Following removal of the posterior part of the basilar part of the occipital bone on both sides and removal of the cerebellum the posterior cranial fossa can be visualised from below, looking up to the tentorium cerebelli. The brainstem can be seen lying against the clivus (figures 142 + 143).

The medulla oblongata extends down to the foramen magnum. The inferior, middle and superior cerebellar peduncles can be seen laterally. The rhomboid fossa, or floor of the fourth ventricle, lies between the cerebellar peduncles on each side and is formed by the dorsal surface of the pons and the cranial half of the medulla. Superiorly the ventricle communicates with the cerebral aqueduct and inferiorly it communicates with the central canal of the spinal cord. A sulcus in the midline divides the floor of the ventricle in two. Either side of the midline sulcus are medial eminences which extend to the sulcus limitans laterally. The facial colliculus forms an expansion of the median sulcus. The vestibular area is located lateral to the inferior fovea (figures 142 + 143).

The ridge formed by the operculum lies superior and medial to the foveate impression in which lies the endolymphatic sac. The ridge is positioned approximately 1 cm inferior to the superior petrosal sinus and 1cm lateral to the internal acoustic meatus. The superior petrosal sinus lies in the attached edge of the tentorium cerebelli, where the tentorium attaches to the petrous part of the temporal bone. Removal of the dura superior and medial to the foveate impression reveals the operculum (figures 144 + 145).

Removal of the bone immediately above and extending onto the lateral part of the vault, and removal of the squamous part of the occipital bone along with the posterior part of the parietal bone, reveals the transverse venous sinus posteriorly and the posterior limb of the middle meningeal artery lying on the dura mater. The sigmoid sinus grooves the inside of the skull where the temporal bone articulates with the occipital bone. From the inside this groove is “s” shaped and runs to the jugular fossa. Removal of the occipital bone and part of the mastoid process from behind reveals the posterior edge of the sigmoid sinus continuing on from the transverse sinus (figures 146 + 147).

The posterior auricular nerve leaves the main trunk of the facial nerve and passes laterally, superior to the posterior belly of digastric. It pierces the fascia and then passes posteriorly over the attachment of sternocleidomastoid to the mastoid and then superiorly behind the pinna (figures 148 + 149).

The branch of the facial nerve that innervates the posterior belly of digastric can be seen leaving the main trunk of the facial nerve posteriorly, inferior to the tip of the mastoid, and passing vertically downwards to the digastric muscle. The facial nerve can then be seen turning forwards to enter the posterior border of the parotid gland (figures 150 + 151).

Drilling of the mastoid now reveals the sigmoid sinus from in front, as the groove which it forms has been removed. The vertical segment of the facial nerve passes superiorly from the stylomastoid foramen to the lateral semicircular canal adjacent to the posterior semicircular canal. The chorda tympani arises from the vertical segment of the facial nerve close to the stylomastoid foramen and passes upwards and anteriorly towards the tympanic membrane (figures 152 + 153).

A thickening of the dura of the posterior cranial fossa is present extending from posterior to the posterior semicircular canal and positioned where the foveate impression would be. The continuation of the transverse venous sinus as the sigmoid sinus can be seen, along

with the point where the superior petrosal sinus drains into the sigmoid sinus. The roof of the mastoid is formed by the dura of the floor of the middle cranial fossa (figures 154 + 155).

The relationship of the petrous temporal bone and the middle and posterior cranial fossae can be seen. The proximal endolymphatic sac can now be visualised from the posterior cranial fossa and the thickening of dura with the distal endolymphatic sac can be seen via the mastoid.

Middle Cranial Fossa Approach

The fan shaped temporalis muscle can be seen lying in the temporal fossa deep to the temporalis fascia. Temporalis muscle is attached to the temporalis fascia superiorly and posteriorly but inferiorly it is separated from the fascia by a fat pad. The superior temporal line where the temporalis fascia inserts is visible and the temporalis can be seen originating from the inferior temporal line. The anterior fibres are vertically arranged, the middle fibres are obliquely arranged and the posterior fibres are almost horizontal. The fibres converge, running deep to the zygomatic arch, anterior to the temporomandibular joint. Temporalis inferiorly lies deep to the thick masseter muscle which takes origin from the lower border of the zygomatic bone and inserts into the mandible at the angle (figures 156 + 157).

Temporalis and the overlying fat pad can be seen to fill the temporal fossa lying between the zygomatic arch and the deeper sphenoid and squamous part of the temporal bone. The zygomatic arch is formed posteriorly by the zygomatic process of the temporal bone which is continuous with the suprameatal line on the lateral aspect of the temporal bone. This line can be seen to mark the level of the floor of the middle cranial fossa (figures 158 + 159).

Lying between the dura mater and the overlying bone are the anterior and posterior branches of the middle meningeal artery. The anterior division is seen to run deep to the pterion, about 2cm above the zygomatic arch and 1½ cm posterior to the frontal process

of the zygomatic bone. The posterior branch is a lot closer to the floor of the middle cranial fossa, lying about 1cm above the suprameatal line (figures 158 + 159).

Raising the dura of the floor of the middle cranial fossa reveals the anterior surface of the petrous temporal bone. This wedge of bone has a wide base where it contacts the squamous part and a narrow apex. Anteriorly the petrous bone is continuous with the cerebral surface of the squamous part and limited by the sphenoid and posteriorly the tentorium cerebelli attaches to the superior edge. The arcuate eminence bulges into the middle cranial fossa. The greater superficial petrosal nerve leaves the temporal bone through the facial hiatus and runs on the bony floor of the cranial floor towards the foramen lacerum and deep to the trigeminal ganglion (figures 158 + 159).

Removal of the dura mater reveals the cerebral cortex covered with pia mater and part of the arachnoid mater. Along the line of the superior sagittal sinus, lateral to it, bridging cerebral veins are present; crossing what would be the subarachnoid space. These bridging veins pass from posterior to anterior before entering the superior sagittal sinus. Arachnoid villi are present lateral to the superior sagittal sinus in the lacunae laterales. A meshwork of cerebral veins and arteries is visible in the pia mater running over the surface of the cerebral cortex. Removal of the pia mater and the superficial vessels reveals the gyri and sulci of the cerebral cortex. The frontal, temporal, parietal and occipital lobes are visible. The lateral sulcus can be seen separating the temporal lobe from the frontal and parietal lobes. The central sulcus separates the frontal and parietal lobes. On the temporal lobe the inferior and the superior temporal gyri can be seen. The inferior temporal gyrus lies closest to the surface of the temporal bone. Over the surface of the cerebral hemisphere the small holes created by the perforating vessels can be seen. Removal of the frontal, parietal and temporal opercula reveals the deeper cortex of the insula. Deep to the insula is the external capsule which lies on the surface of the putamen of the lentiform nucleus. Inferior to the external capsule, and running from front to back is the inferior occipitofrontal fasciculus and anteriorly the uncinate fasciculus. The corona radiata can be seen superiorly extending radially from the internal capsule out towards the cortex. The internal capsule lies deep to the putamen and passes inferiorly

towards the cerebral peduncle, deep to the optic tract. The injected perforating vessels are visible in the substance of the brain. At the anterior part of the optic tract, close to the optic chiasm is the middle cerebral artery which has been divided. The posterior cerebral artery lies inferior to the optic tract passing from the circle of Willis posteriorly. With removal of the undersurface of the temporal lobe of the brain the dura of the floor of the middle cranial fossa can be seen. Cerebral veins are also evident (figures 160 + 161).

The superior semicircular canal lies under the arcuate eminence, forming the eminence. The removal of the bone approximately 60 degrees anterior and medial to the superior canal reveals the roof of the internal auditory meatus. Underlying the facial hiatus is the greater superficial petrosal nerve. This can be traced posteriorly and laterally to the genicular ganglion. The horizontal, perilyabyrinthine segment of the facial nerve continues laterally and posteriorly from the genicular ganglion. Drilling above the internal acoustic meatus reveals the dura which lines the roof of the meatus. The contents of the internal acoustic meatus can be seen once the dura, which lined, the roof has been excised. The facial nerve is in the superior and medial (anterior) aspect of the internal acoustic meatus and the superior vestibular nerve is in the superior and lateral (posterior) part. Drilling anterior to the fundus of the canal reveals the cochlea. The facial nerve can be seen winding around the cochlea towards the genicular ganglion. A vertical bar of bone, the vertical crest, separates the facial nerve from the superior vestibular nerve at the fundus (figures 162 + 163).

The cochlear nerve lies in the meatus inferior to the facial nerve and the inferior vestibular nerve lies inferior to the superior vestibular nerve. The cochlear and vestibular arteries which are branches of the labyrinthine artery are visible within the meatus. A small artery can be seen lying on the surface of the cochlea and inferior vestibular nerves. At the fundus a horizontal bridge of bone, the transverse crest separates the facial and superior vestibular nerves from the cochlea and inferior vestibular nerves (figures 162 + 163).

Removal of the dura reveals the petrous temporal bone, the base of which lies at the junction of the petrous and squamous parts, with the apex lying medially and anteriorly close to the impression for the trigeminal nerve. Removal of the roof of the trigeminal cave and the surrounding dura reveals the fibres of the trigeminal nerve which expand into a large flattened ganglion, the trigeminal ganglion. Arising from the ganglion are the three divisions, the mandibular passing to the foramen ovale, the maxillary passing to the foramen rotundum and the ophthalmic which runs forward in the wall of the cavernous sinus. The cavernous sinus can be seen medial and anterior to the ganglion. Immediately lateral and posterior to the foramen ovale is the foramen spinosum which is transmitting the middle meningeal artery (figures 164 + 165).

The greater superficial petrosal nerve runs from the genicular ganglion anteriorly and medially to pass deep to the trigeminal ganglion. Medial to the nerve and deeper within the petrous bone is the horizontal segment of the internal carotid artery within the carotid canal (figures 164 + 165).

The tegmen tympani forms the roof of the tympanic cavity. Within the tympanic cavity the malleus articulates with the incus and incus articulates with the stapes. The head of the malleus can be seen anterior to the incus and it articulates with the body of the incus. Inferiorly the long process of the incus can be seen articulating with the head of the stapes. The short process of the incus is directed posteriorly and is attached to the fossa incudis in the epitympanic recess. The Eustachian tube opens into the tympanic cavity at the anterior tympanic wall (figures 164 + 165).

Perpendicular to the axis of the superior canal, posteriorly, lies the posterior semicircular canal. Anterior to the posterior canal and deep and lateral to the superior canal is the lateral semicircular canal (figures 164 + 165).

Removal of the mastoid air cells and bone posterior to the posterior semicircular canal reveals the dura of the posterior cranial fossa from the posterior canal to the sigmoid sinus. Anterior to the mastoid is the external auditory canal. The sigmoid sinus extends

inferiorly, medially and anteriorly towards the jugular bulb. The upper part of the thickening in the dura of the posterior cranial fossa is identifiable (figures 164 + 165).

CLINICAL PROCEDURES

Retrosigmoid / suboccipital acoustic neuroma resection

A retrosigmoid craniotomy allows the surgeon to enter the posterior cranial fossa. Division of the tissues in the back of the neck resulted in bleeding from a rich venous plexus in the sub-occipital region along with bleeding from the emissary veins. The anterior margin of the craniotomy is the sigmoid sinus and superior margin the transverse sinus. The dura mater and the arachnoid mater has to be opened and the cerebellum retracted to visualise the posterior surface of the petrous temporal bone (figure 166).

In the cerebellopontine angle, the vestibulocochlear and facial nerves are revealed coursing into the internal acoustic meatus, and the trigeminal nerve coursing to the trigeminal cave. The abducens nerve is seen to pass through a hole in the dura posterior to the cavernous sinus. Inferiorly the glossopharyngeal, vagus and accessory nerves are seen.

The foveate impression is seen with the bulge formed by the operculum more superior and medial on the surface of the petrous temporal bone.

Glomus jugulare resection by lateral approach

With the external auditory meatus divided through the cartilaginous portion and sewn shut it can be retracted anteriorly with the skin flap. The root of the zygomatic process can be seen superior to the bony part of the external auditory meatus and can be seen to be continuous with the supramastoid crest. Sternocleidomastoid can be seen attaching to the mastoid process with the great auricular nerve crossing in front of the muscle from posterior to anterior (figure 167).

With the superficial part of the parotid gland removed and the facial nerve dissected out of the vertical segment of the fallopian canal it can be seen transposed into a new canal drilled in the attic of the tympanic cavity. The remains of the mastoid and tympanic cavities are continuous, filled with tumour. The sigmoid sinus forms the posterior limit of the mastoid, however the posterior cranial fossa dura is visible posterior to the sigmoid sinus (figure 168).

Division of the posterior belly of digastric and fracturing of the styloid process allows visualisation of the infratemporal fossa and the structures deep to the infratemporal fossa from behind. Ties can be seen around the internal jugular vein and the internal carotid artery. The lower four cranial nerves are visible as they enter the neck. The glossopharyngeal is visible passing superficial to the internal carotid artery as it travels downwards and forwards. The vagus and the hypoglossal nerves pass into the neck deep to the internal jugular vein and then move downwards. The accessory nerve loops around the anterior border of the internal jugular vein from medial to lateral and then passes backwards and downwards (figure 168).

This surgical procedure then allowed for removal of the lateral part of the petrous temporal bone.



Figure 13 Photograph showing an oblique posterior and lateral view of the skeleton of the head and neck

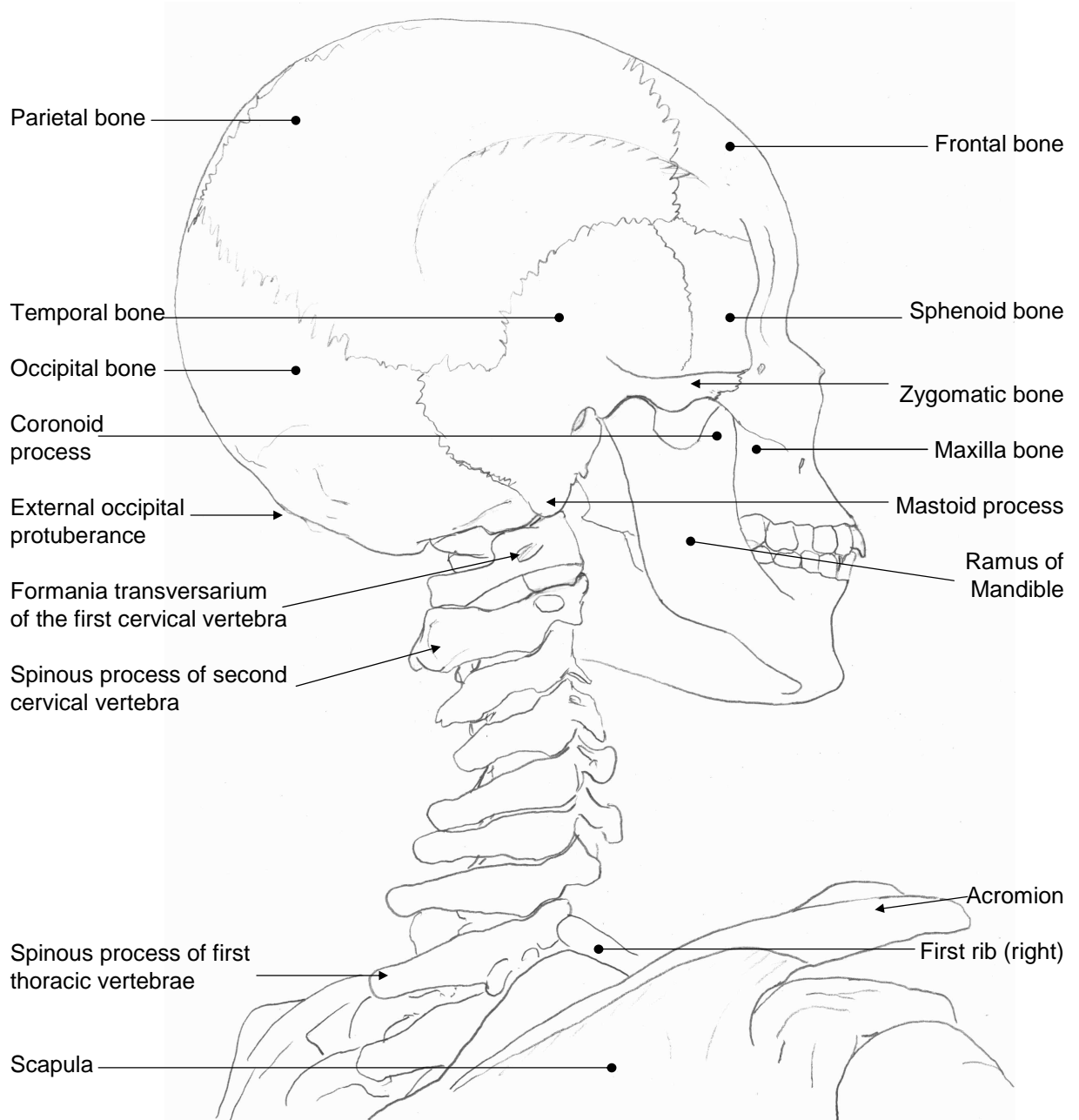


Figure 14 Diagram showing an oblique posterior and lateral view of the skeleton of the head and neck



Figure 15 Photograph of lateral view of right temporal bone

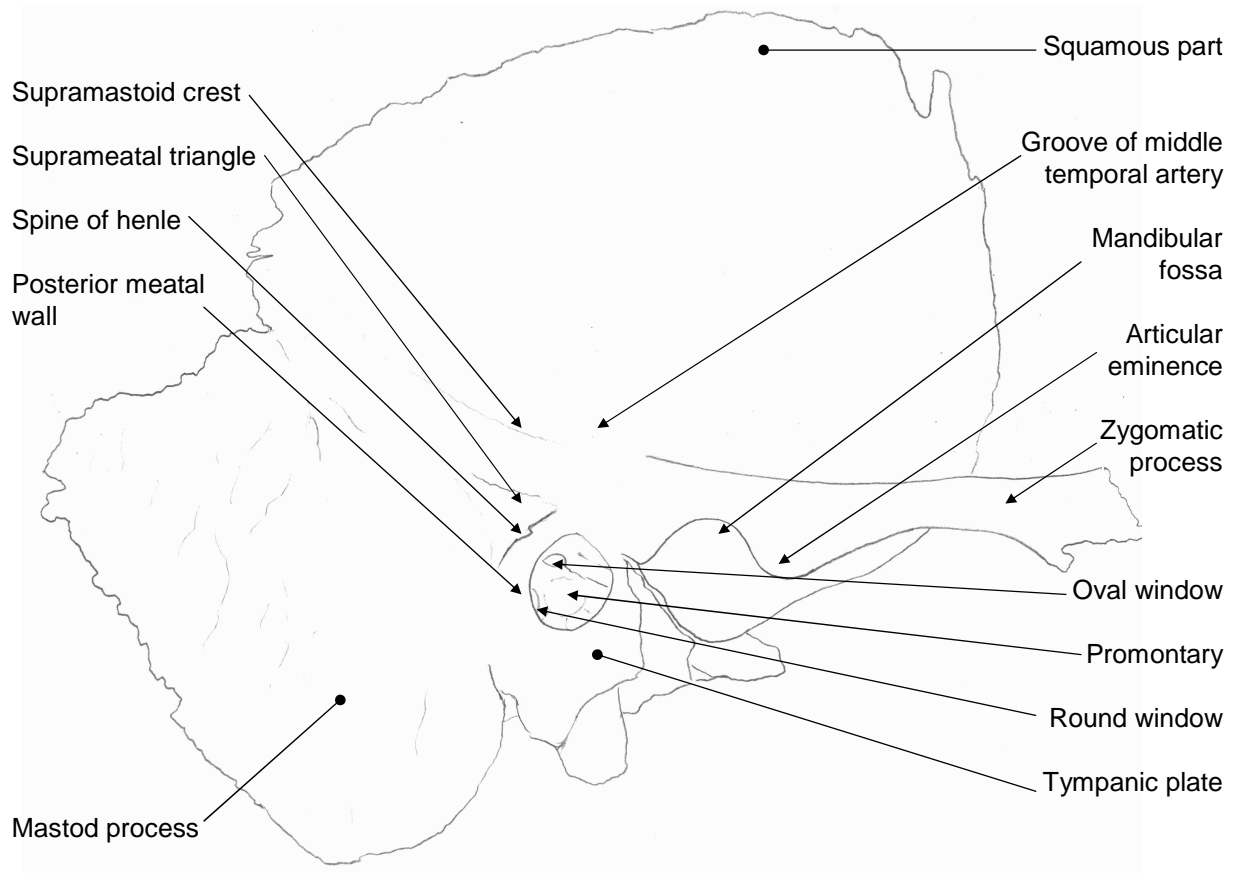


Figure 16 Drawing of lateral view of right temporal bone



Figure 17 Photograph of superior view of right temporal bone

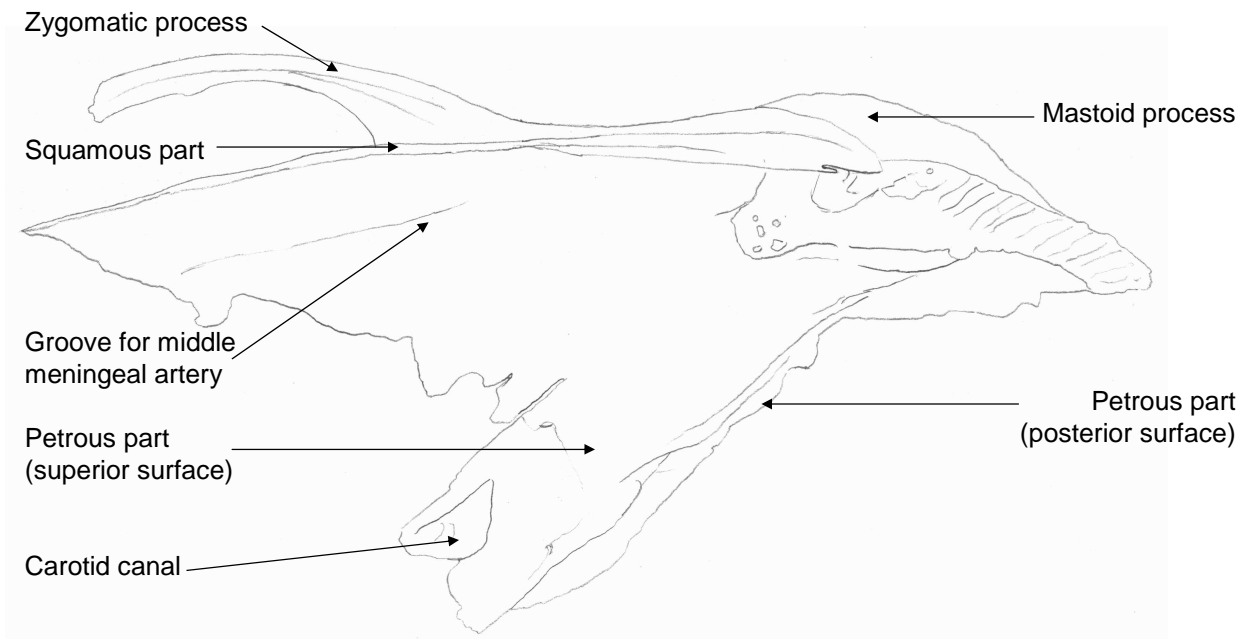


Figure 18 Drawing of superior view of right temporal bone



Figure 19 Photograph of inferior view of right temporal bone

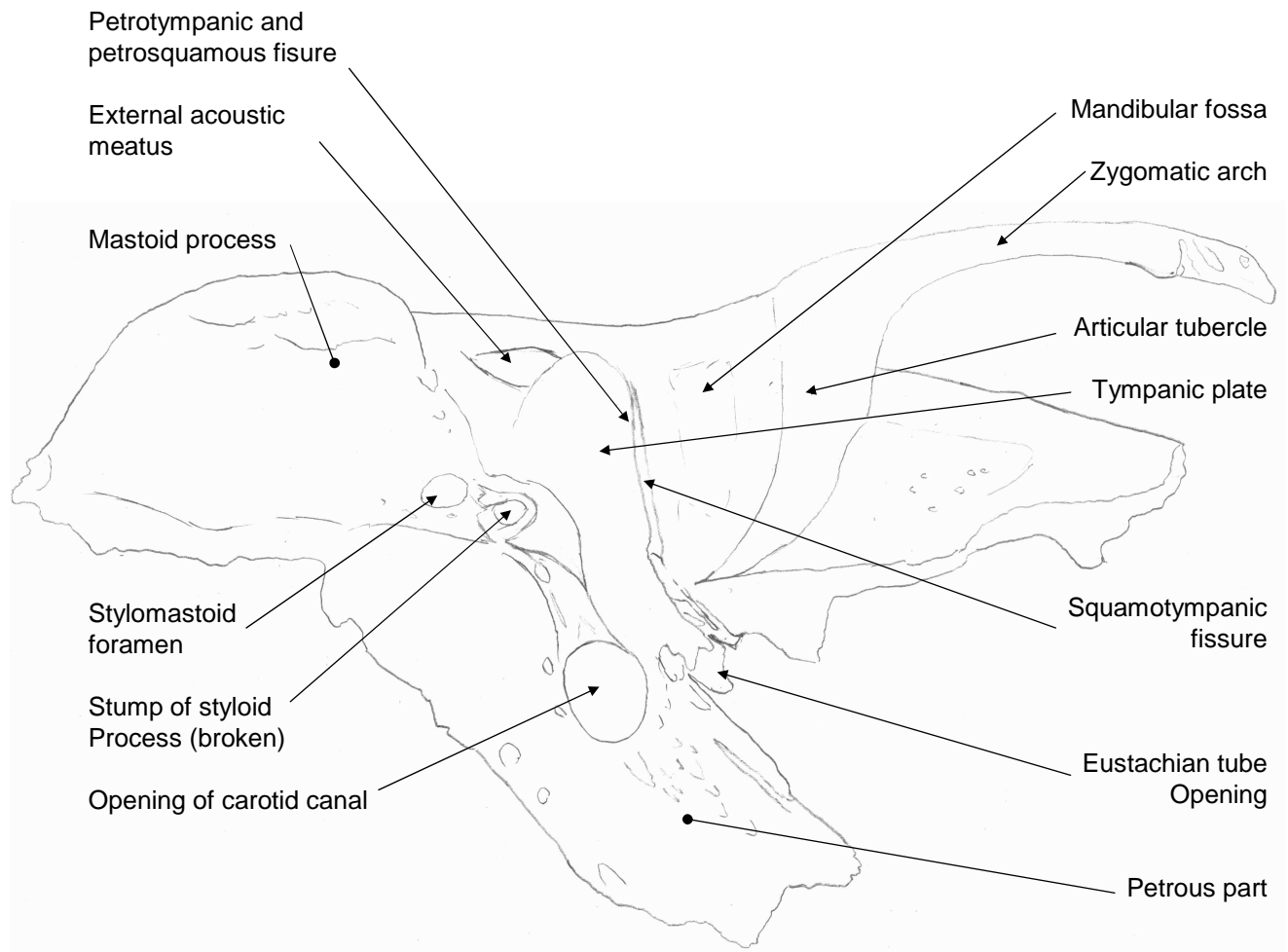


Figure 20 Drawing of lateral view of right temporal bone



Figure 21 Photograph of posterior view of right temporal bone

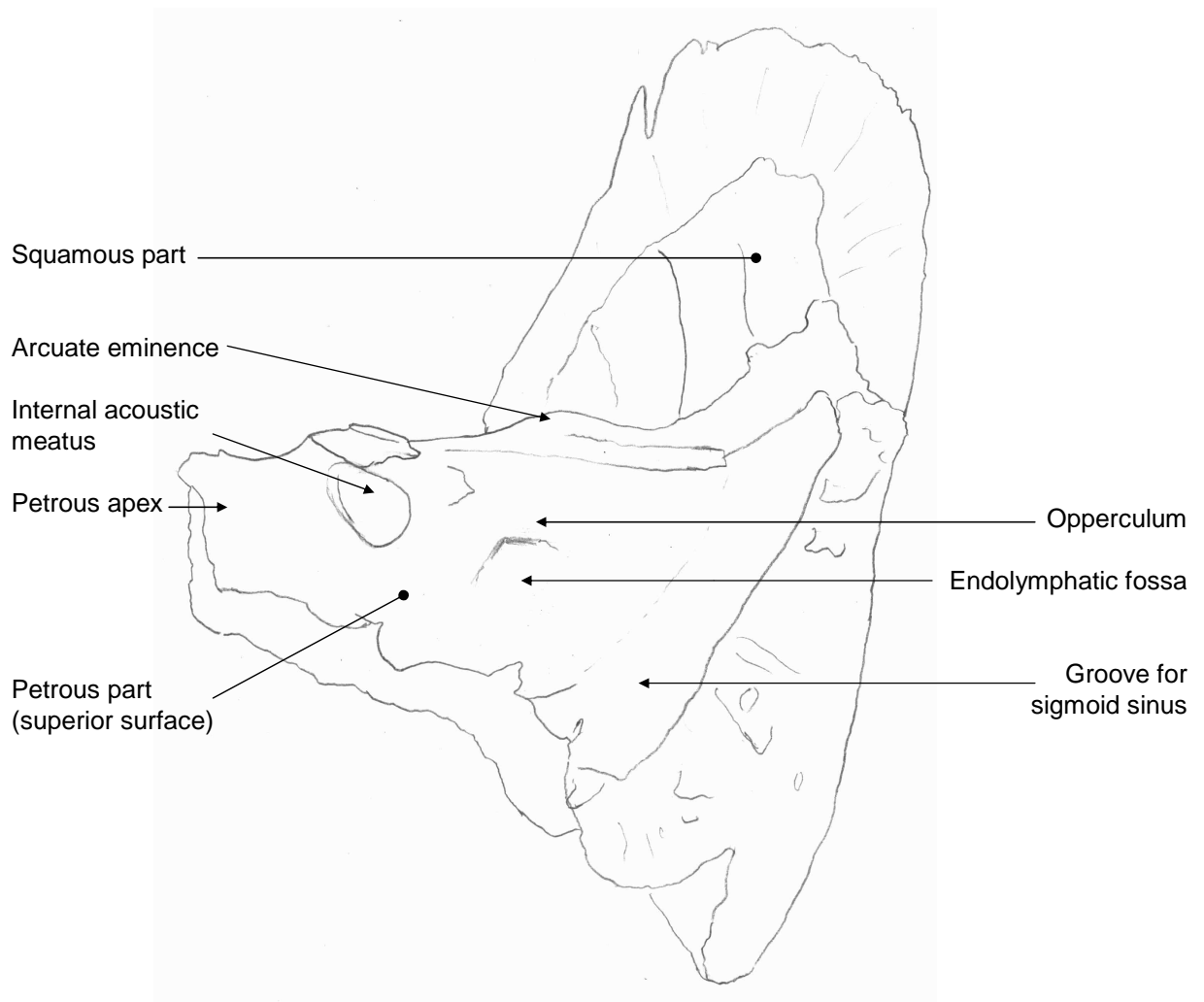


Figure 22 Diagram of posterior view of right temporal bone



Figure 23 Photograph of posterior view of left anterior, middle and posterior cranial fossae

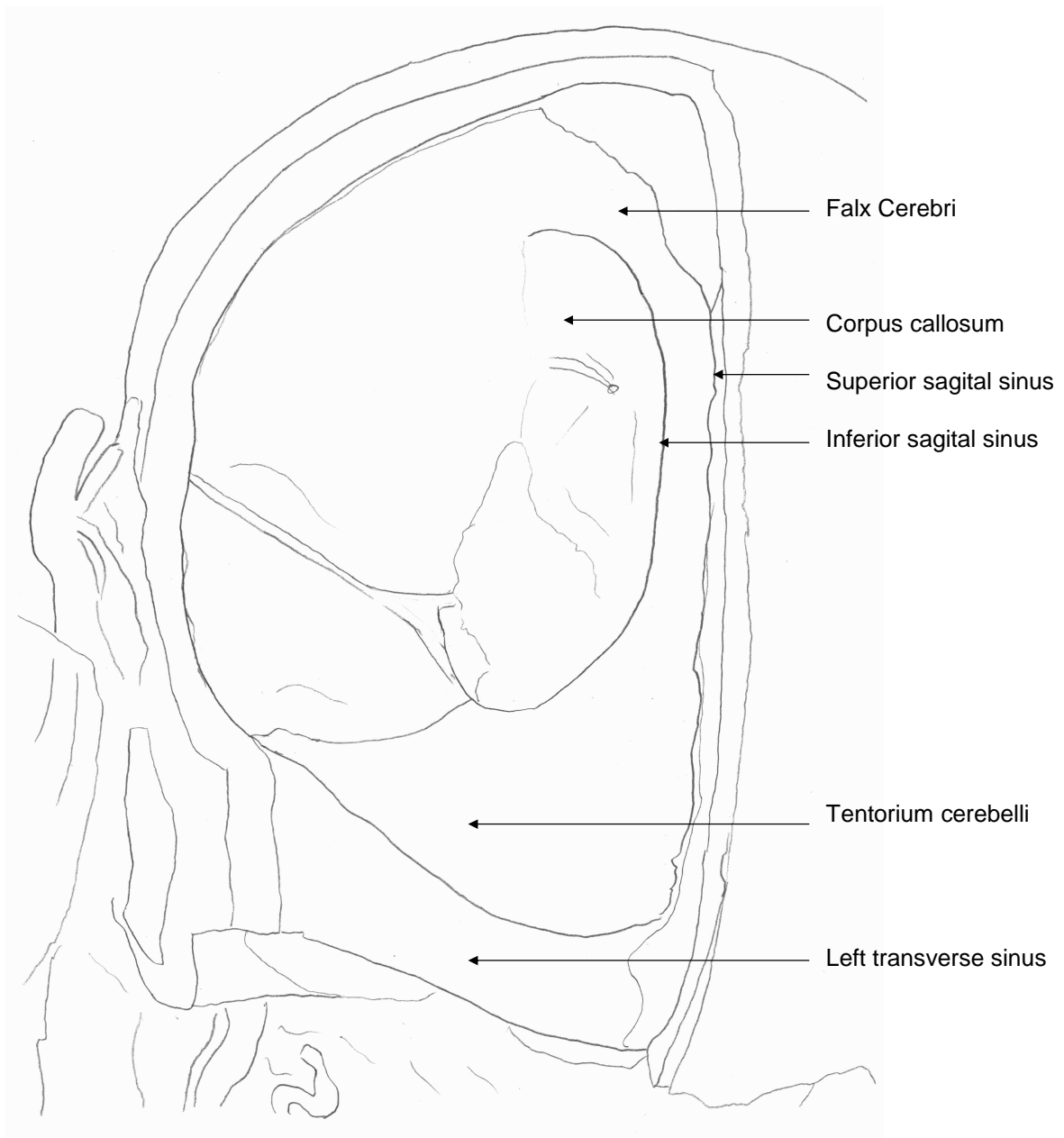


Figure 24 Diagram of posterior view of left anterior, middle and posterior cranial fossae

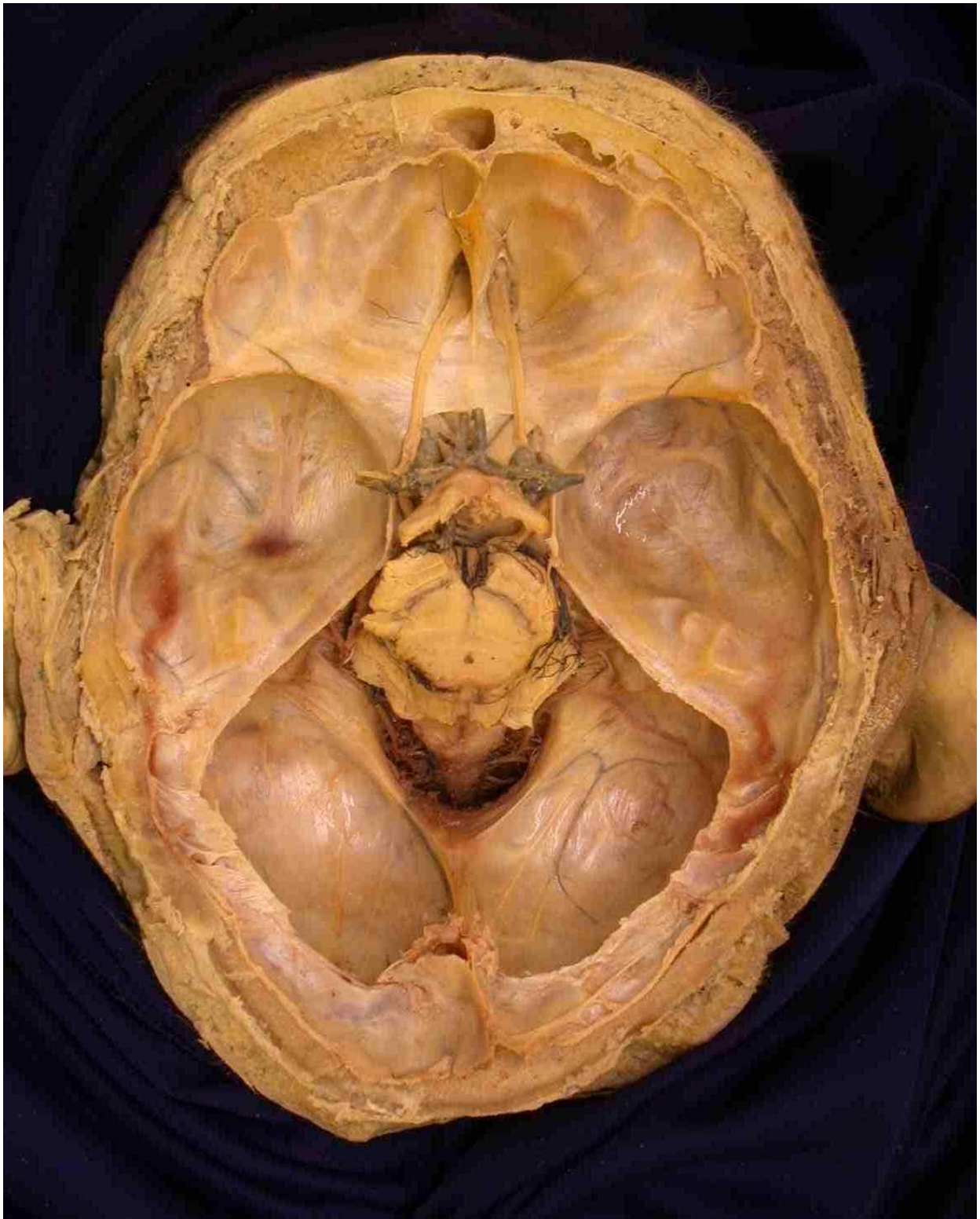


Figure 25 Photograph of floor of cranial cavity showing anterior, middle and posterior cranial fossae

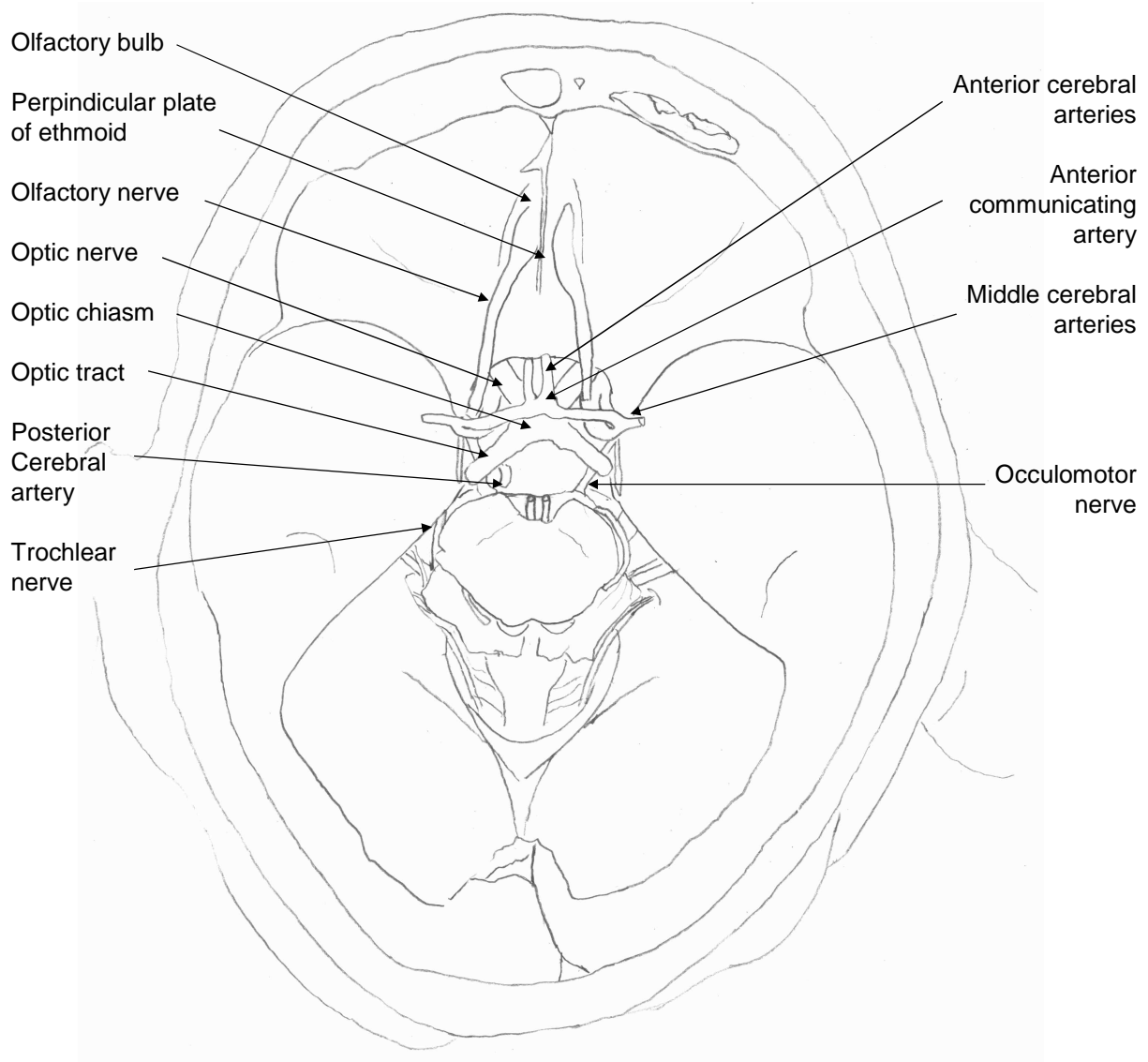


Figure 26 Diagram of floor of cranial cavity showing anterior, middle and posterior cranial fossae



Figure 27 Photograph of posterior aspect of left temporal bone with internal acoustic meatus and jugular foramen

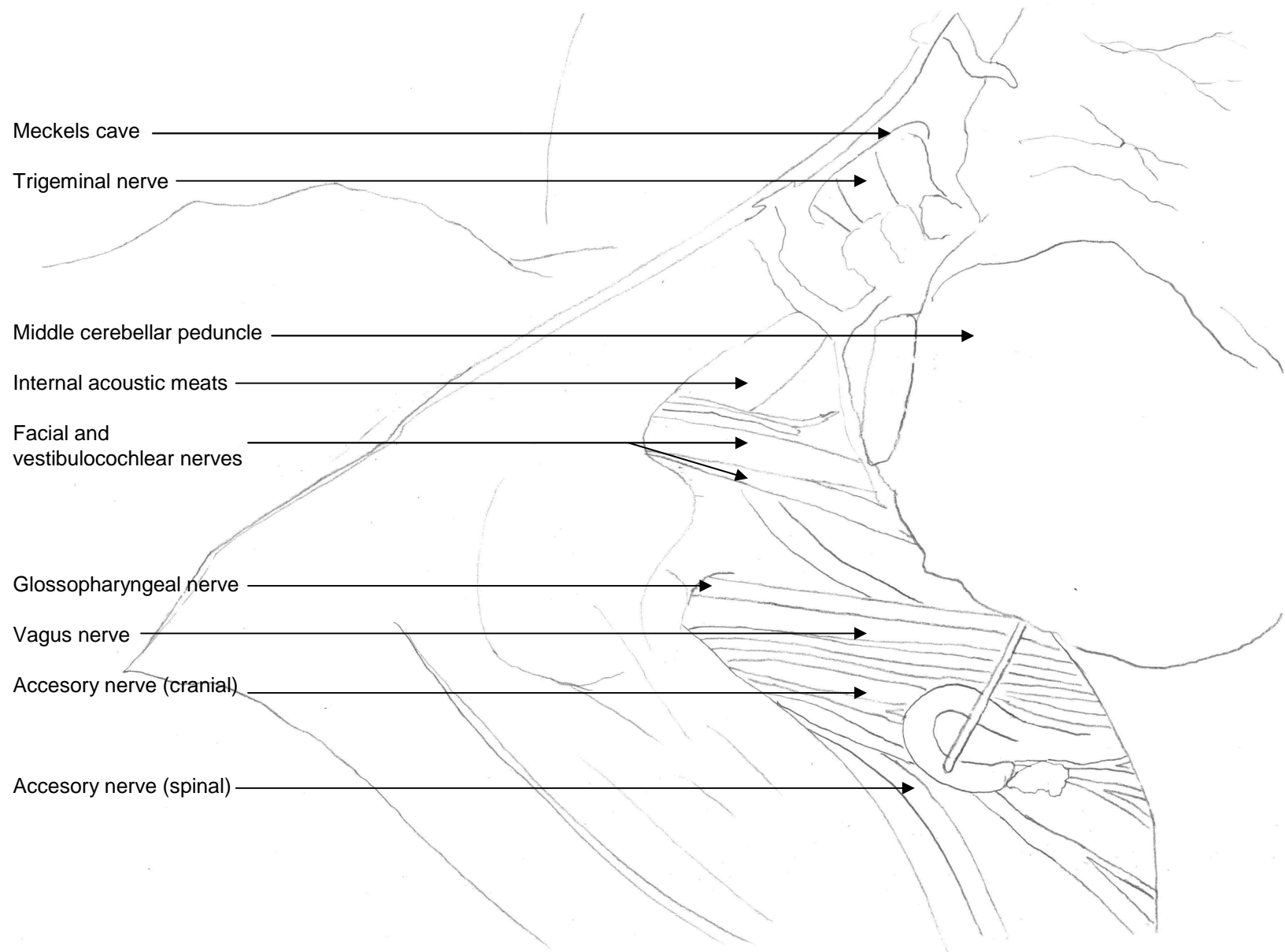


Figure 28 Diagram of posterior aspect of left temporal bone with internal acoustic meatus and jugular foramen

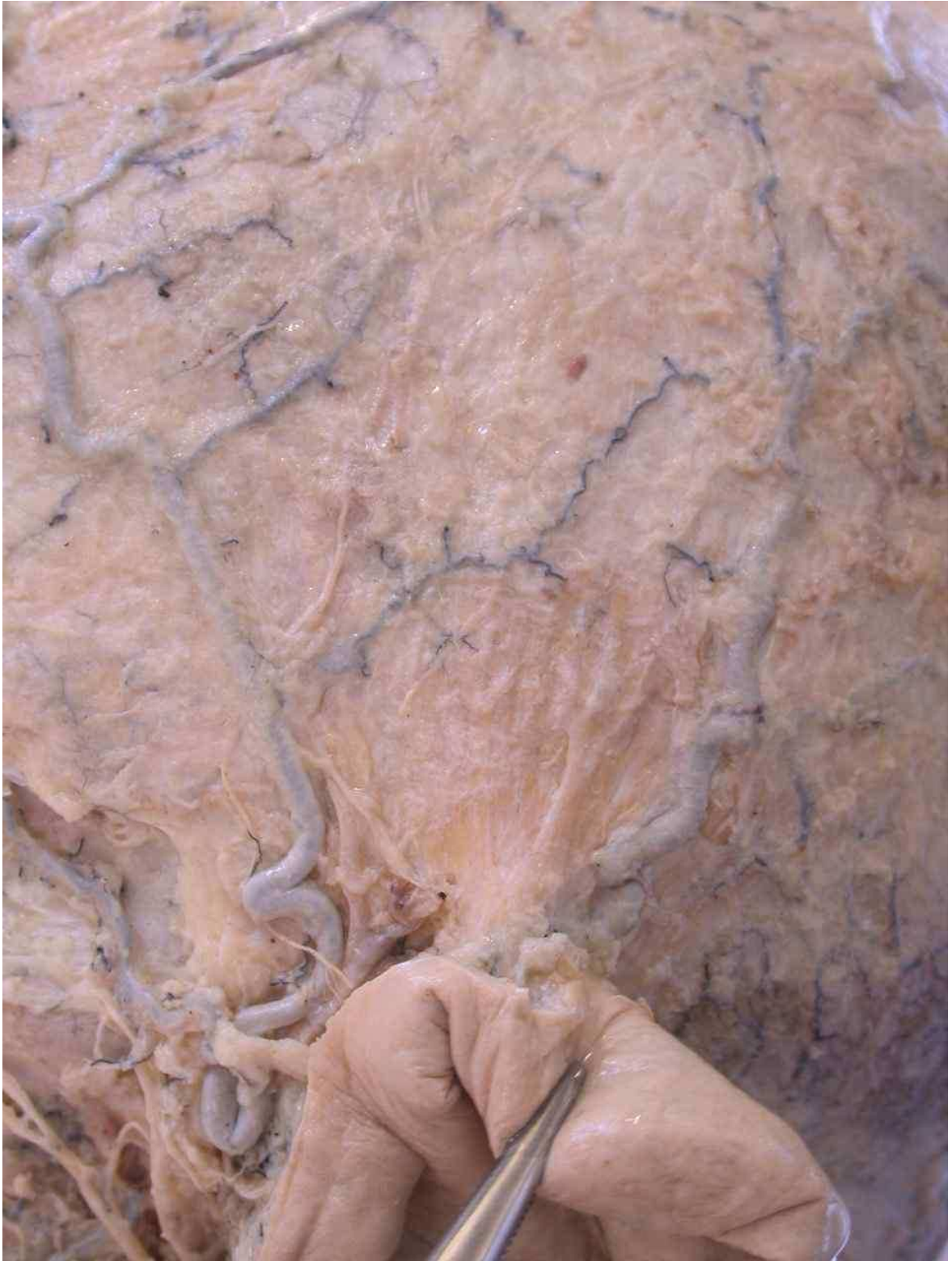


Figure 29 Photograph of left superficial temporal region

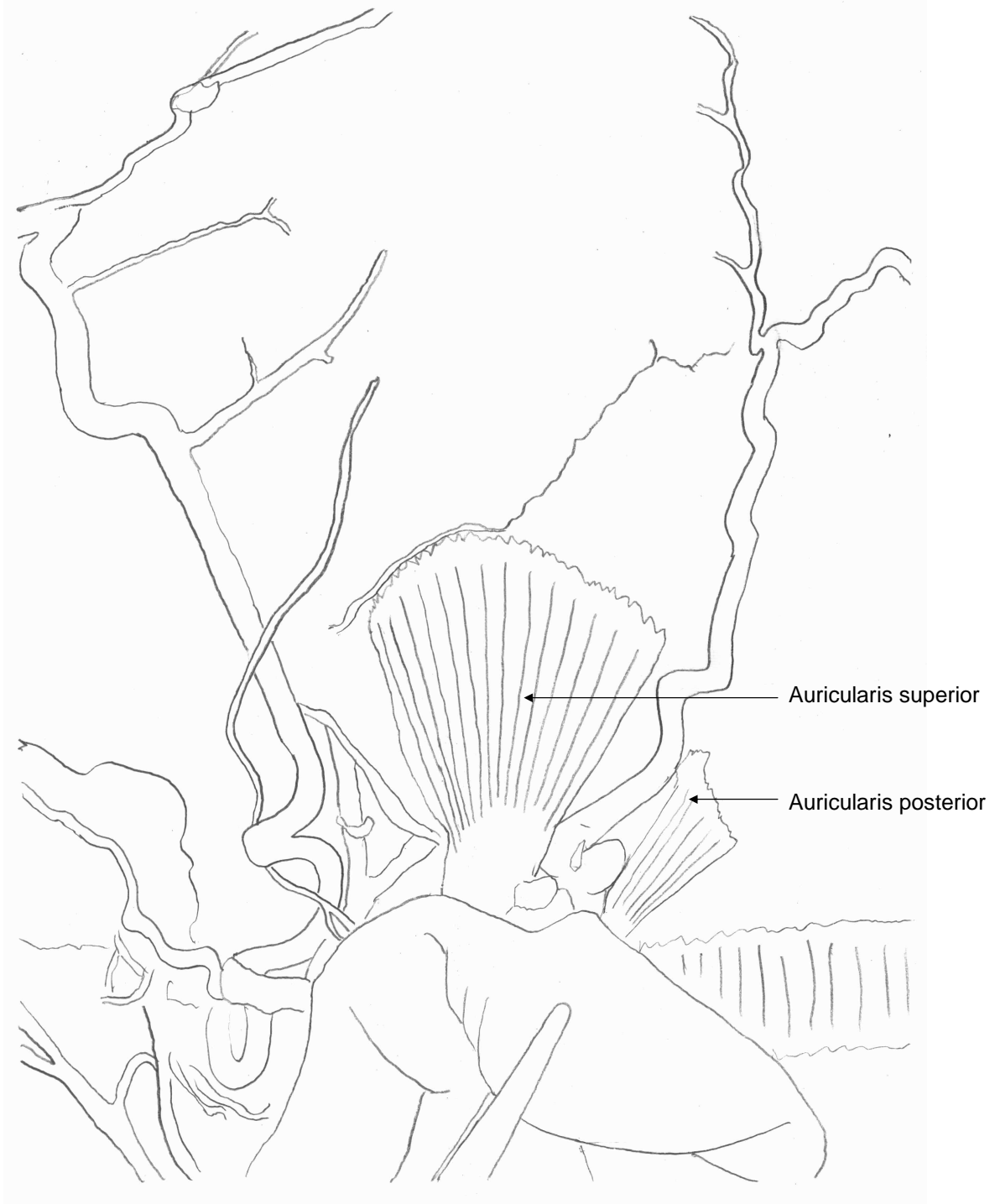


Figure 30 Diagram of superficial left head and neck dissection

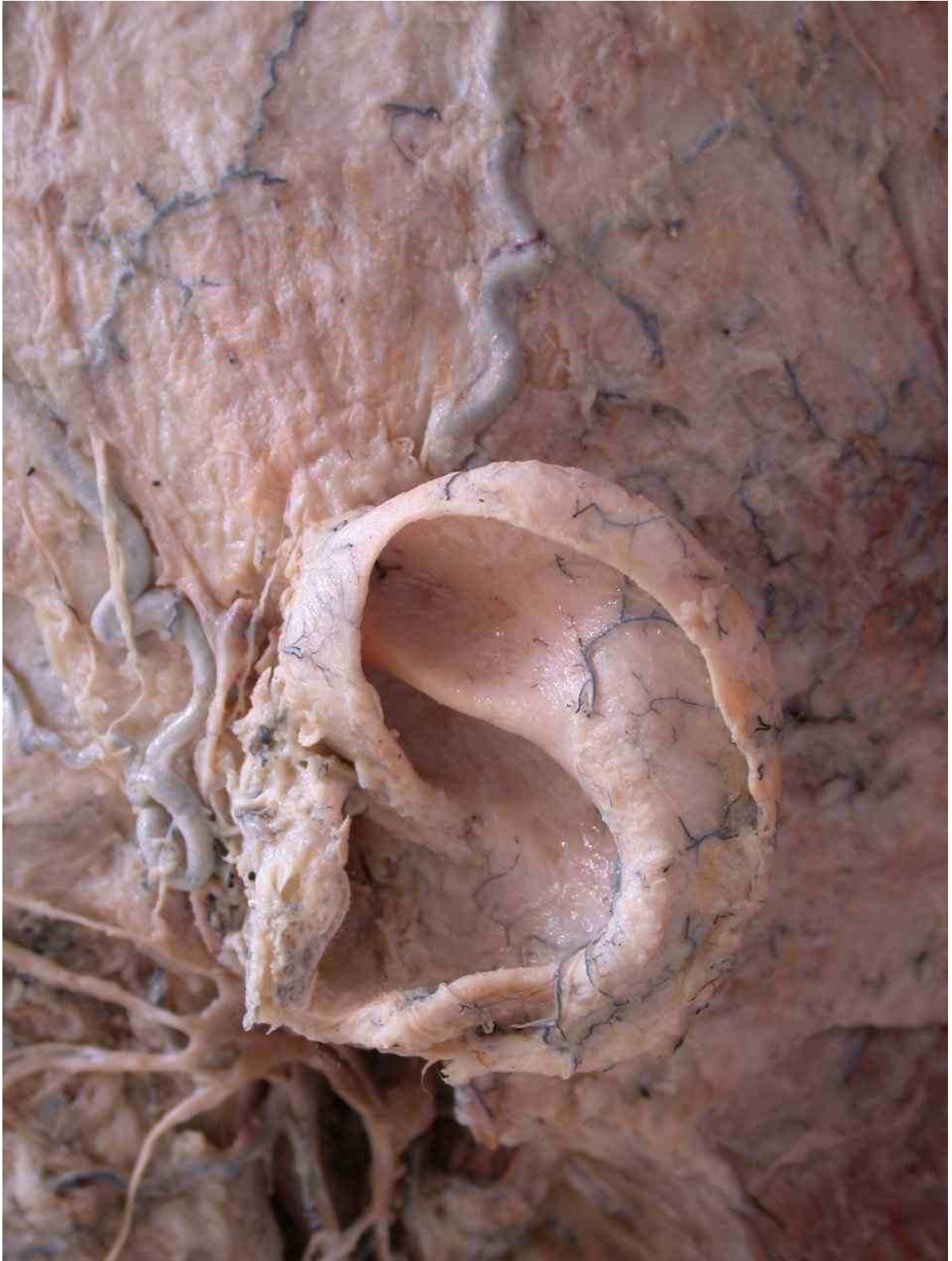


Figure 31 Photograph of left pinna dissection

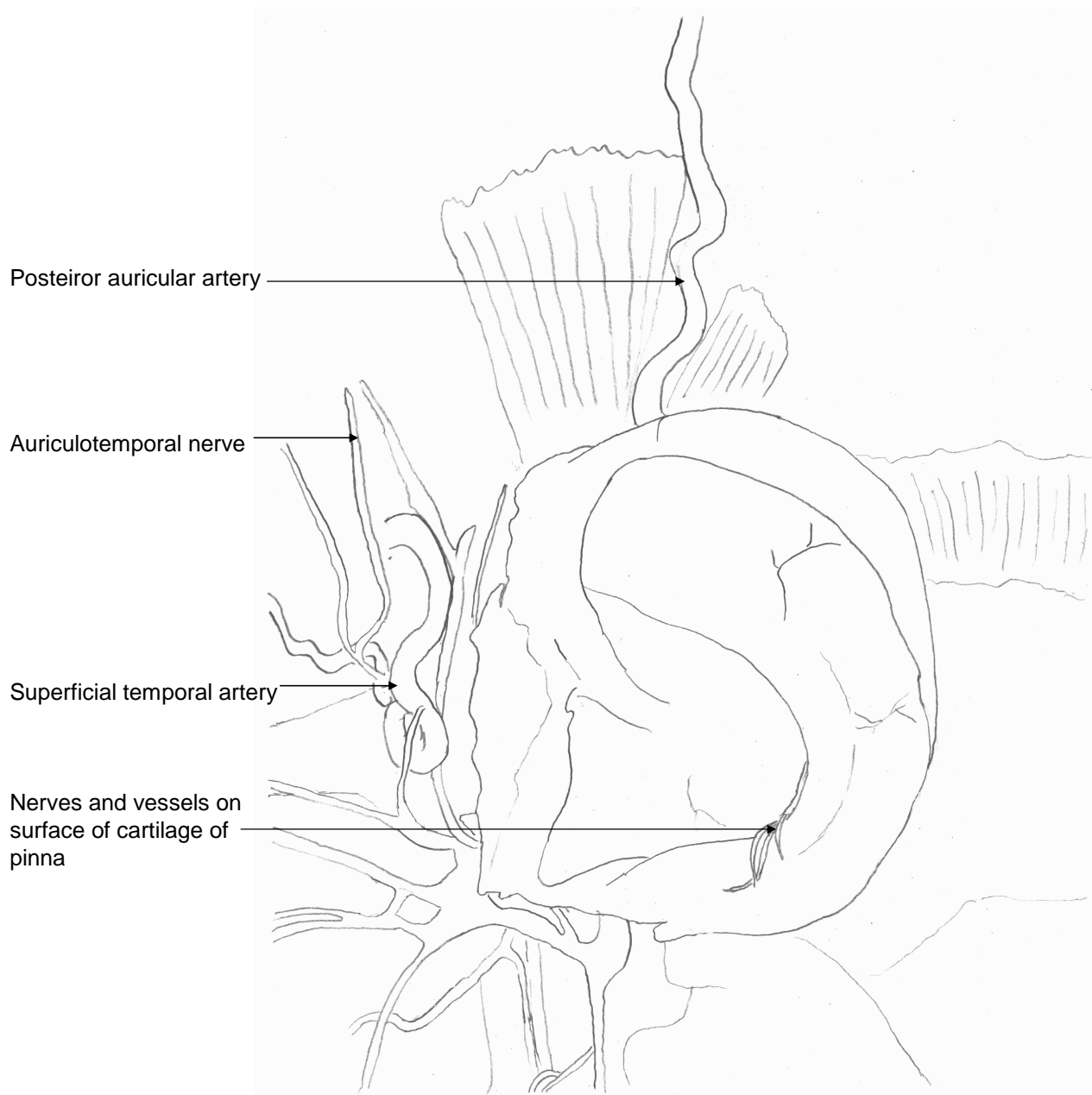


Figure 32 Diagram of left pinna dissection

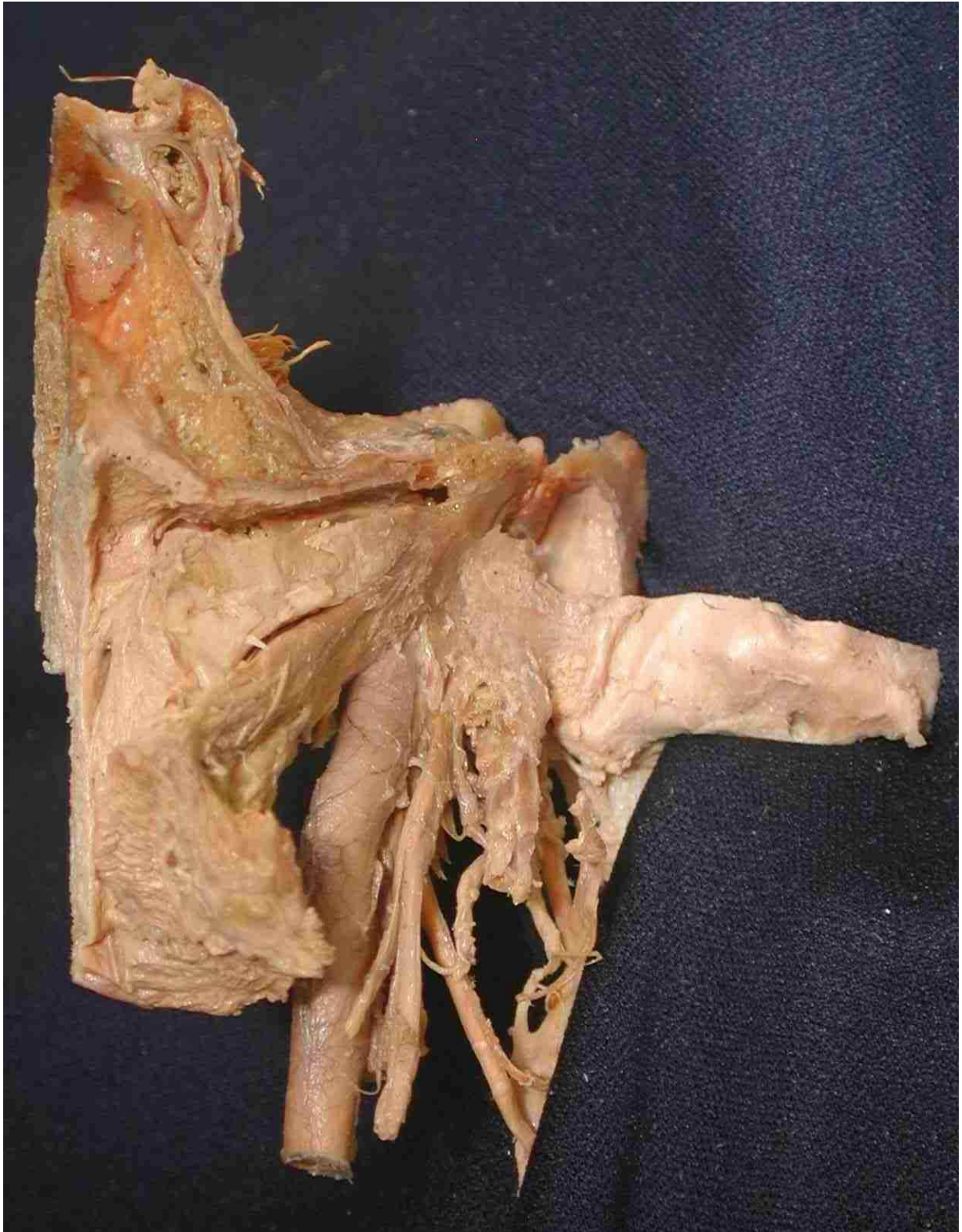


Figure 33 Photograph of anterior view of superior view of left temporal bone with tympanic cavity de-roofed and genicular ganglion exposed

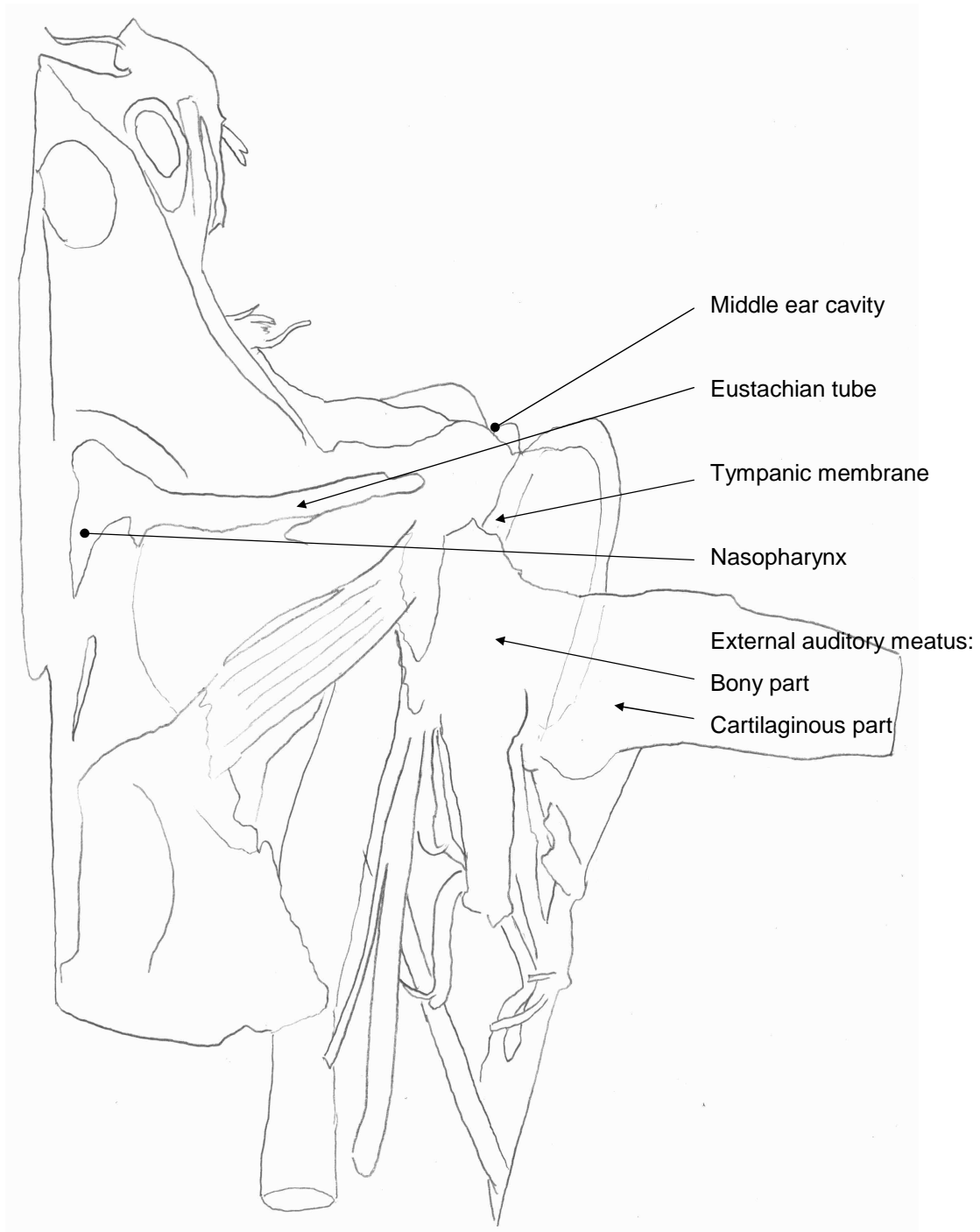


Figure 34 Diagram of anterior view of superior view of left temporal bone with tympanic cavity de-roofed and genicular ganglion exposed

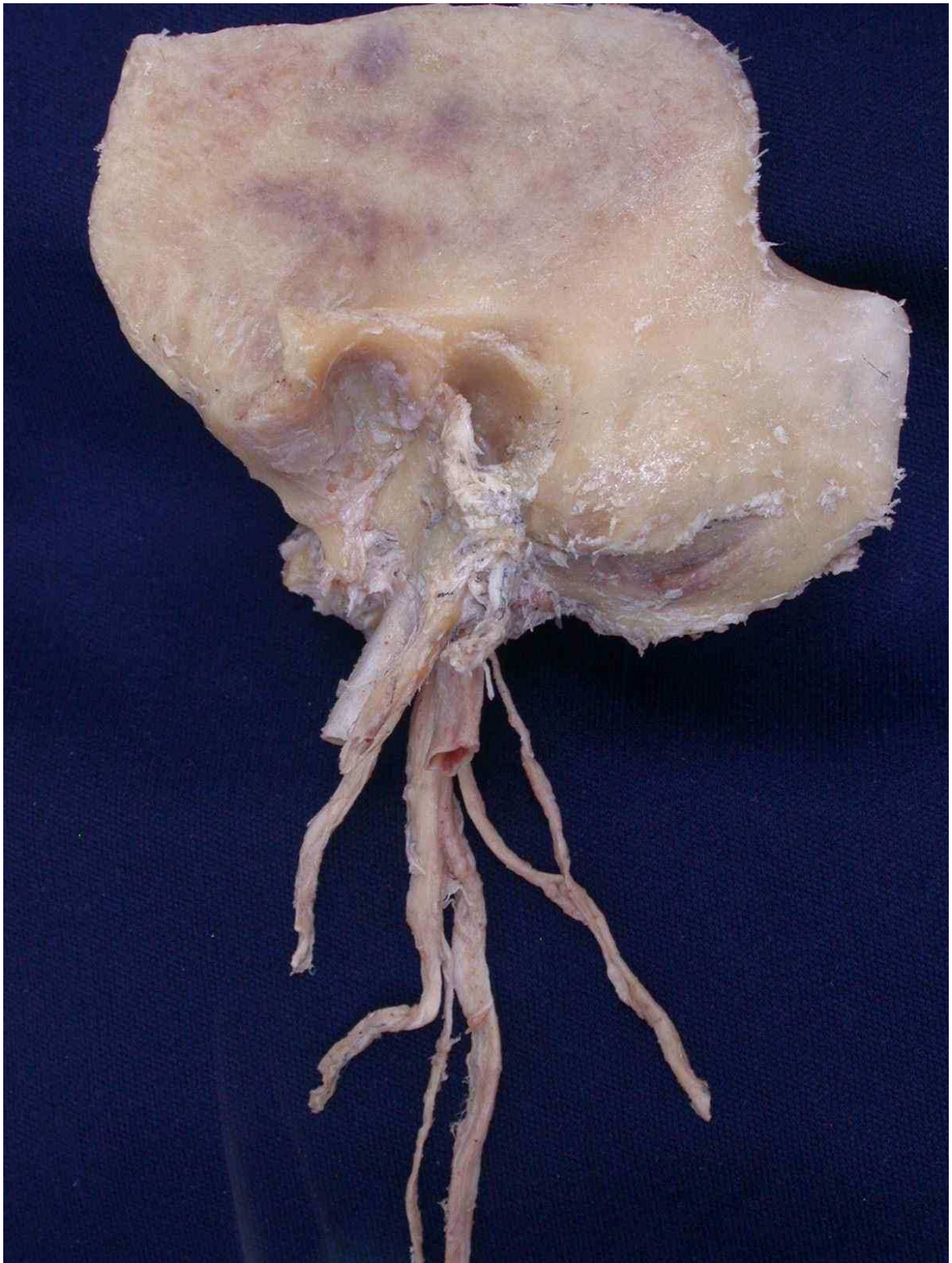


Figure 35 Photograph of lateral view of left temporal bone with glossopharyngeal, hypoglossal, vagus and accessory nerves and the internal jugular vein and internal carotid artery

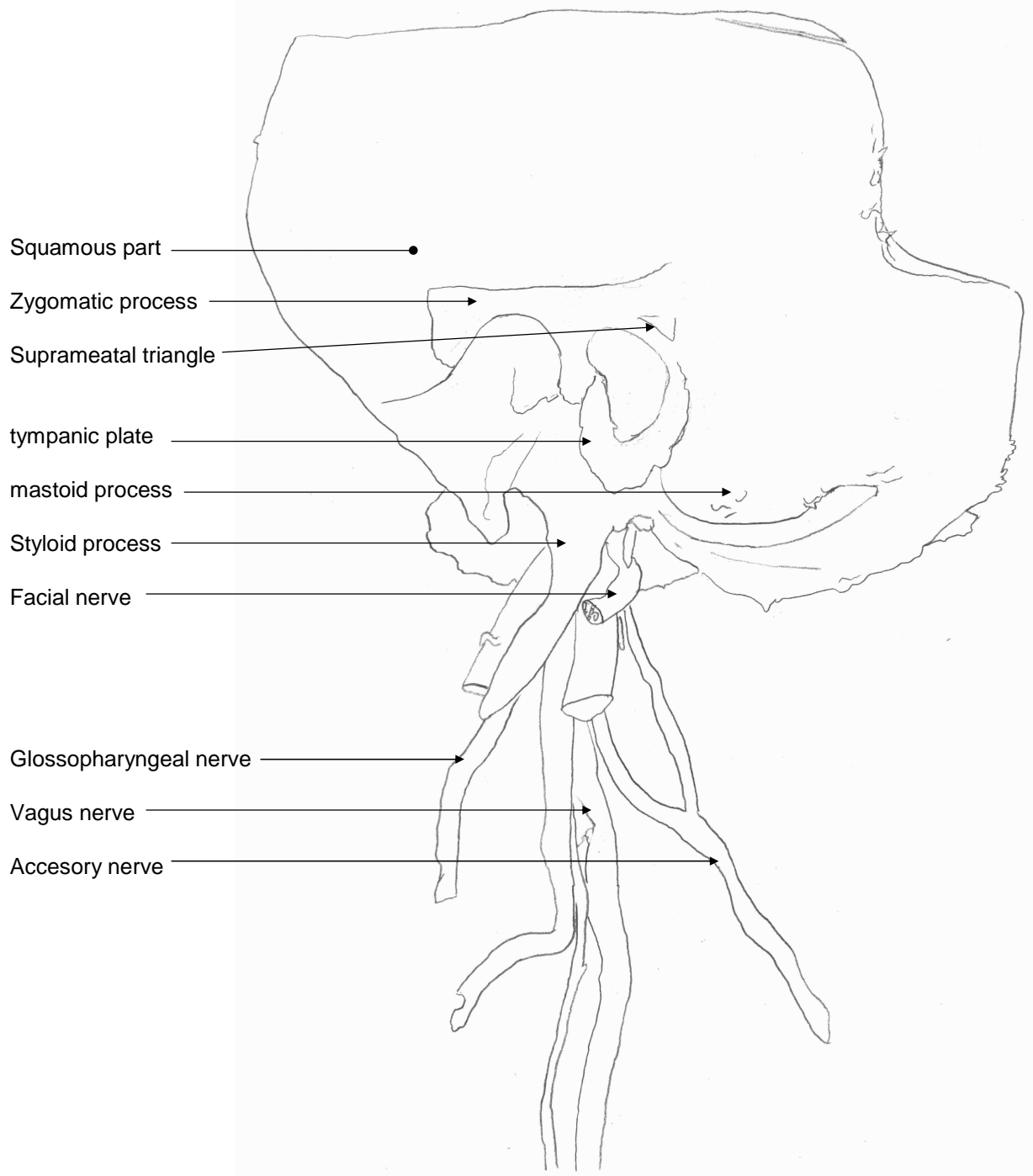


Figure 36 Photograph of lateral view of left temporal bone with glossopharyngeal, hypoglossal, vagus and accessory nerves and the internal jugular vein and internal carotid artery



Figure 37 Photograph of inferior view of the jugular fossa and the parts of the ear

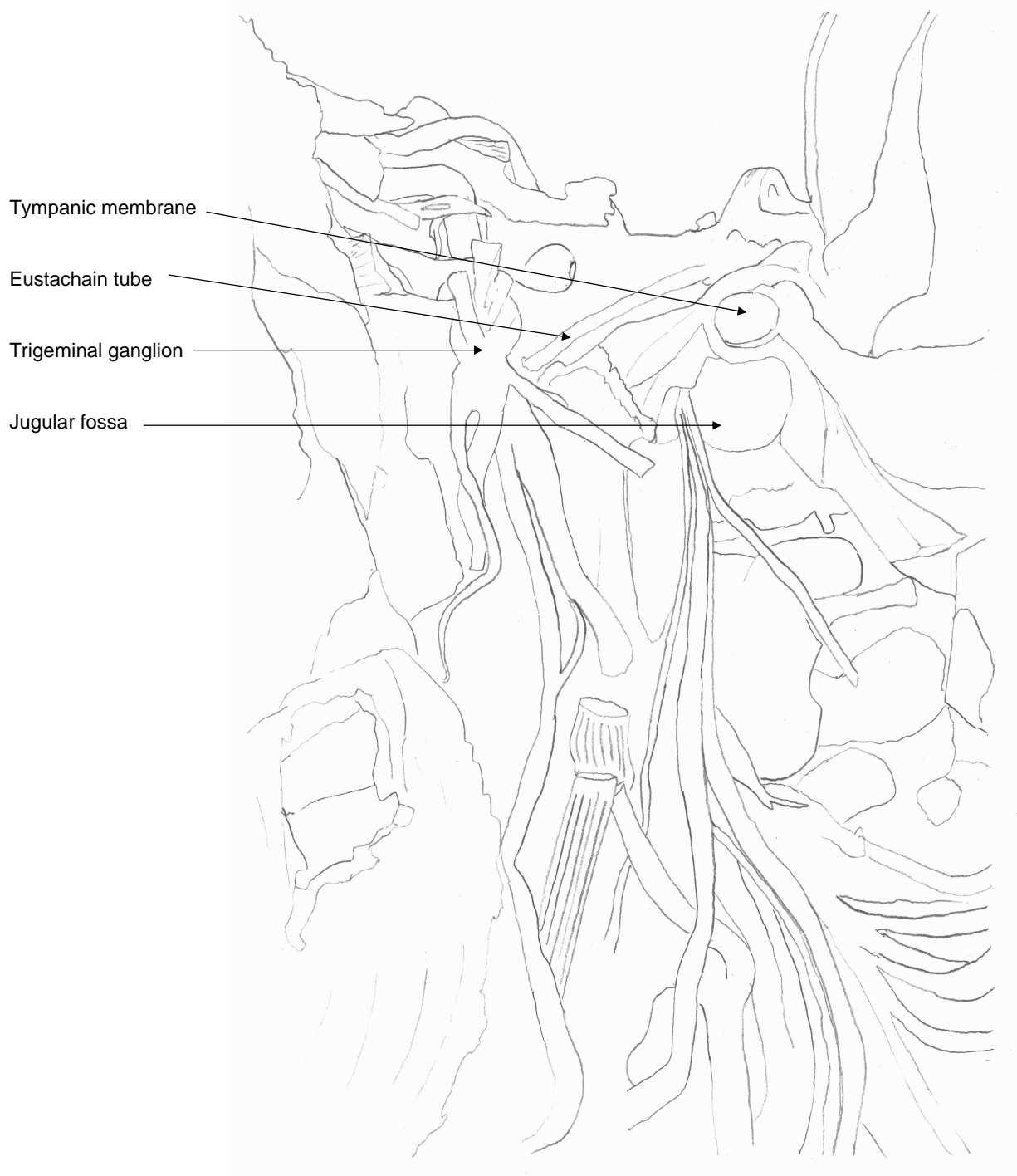


Figure 38 Diagram of inferior view of the jugular fossa and the parts of the ear



Figure 39 Photograph of inferior view of nerves within the jugular fossa

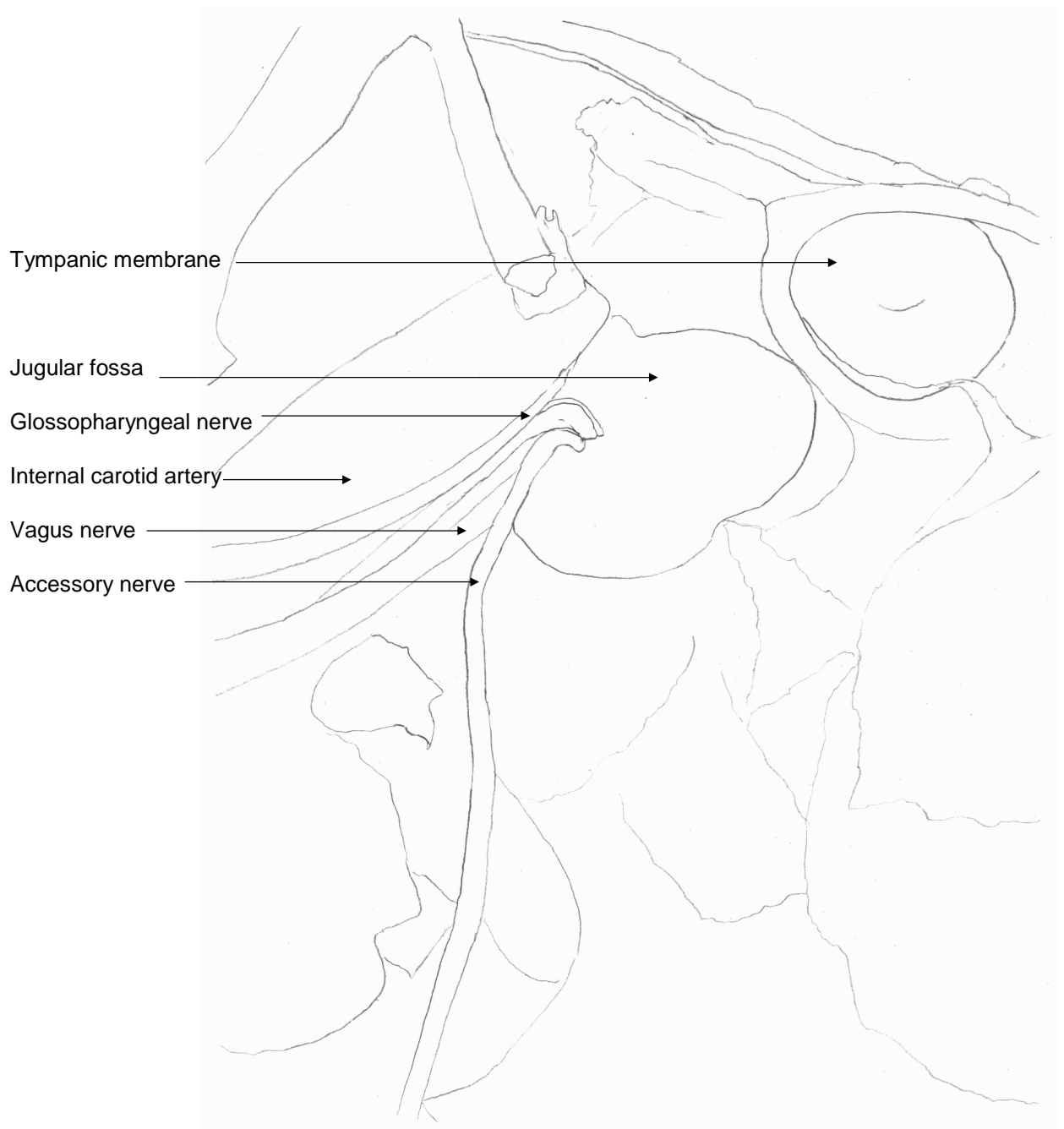


Figure 40 Diagram of inferior view of nerves within the jugular fossa



Figure 41 Photograph of lateral view of tympanic membrane, tympanic cavity and superior semicircular canal

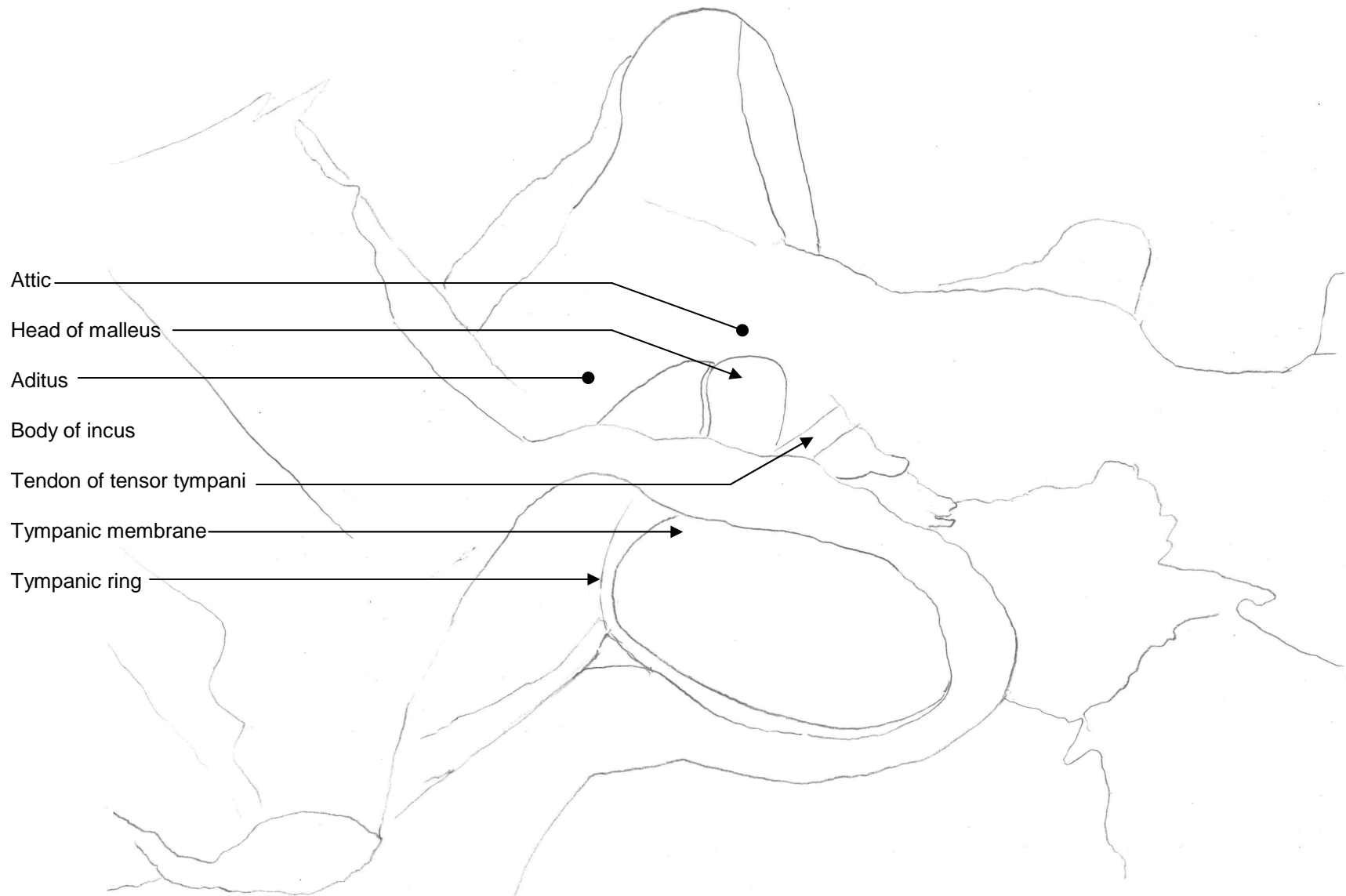


Figure 42 Diagram of lateral view of tympanic membrane, tympanic cavity and superior semicircular canal



Figure 43 Photograph of medial view of the course of the internal carotid artery

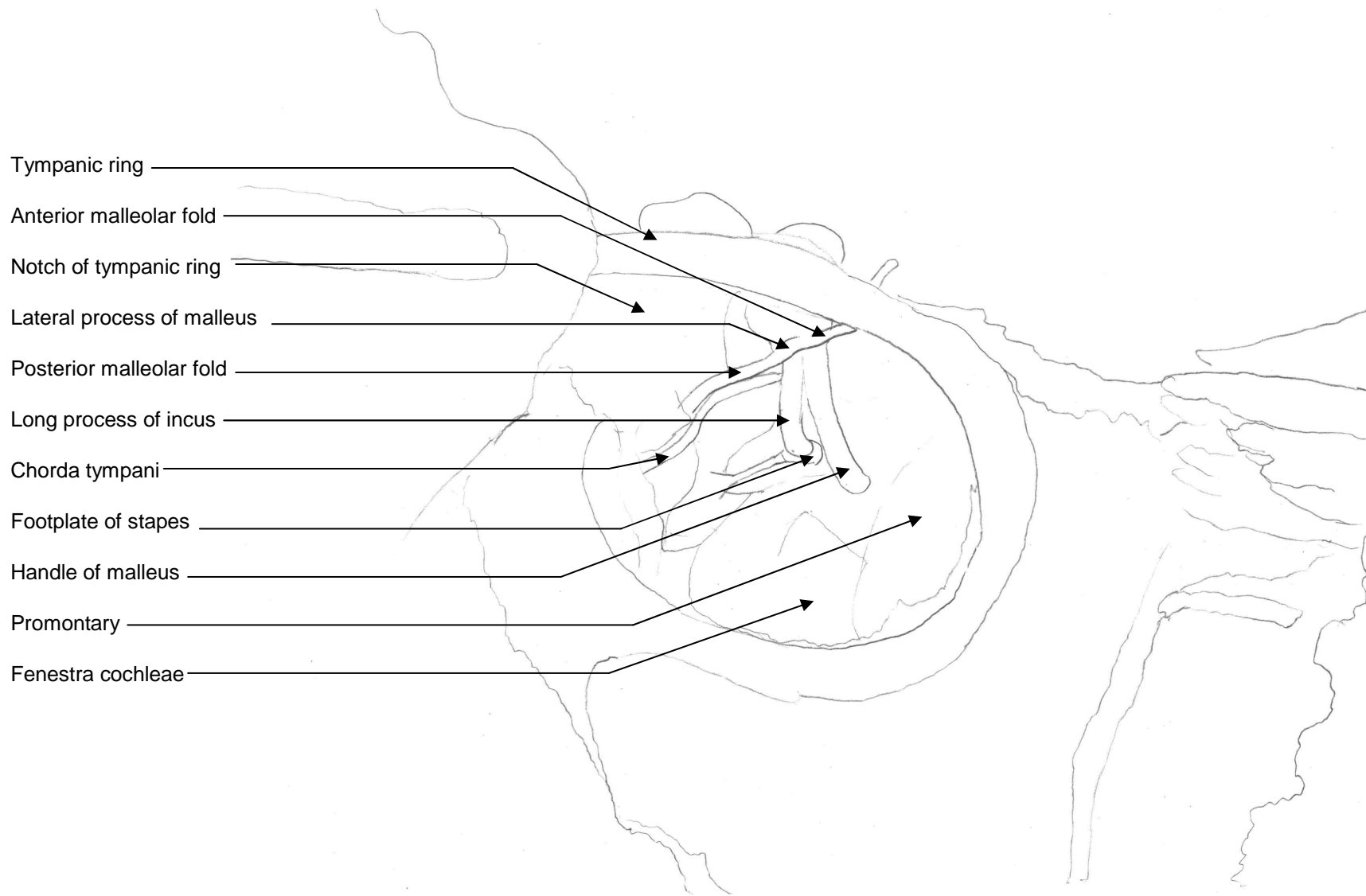


Figure 44 Diagram of medial view of the course of the internal carotid artery



Figure 45 Photograph of cochlea after removal of the bony wall of the promontory

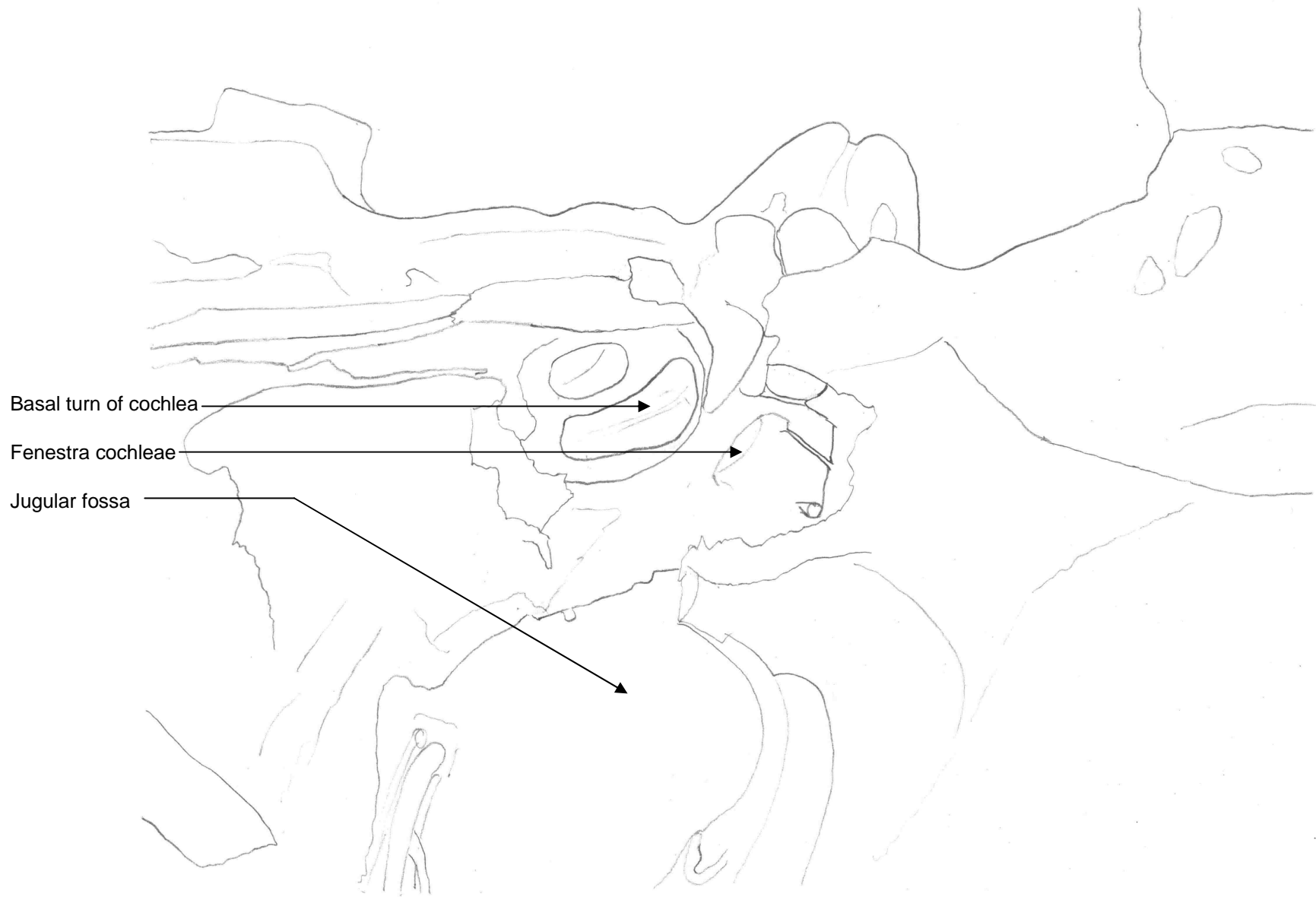


Figure 46 Diagram of cochlea after removal of the bony wall of the promontory



Figure 47 Photograph of superior view of left temporal bone with tympanic cavity de-roofed and genicular ganglion exposed

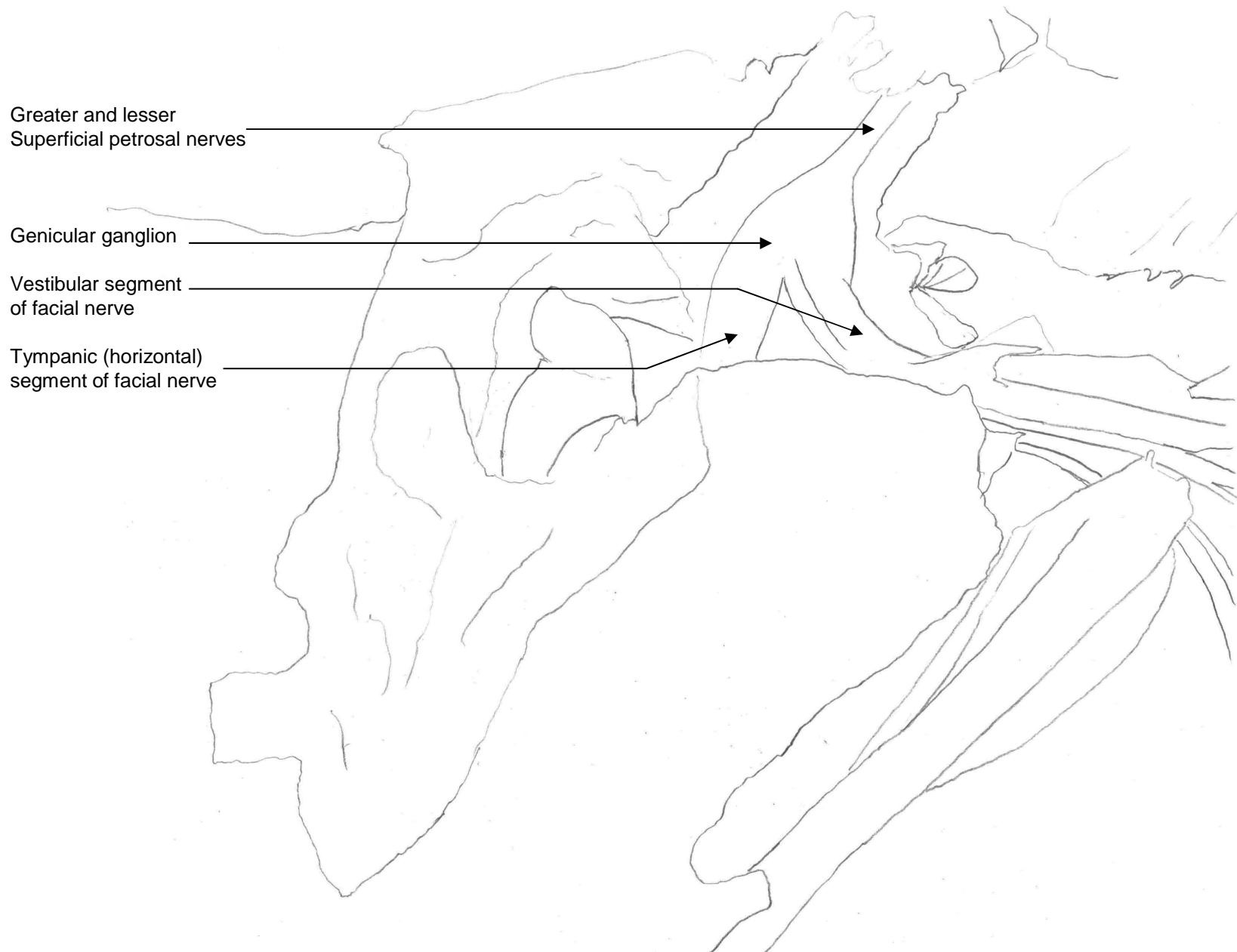


Figure 48 Diagram of superior view of left temporal bone with tympanic cavity de-roofed and genicular ganglion exposed



Figure 49 Photograph of vertical segment of facial nerve visualised through mastoid

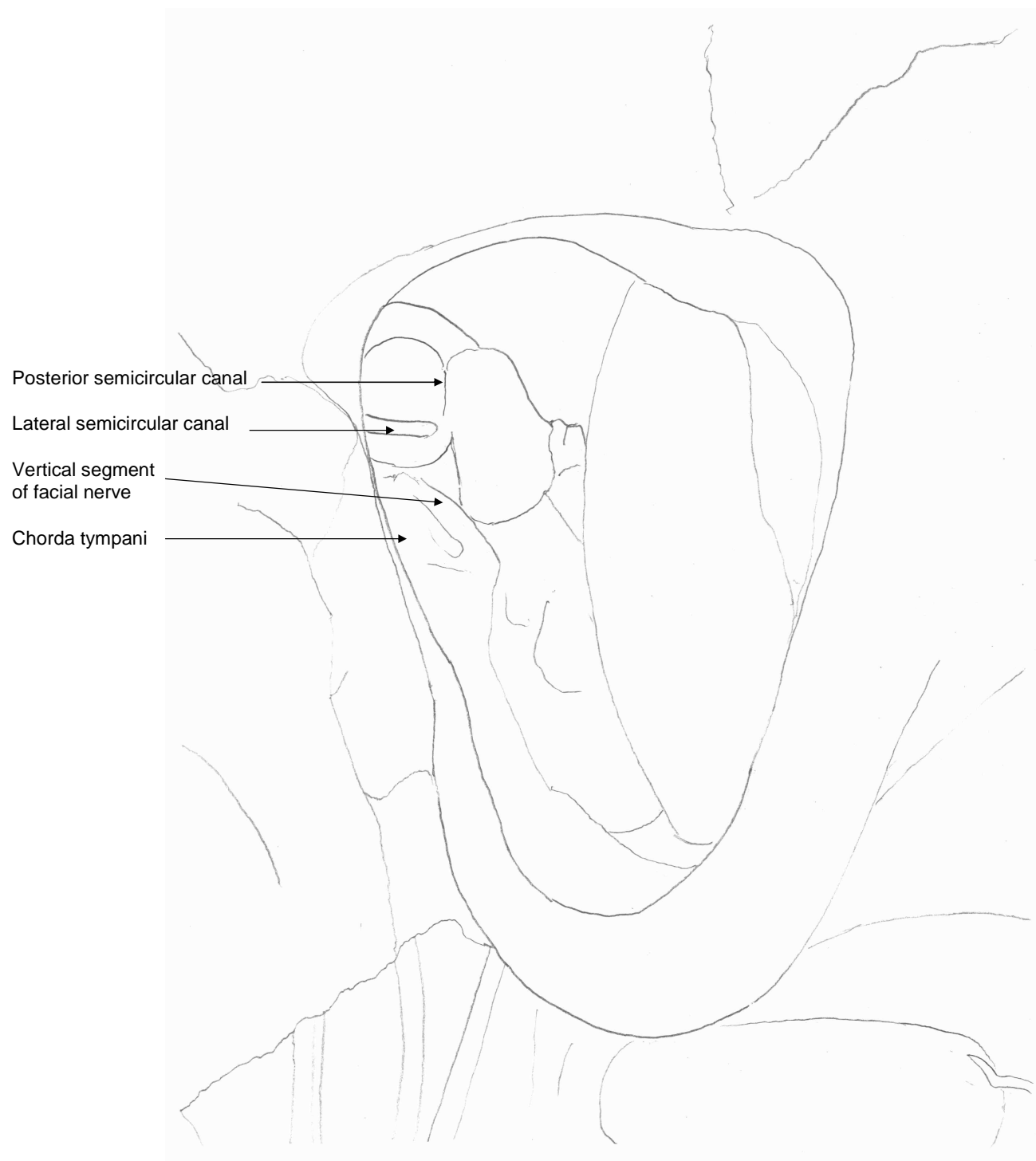


Figure 50 Diagram of vertical segment of the facial nerve visualised through mastoid cavity



Figure 51 Photograph of medial view of nasopharynx

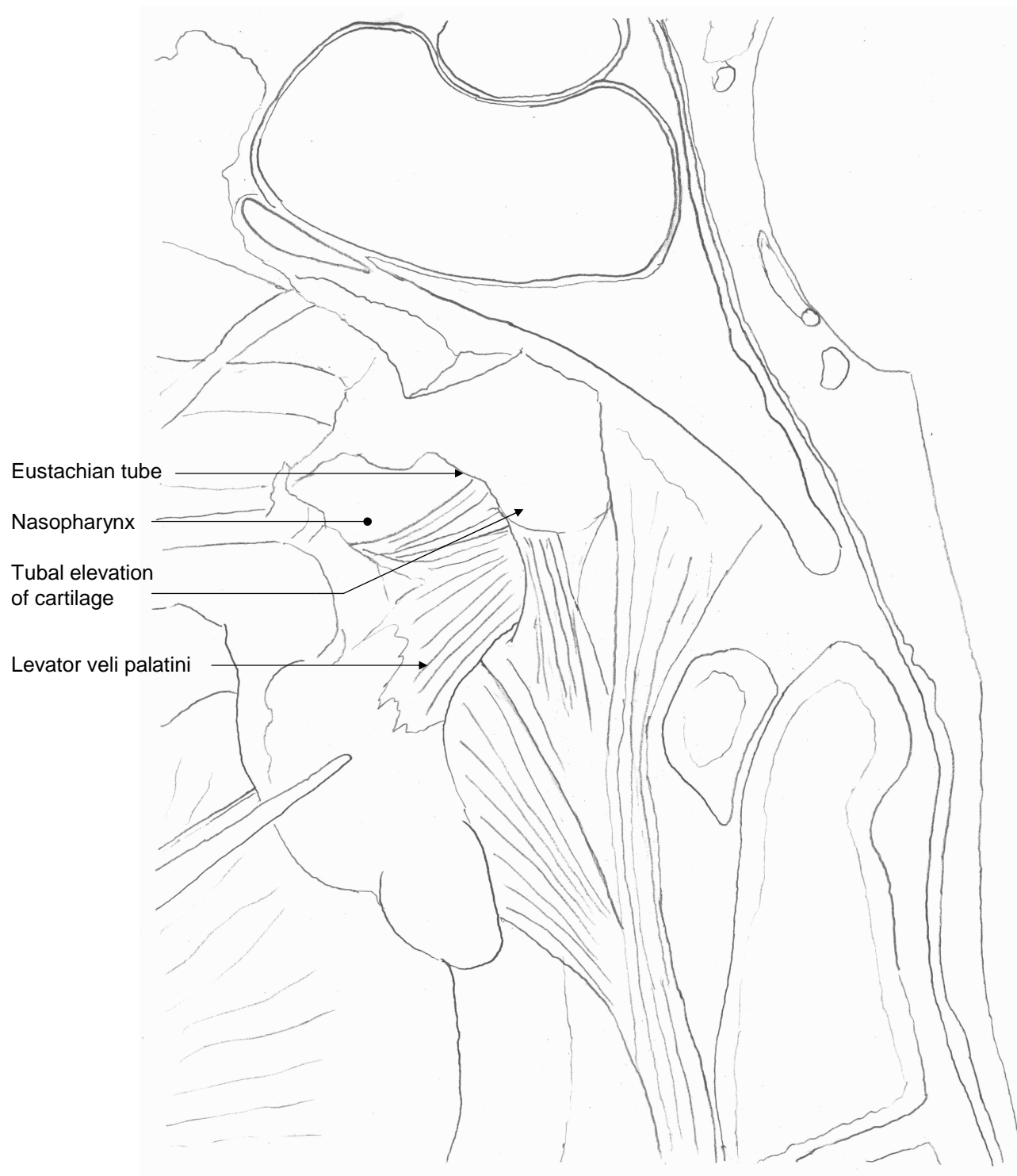


Figure 52 Diagram of medial view of nasopharynx



Figure 53 Photograph of medial view of intraosseous course internal carotid artery



Figure 54 Diagram of medial view of intraosseous course internal carotid artery



Figure 55 Photograph of medial view of the course of the internal carotid artery

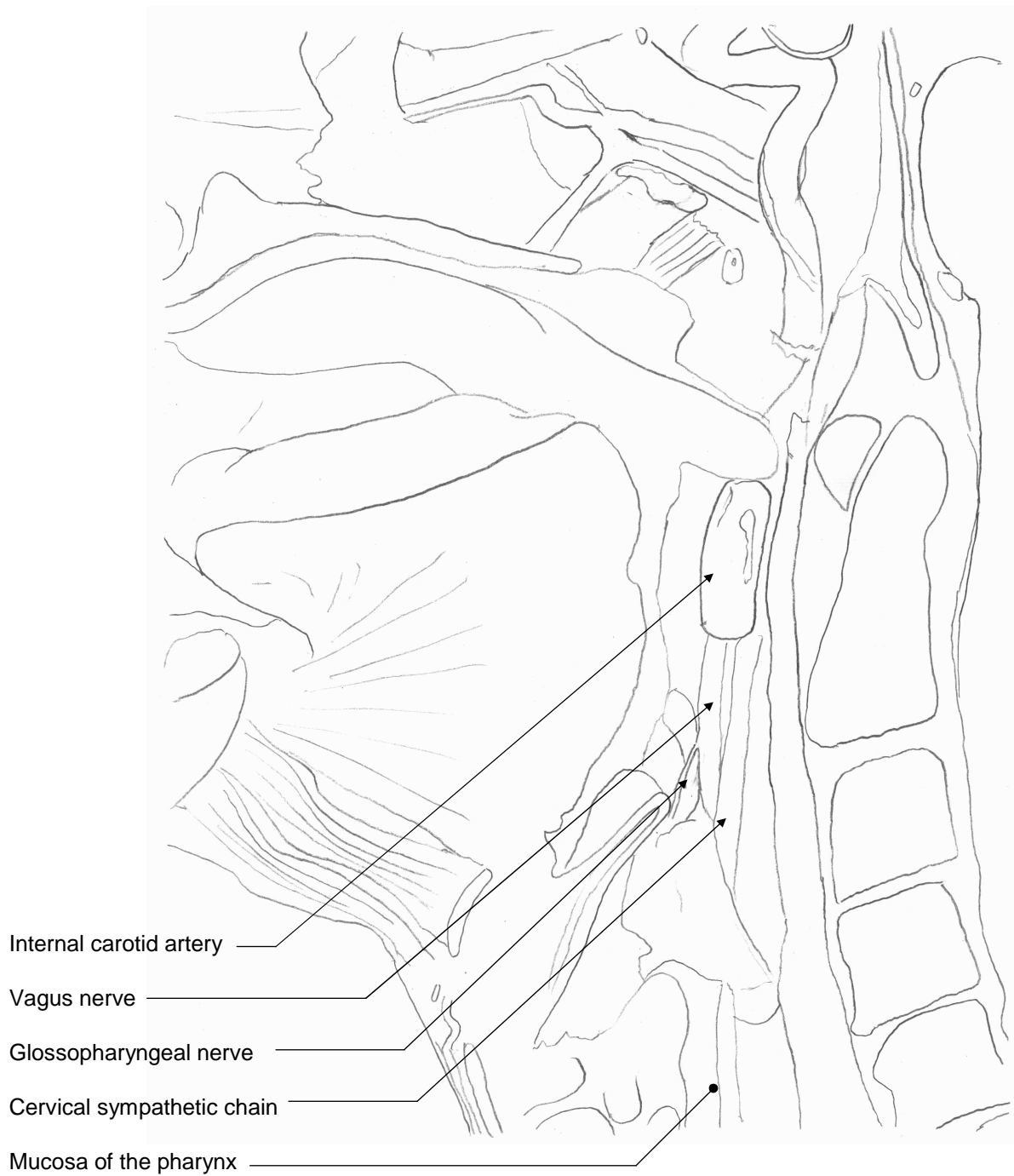


Figure 56 Diagram of medial view of the course of the internal carotid artery



Figure 57 Photograph of right temporal bone showing opened internal acoustic meatus, cochlea and semicircular canals

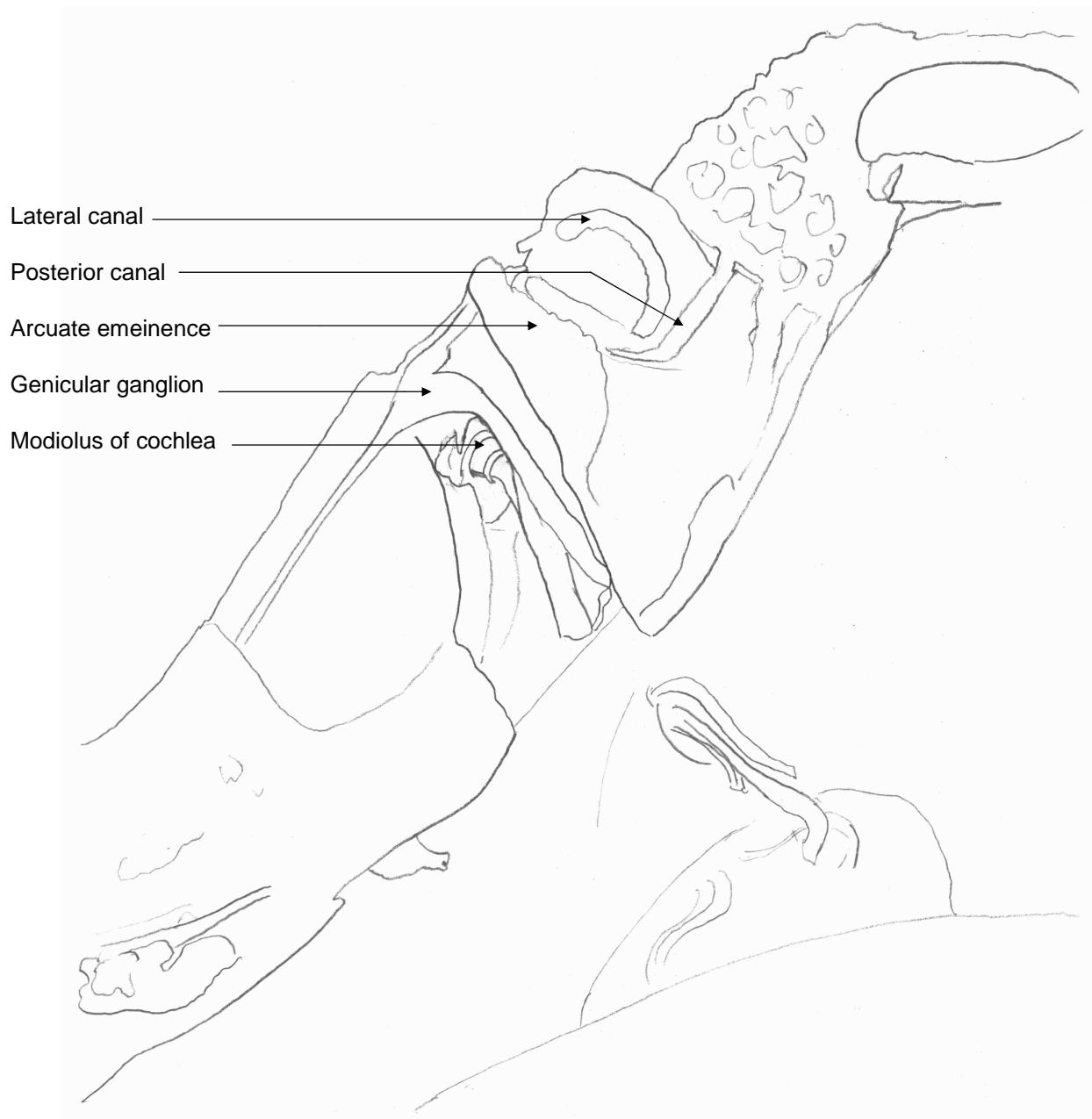


Figure 58 Diagram of right temporal bone showing opened internal acoustic meatus, cochlea and semicircular canals



Figure 59 Photograph of left superior, lateral and posterior semicircular canals opened

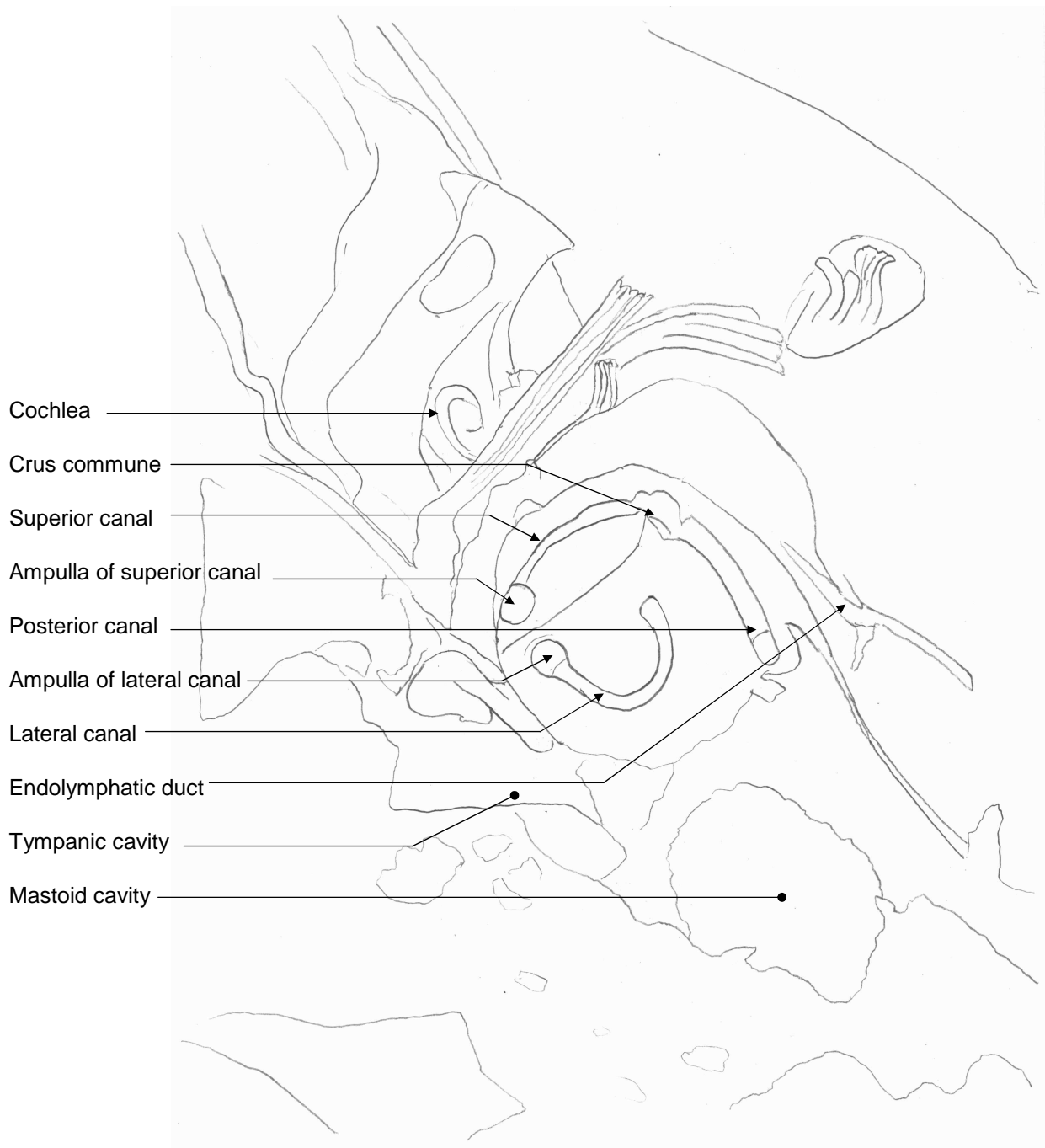


Figure 60 Diagram of left superior, lateral and posterior semicircular canals opened



Figure 61 Photograph of membranous labyrinth within the bony labyrinth

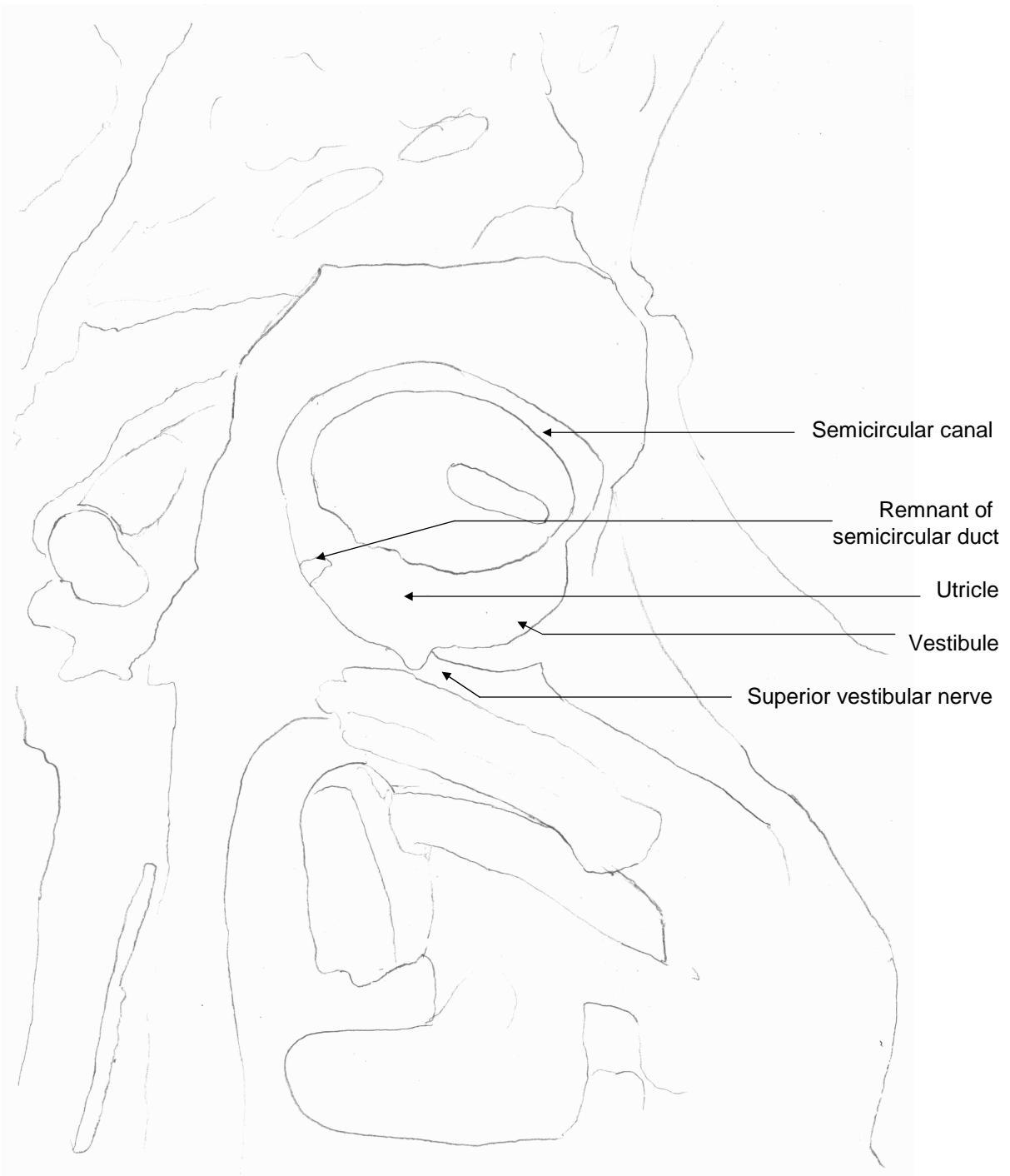


Figure 62 Photograph of membranous labyrinth within the bony labyrinth

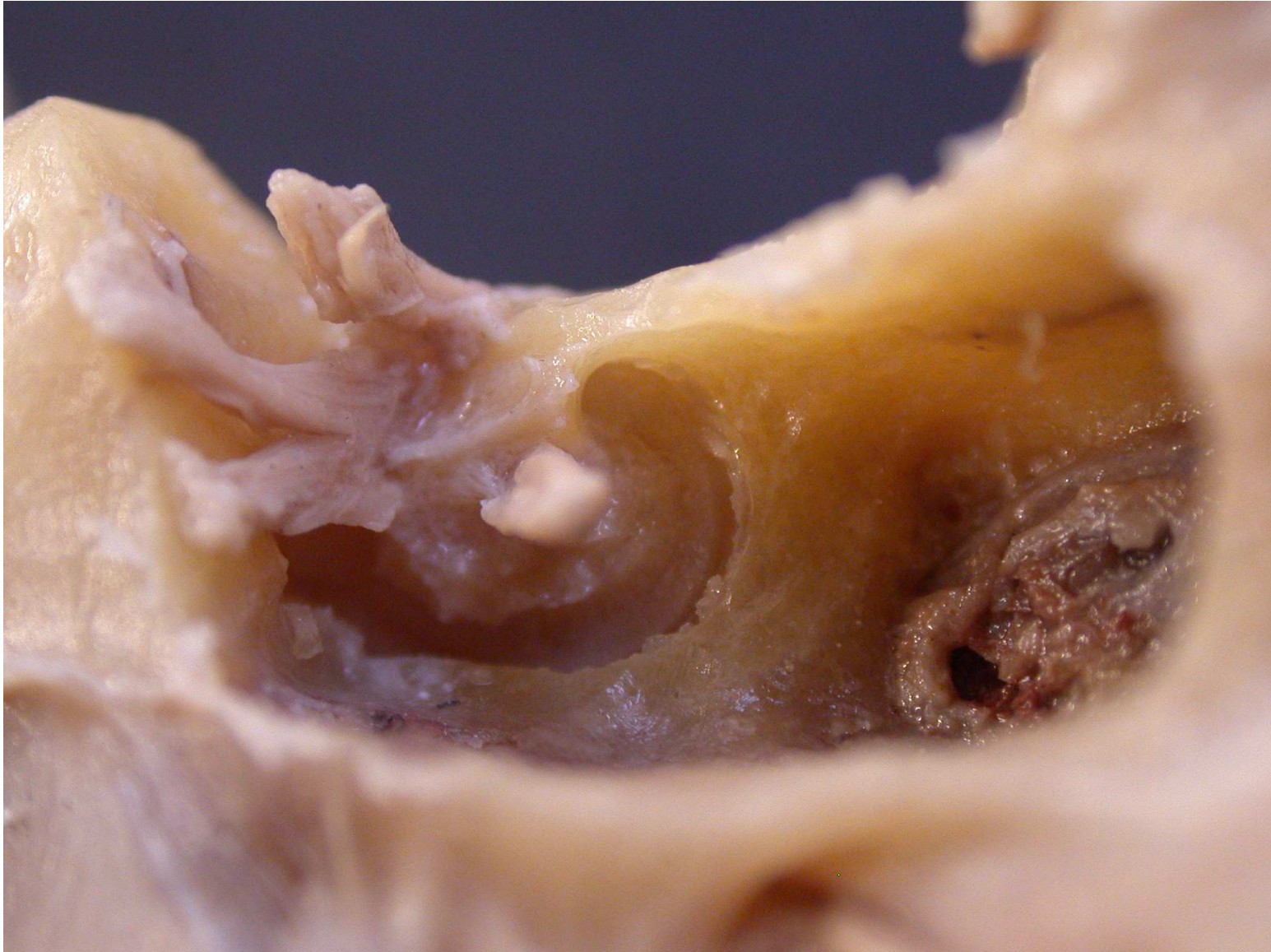


Figure 63 Photograph cochlea and cochlear nerve

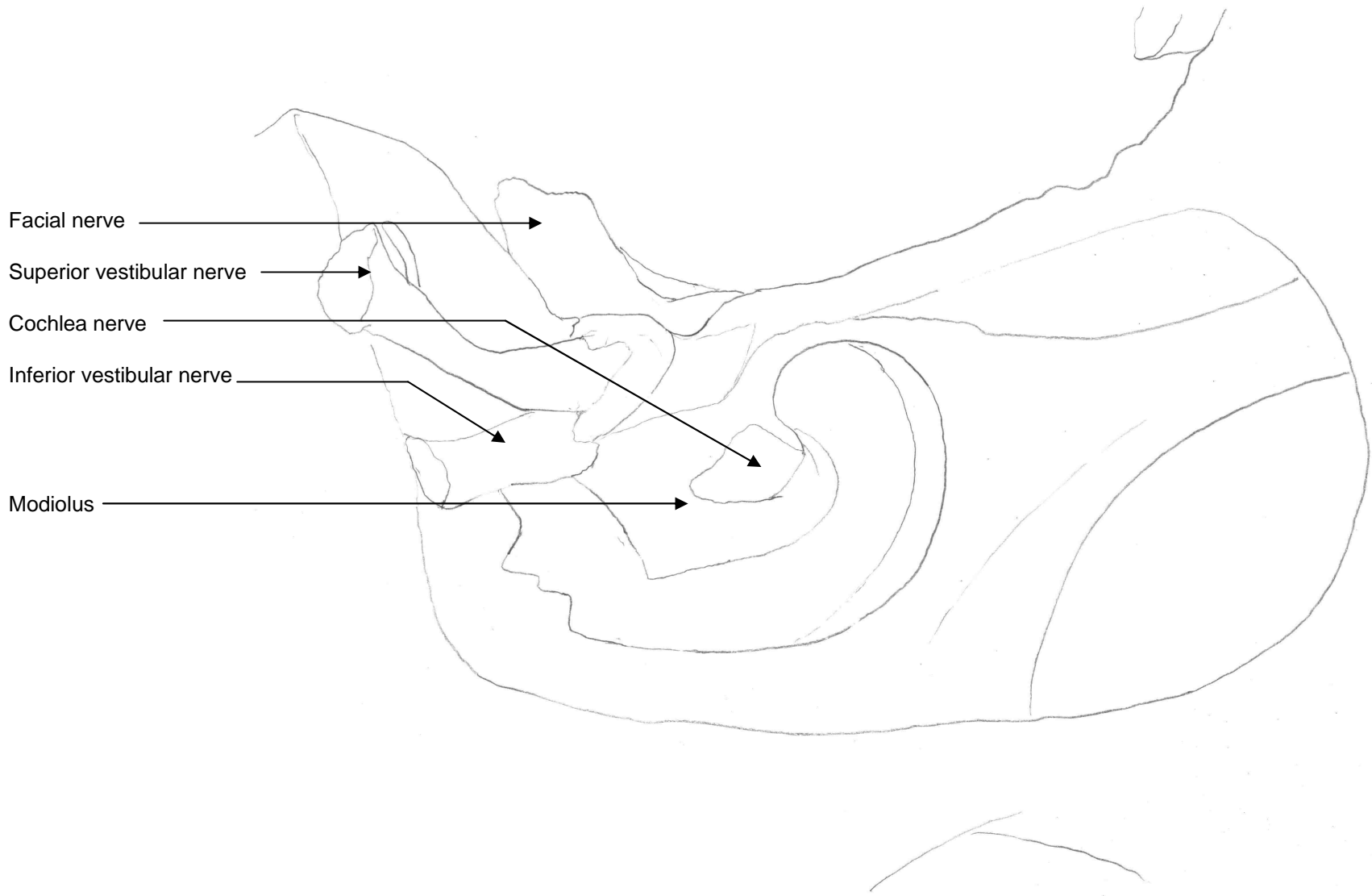


Figure 64 Diagram of cochlea and cochlear nerve

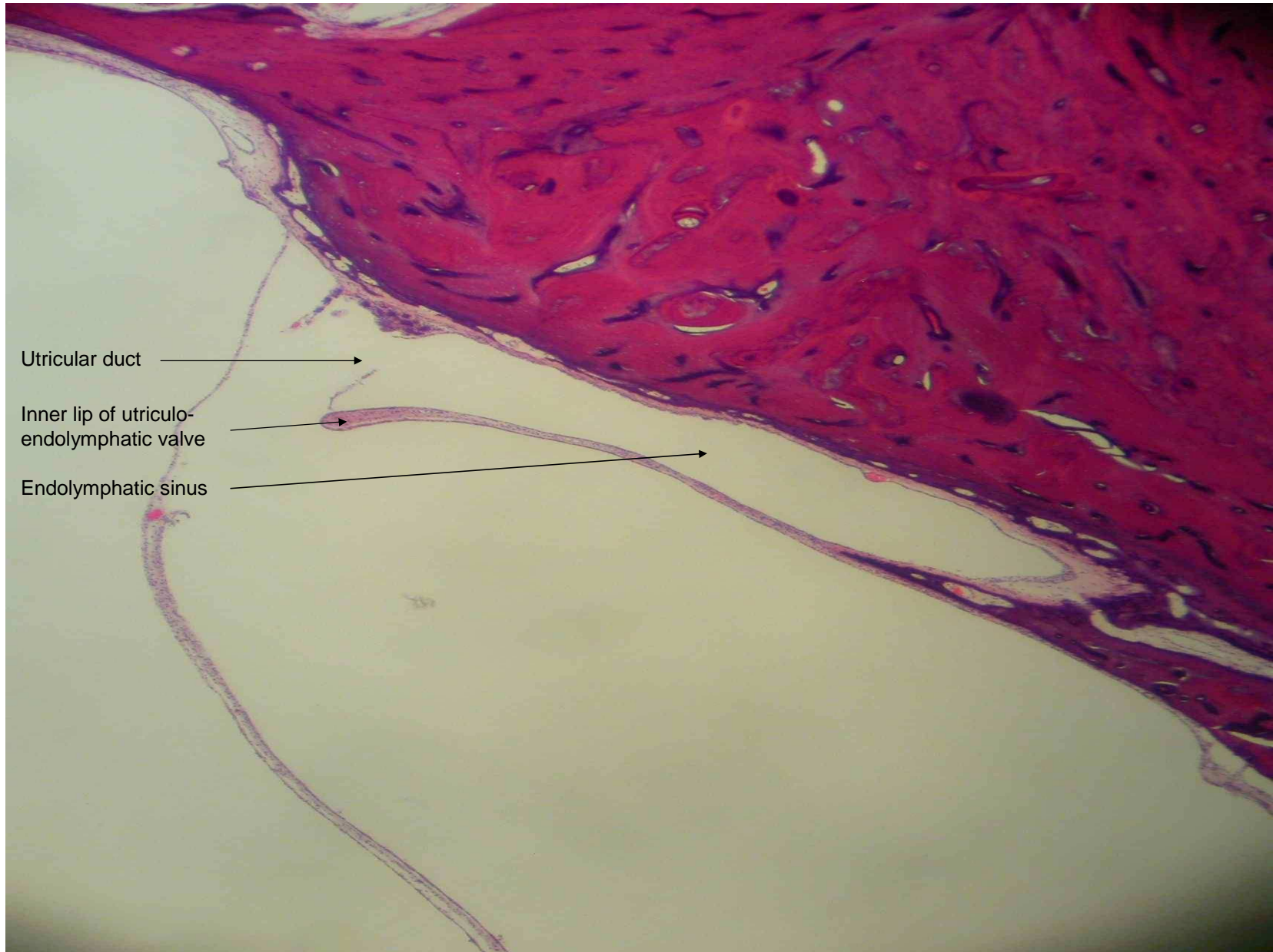


Figure 65 Photograph of histological specimen of saccule, utricle and endolymphatic duct stained with haemotoxylin and eosin



Figure 66 Photograph of posterior aspect of right temporal bone with dura mater partly removed

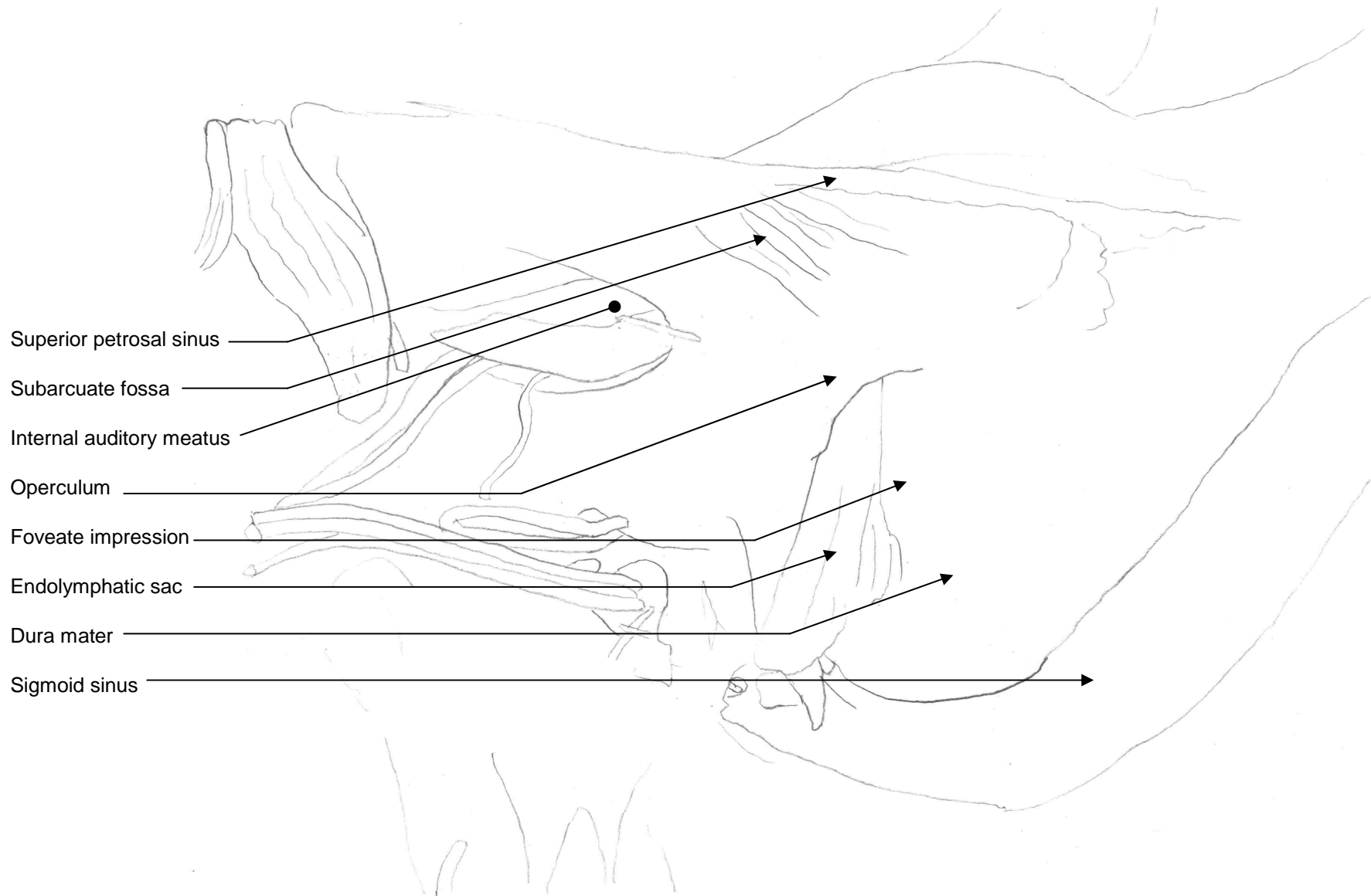


Figure 67 Diagram of posterior aspect of right temporal bone with dura mater partly removed

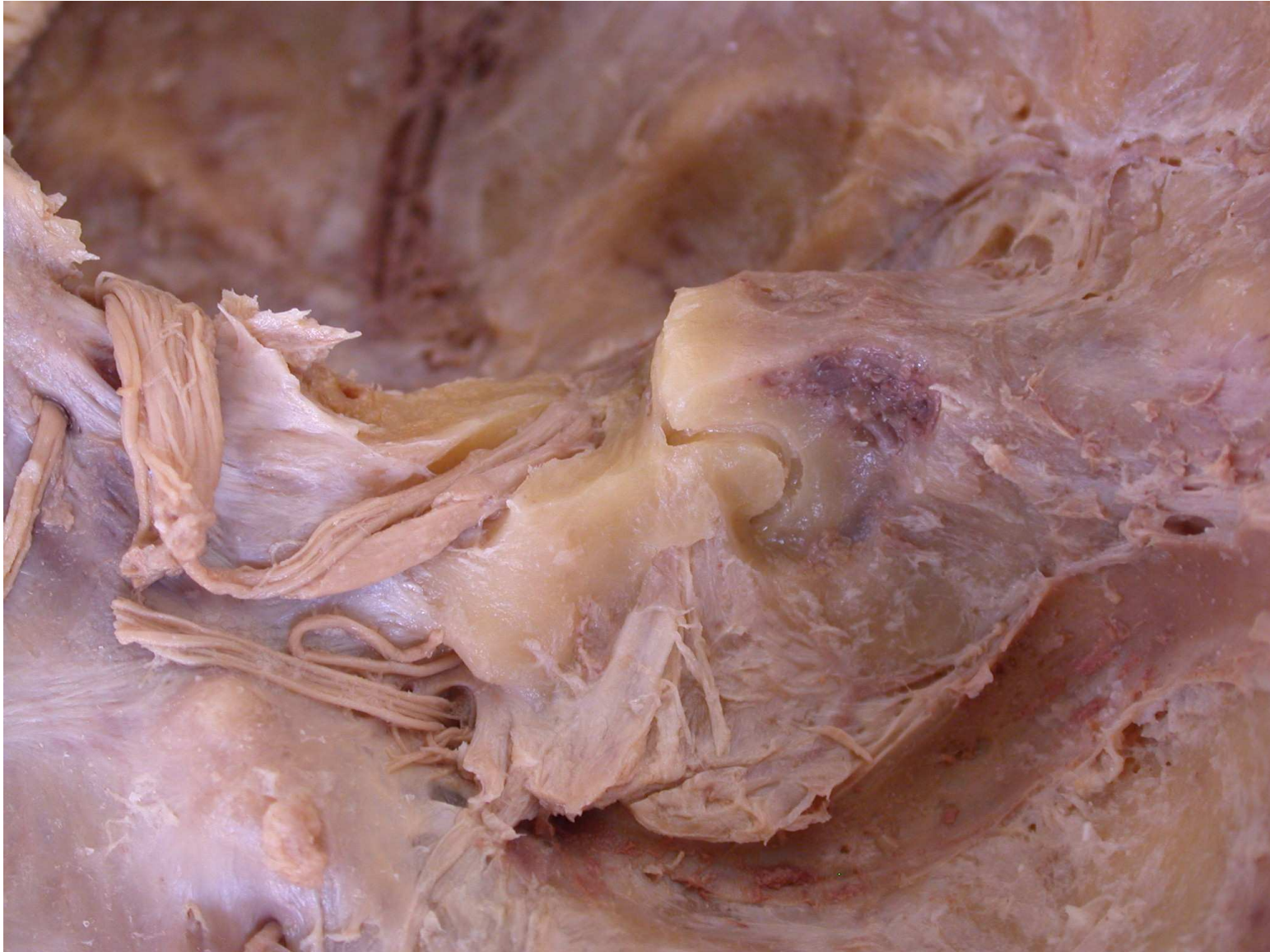


Figure 68 Photograph of posterior aspect of right temporal bone showing intra and extra osseous parts of the endolymphatic sac

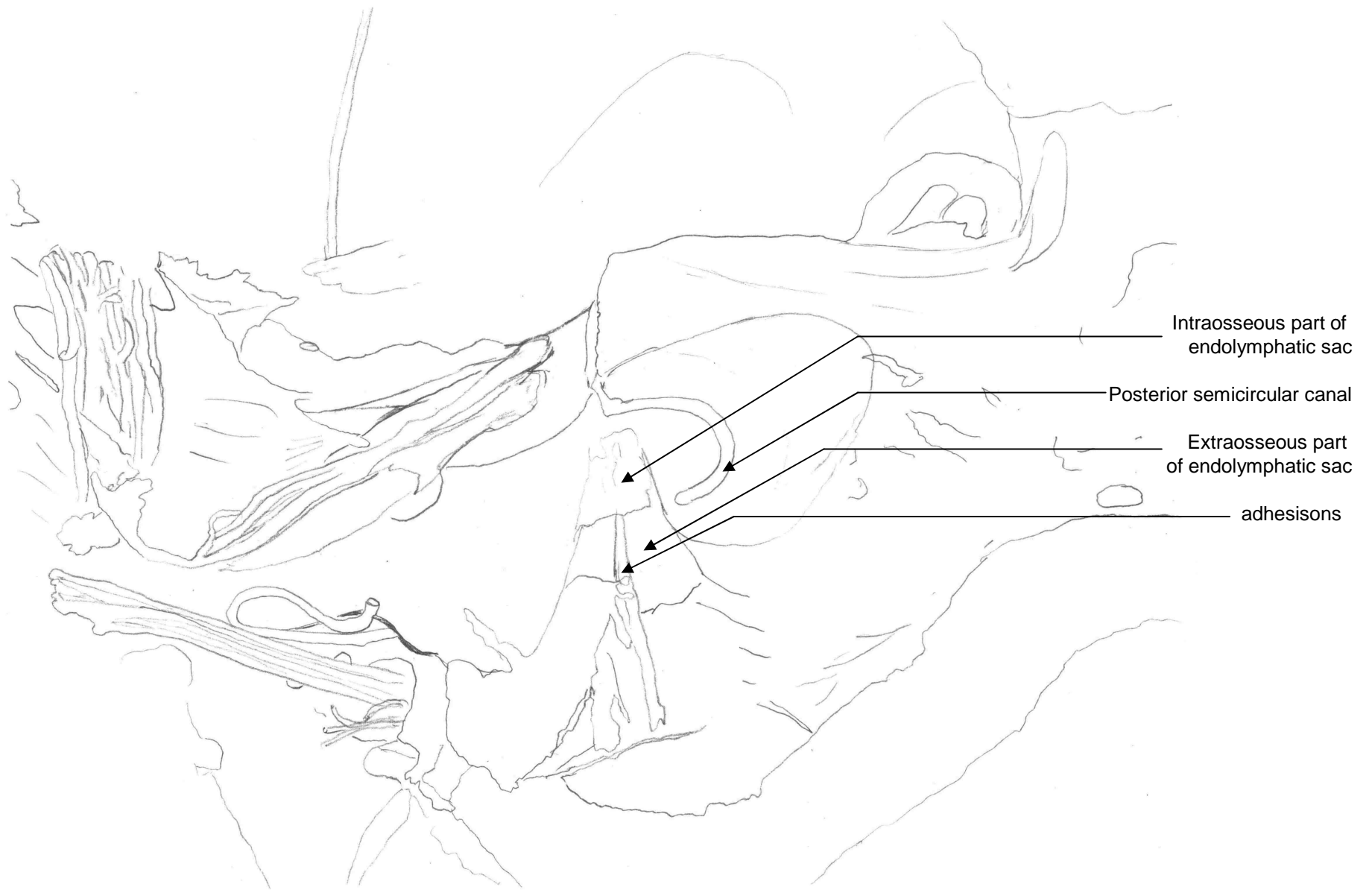


Figure 69 Diagram of posterior aspect of right temporal bone showing intra and extra osseous parts of the endolymphatic sac



Figure 70 Photograph of the intraosseous part of the endolymphatic sac

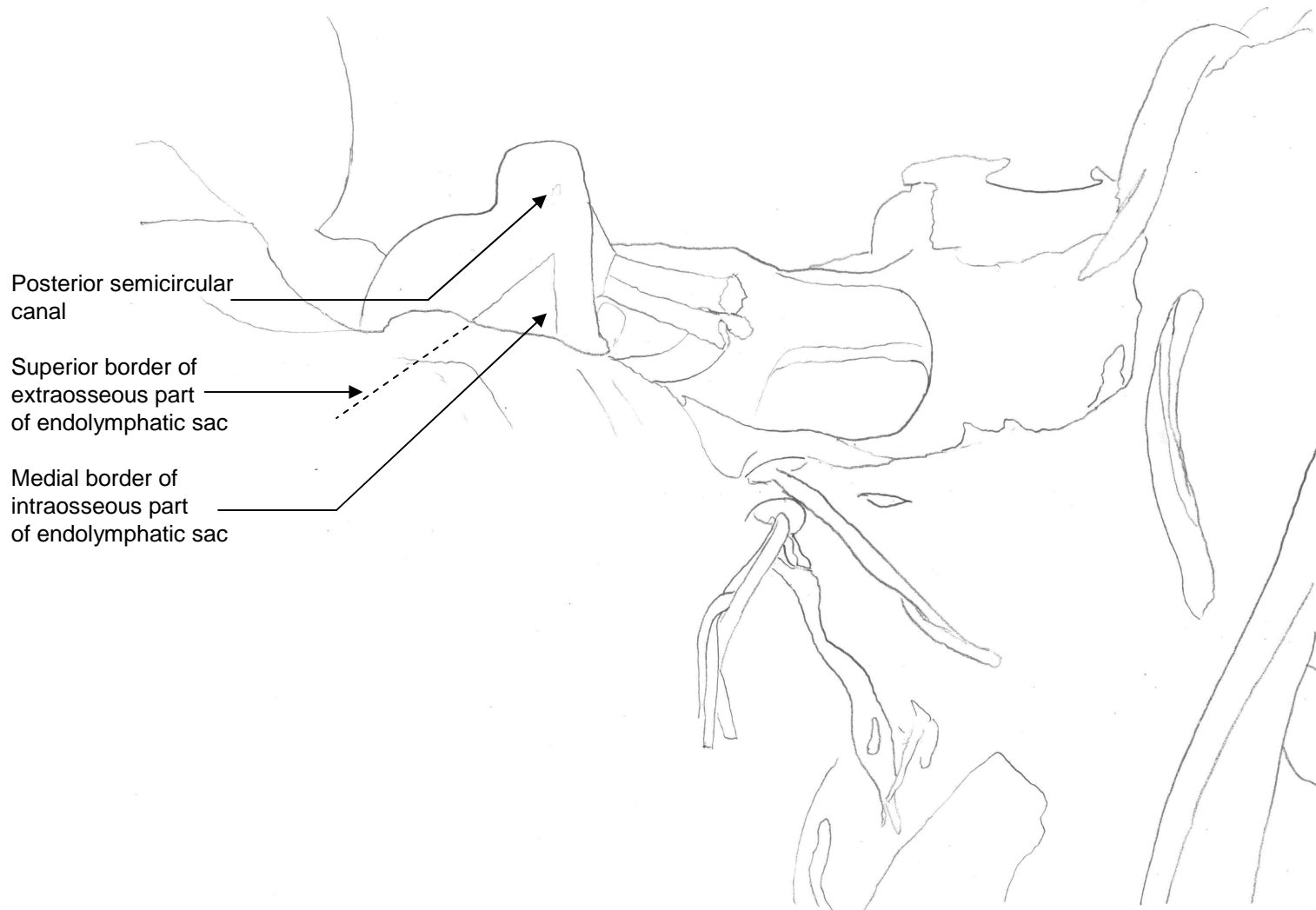


Figure 71 Diagram of the intraosseous part of the endolymphatic sac



Figure 72 Photograph of posterior view of right temporal bone revealing labyrinth

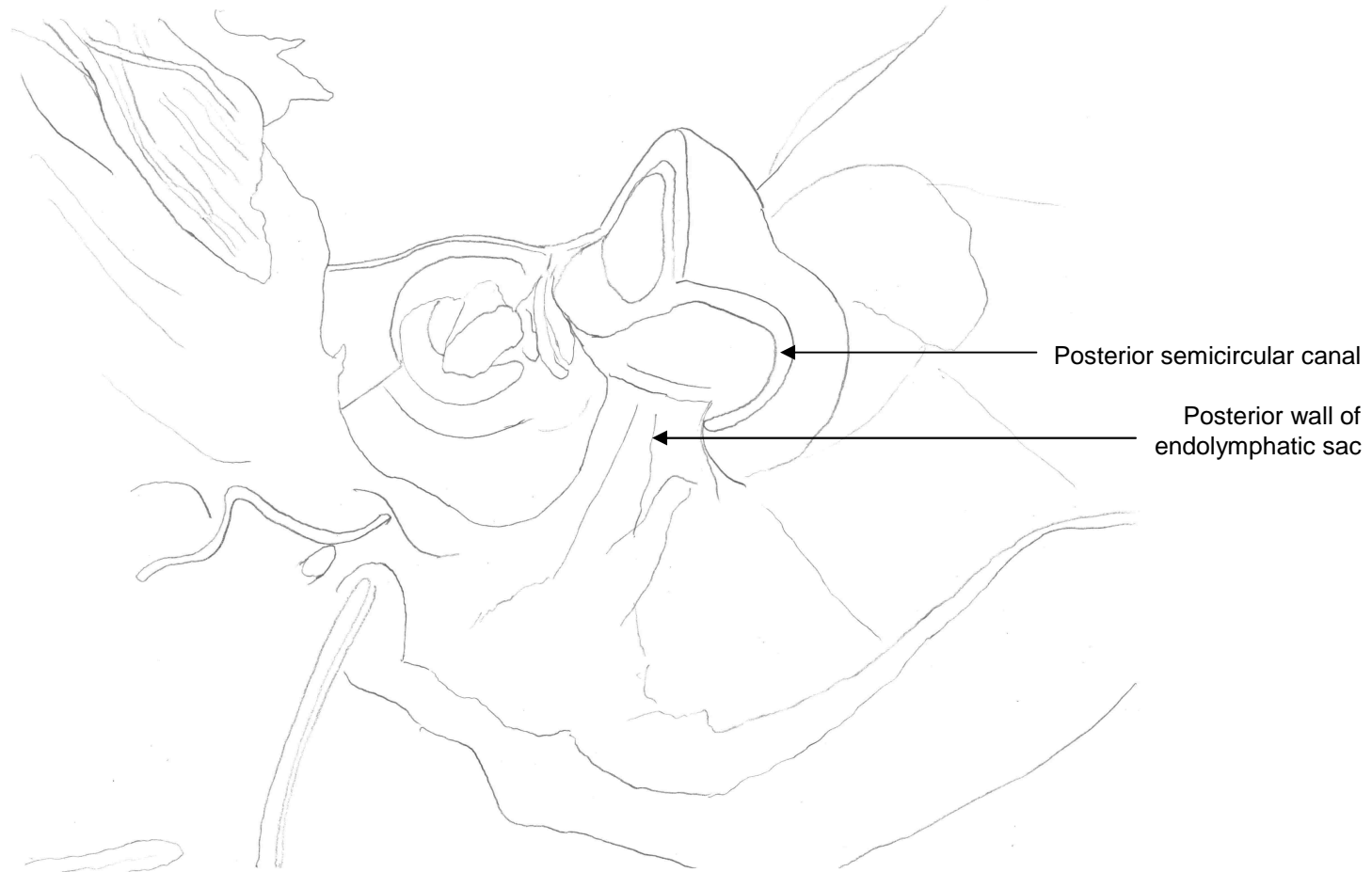


Figure 73 Diagram of posterior view of right temporal bone revealing labyrinth



Figure 74 Photograph of superior view of drilled left temporal bone

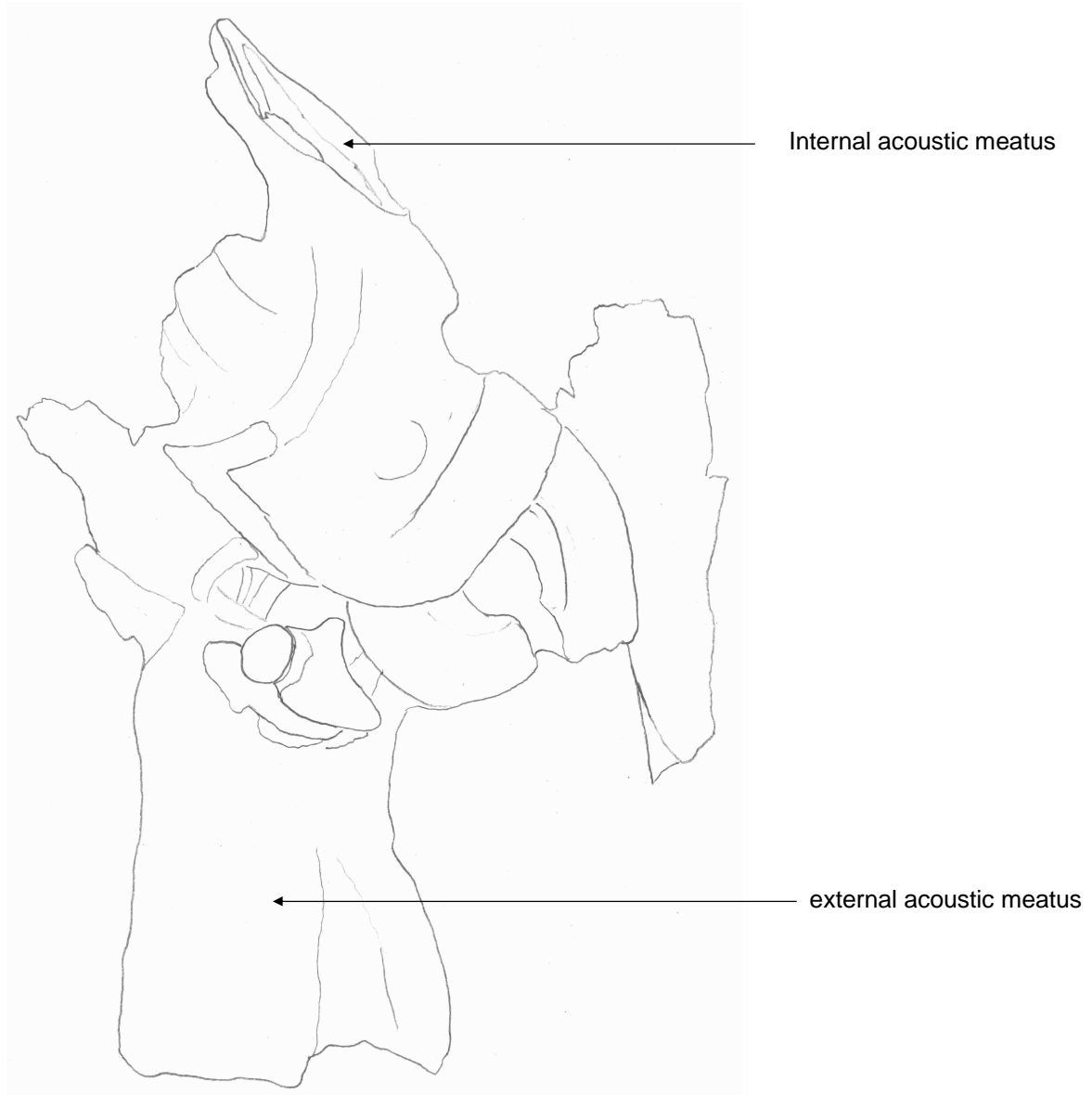


Figure 75 Diagram of superior view of drilled left temporal bone

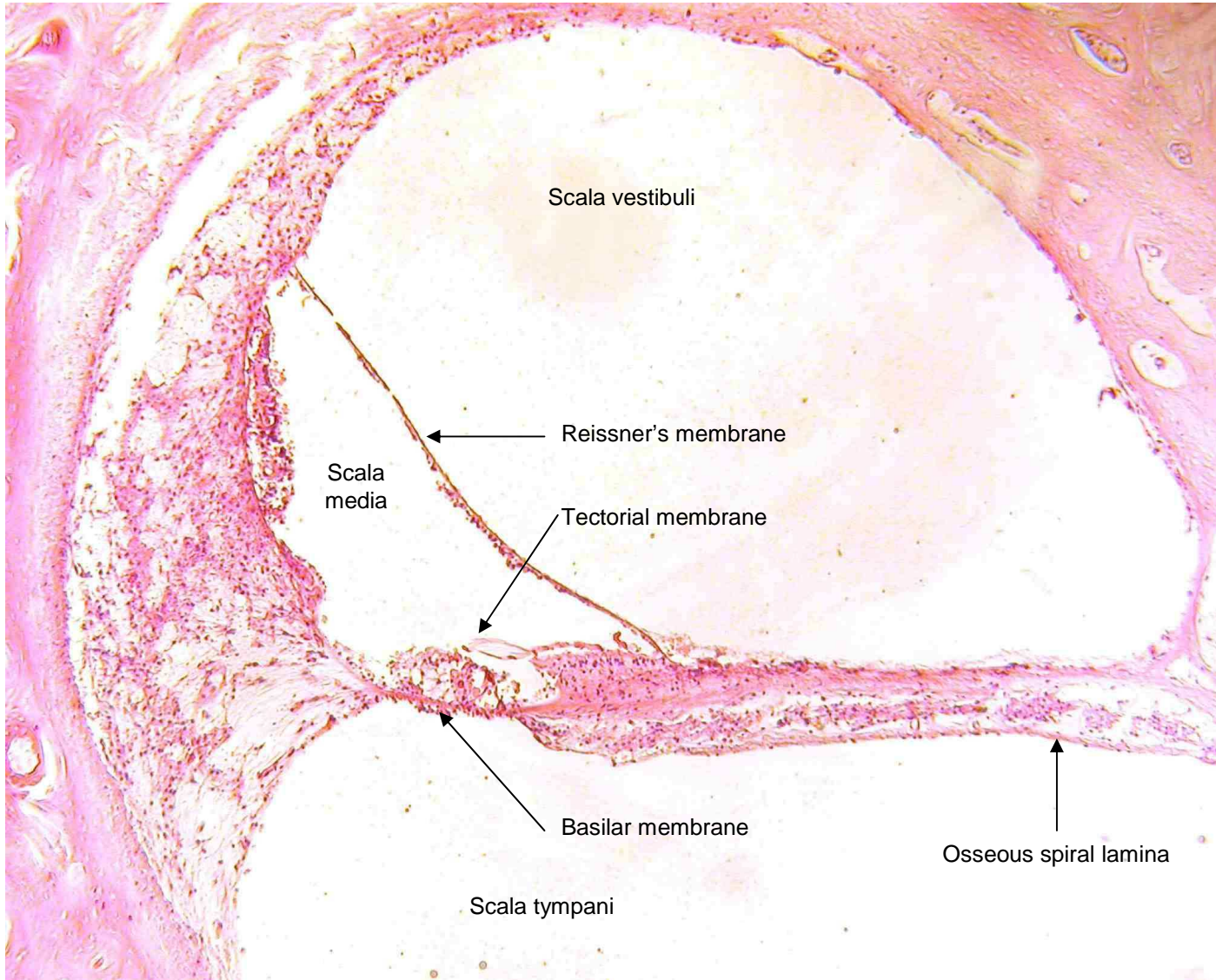


Figure 76 Photograph of section of cochlea stained with haematoxylin and eosin

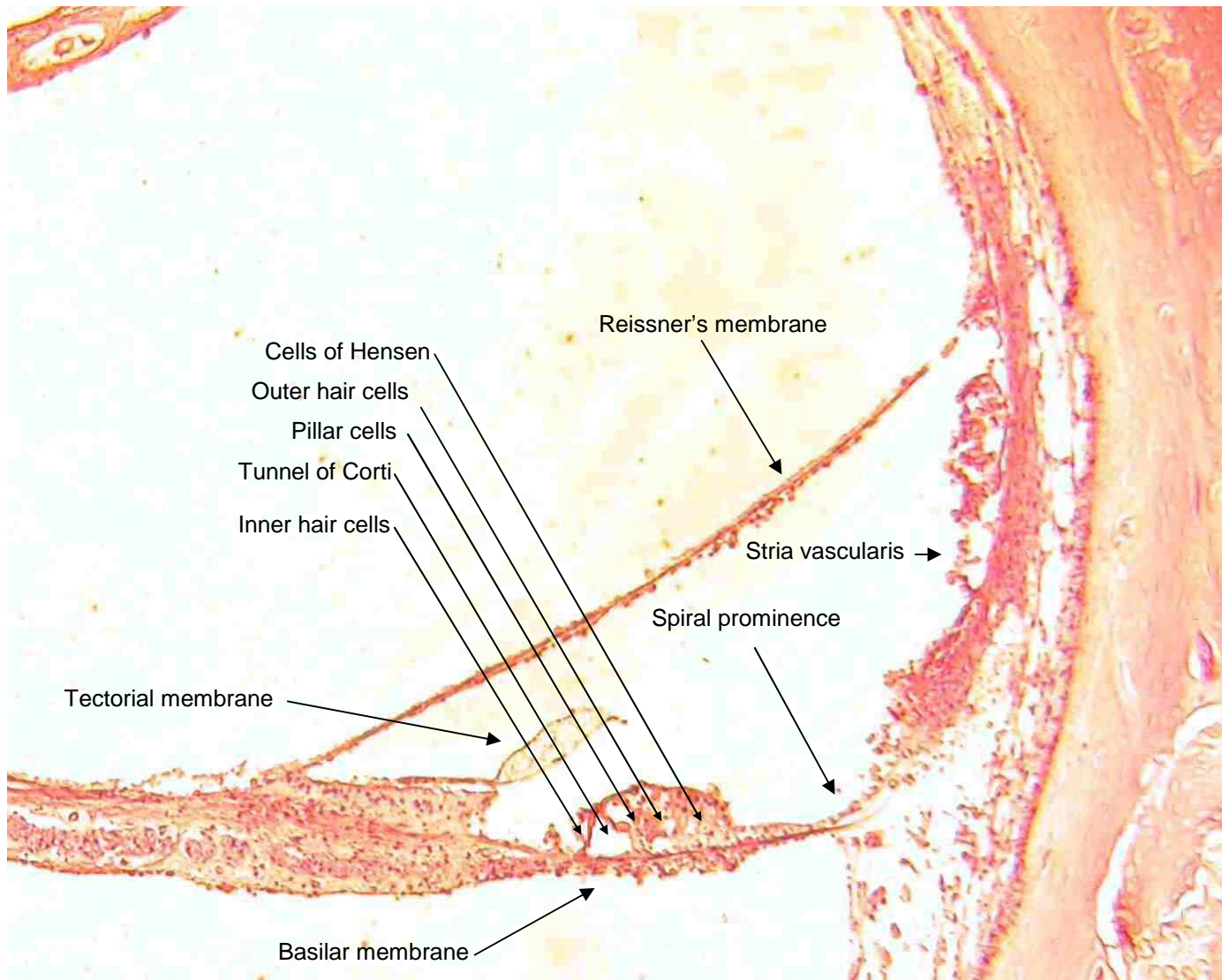


Figure 77 Photograph of section of cochlea duct stained with haematoxylin and eosin



Figure 78 Photograph of section of cochlea stained with massons trichrome



Tubules of endolymphatic sac

Figure 79 Photograph of section of intermediate endolymphatic sac stained with haematoxylin and eosin



Figure 80 Photograph of section of distal endolymphatic sac stained with haematoxylin and eosin

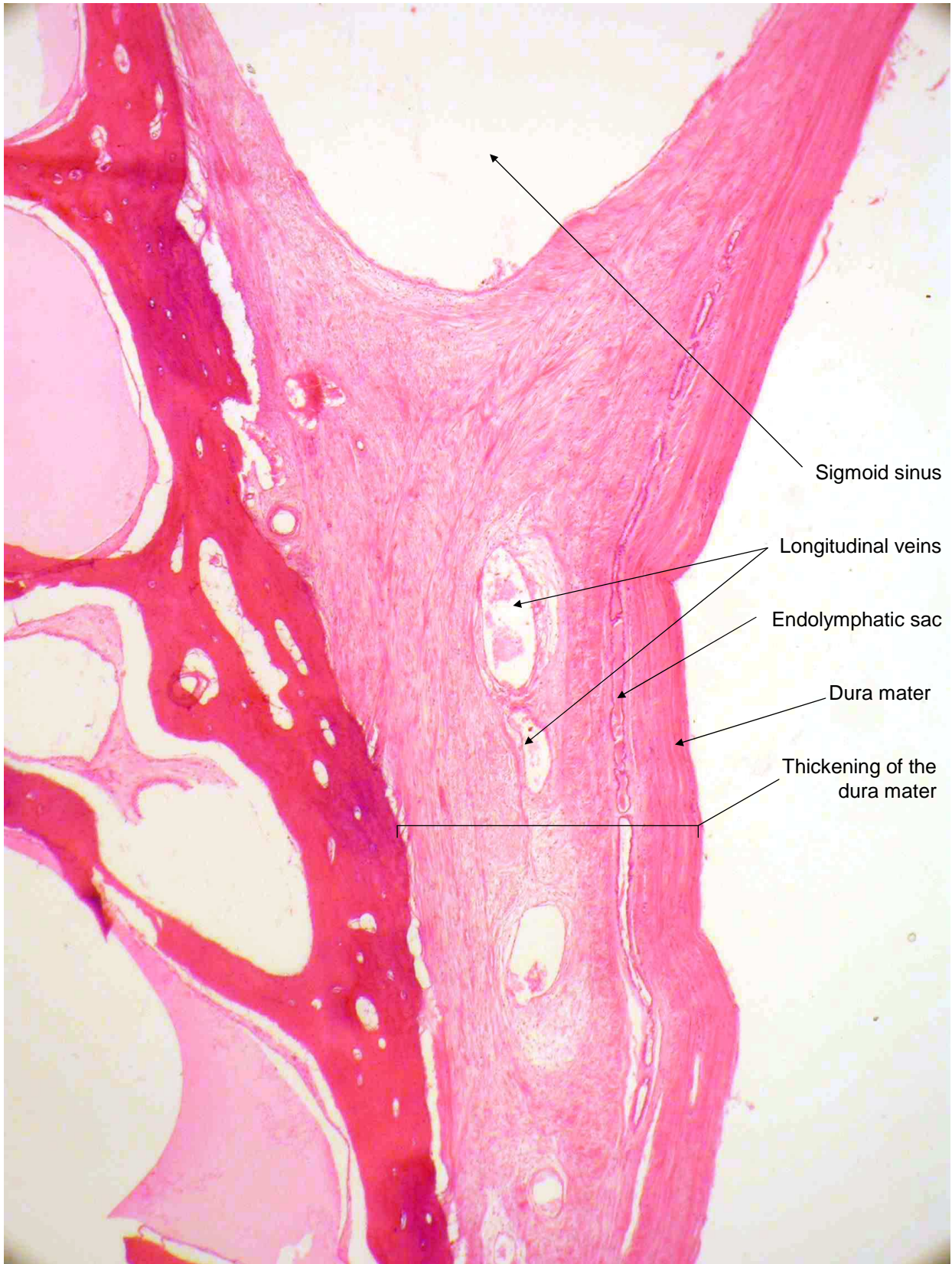


Figure 81 Photograph of section of distal endolymphatic sac stained with haemotoxylin and eosin

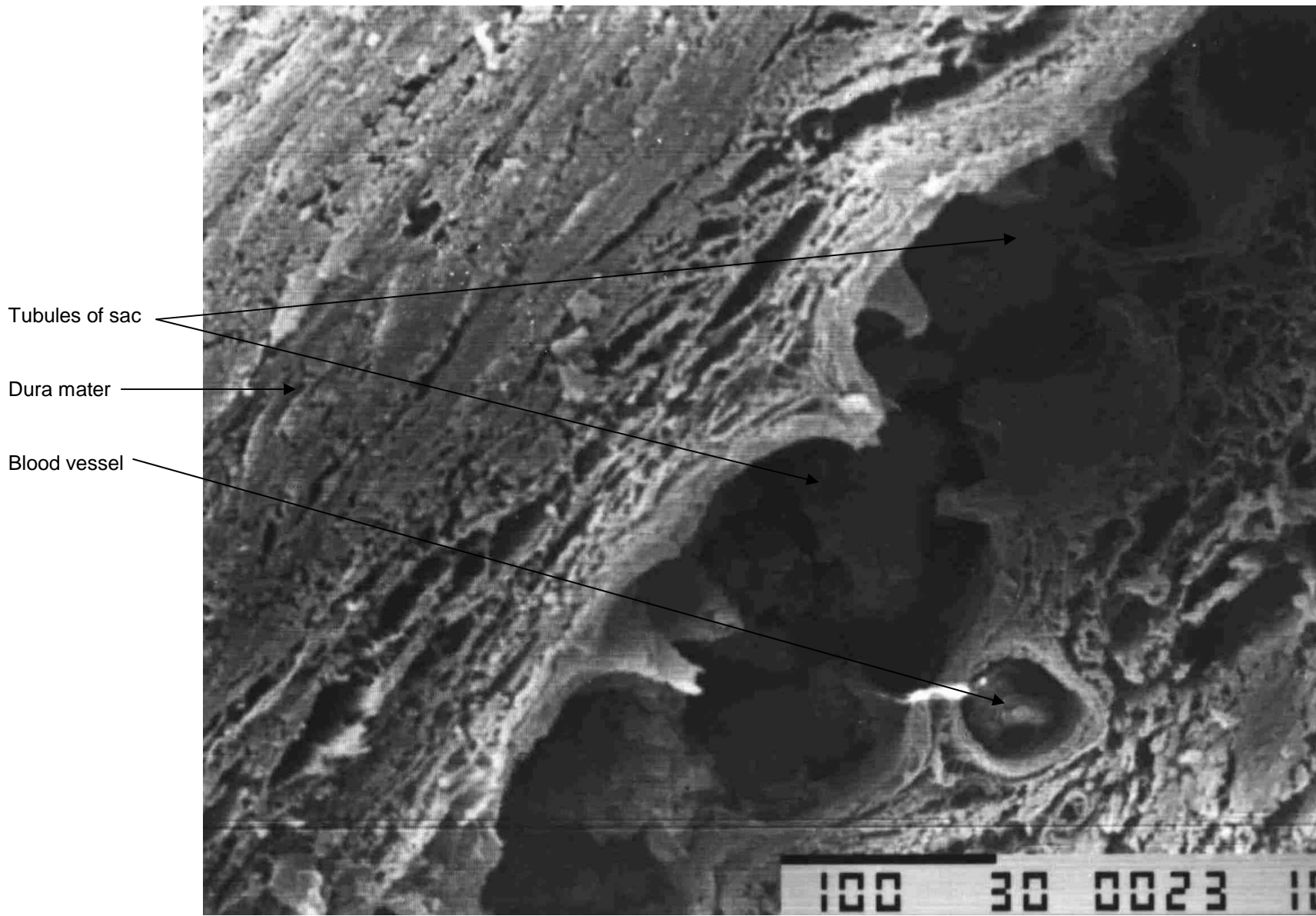


Figure 82 Electron micrograph of transverse section of endolymphatic sac

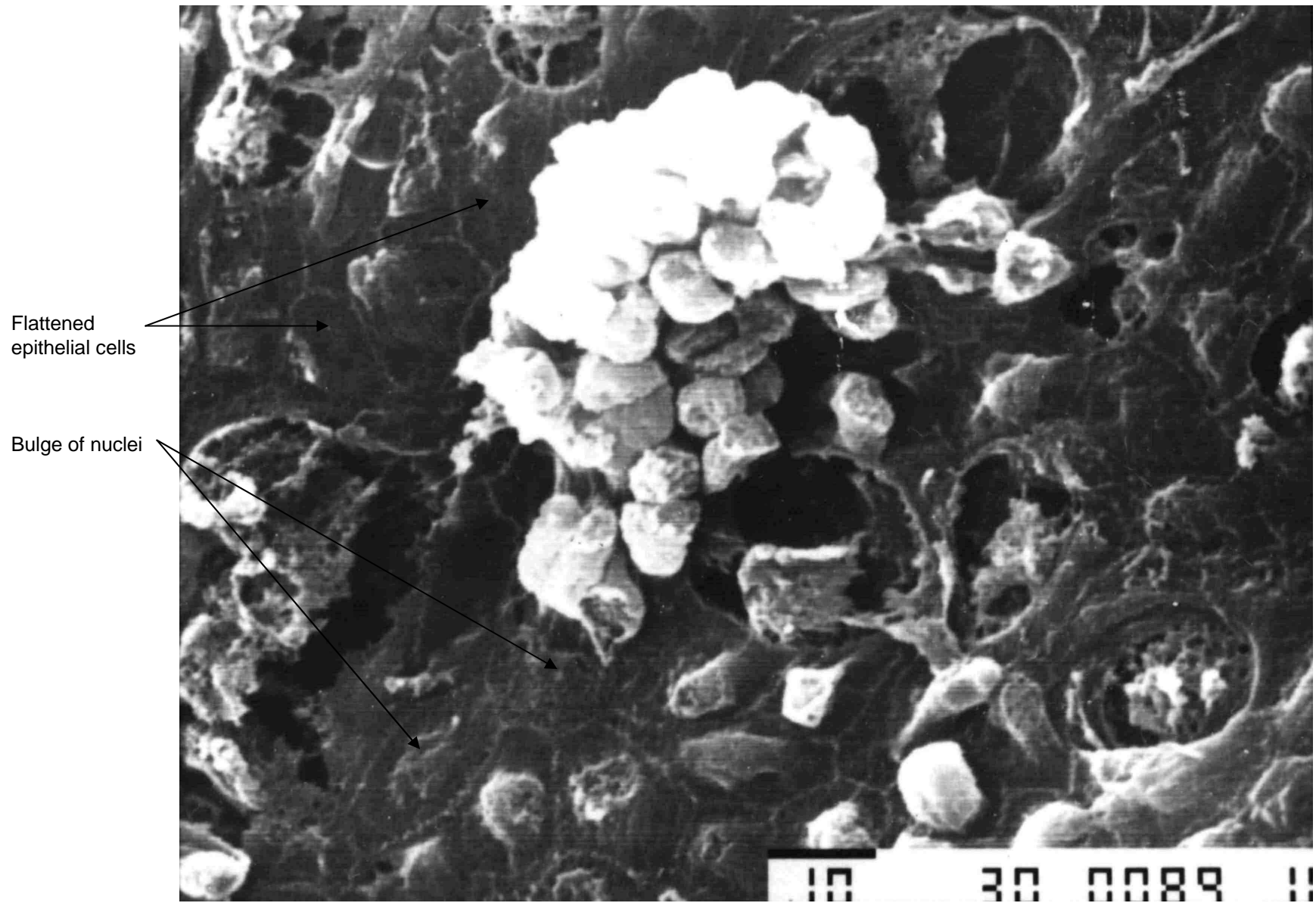


Figure 83 Electron micrograph of the internal surface of the endolymphatic sac

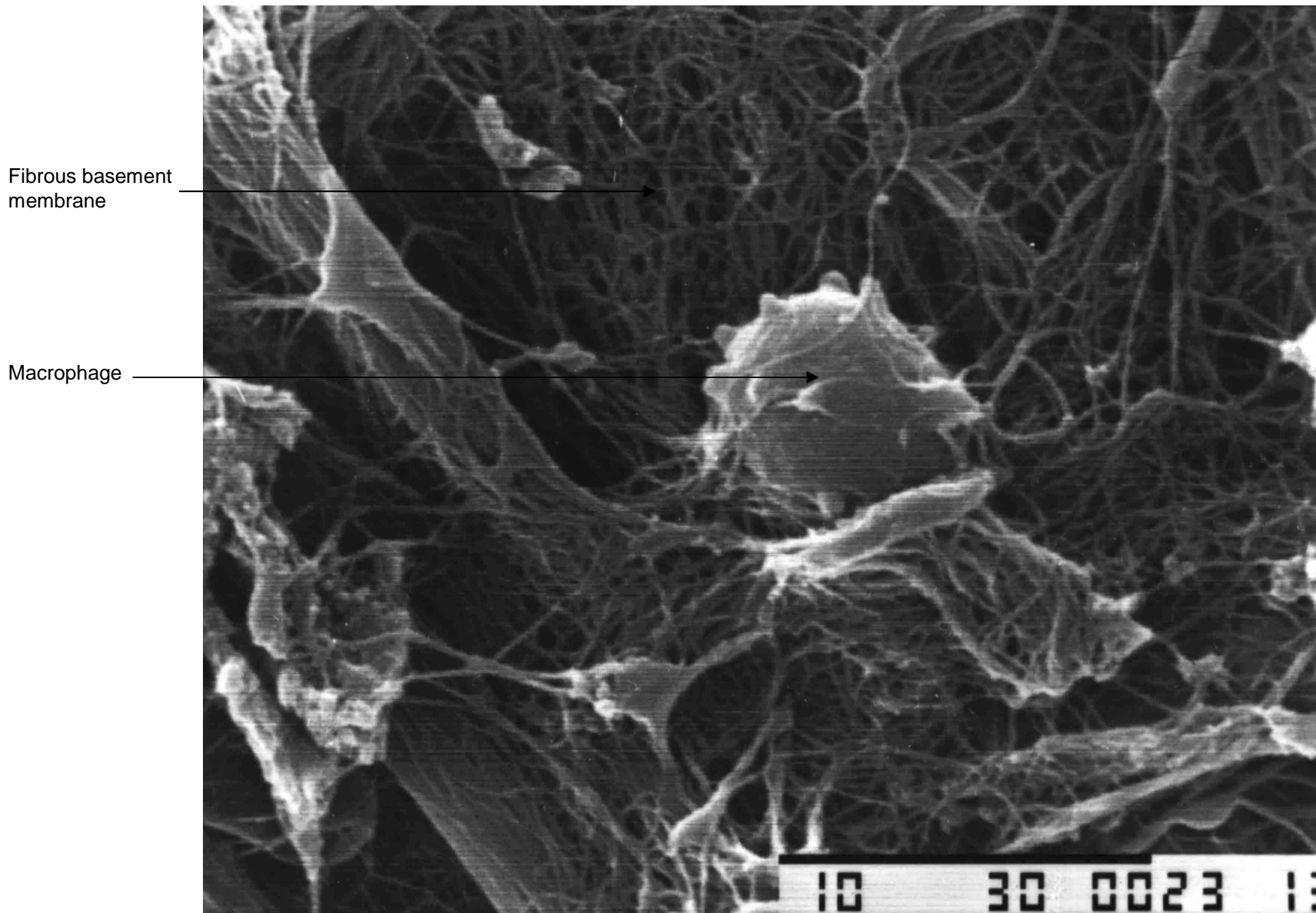


Figure 84 Electron micrograph of the basement membrane of the endolymphatic sac

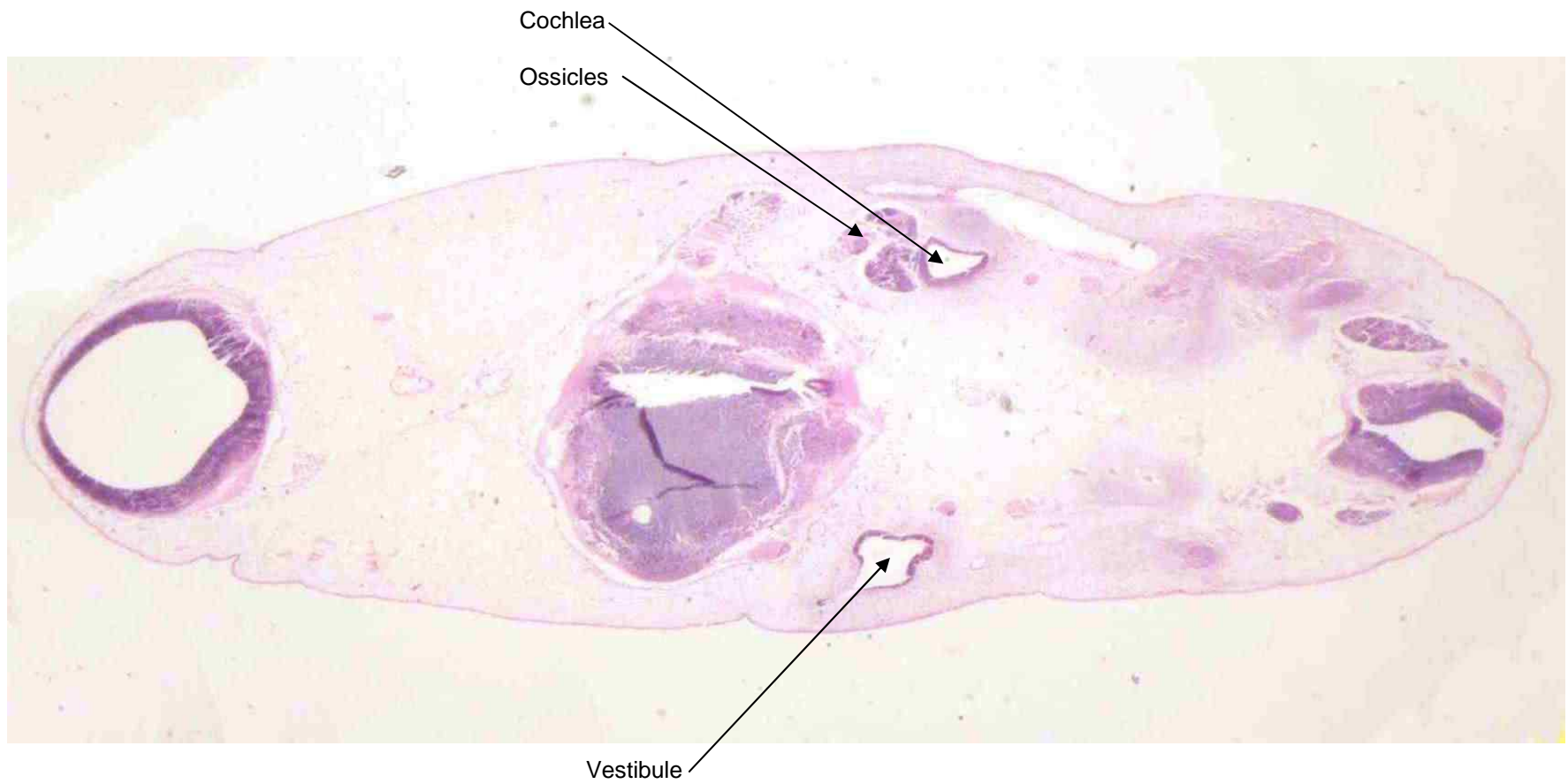


Figure 85 Photograph of a section of a 27mm human embryo head stained with haematoxylin and eosin



Figure 86 Photograph of a section of a 55mm human embryo head stained with haemotoxylin and eosin

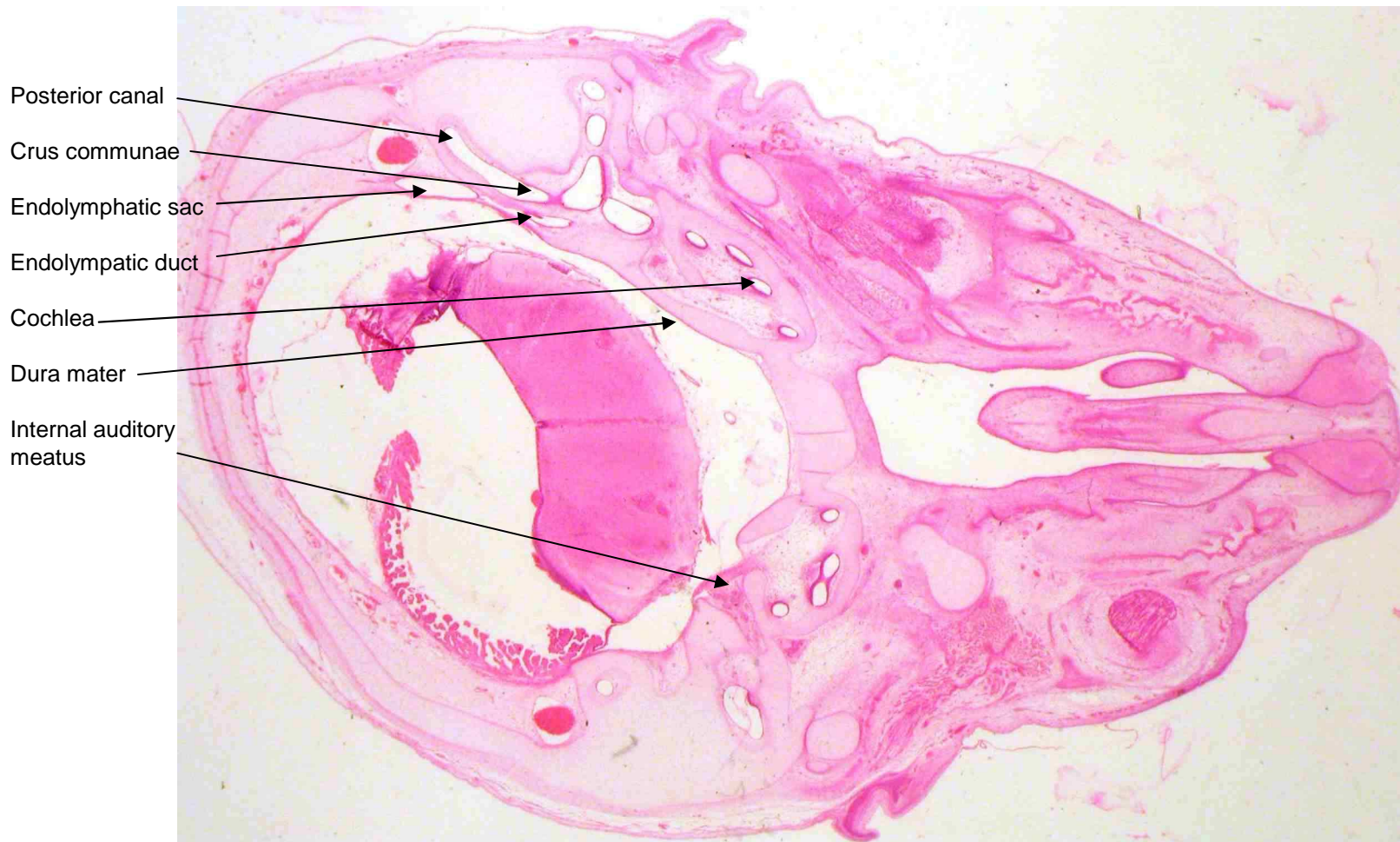


Figure 87 Photograph of a section of a 55mm human embryo head stained with haemotoxylin and eosin

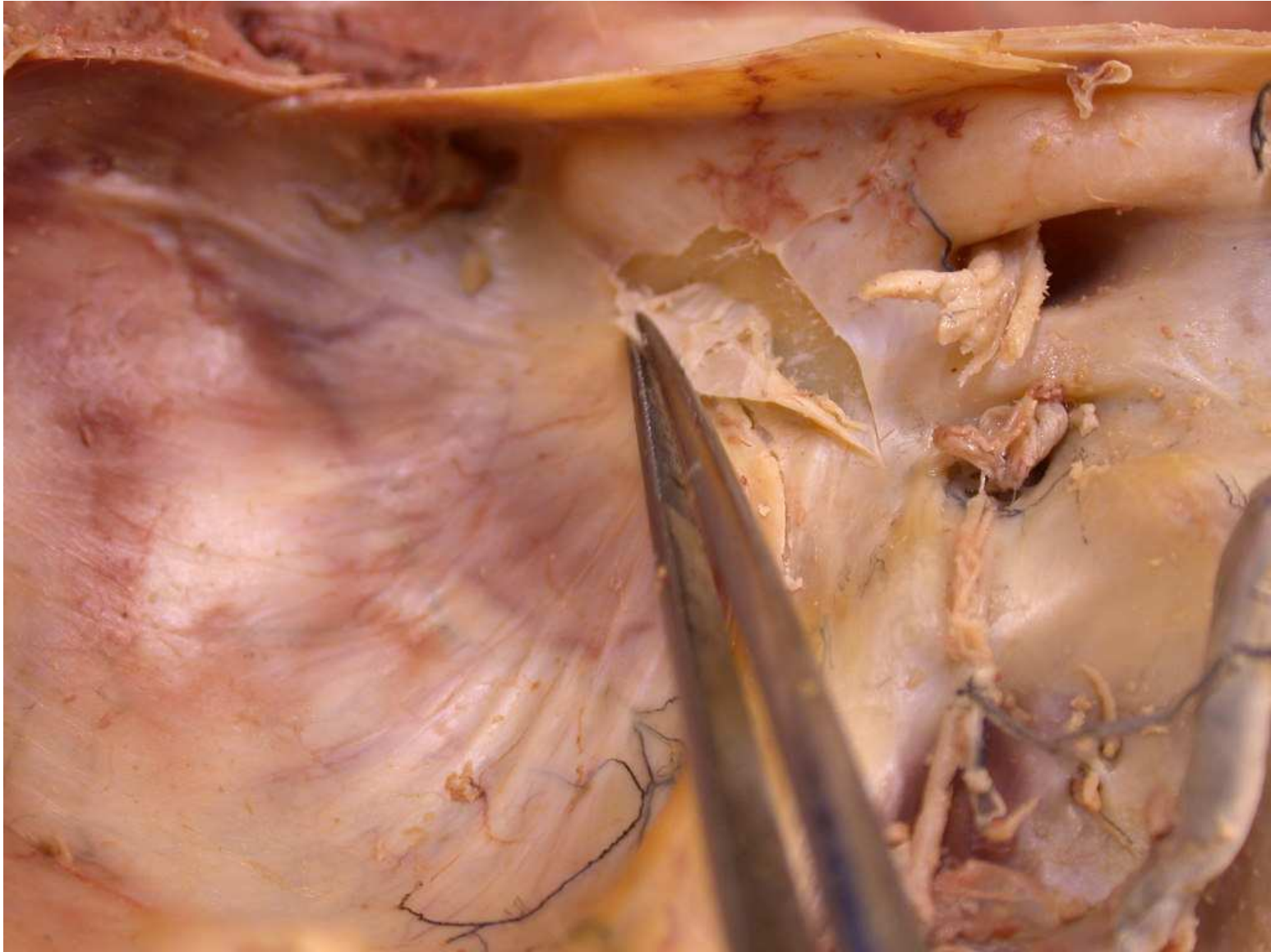


Figure 88 Photograph of the operculum and endolymphatic sac

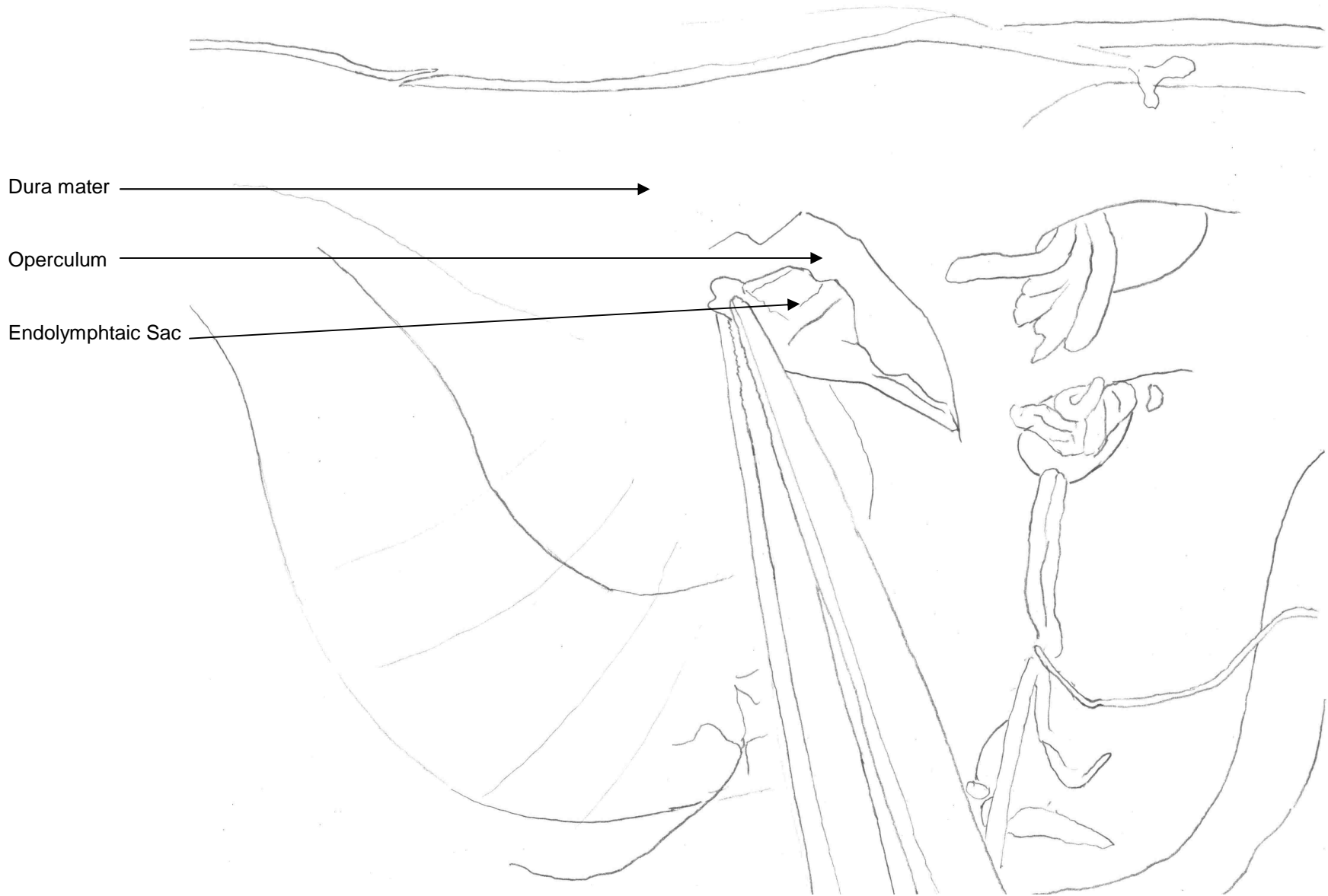


Figure 89 Diagram of the operculum and endolymphatic sac



Figure 90 Photograph of the endolymphatic sac with the lumen opened

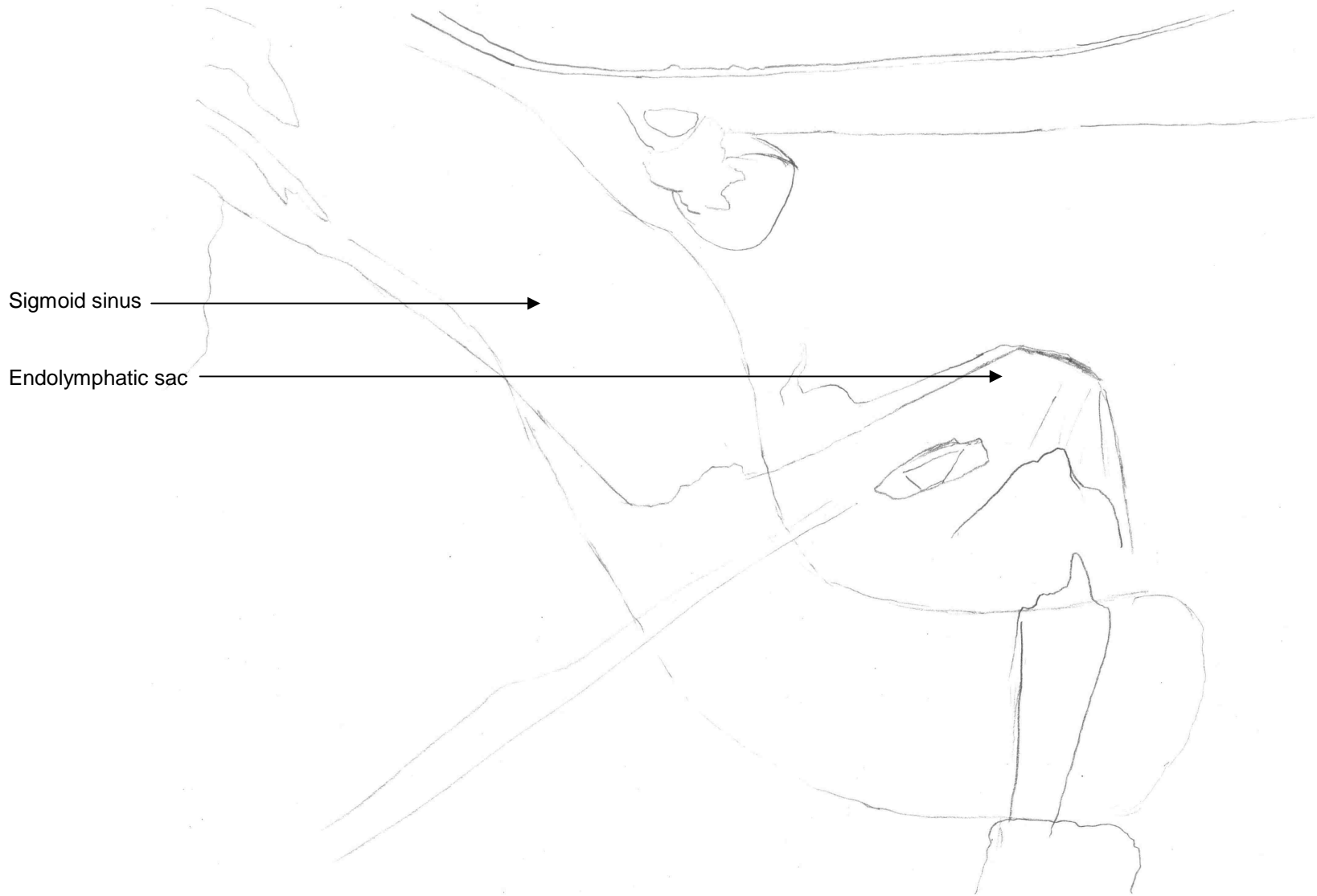


Figure 91 Diagram of the endolymphatic sac with the lumen opened

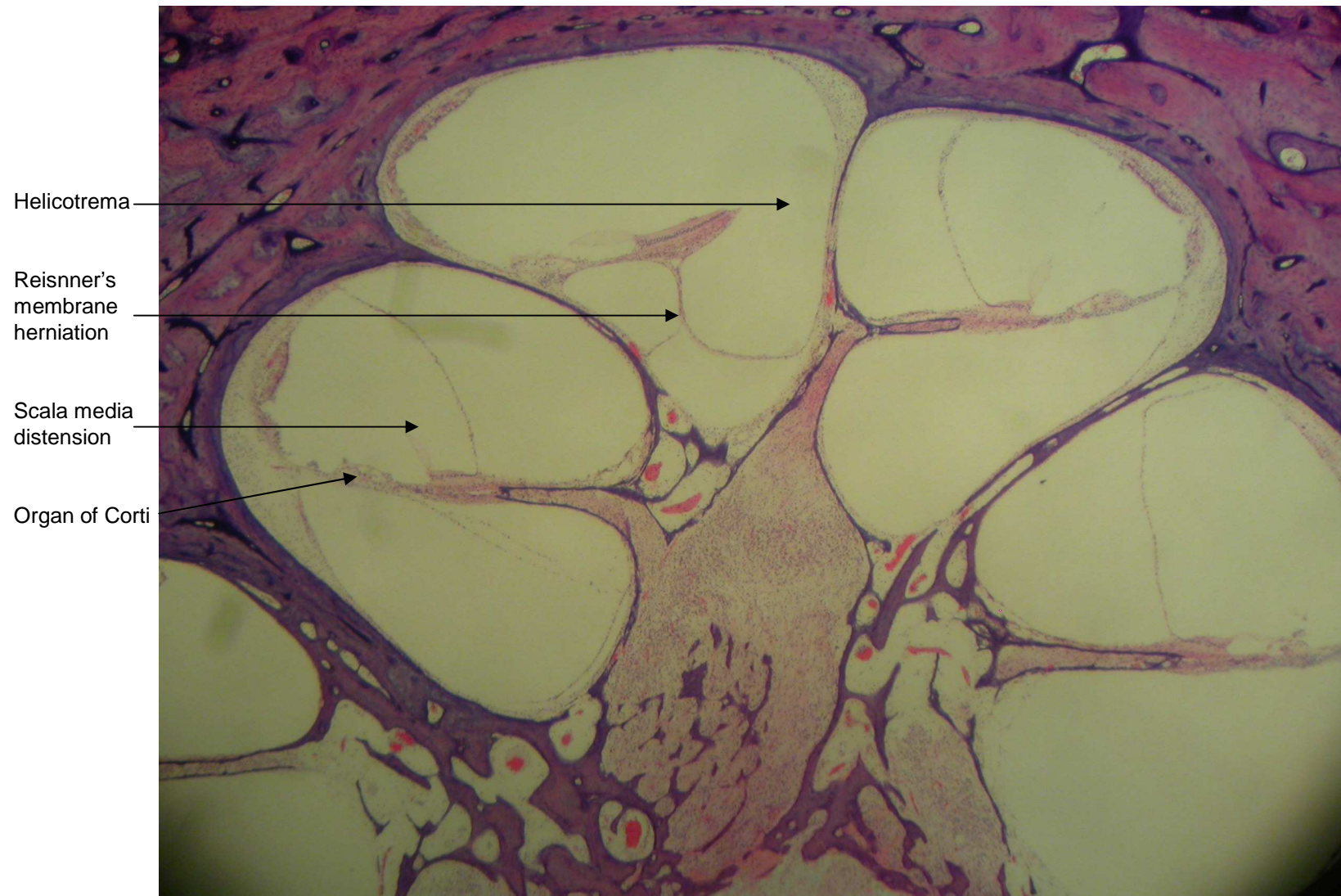


Figure 92 Photograph of a section of the affected cochlea, right, from a patient with unilateral Ménière's disease stained with haematoxylin and eosin

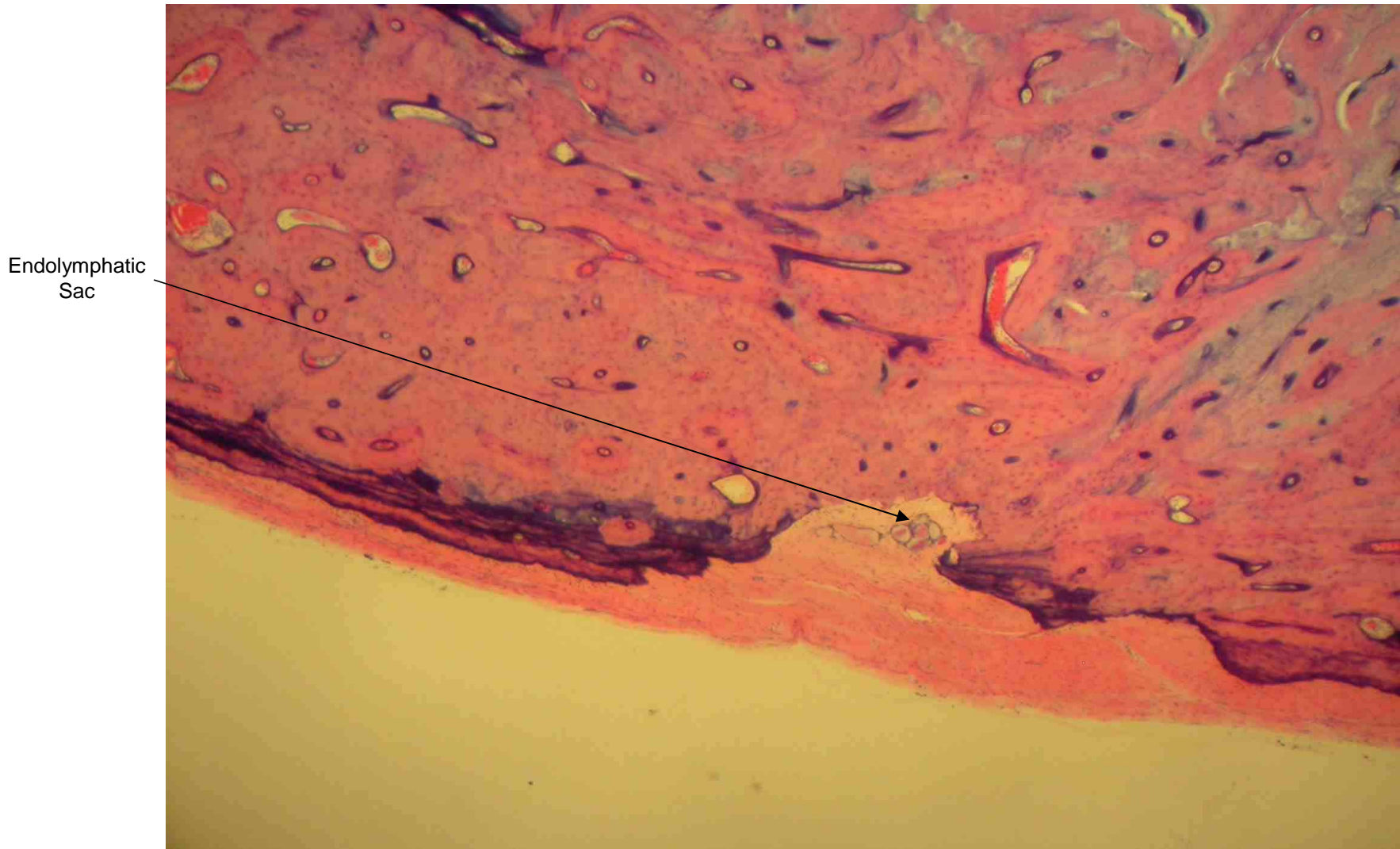


Figure 93 Photograph of a section of the left temporal bone showing the endolymphatic sac from a patient with long standing menieres disease, stained with haemotoxylin and eosin

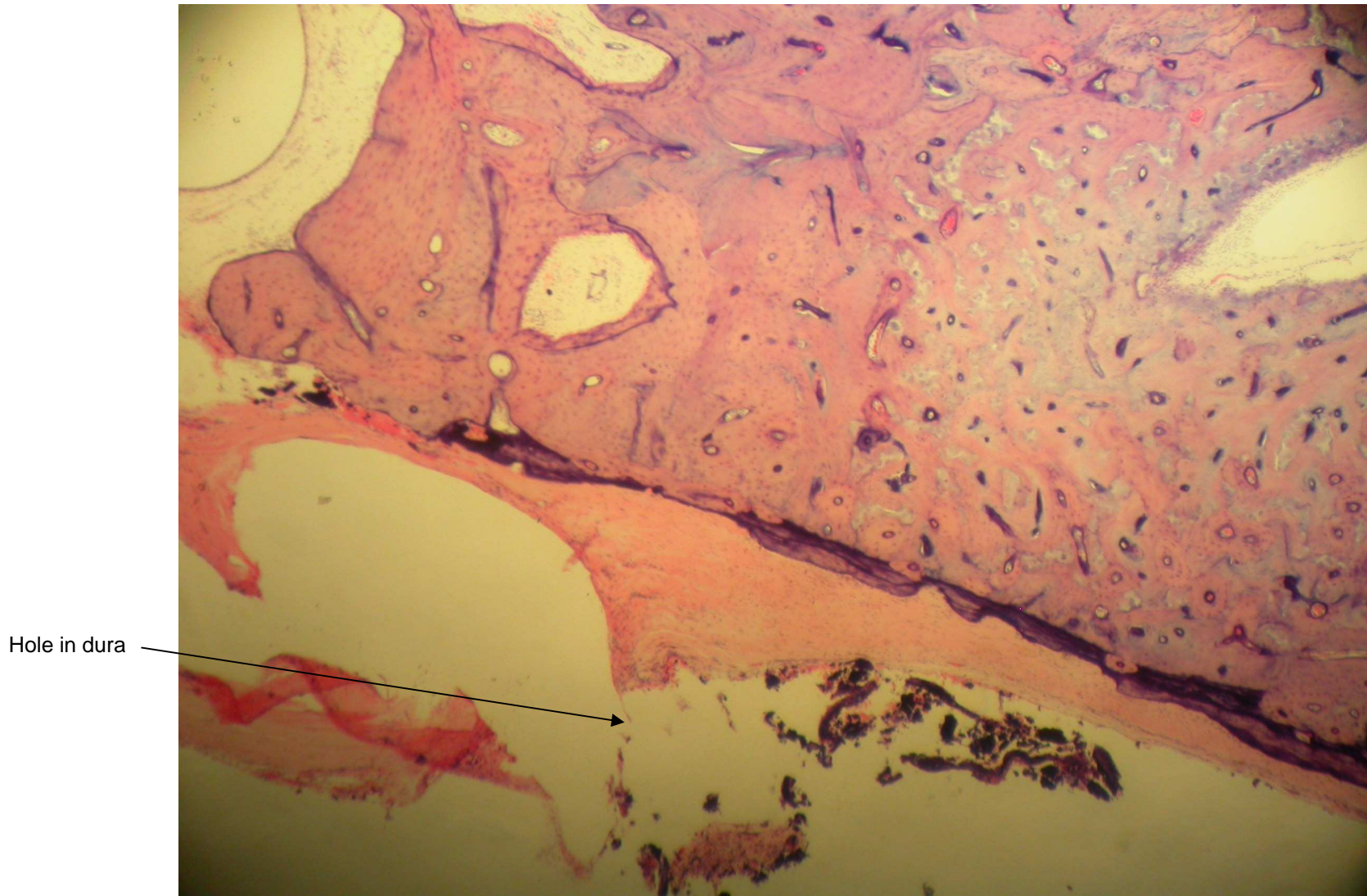


Figure 94 Photograph of a section of the right temporal bone from a patient with previous endolymphatic sac decompression and stent insertion stained with haematoxylin and eosin

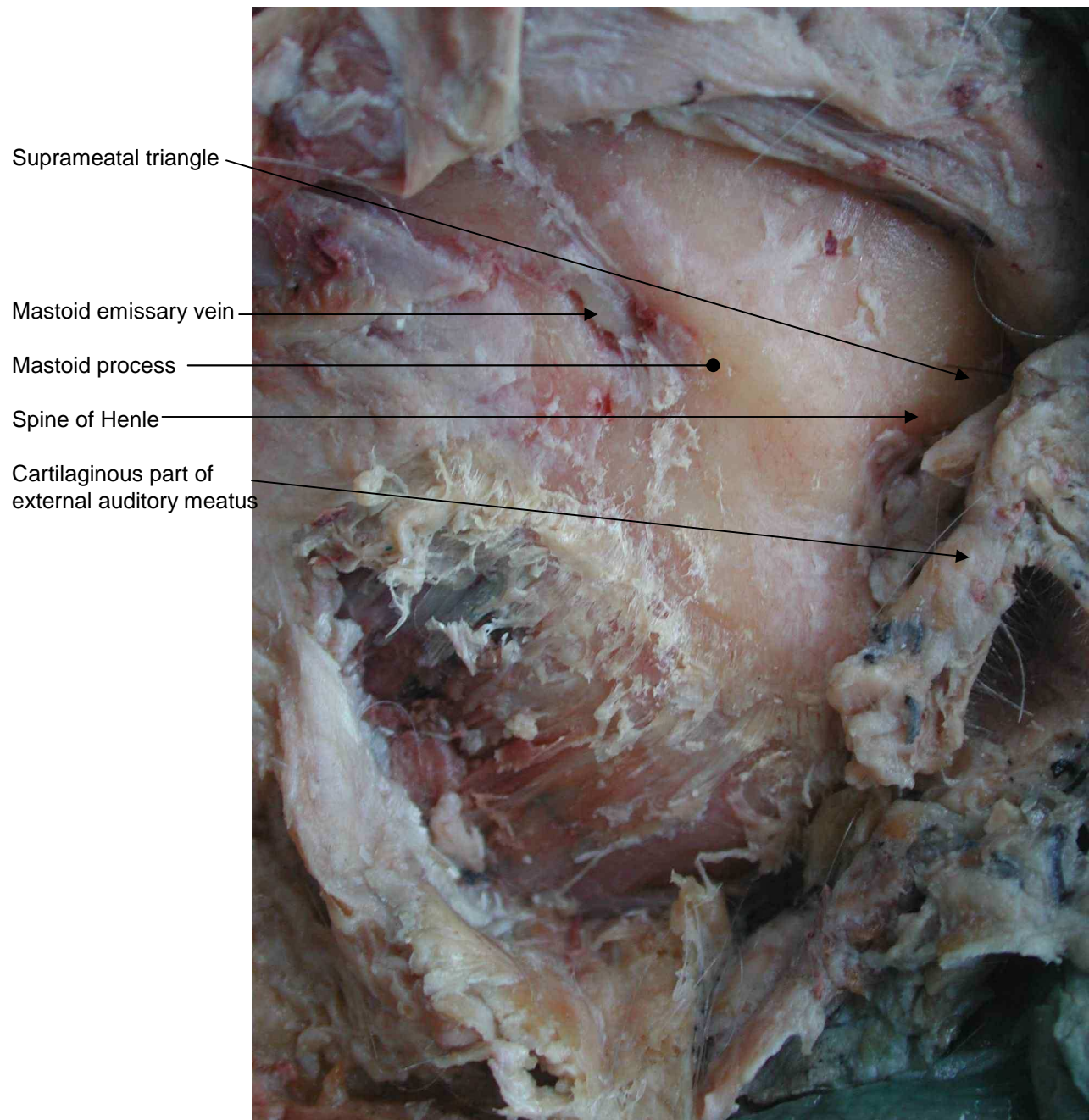


Figure 95 Photograph of a right mastoid process

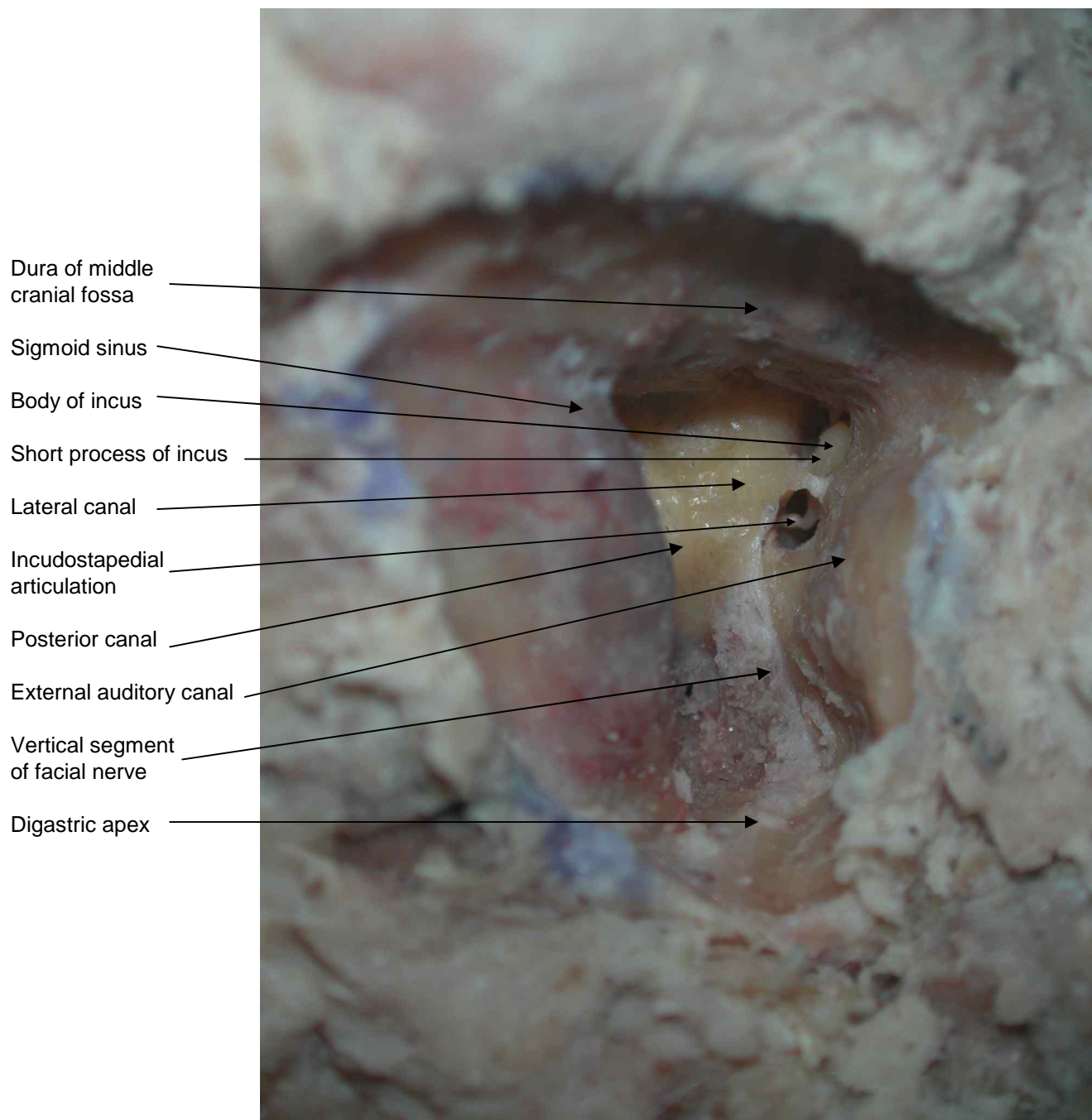


Figure 96 Photograph of a right cortical mastoidectomy and endolymphatic sac decompression

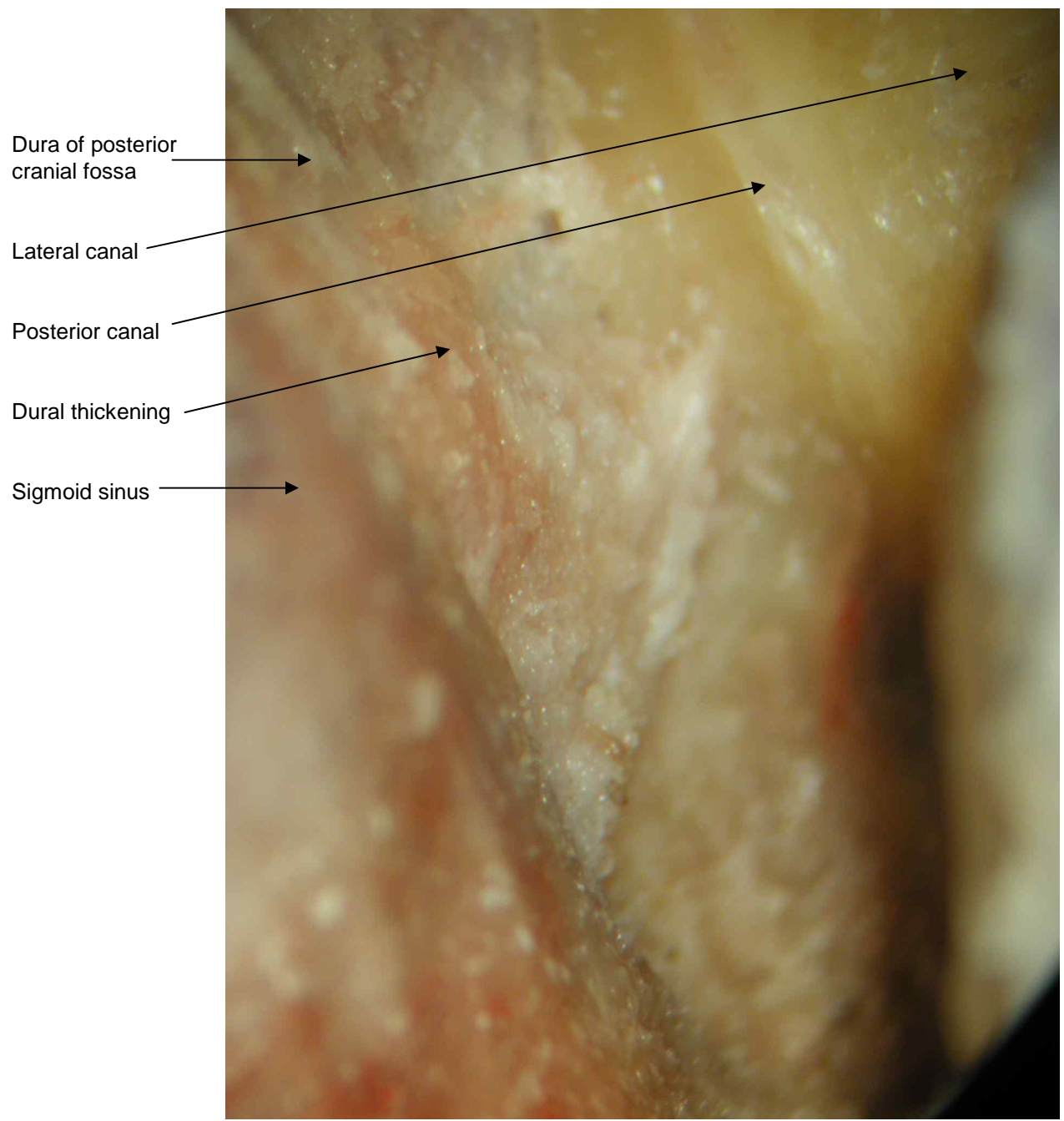


Figure 97 Photograph of a right cortical mastoidectomy and endolymphatic sac decompression



Figure 98 Photograph of a right superficial head dissection

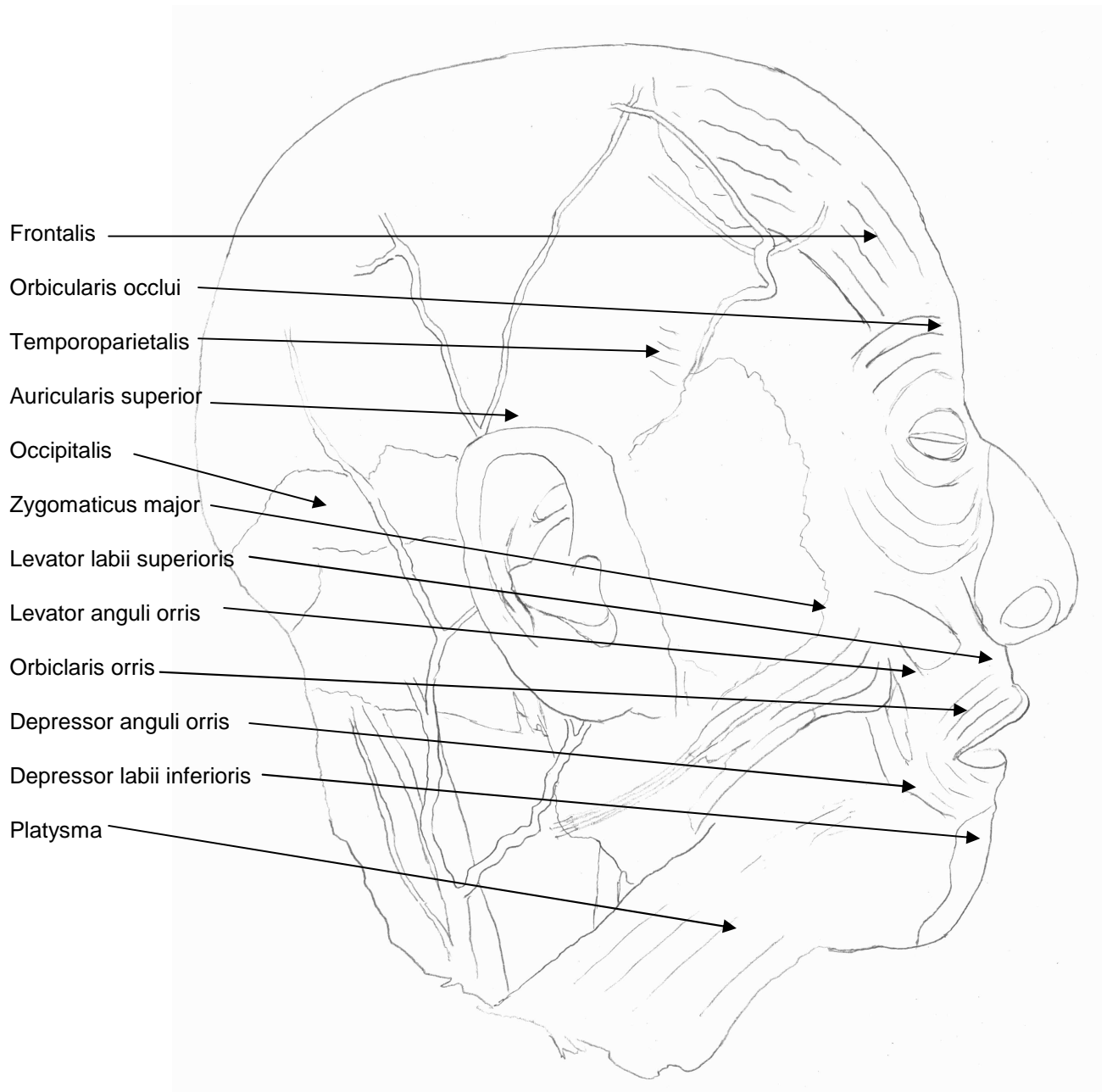


Figure 99 Diagram of a right superficial head dissection



Figure 100 Photograph of the superficial structures behind the pinna

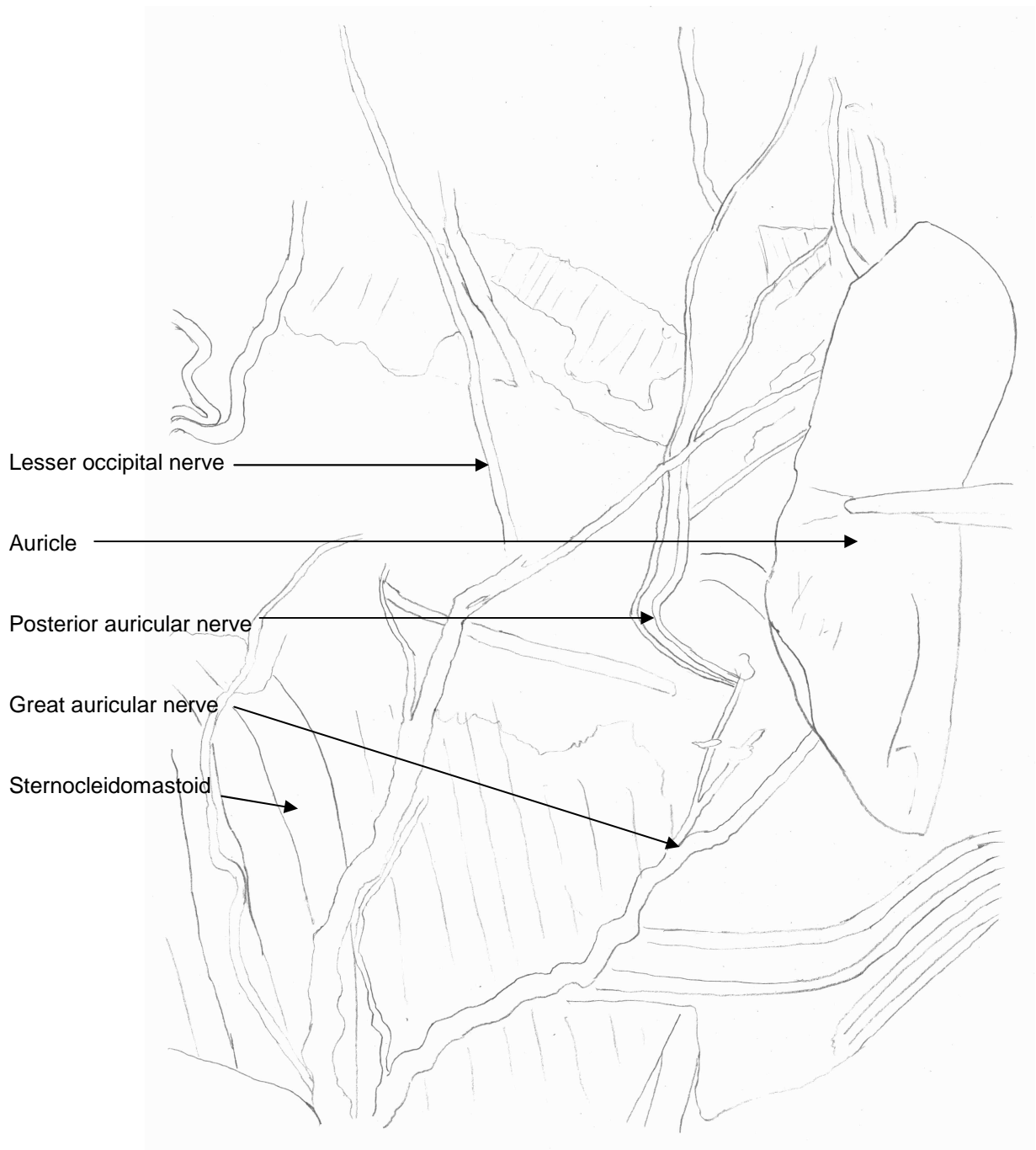


Figure 101 Photograph of the superficial structures behind the pinna



Figure 102 Photograph of superficial left head and neck dissection

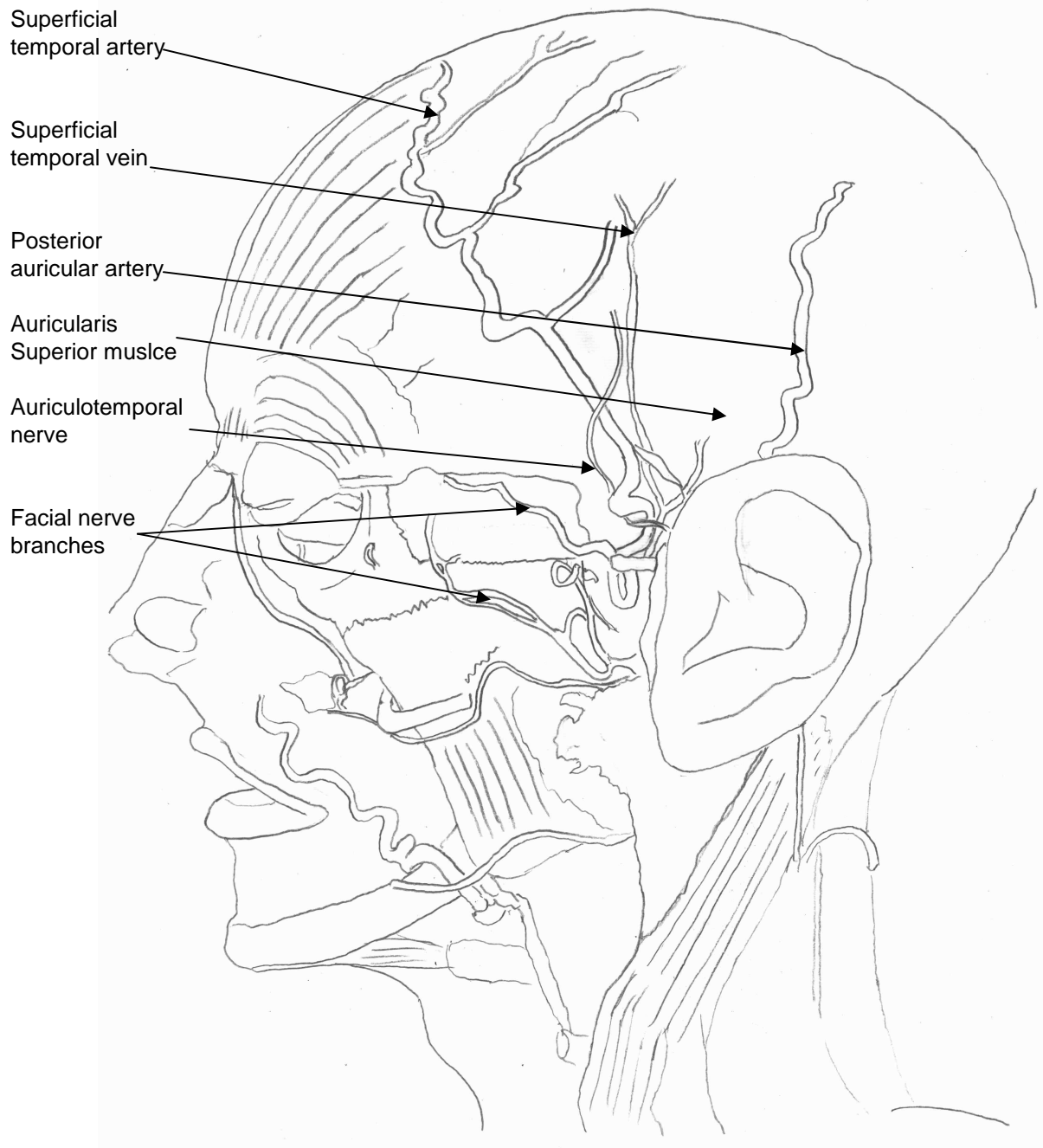


Figure 103 Diagram of superficial left head and neck dissection



Figure 104 Photograph of posterior view of left pinna dissection

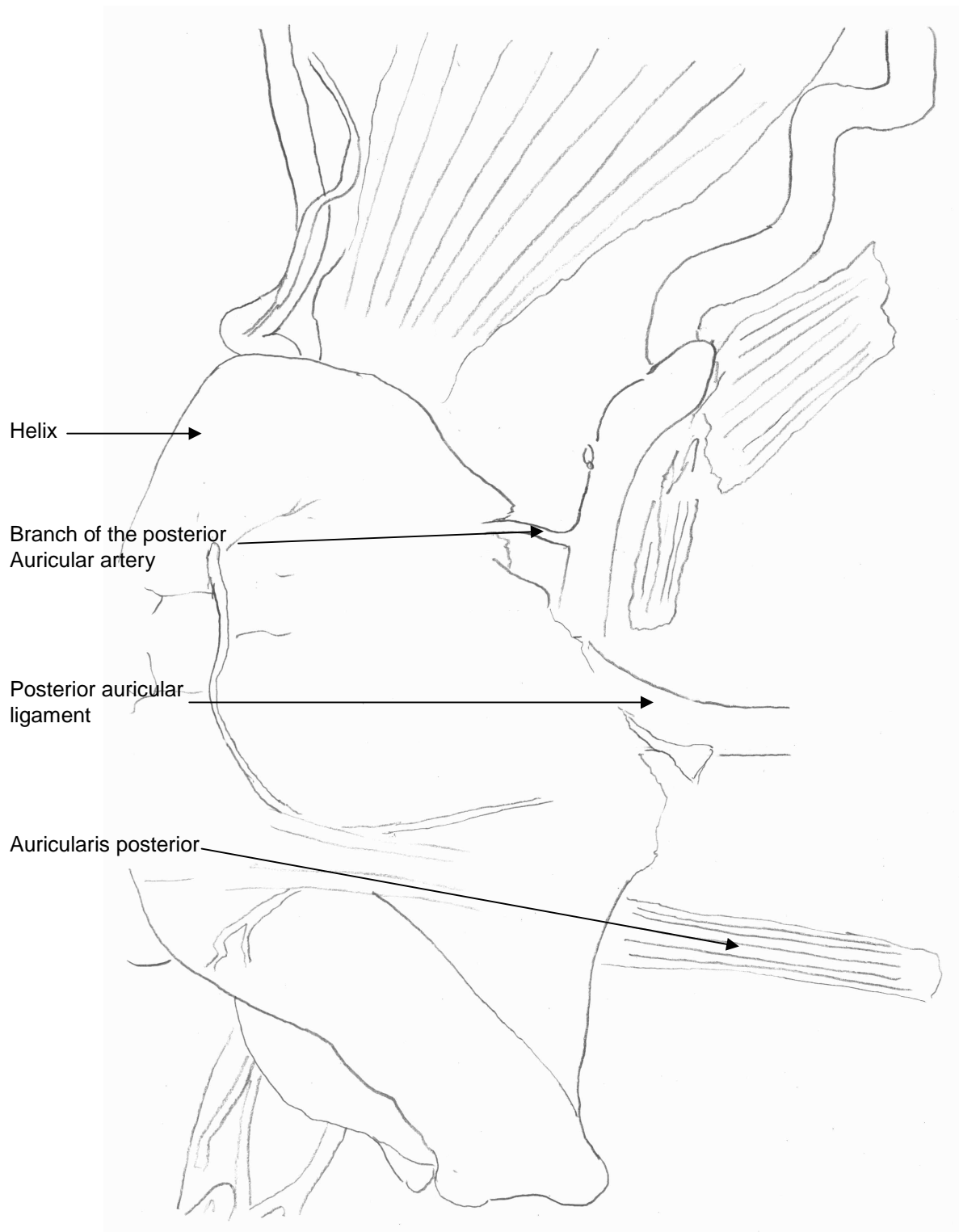


Figure 105 Diagram of posterior view of left pinna dissection

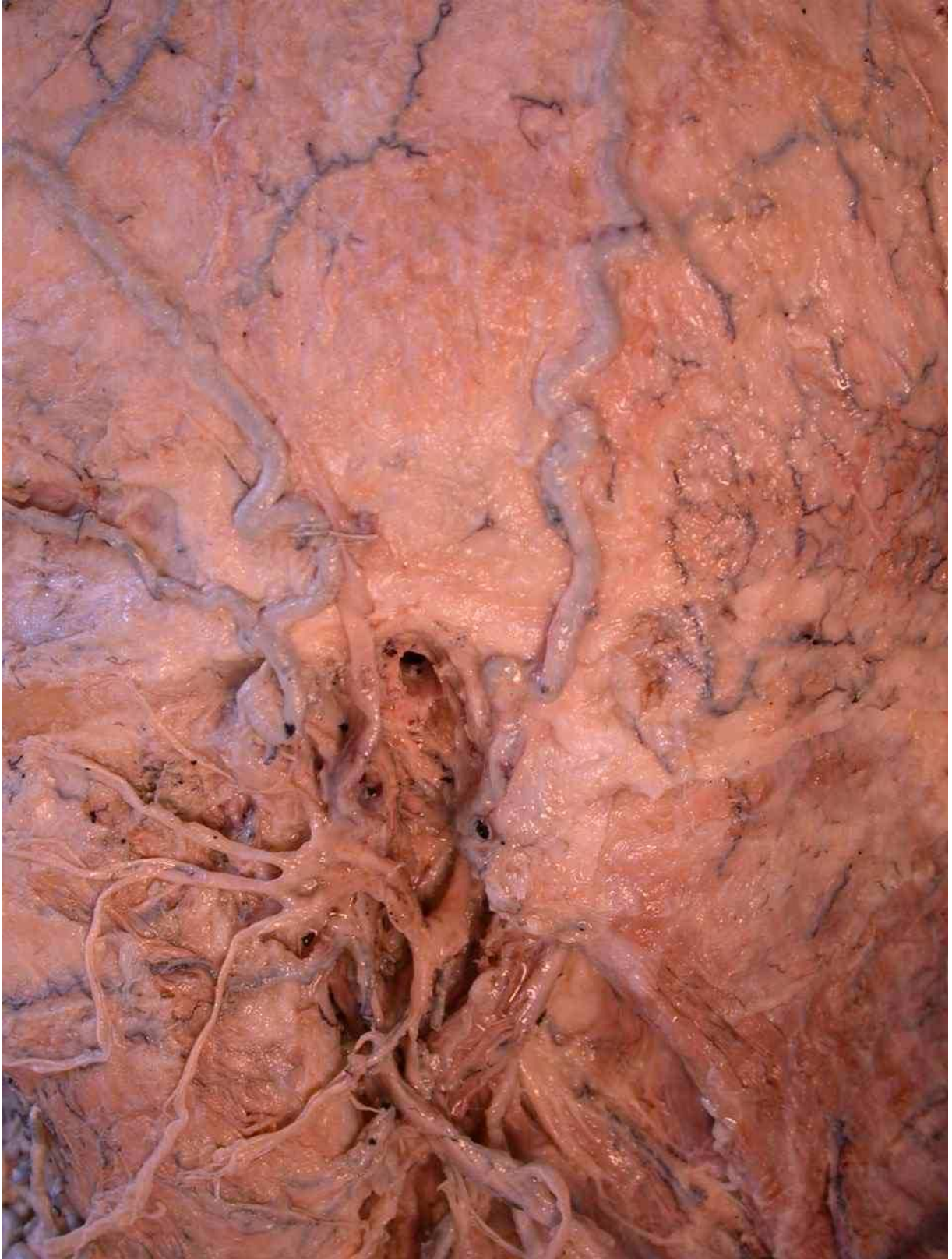


Figure 106 Photograph of left bony external acoustic meatus

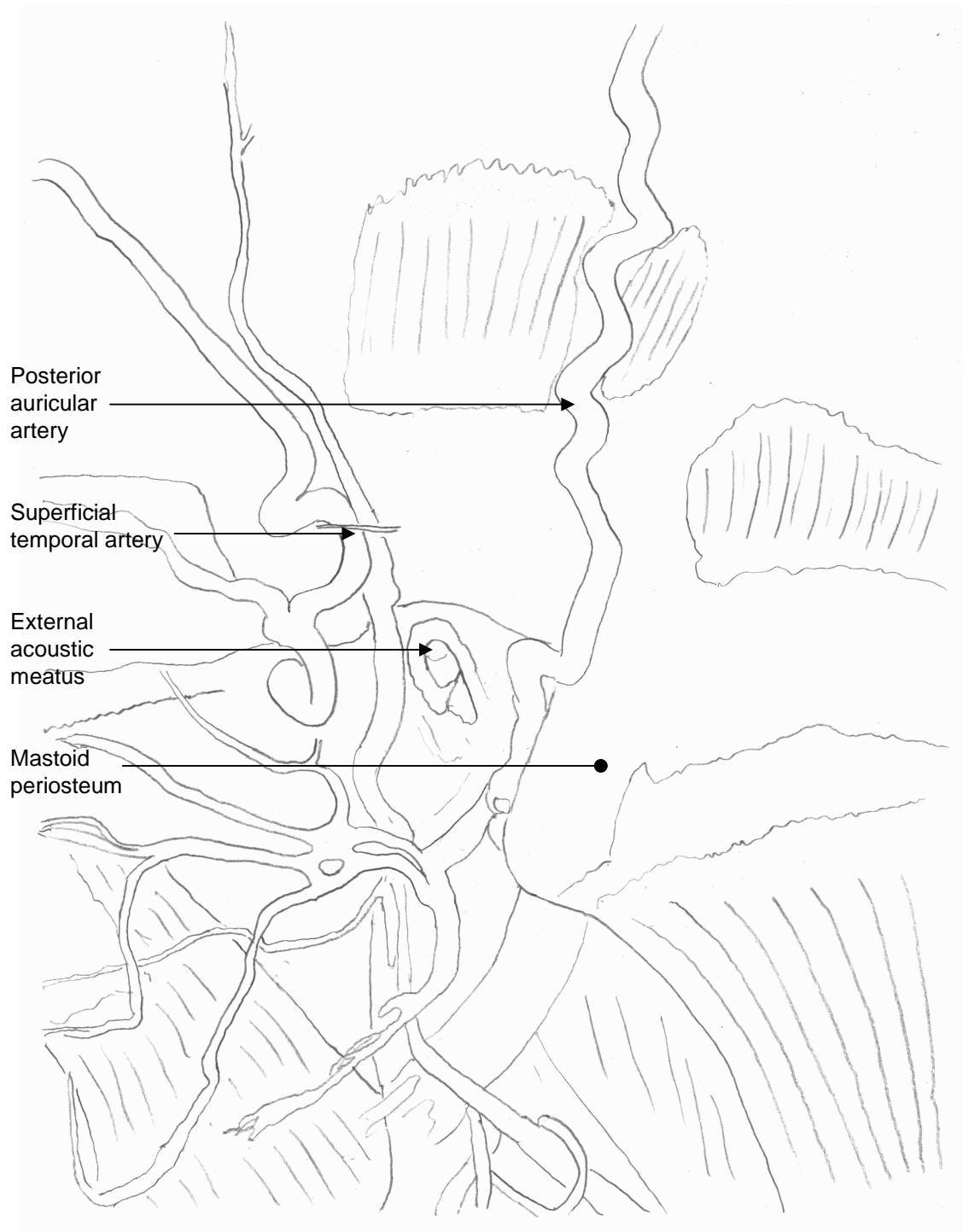


Figure 107 Diagram of left bony external acoustic meatus

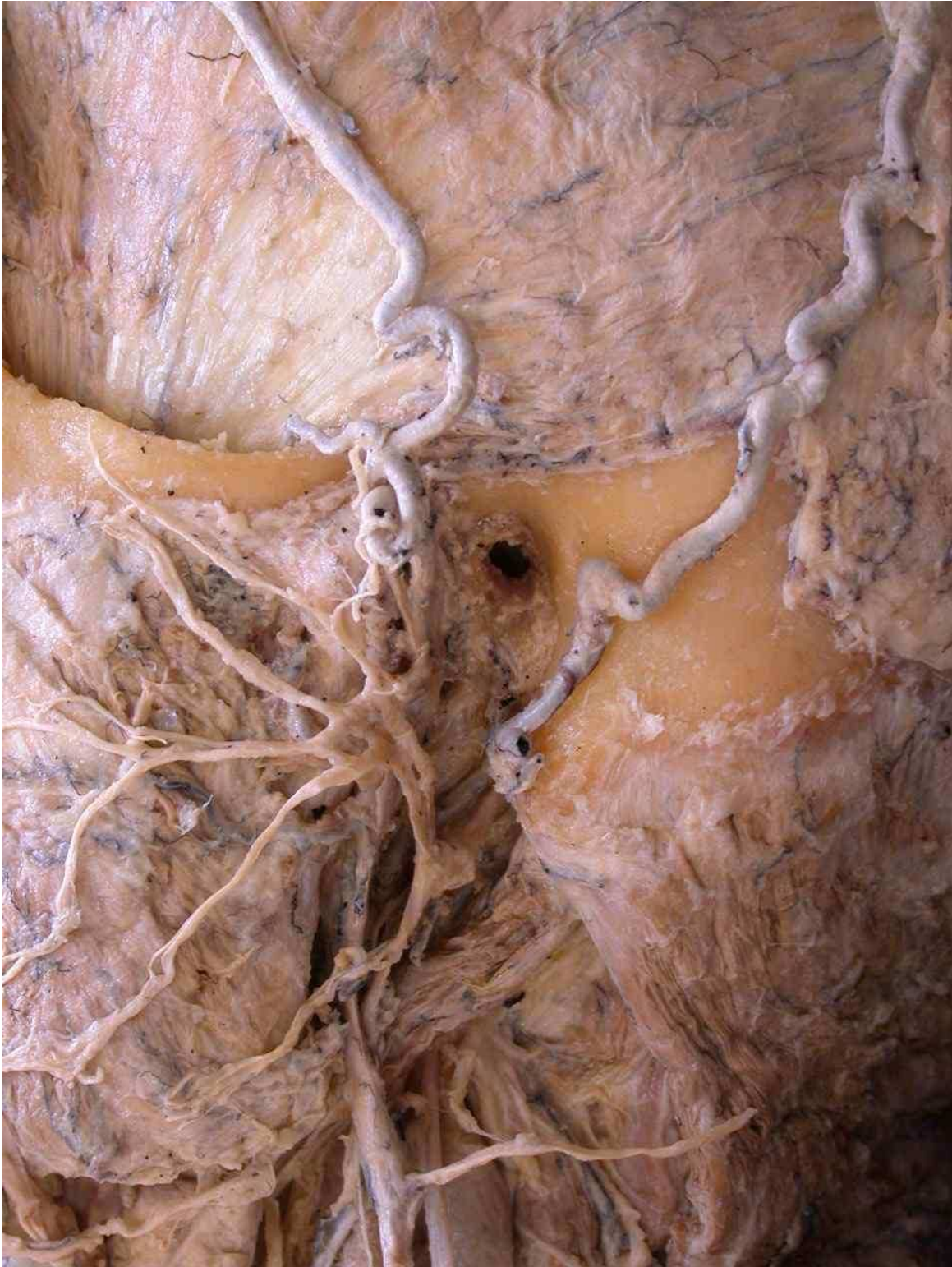


Figure 108 Photograph of left mastoid process with periosteum removed

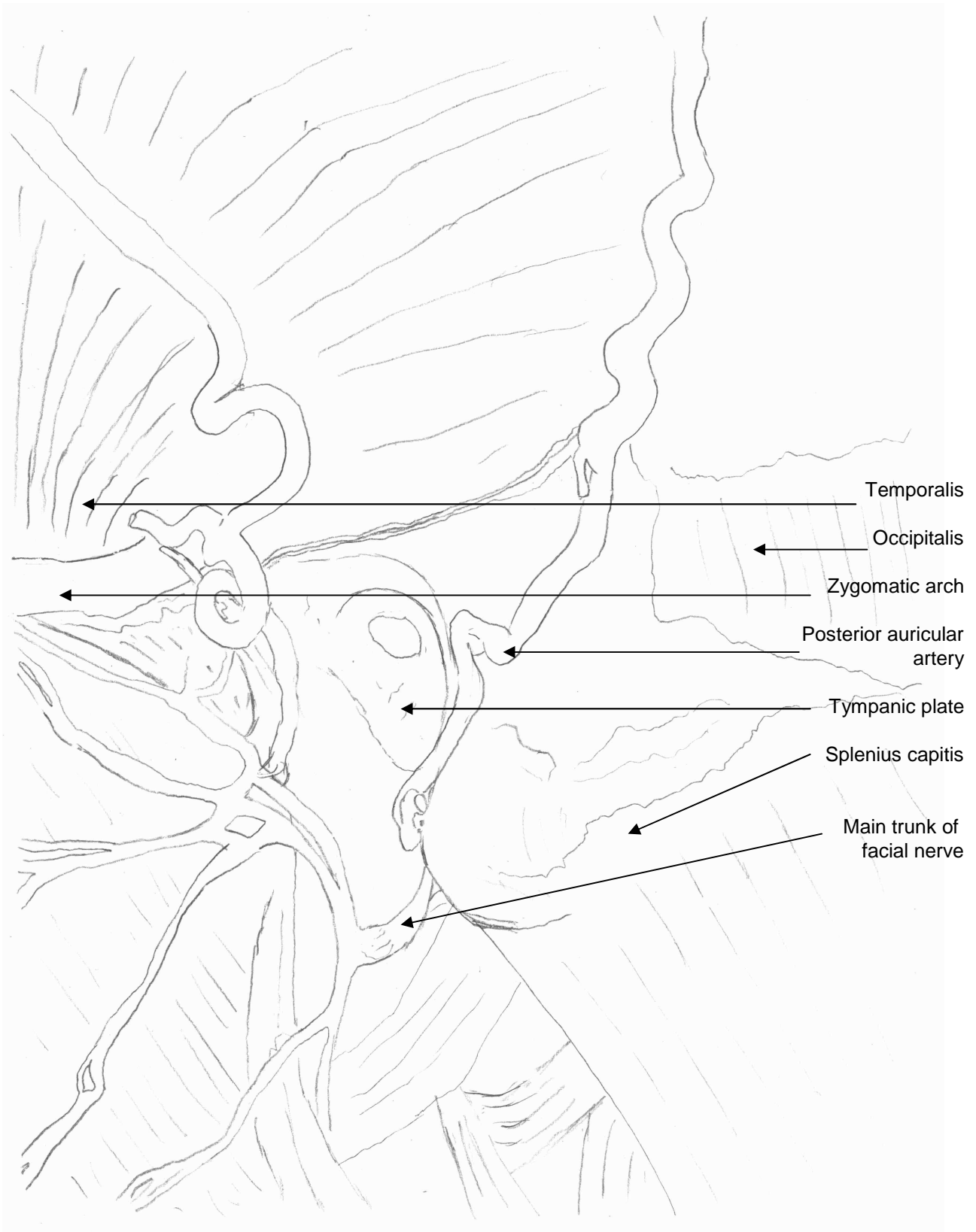


Figure 109 Diagram of left mastoid process with periosteum removed

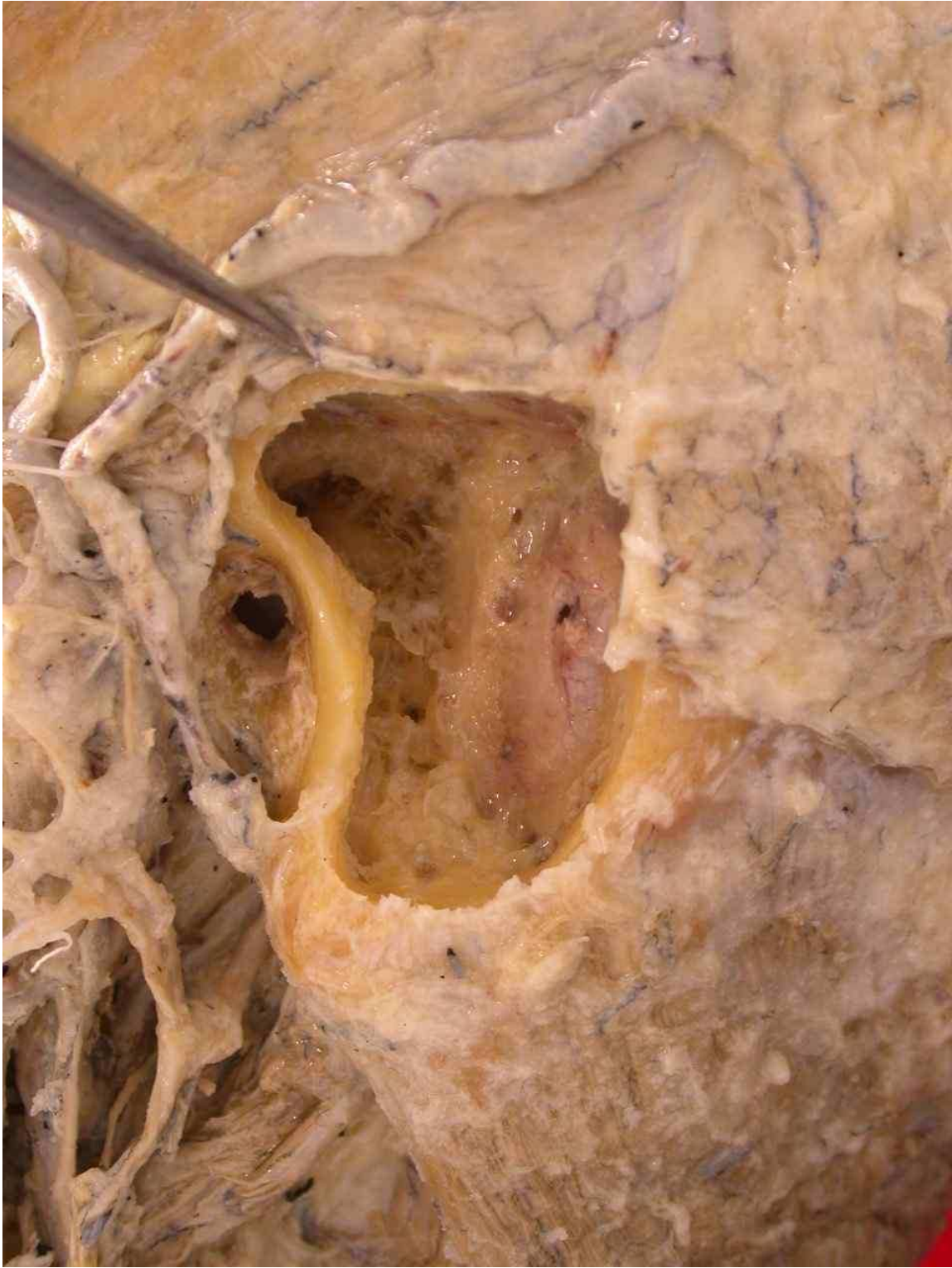


Figure 110 Photograph of left mastoid process with cortex removed

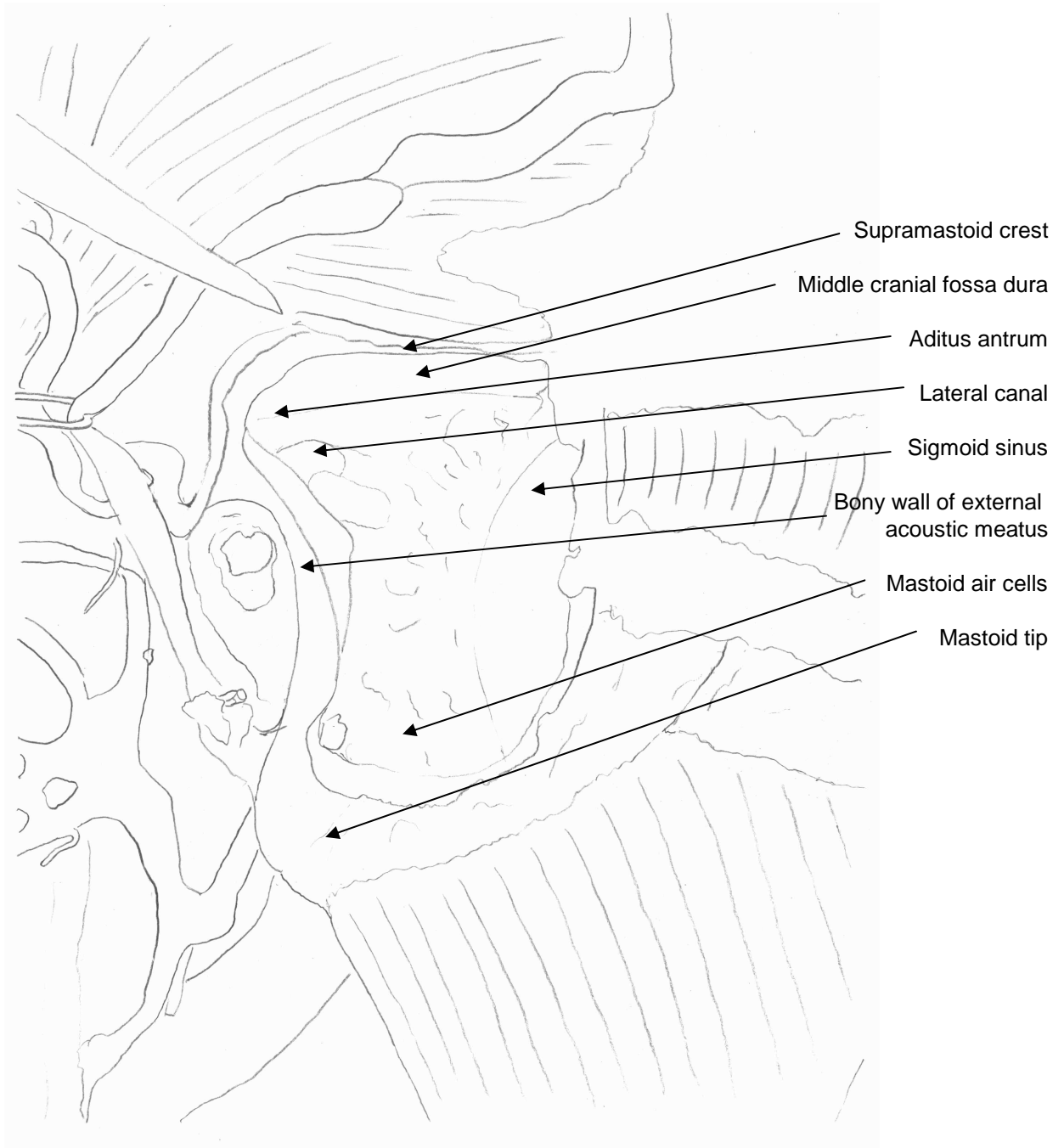


Figure 111 Diagram of left mastoid process with cortex removed

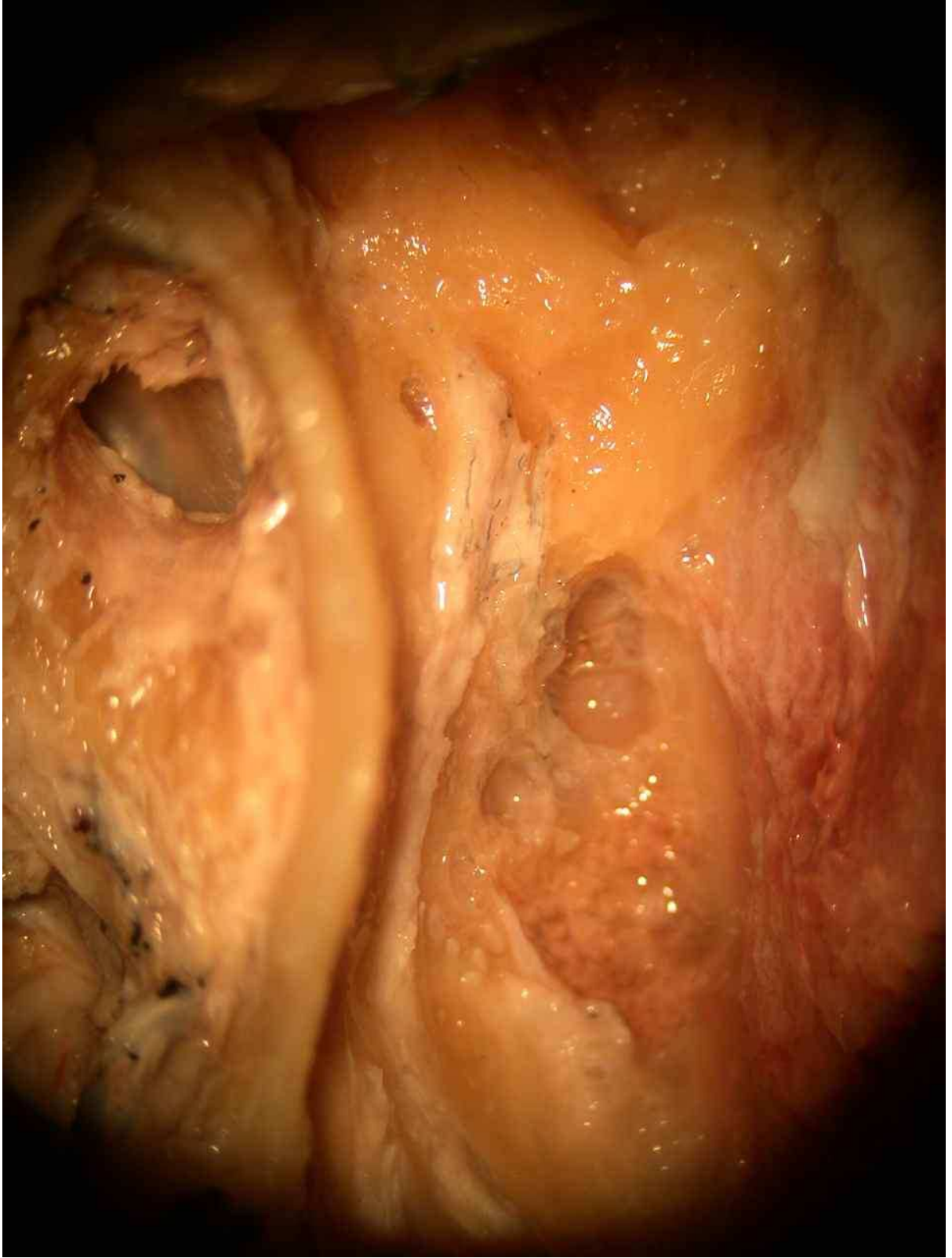


Figure 112 Photograph of left cortical mastoidectomy and endolymphatic sac decompression

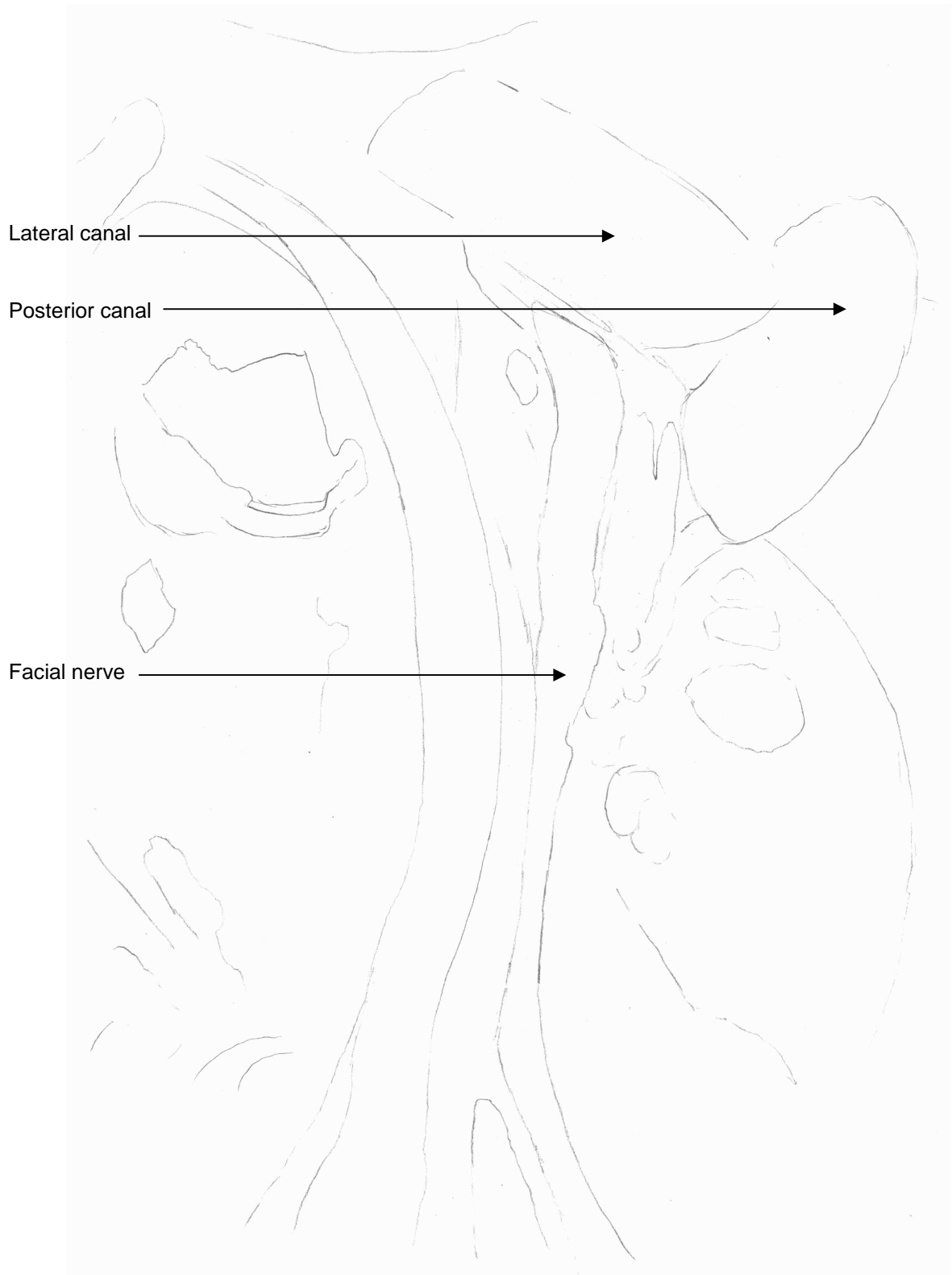


Figure 113 Photograph of left cortical mastoidectomy and endolymphatic sac decompression

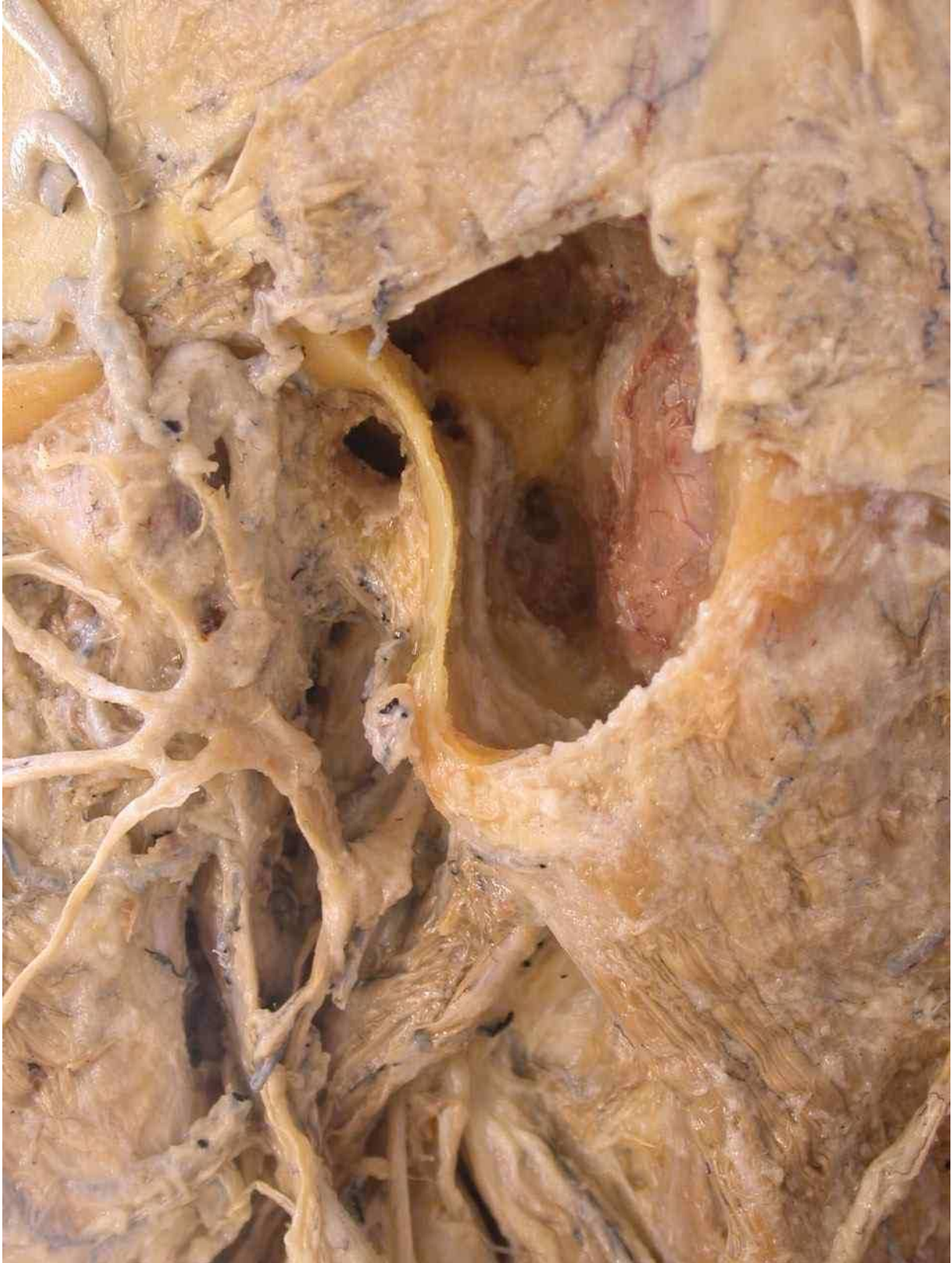


Figure 114 Photograph of left mastoid post endolymphatic sac decompression

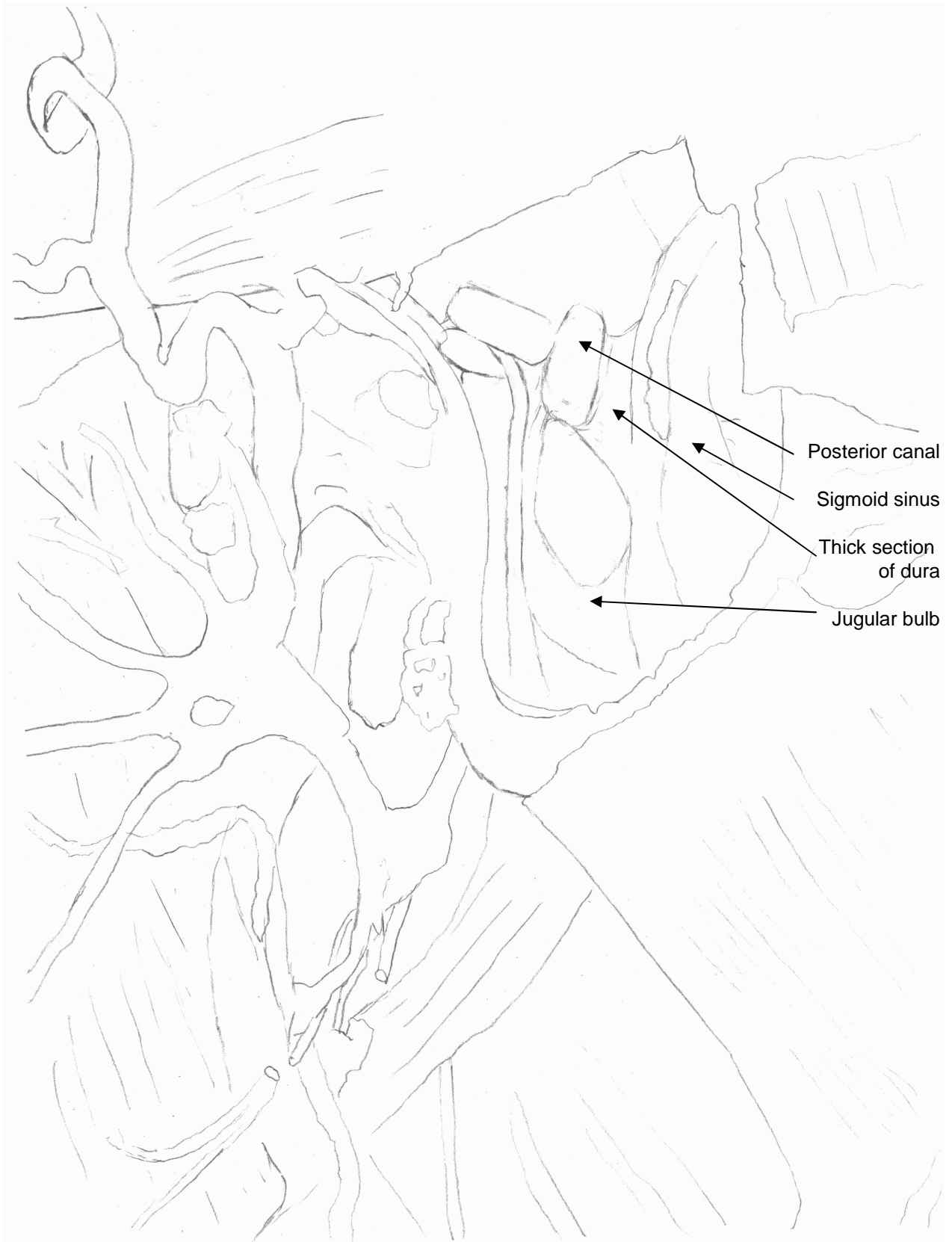


Figure 115 Diagram of left mastoid post endolymphatic sac decompression



Figure 116 Photograph of superficial back of head and neck dissection2

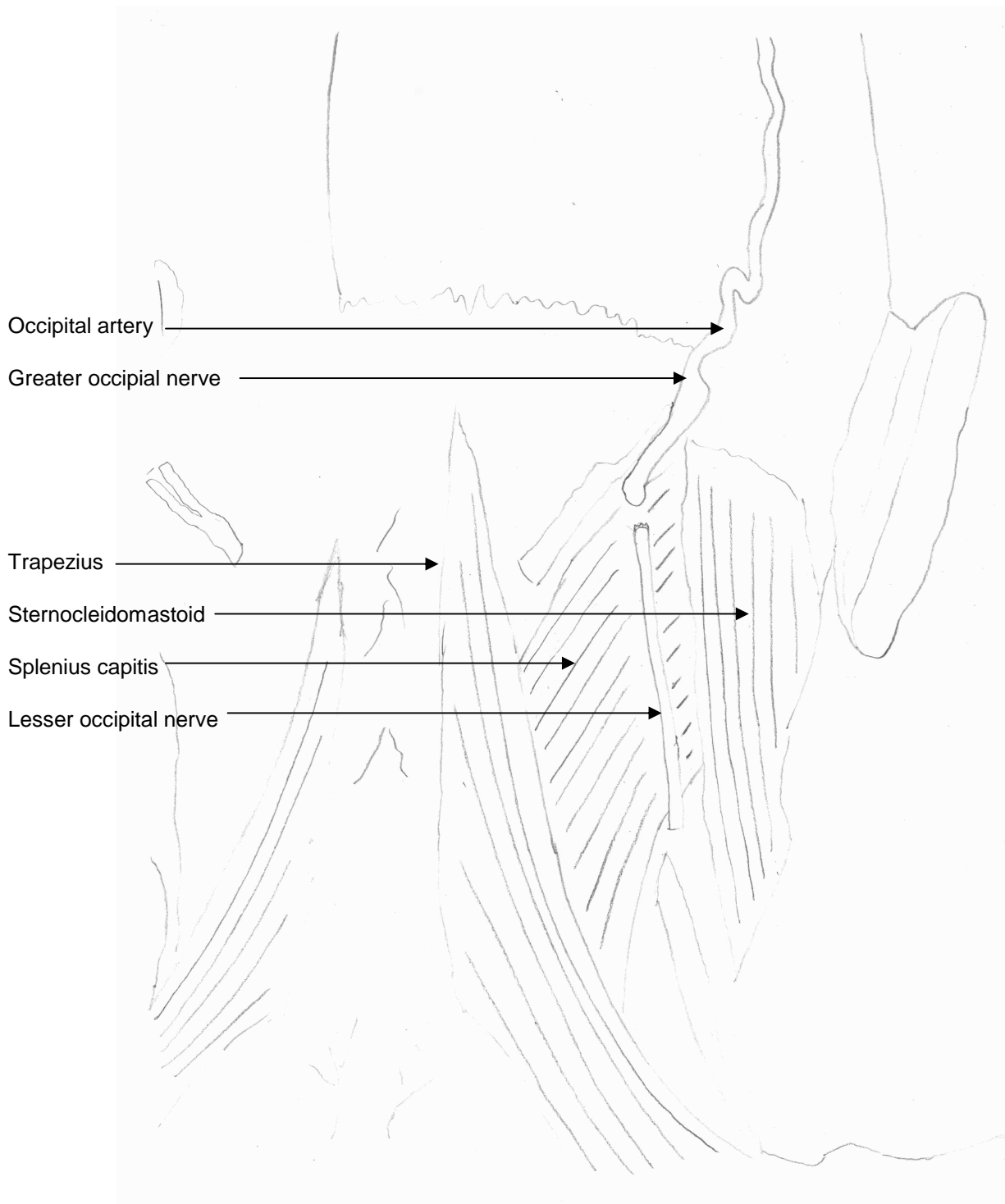


Figure 117 Diagram of superficial back of head and neck dissection



Figure 118 Photograph of neck dissection following removal of trapezius

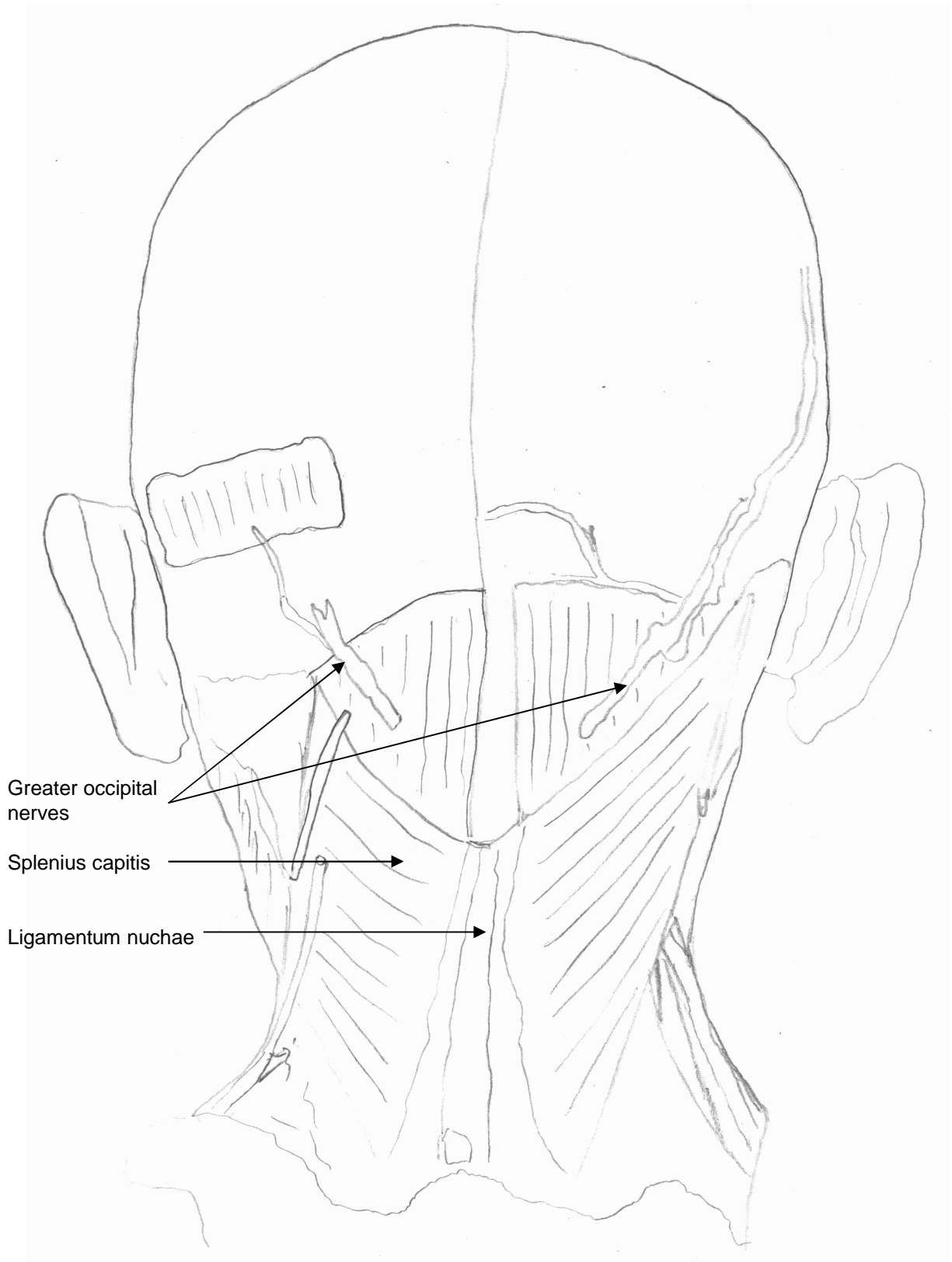


Figure 119 Photograph of neck dissection following removal of trapezius

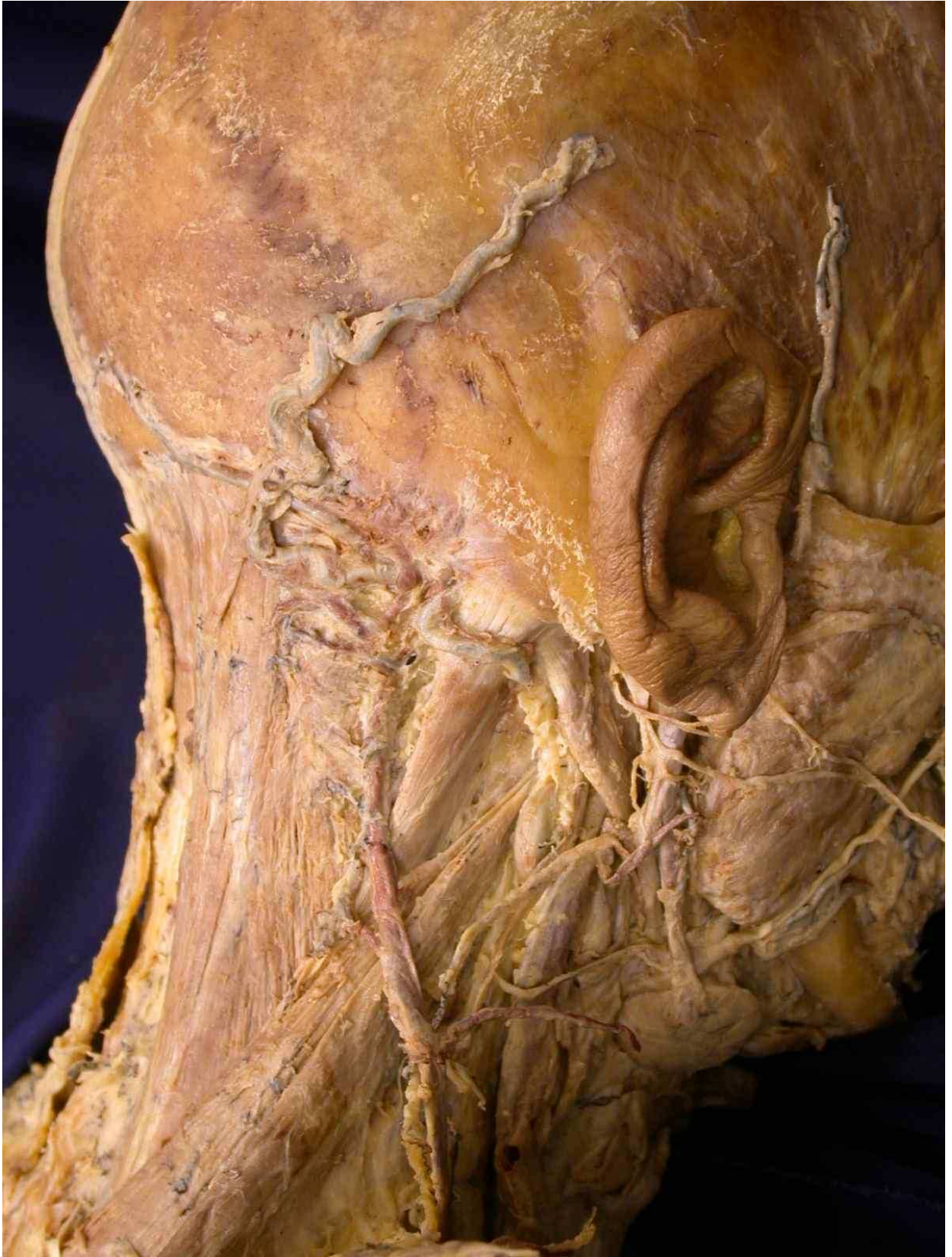


Figure 120 Photograph of lateral view of neck dissection



Figure 121 Diagram of lateral view of neck dissection



Figure 122 Photograph of longissimus capitis

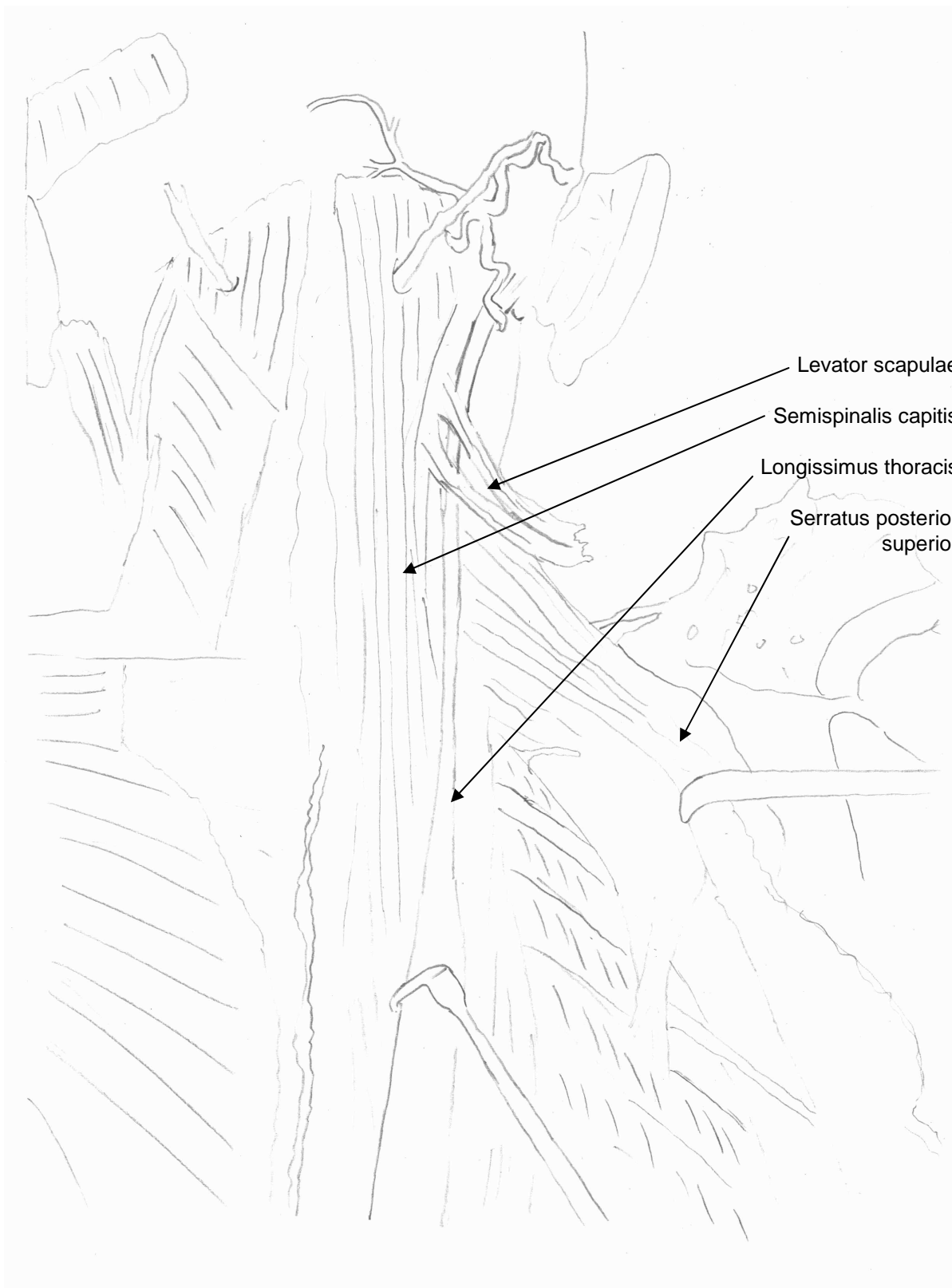


Figure 123 Diagram of longissimus capitis

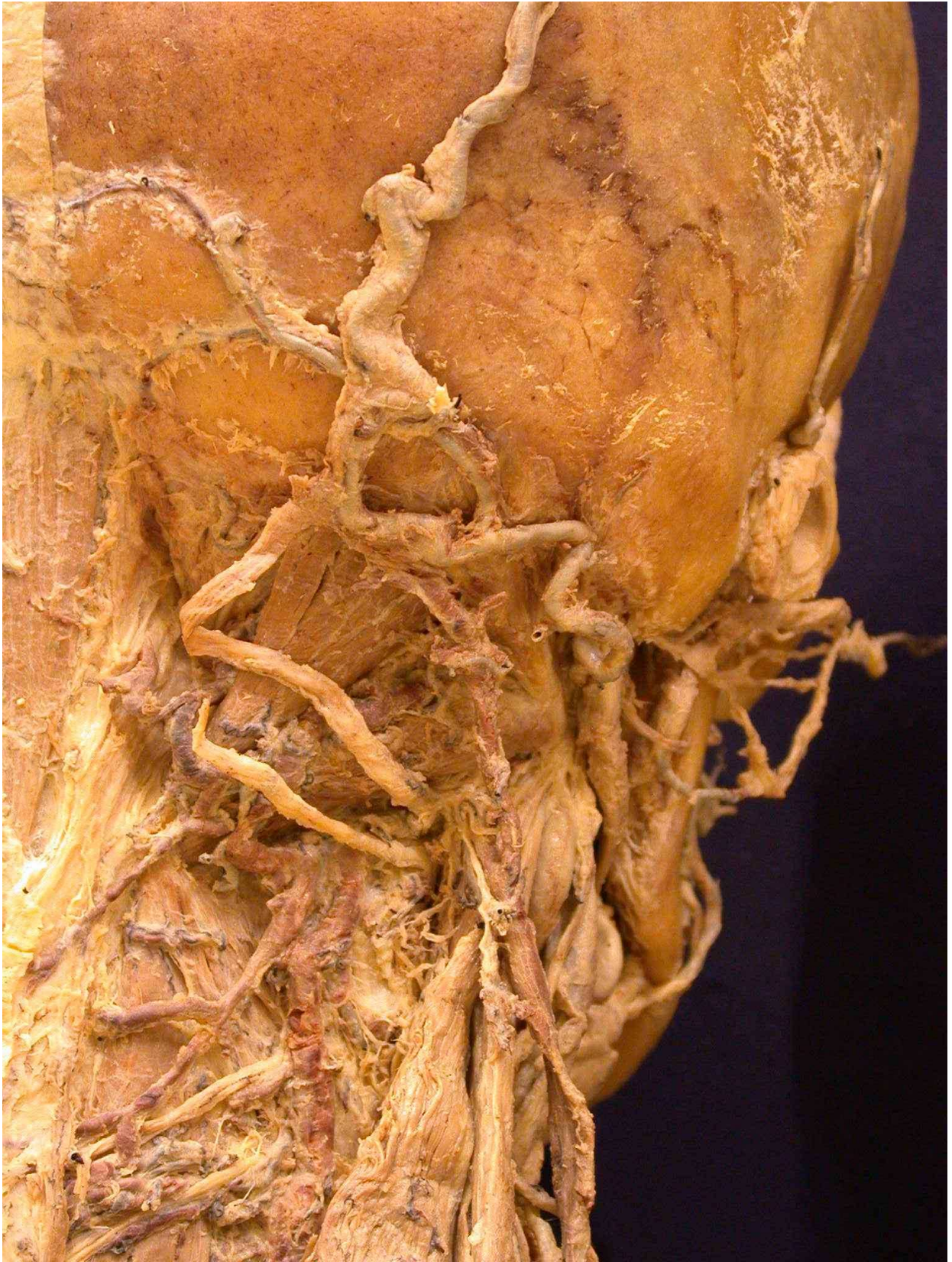


Figure 124 Photograph of posterior view of right suboccipital triangle

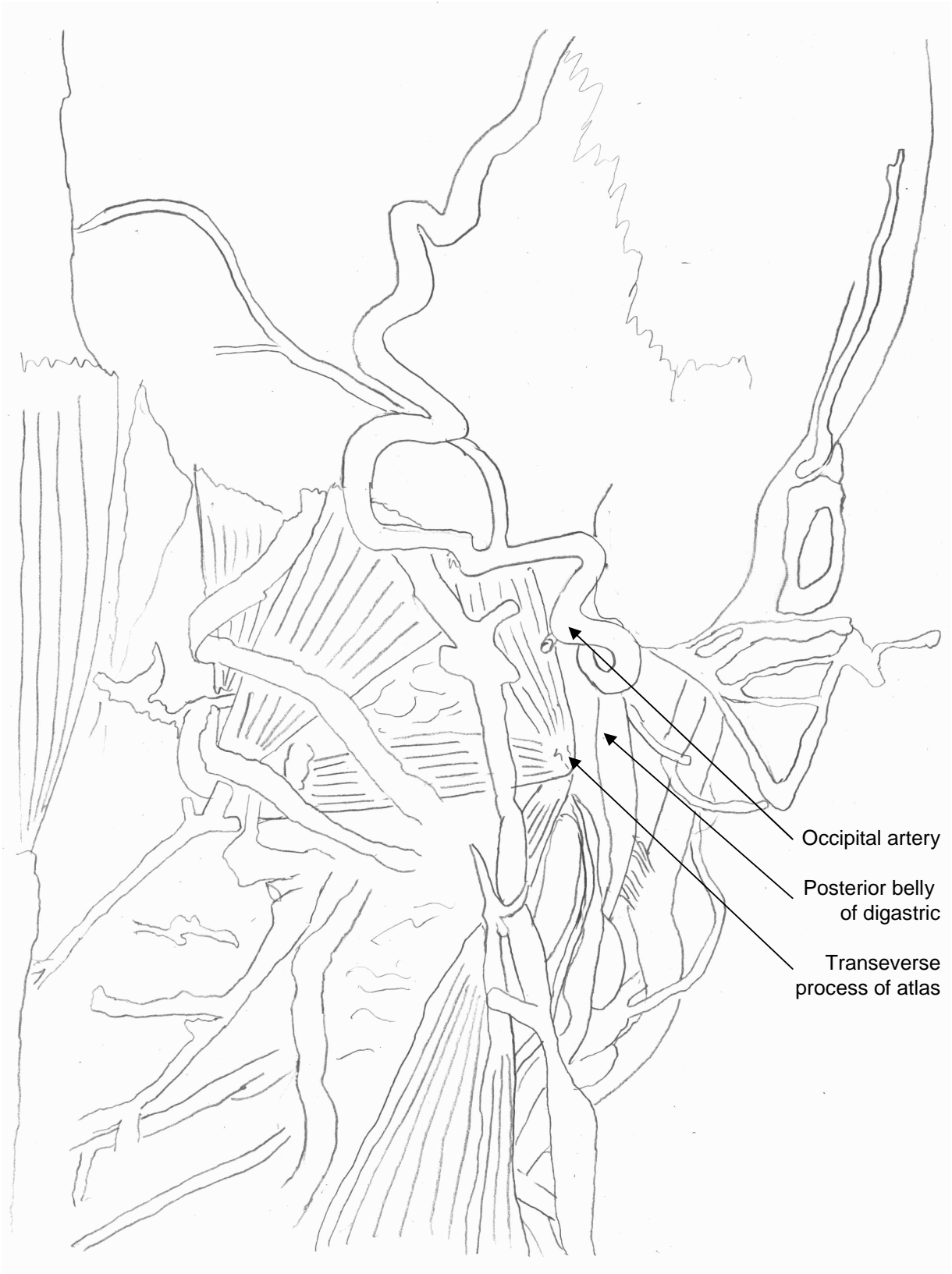


Figure 125 Diagram of posterior view of right suboccipital triangle



Figure 126 Photograph of posterior view of left suboccipital triangle

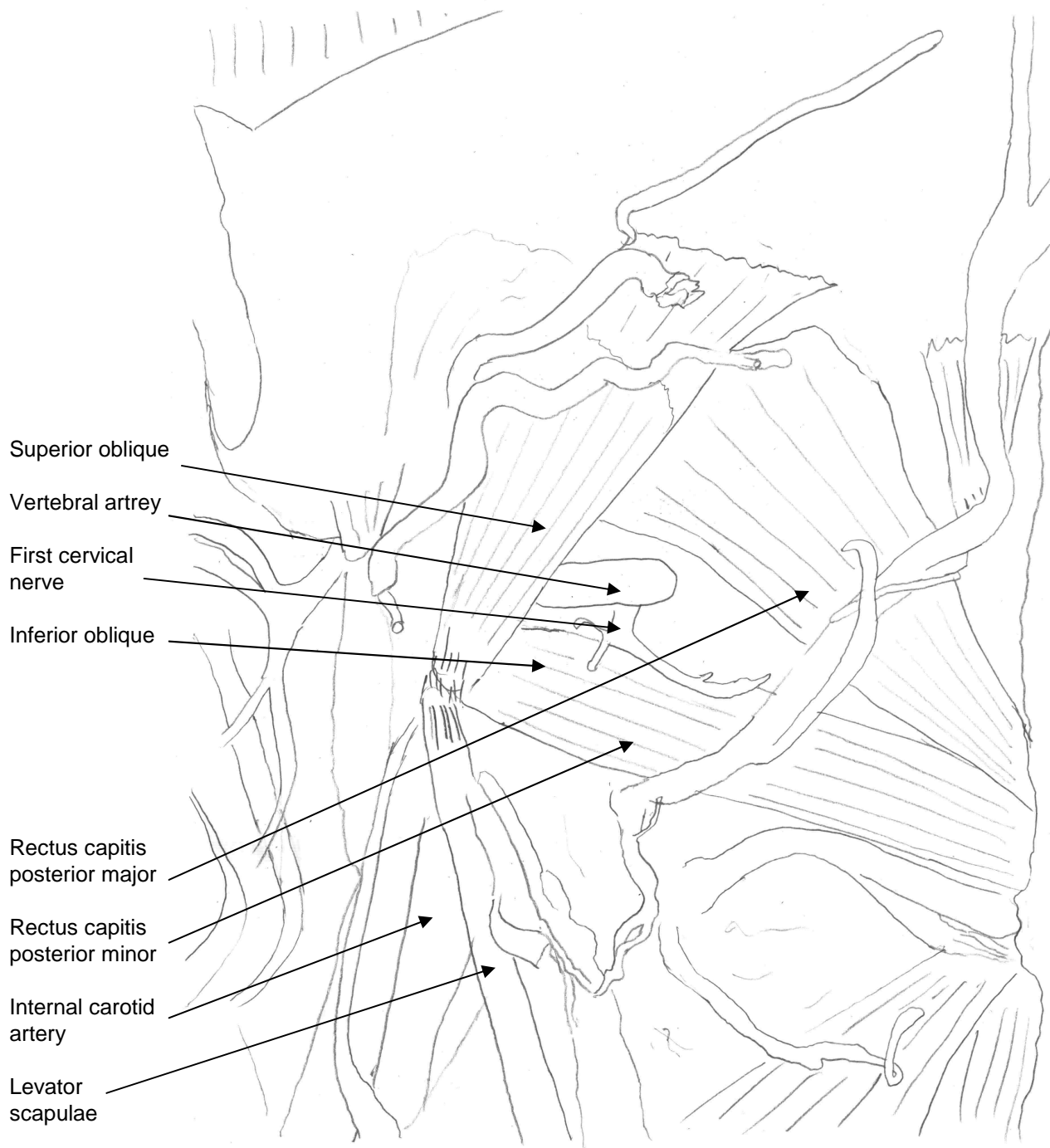


Figure 127 Diagram of posterior view of left suboccipital triangle



Figure 128 Photograph of posterior view of deep neck dissection

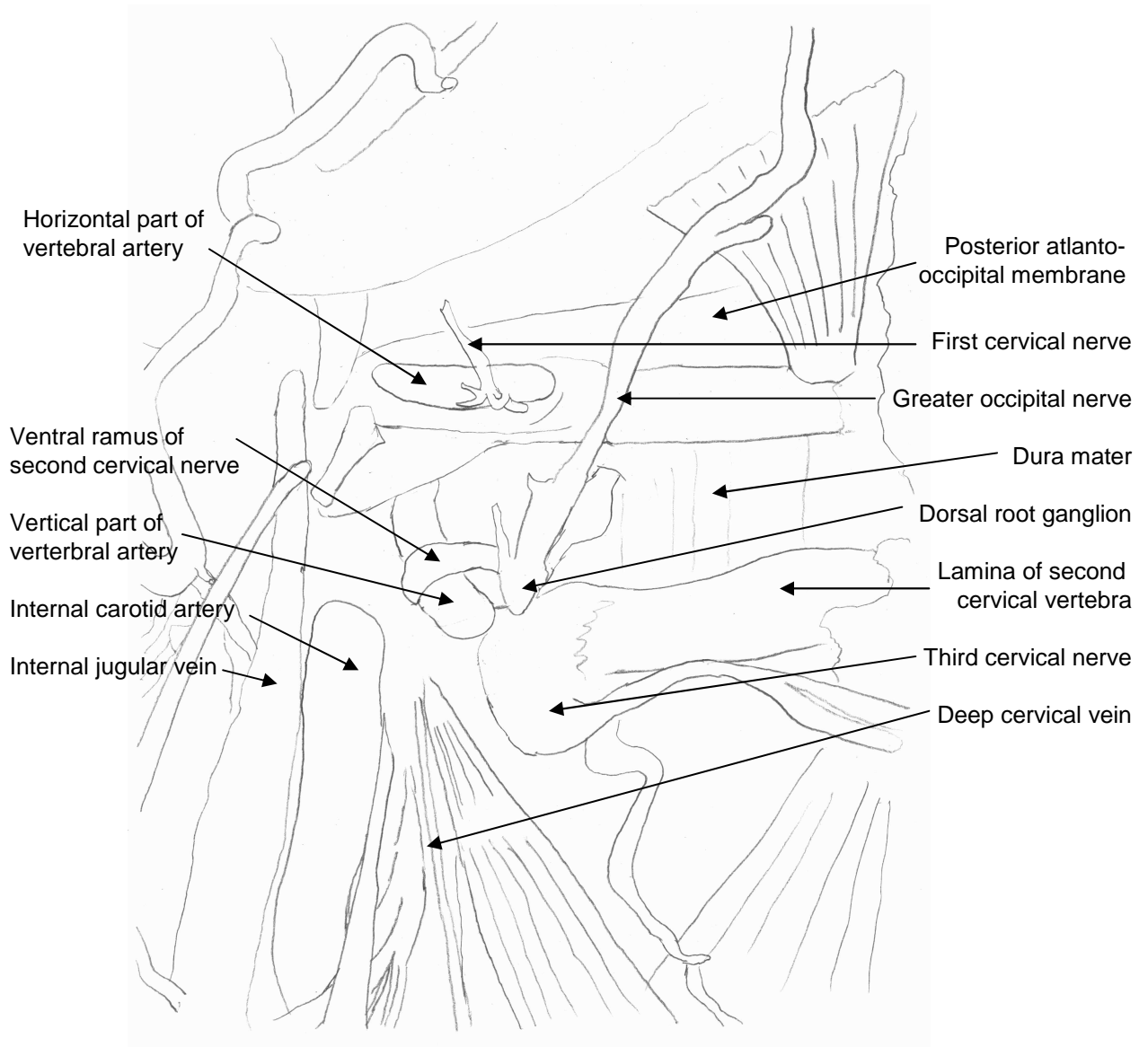


Figure 129 Diagram of posterior view of deep neck dissection



Figure 130 Photograph of lateral view of posterior cranial fossa opened

Dura of middle fossa

Posterior limb of
middle meningeal artery

Transverse
venous sinus

Dura of posterior
fossa

Sigmoid sinus

Mastoid process

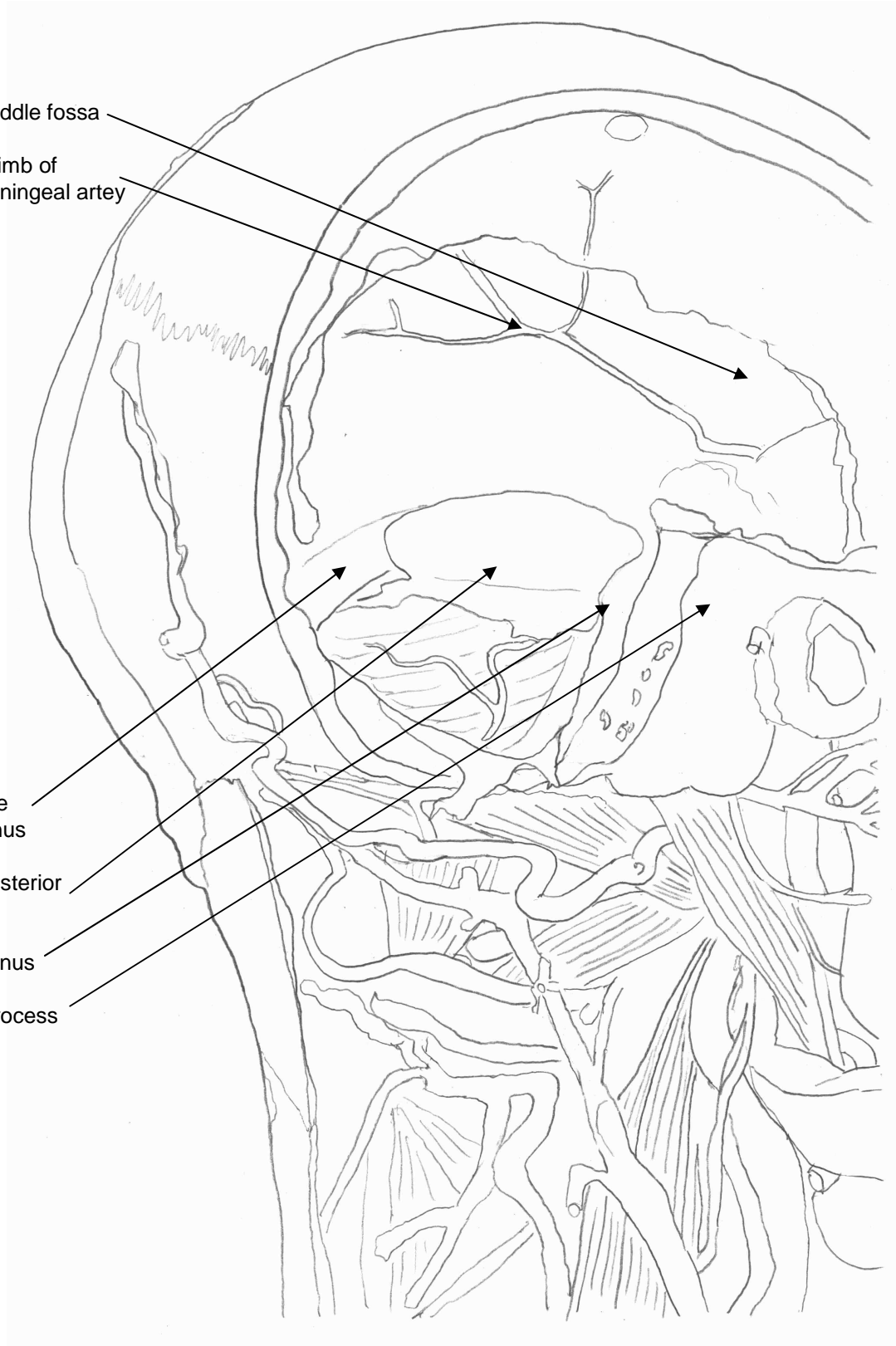


Figure 131 Diagram of lateral view of posterior cranial fossa opened

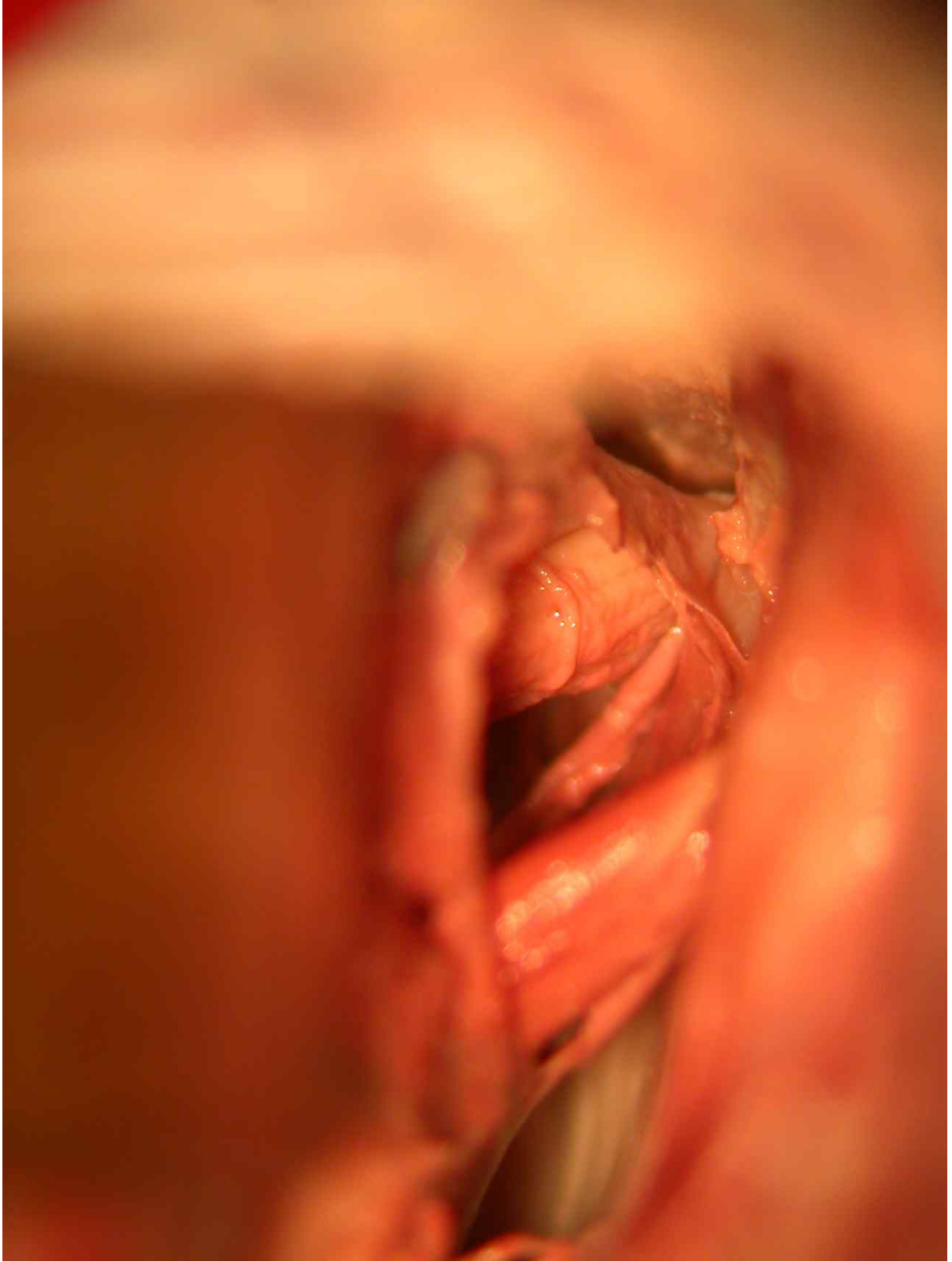


Figure 132 Photograph of superior aspect of space between hind brain and clivus

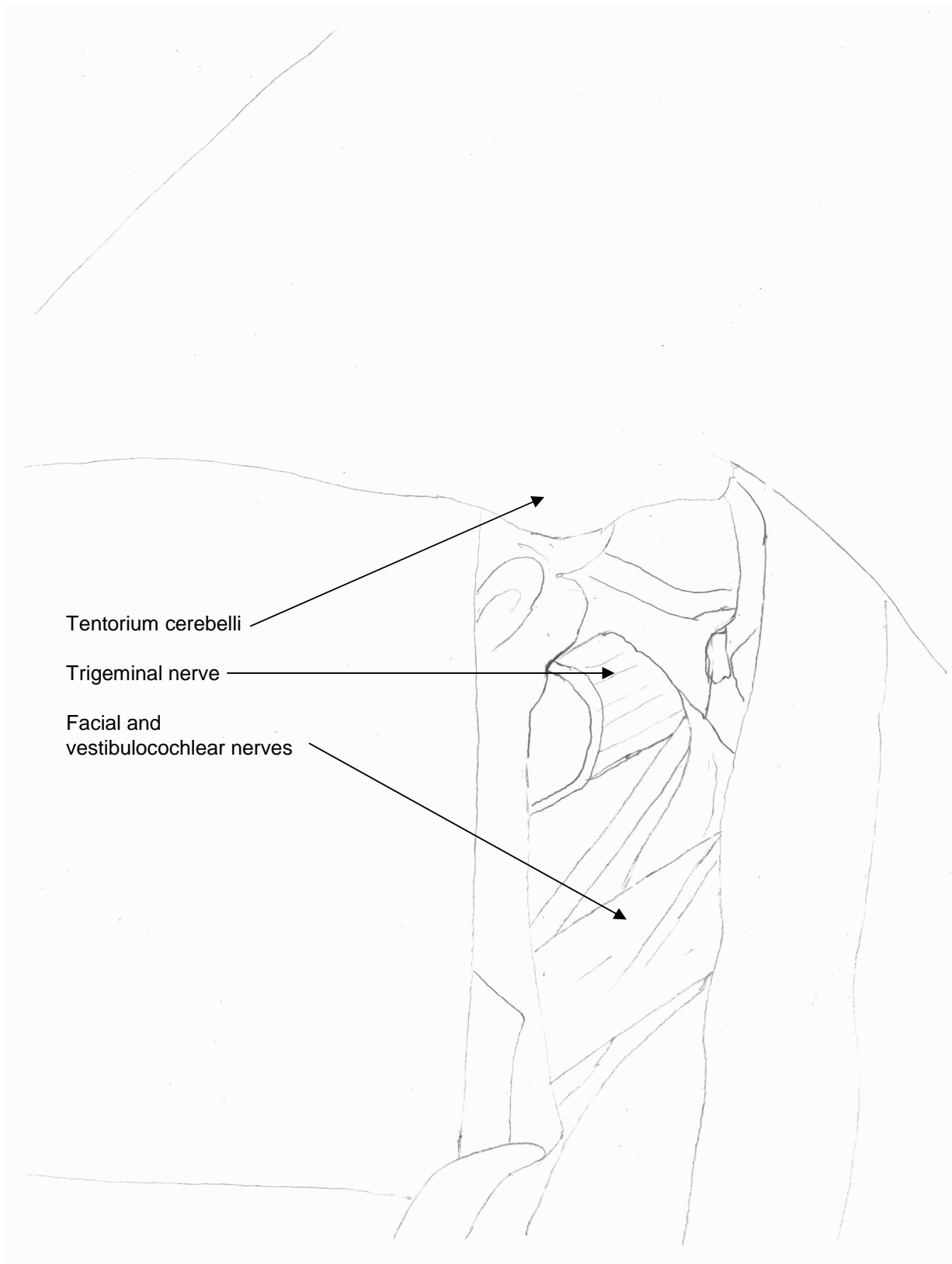


Figure 133 Diagram of superior aspect of space between hind brain and clivus

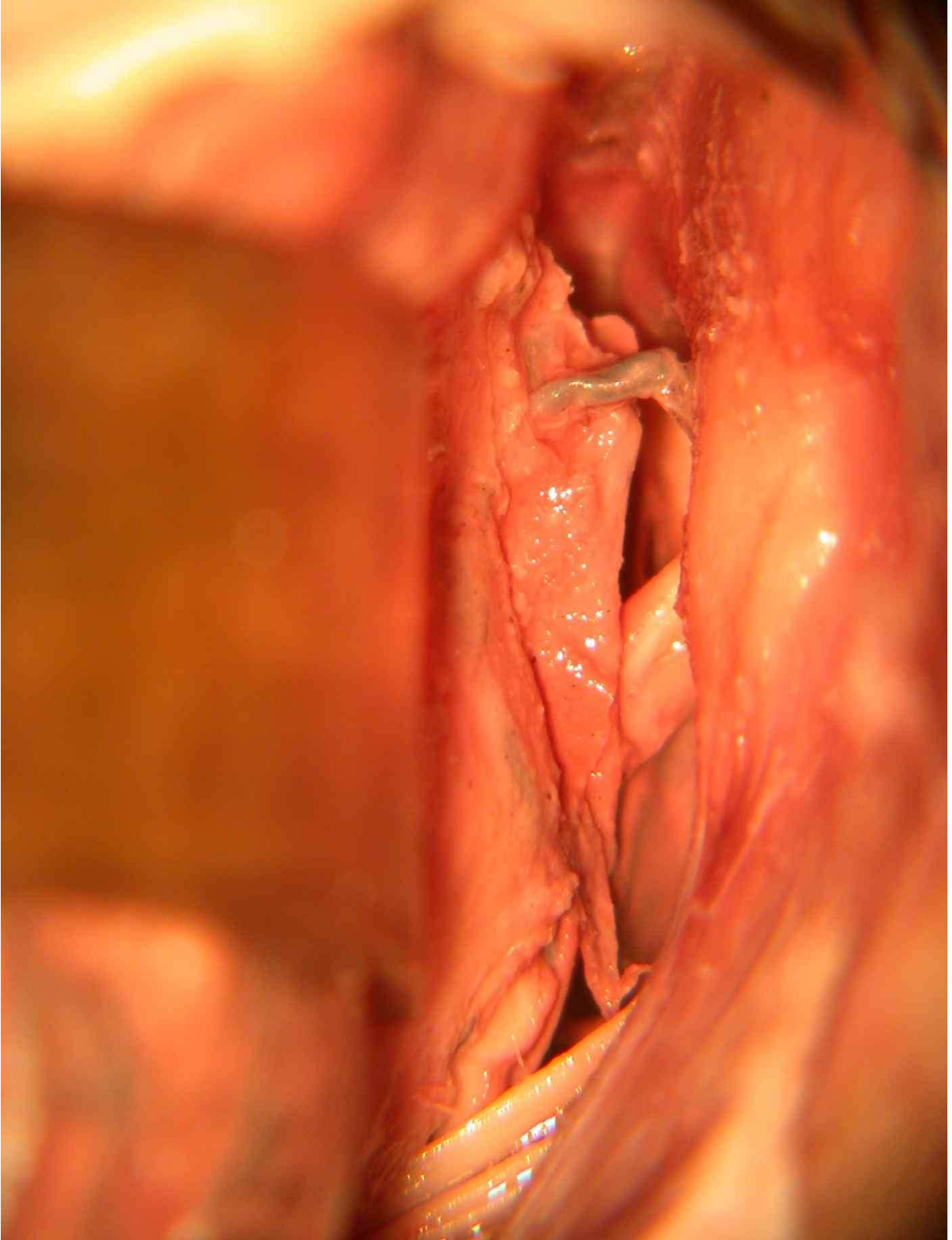


Figure 134 Photograph of space between hindbrain and anterior wall of the posterior cranial fossa

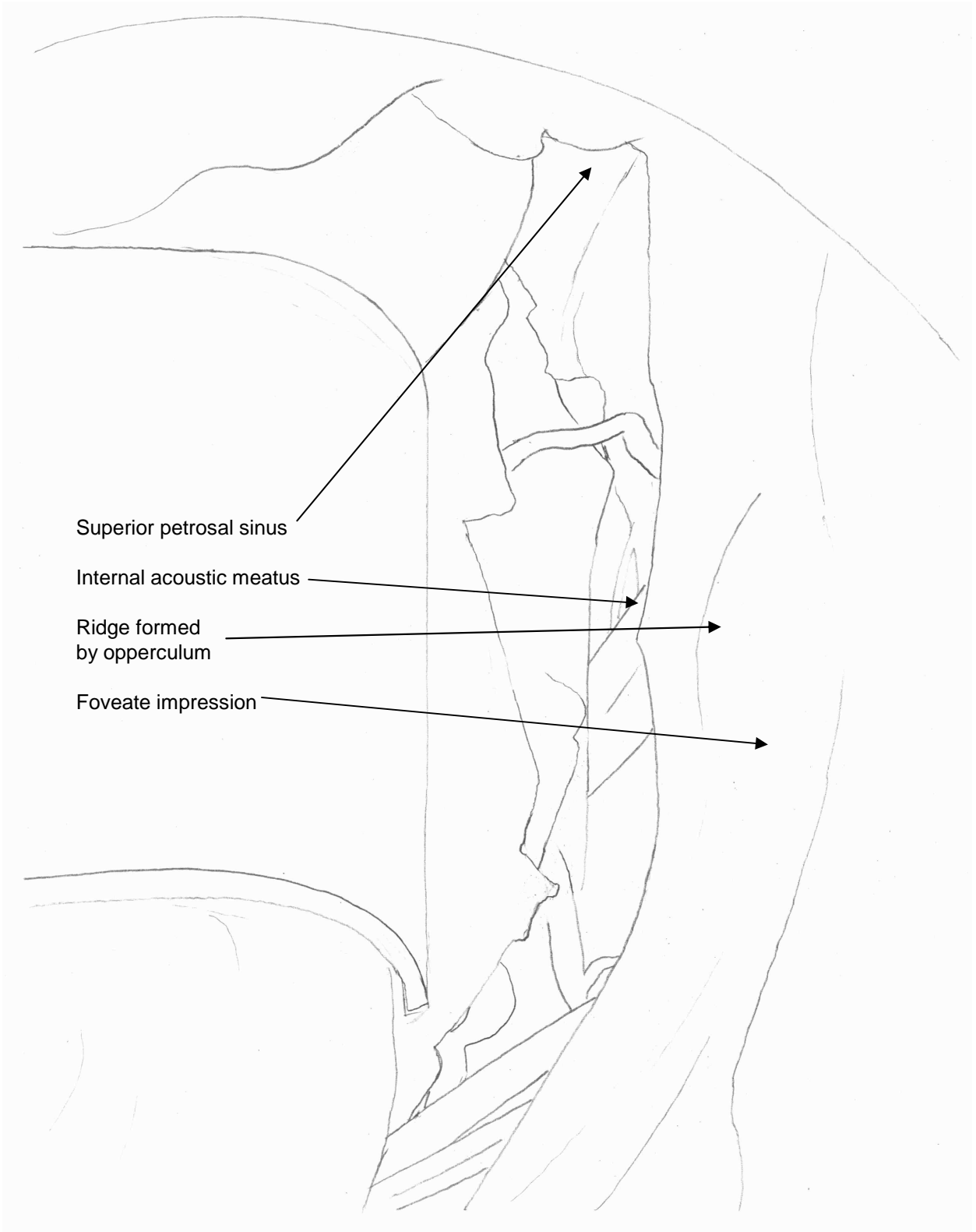


Figure 135 Diagram of space between hindbrain and anterior wall of the posterior cranial fossa



Figure 136 Photograph of left and right suboccipital triangles

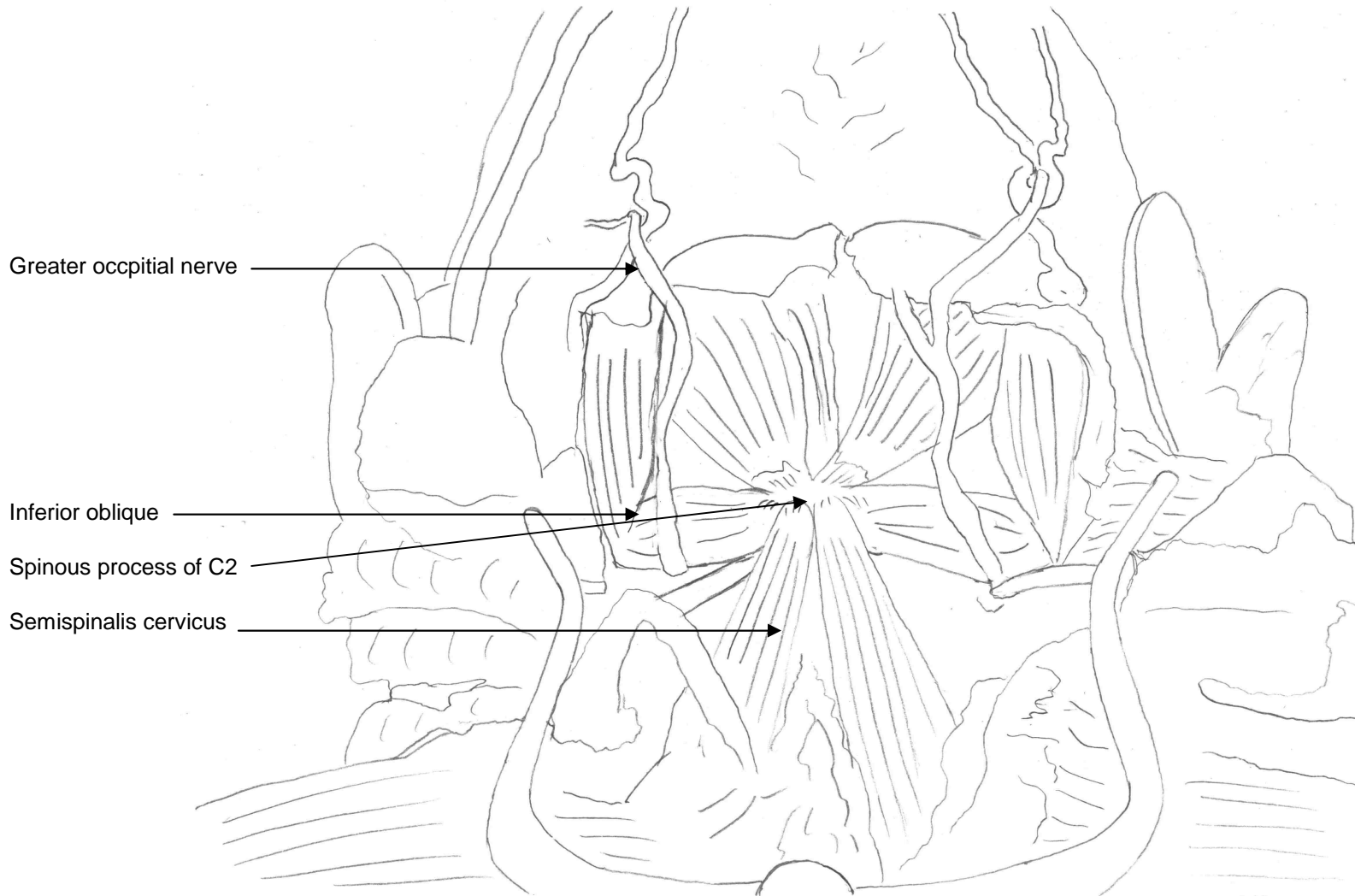


Figure 137 Photograph of left and right suboccipital triangles



Figure 138 Photograph of right deep suboccipital dissection

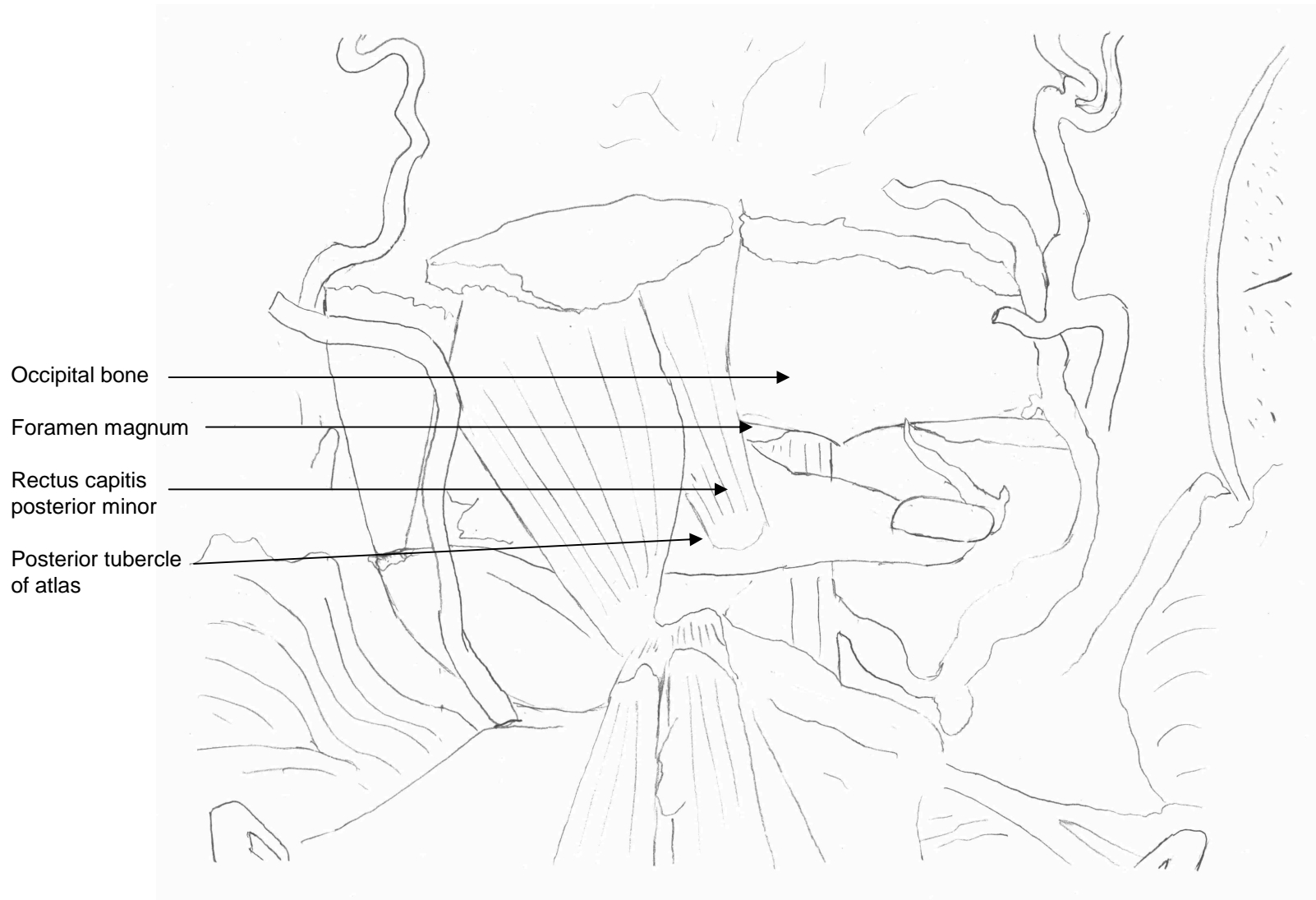


Figure 139 Diagram of right deep suboccipital dissection



Figure 140 Photograph of posterior view of right posterior cranial fossa opened

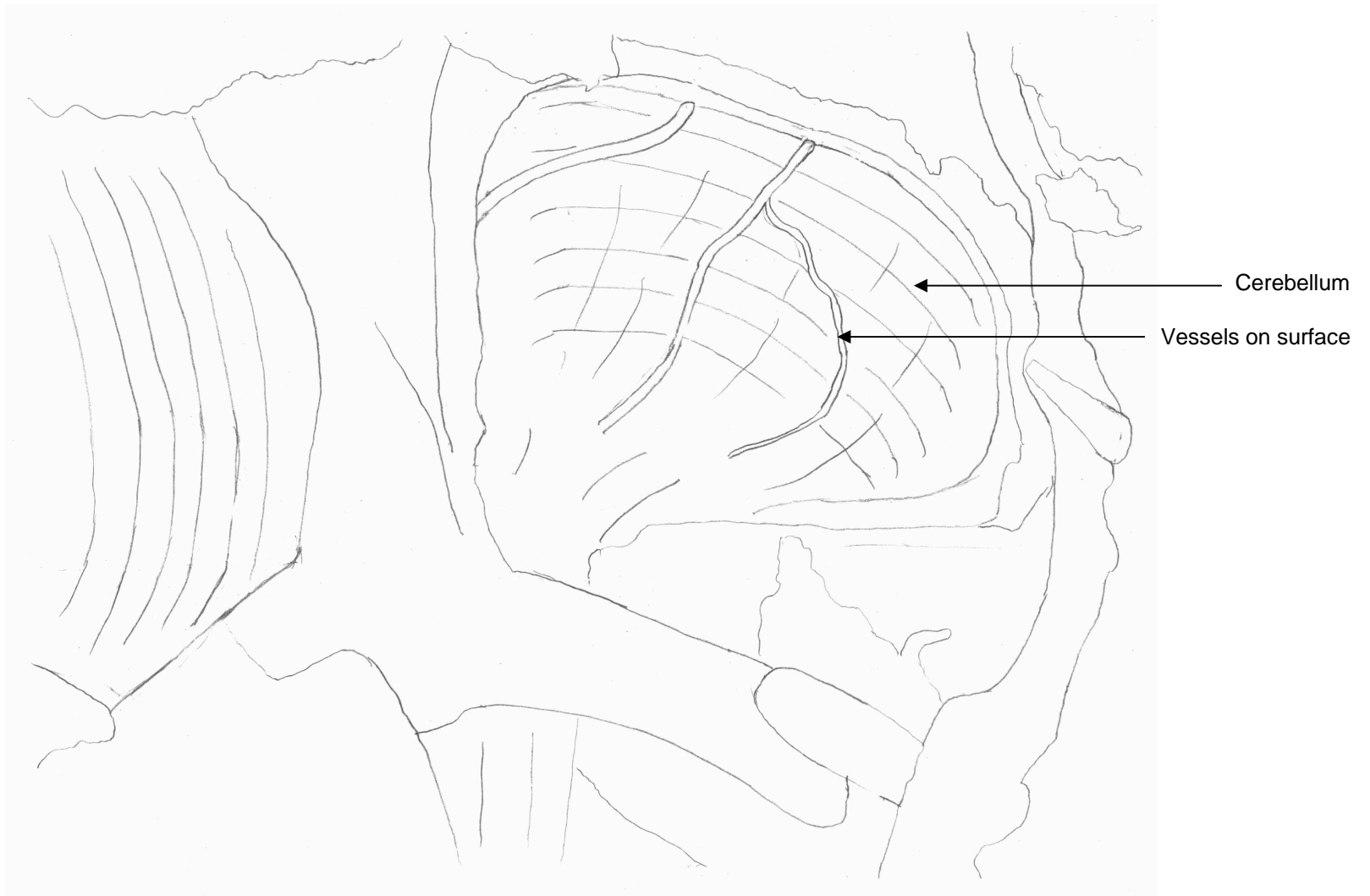


Figure 141 Diagram of posterior view of right posterior cranial fossa opened

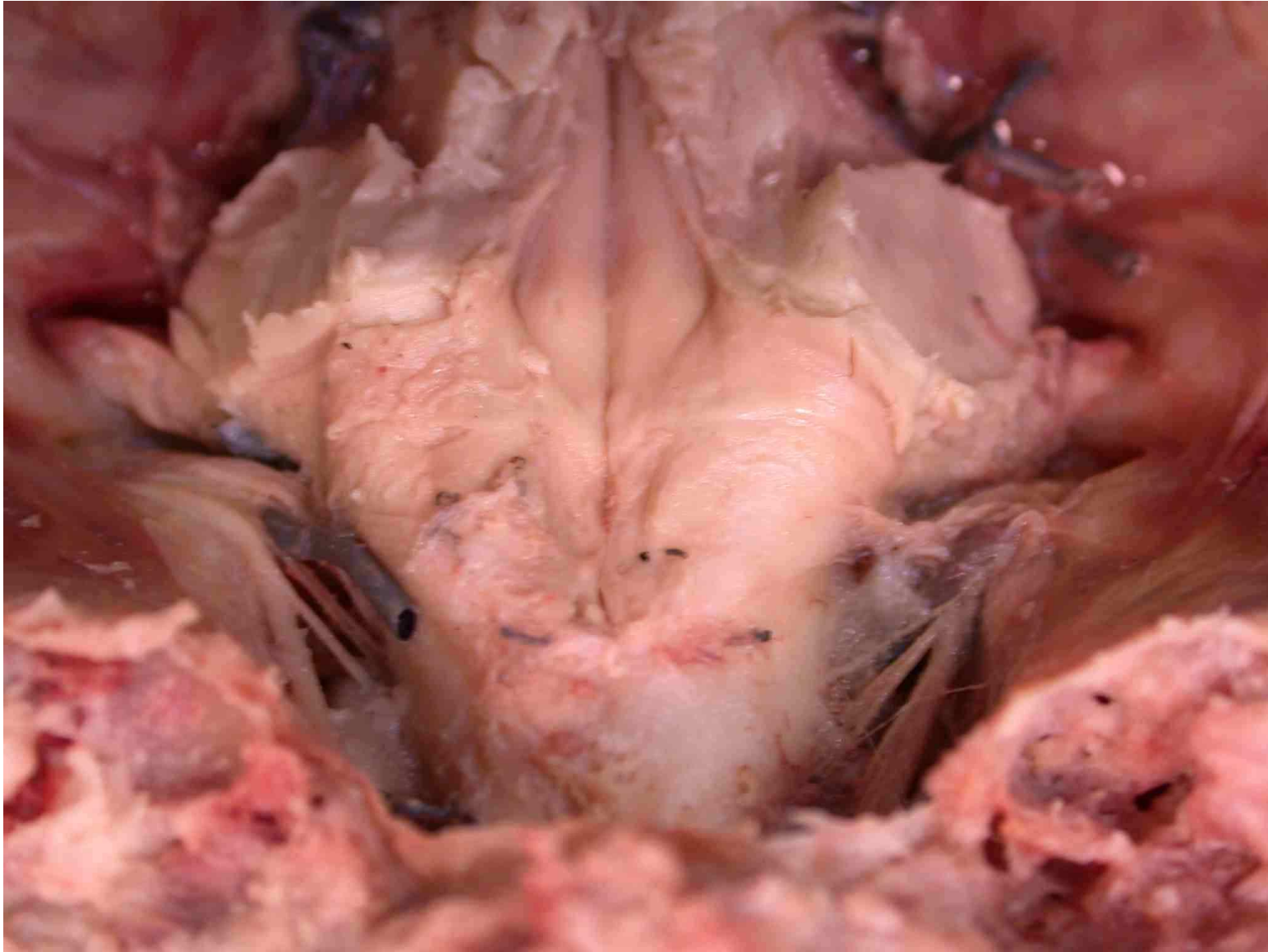


Figure 142 Photograph of posterior view of hindbrain with cerebellum removed

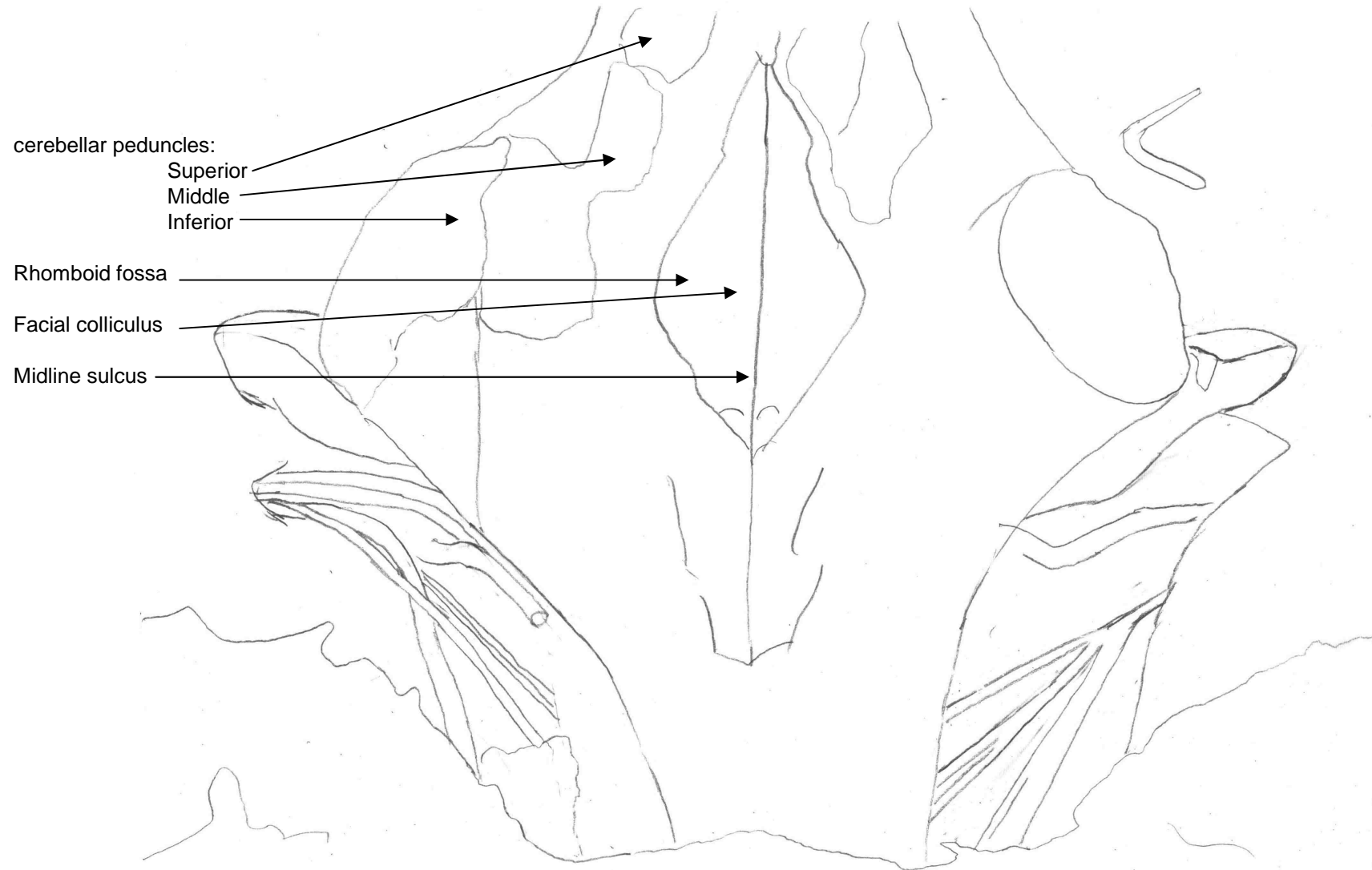


Figure 143 Photograph of posterior view of hindbrain with cerebellum removed



Figure 144 Photograph of posterior view of anterior wall of left posterior cranial fossa

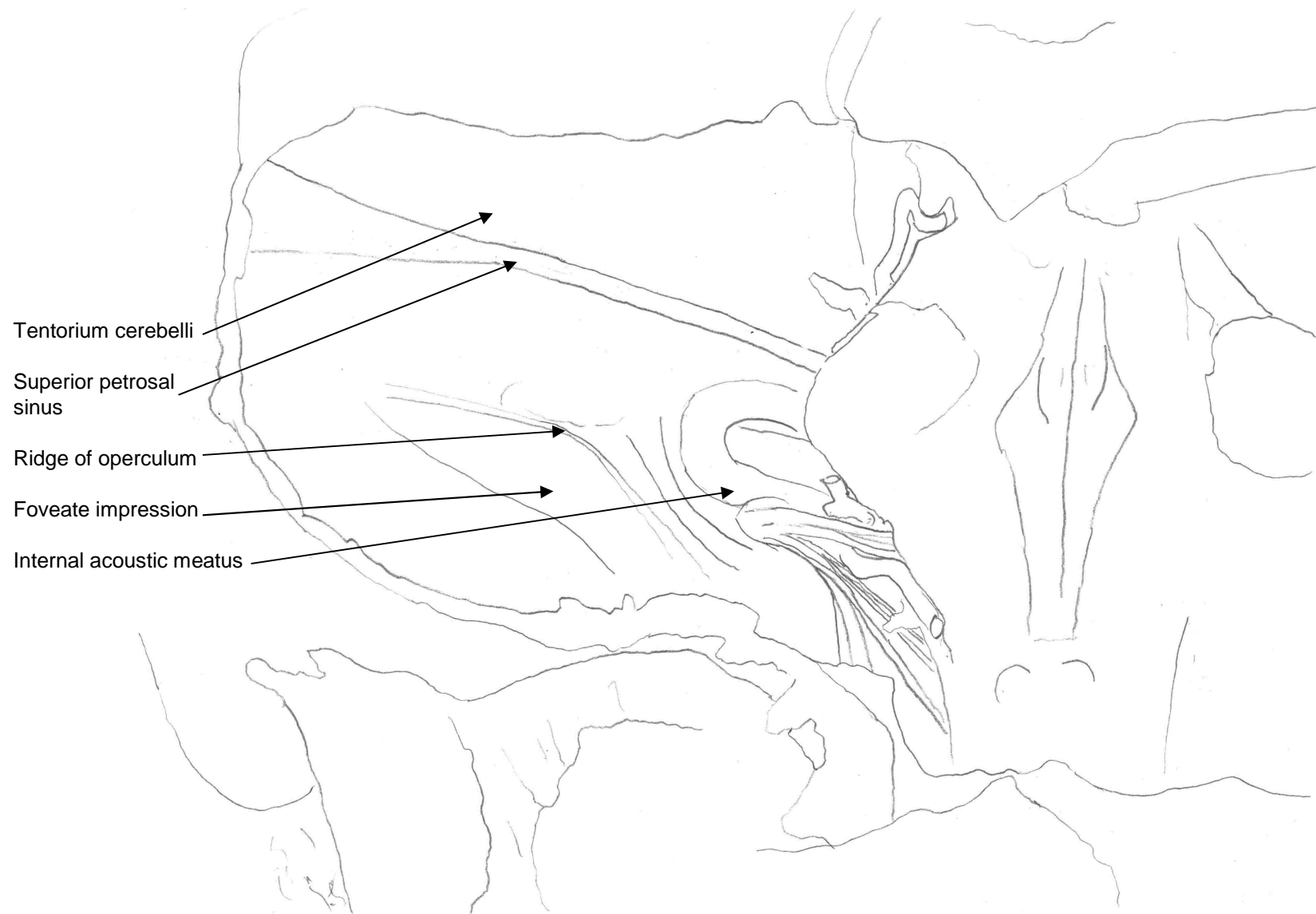


Figure 145 Diagram of posterior view of anterior wall of left posterior cranial fossa

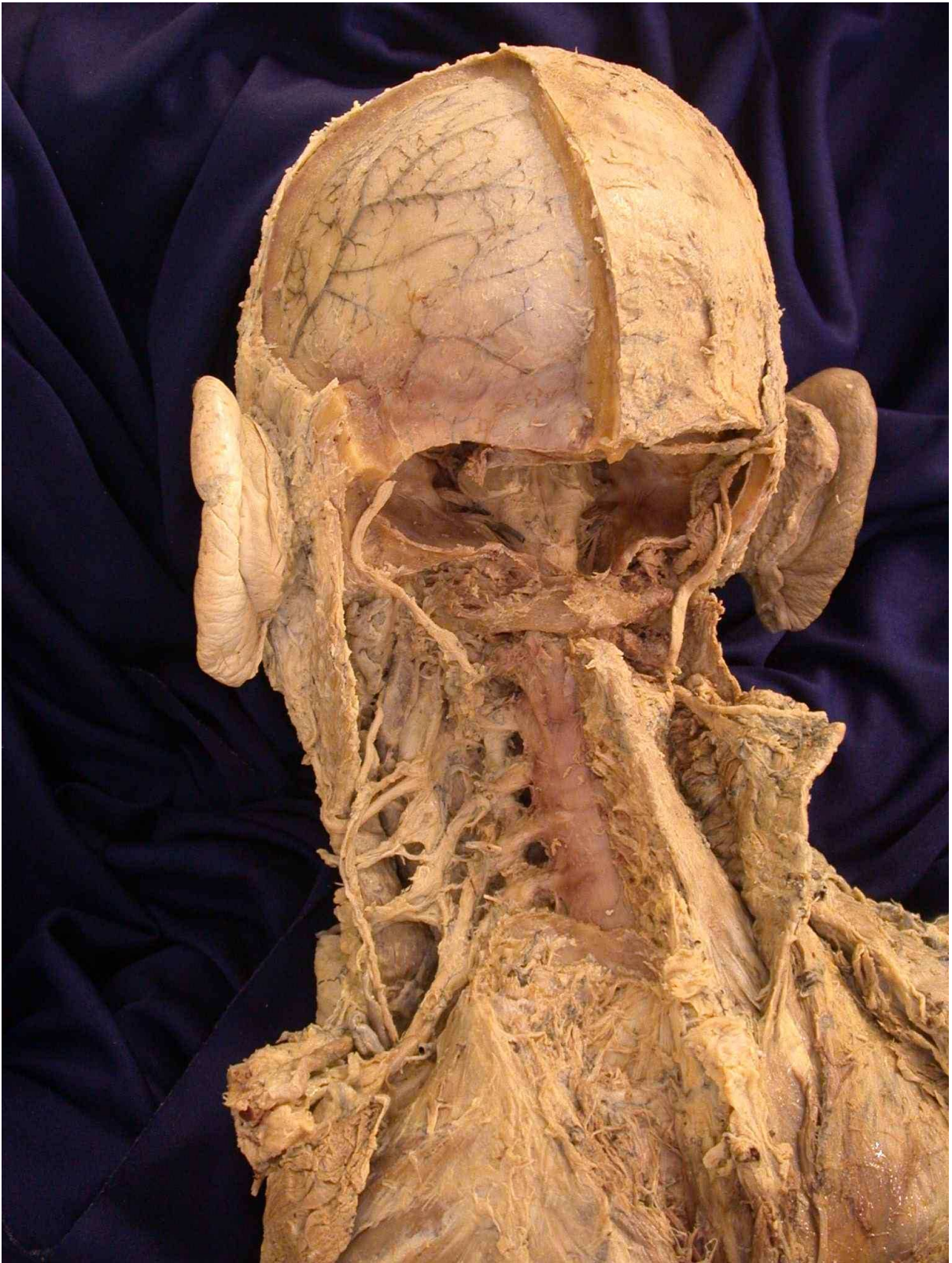


Figure 146 Photograph of posterior view of deep back of head and neck dissection

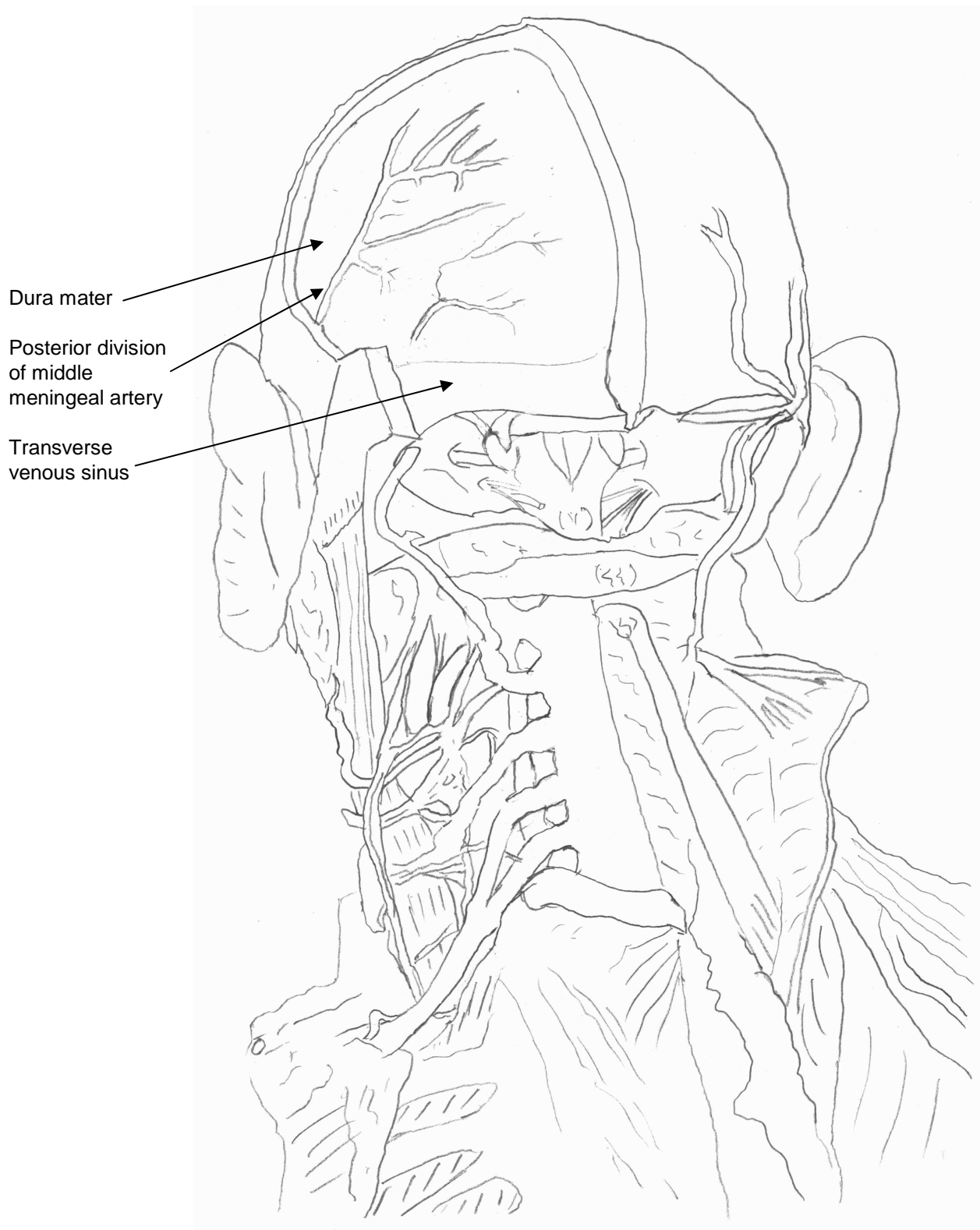


Figure 147 Diagram of posterior view of deep back of head and neck dissection



Figure 148 Photograph of left parotid gland

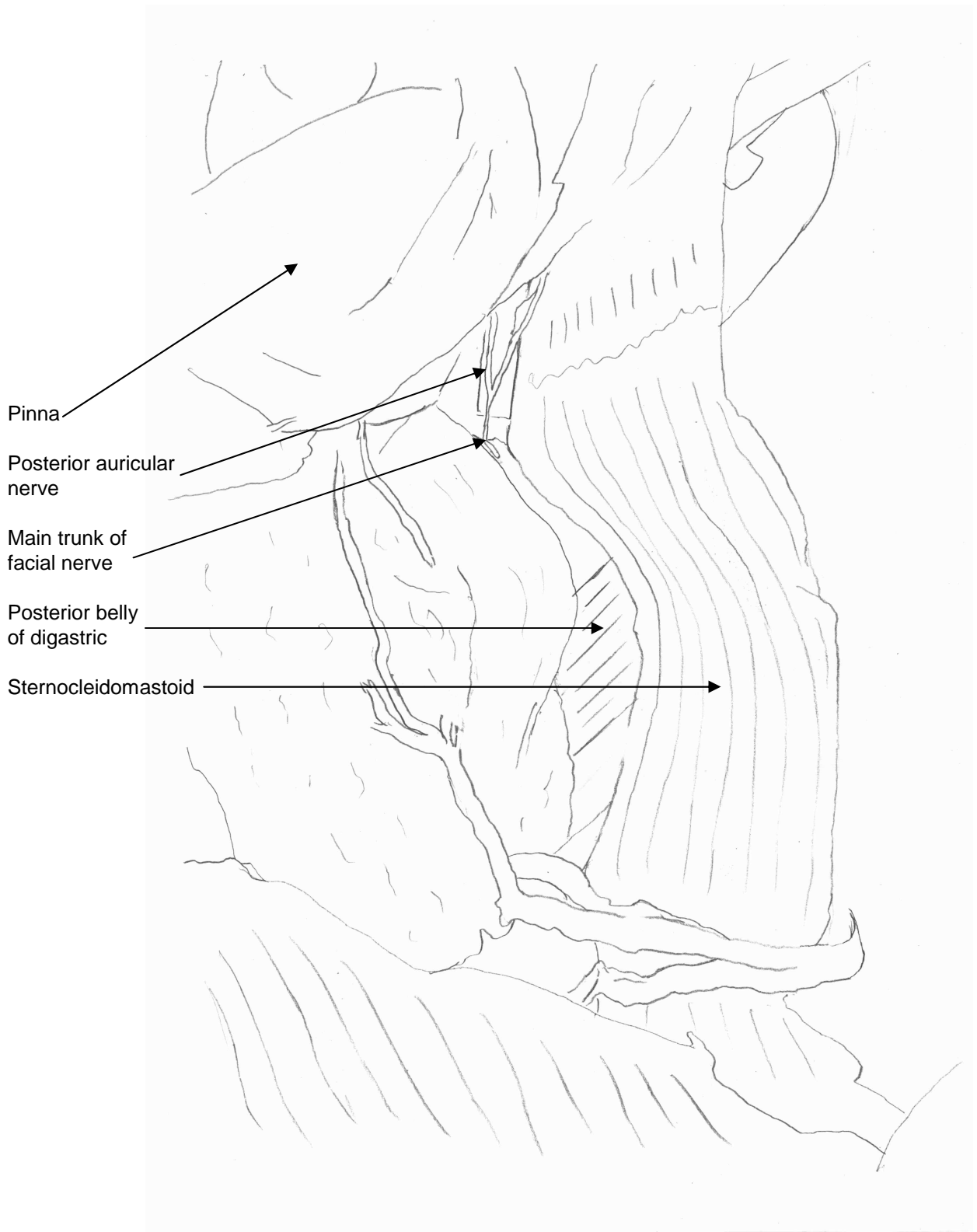


Figure 149 Diagram of left parotid gland



Figure 150 Photograph of left parotid gland with main trunk of facial nerve

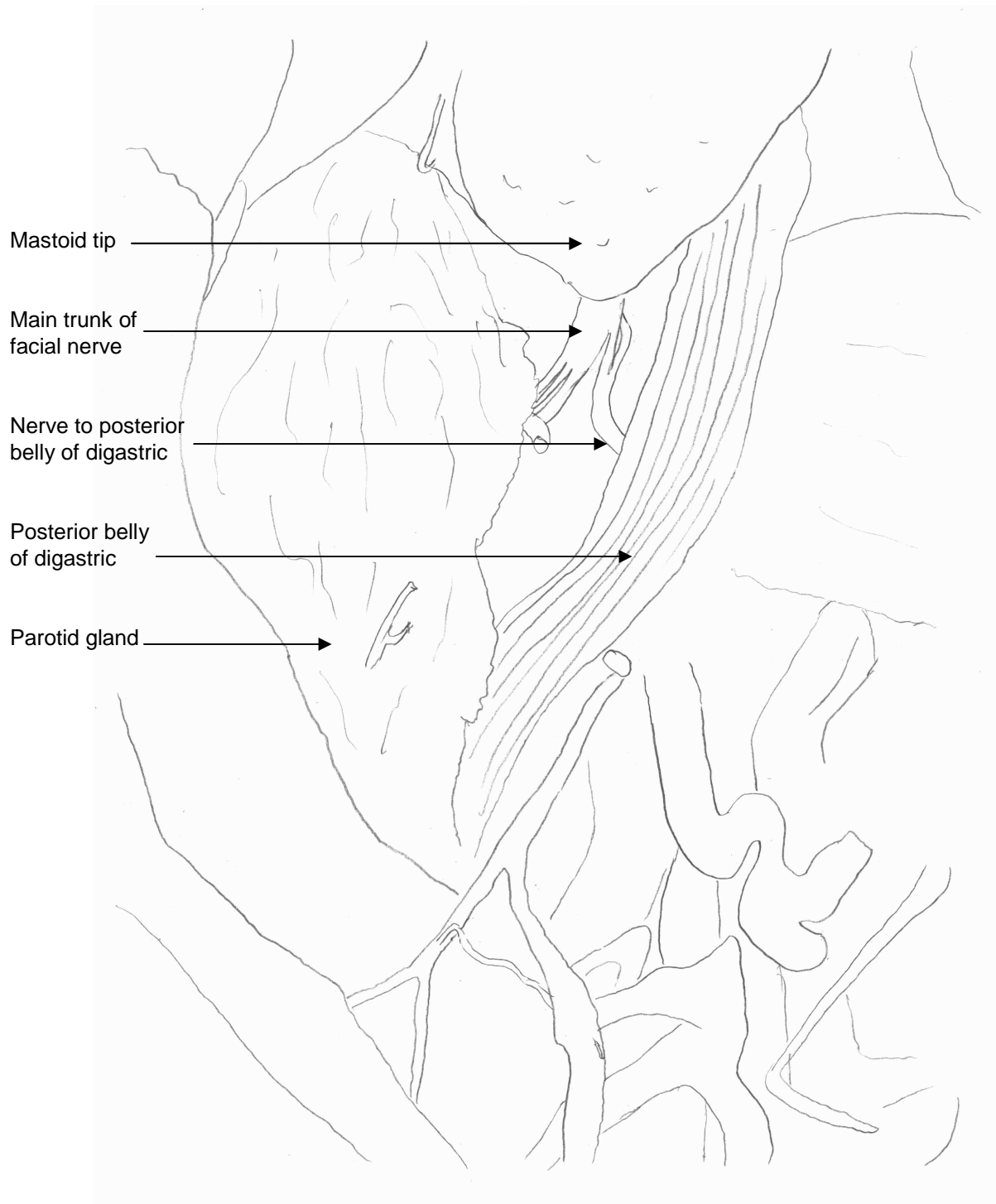


Figure 151 Diagram of left parotid gland with main trunk of facial nerve



Figure 152 Photograph of left vertical segment of the facial nerve

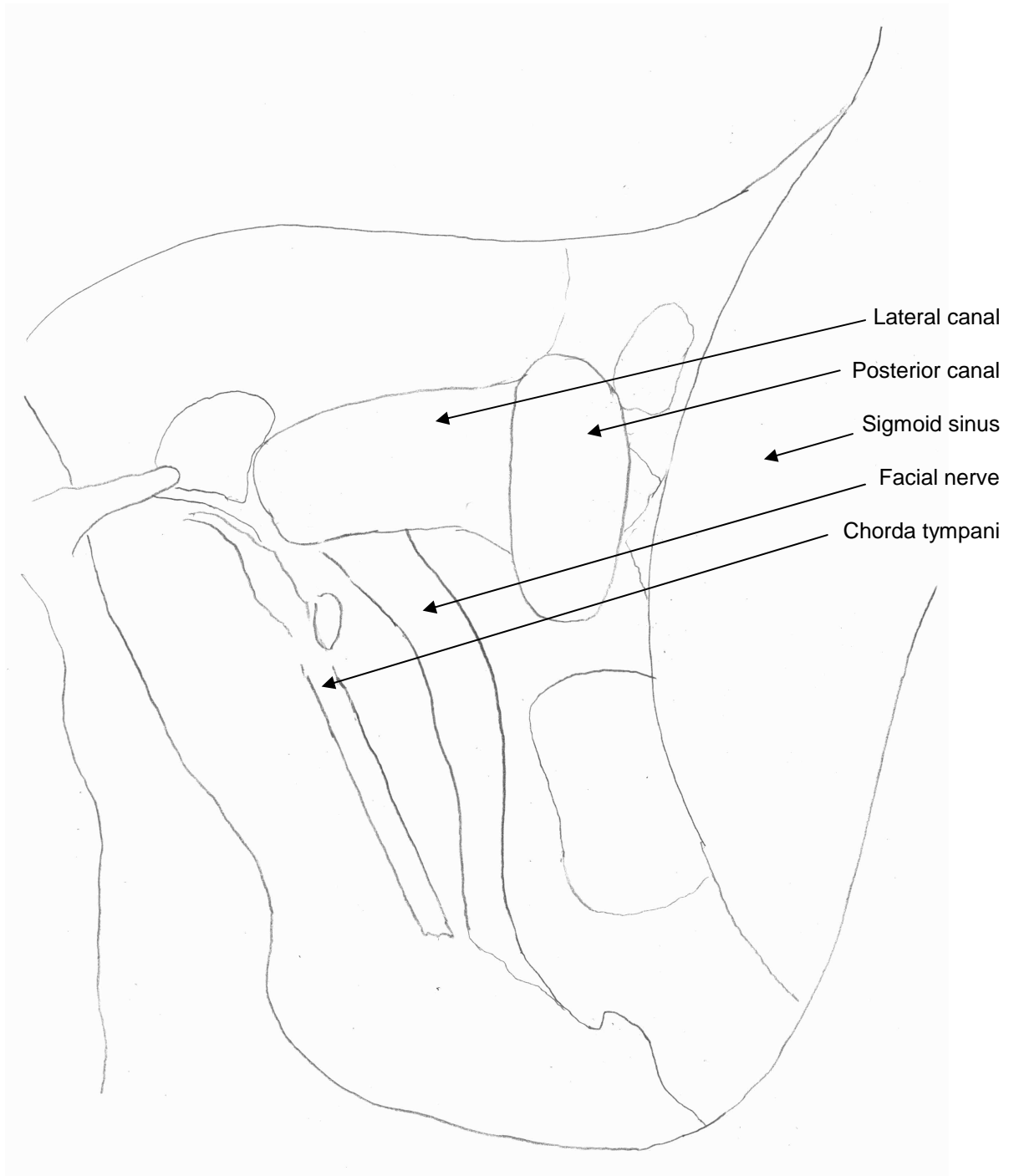


Figure 153 Diagram of left vertical segment of the facial nerve



Figure 154 Photograph of left temporal bone and suboccipital dissection

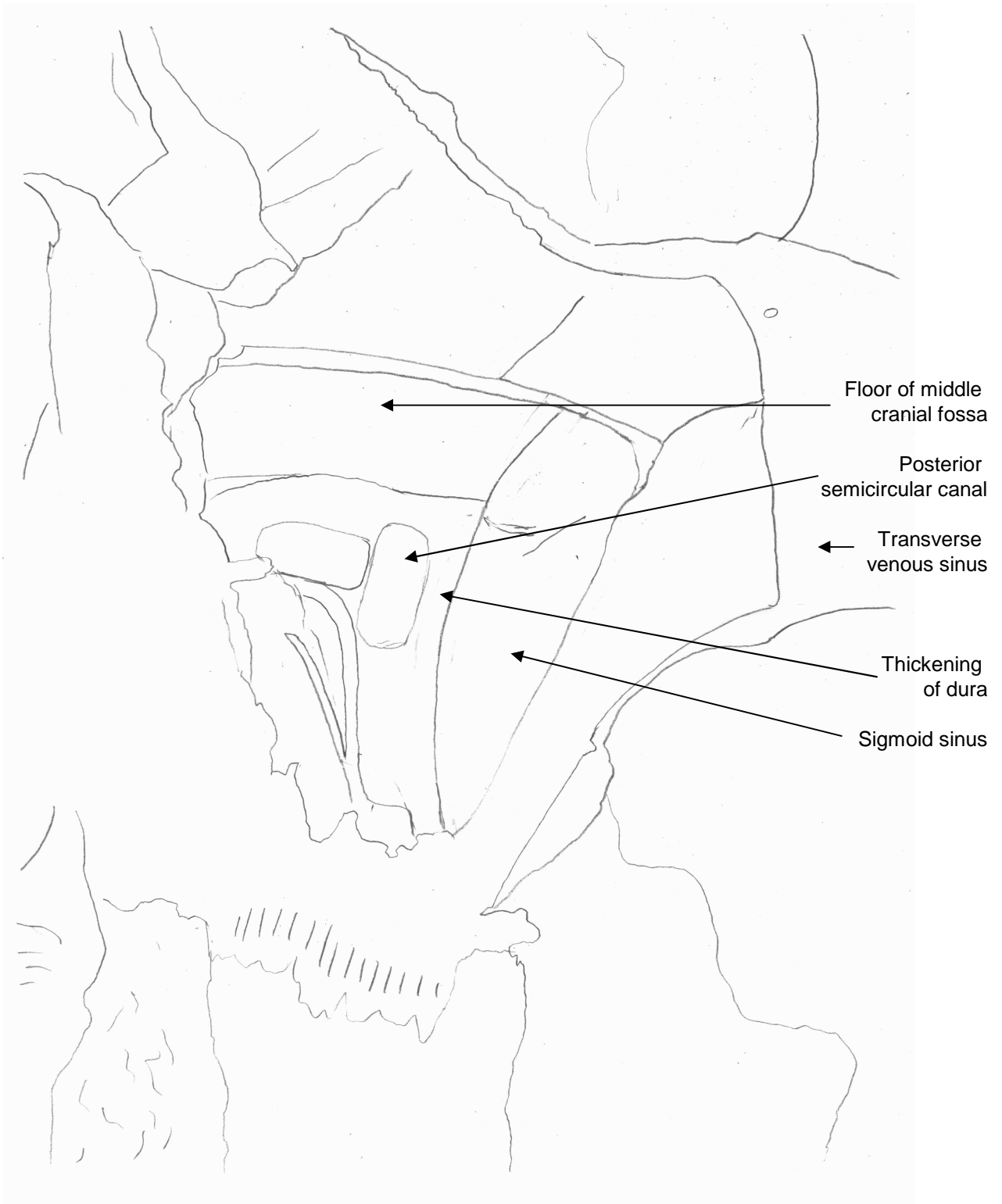


Figure 155 Diagram of left temporal bone and suboccipital dissection

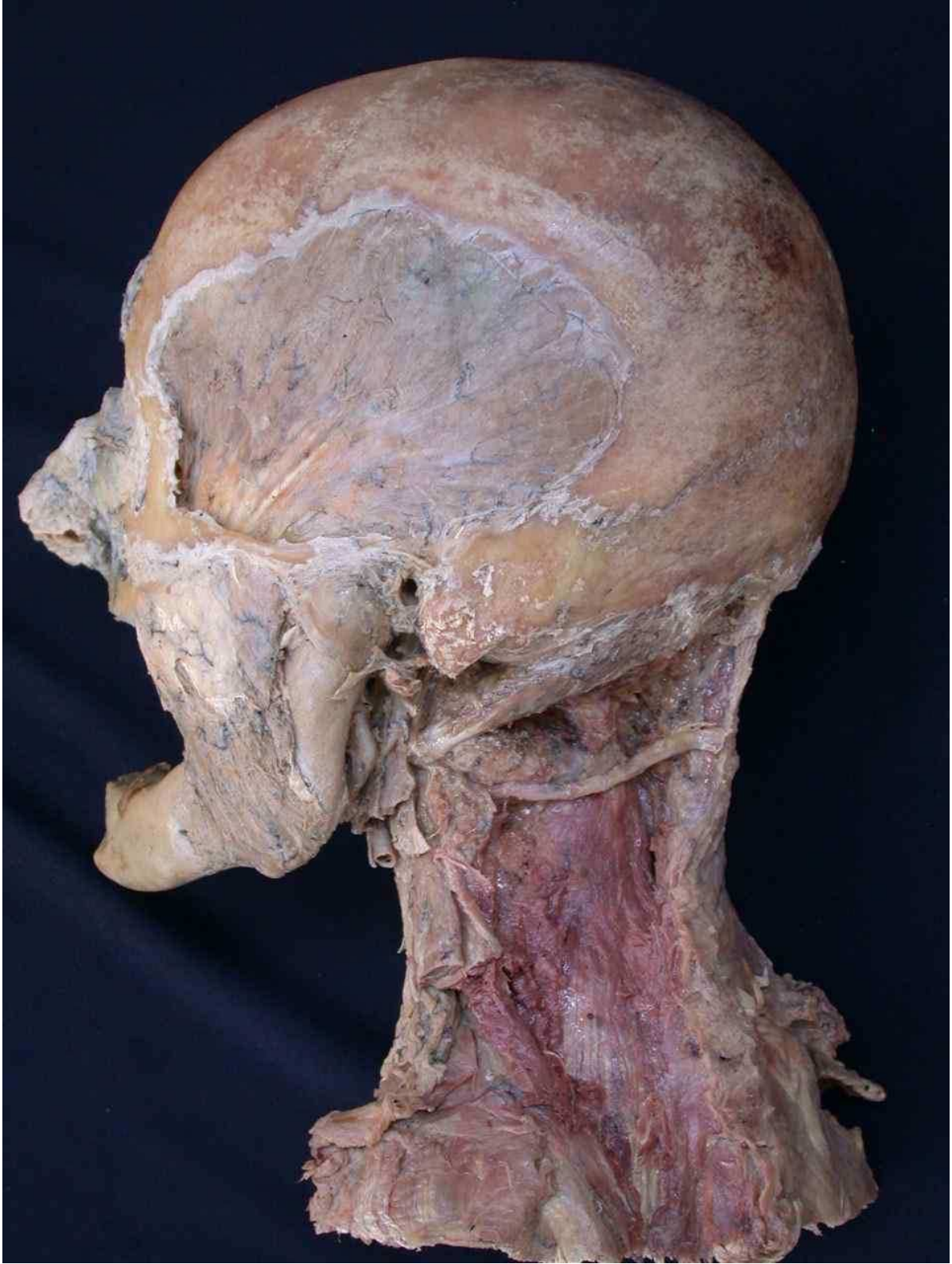


Figure 156 Photograph of left view of head and neck dissection

Temporalis

Superior
temporal line

Zygomatic arch

Masseter

Temporomandibular
joint

Angle of mandible

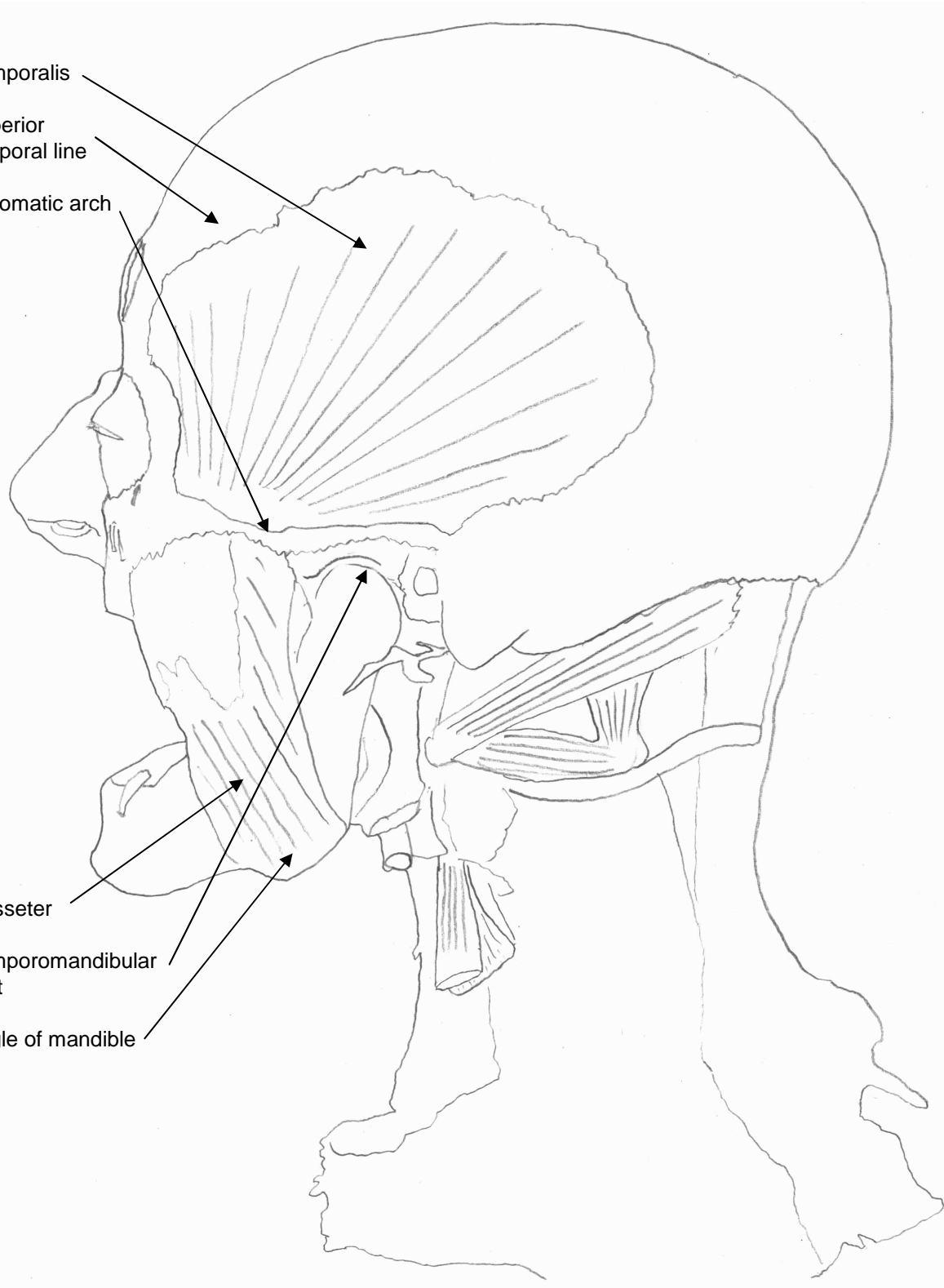


Figure 157 Diagram of left view of head and neck dissection

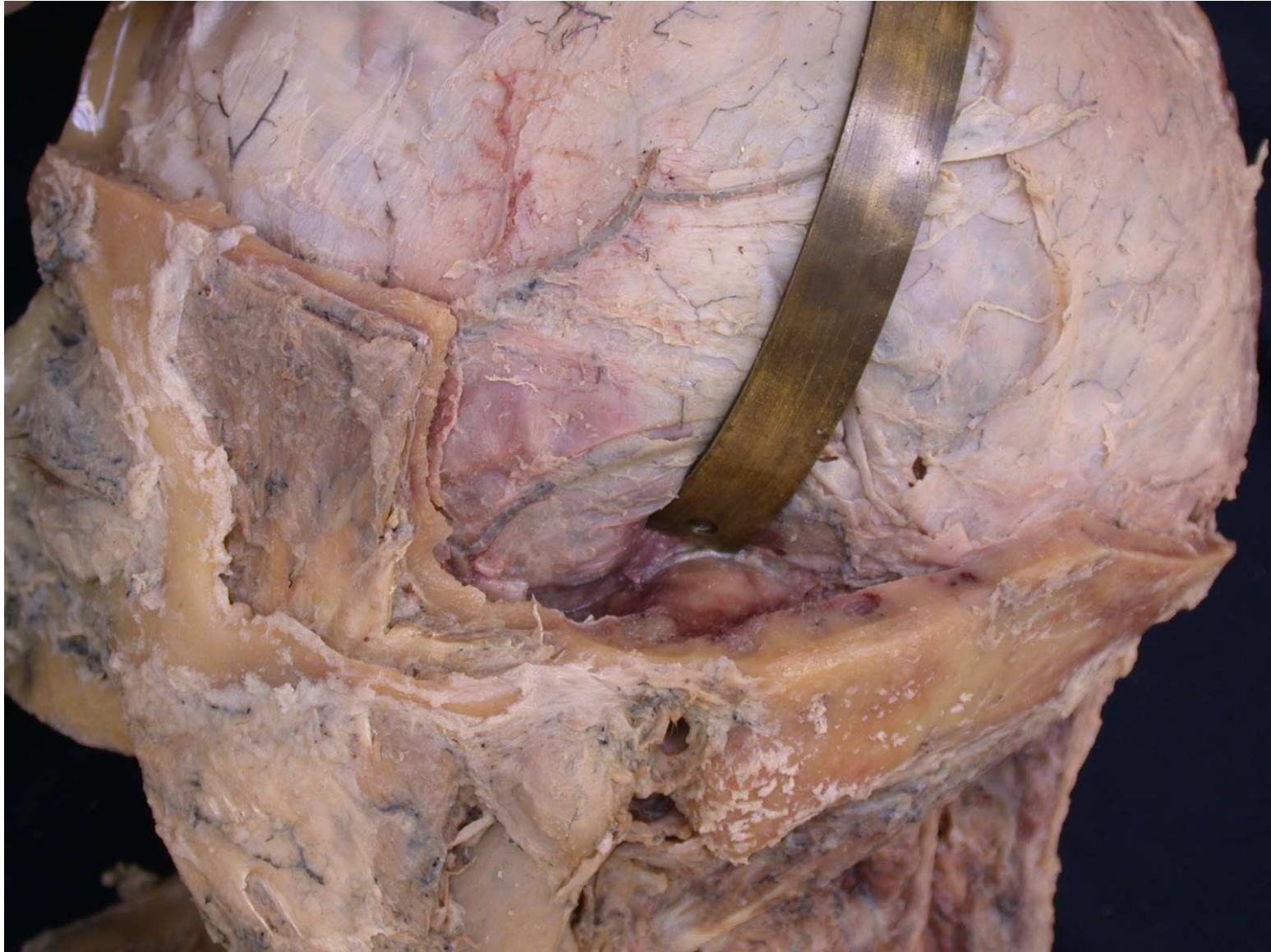


Figure 158 Photograph of dura mater being elevated from the floor of the cranial cavity

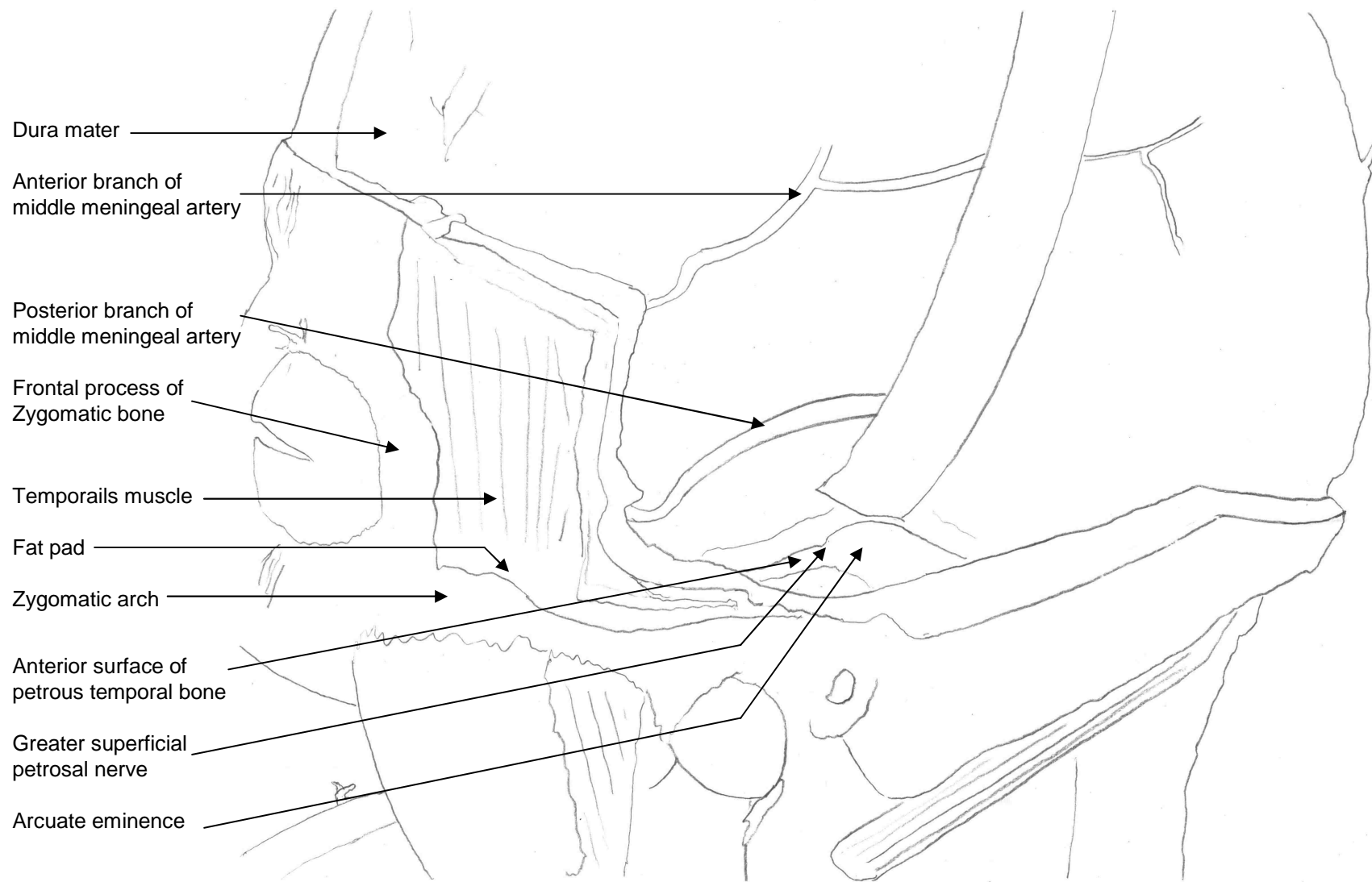


Figure 159 Diagram of dura mater being elevated from the floor of the cranial cavity



Figure 160 Photograph of lateral view of left middle cranial fossa

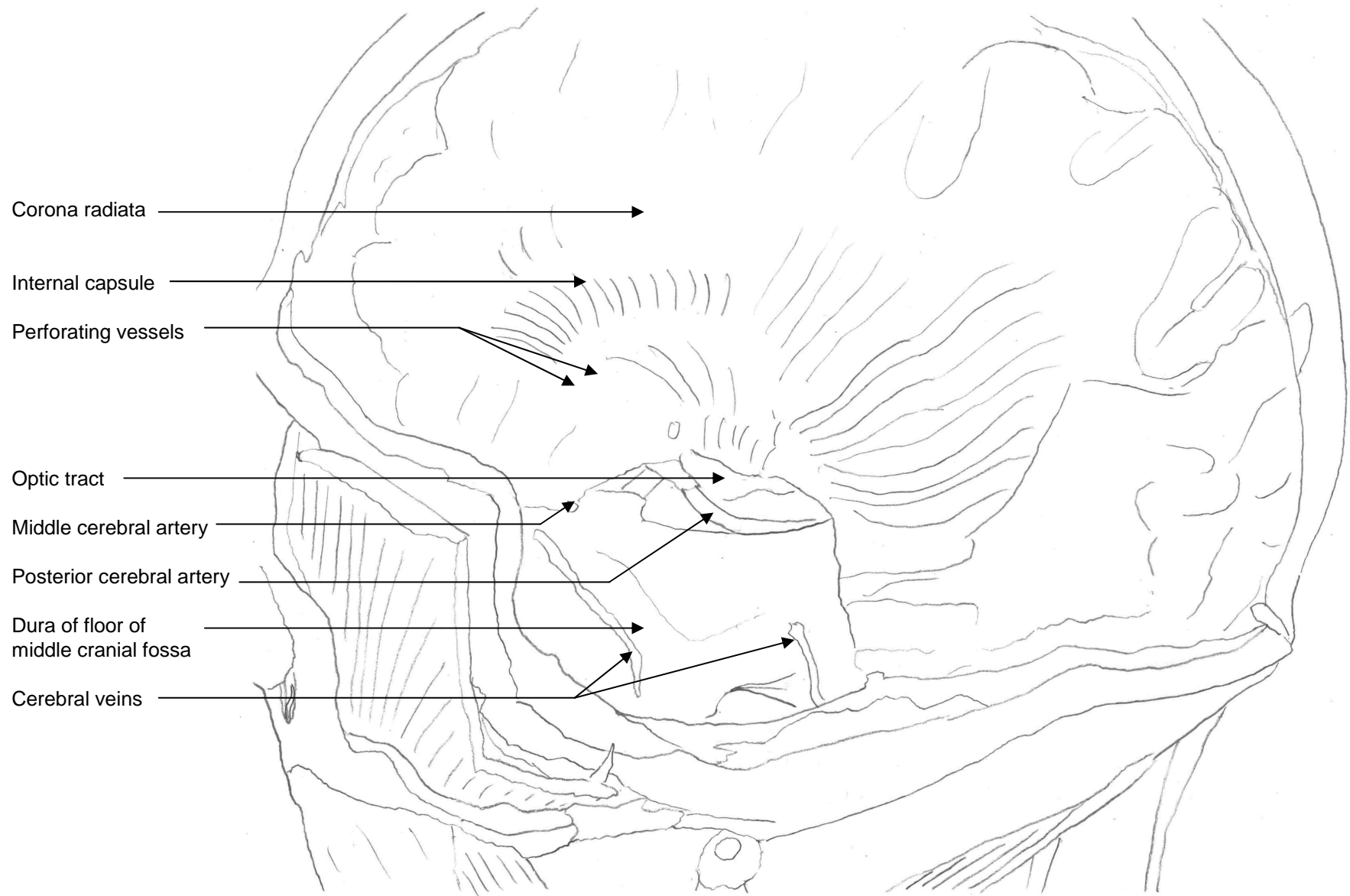


Figure 161 Diagram of lateral view of left middle cranial fossa



Figure 162 Photograph of left internal acoustic meatus de-roofed and facial nerve retracted

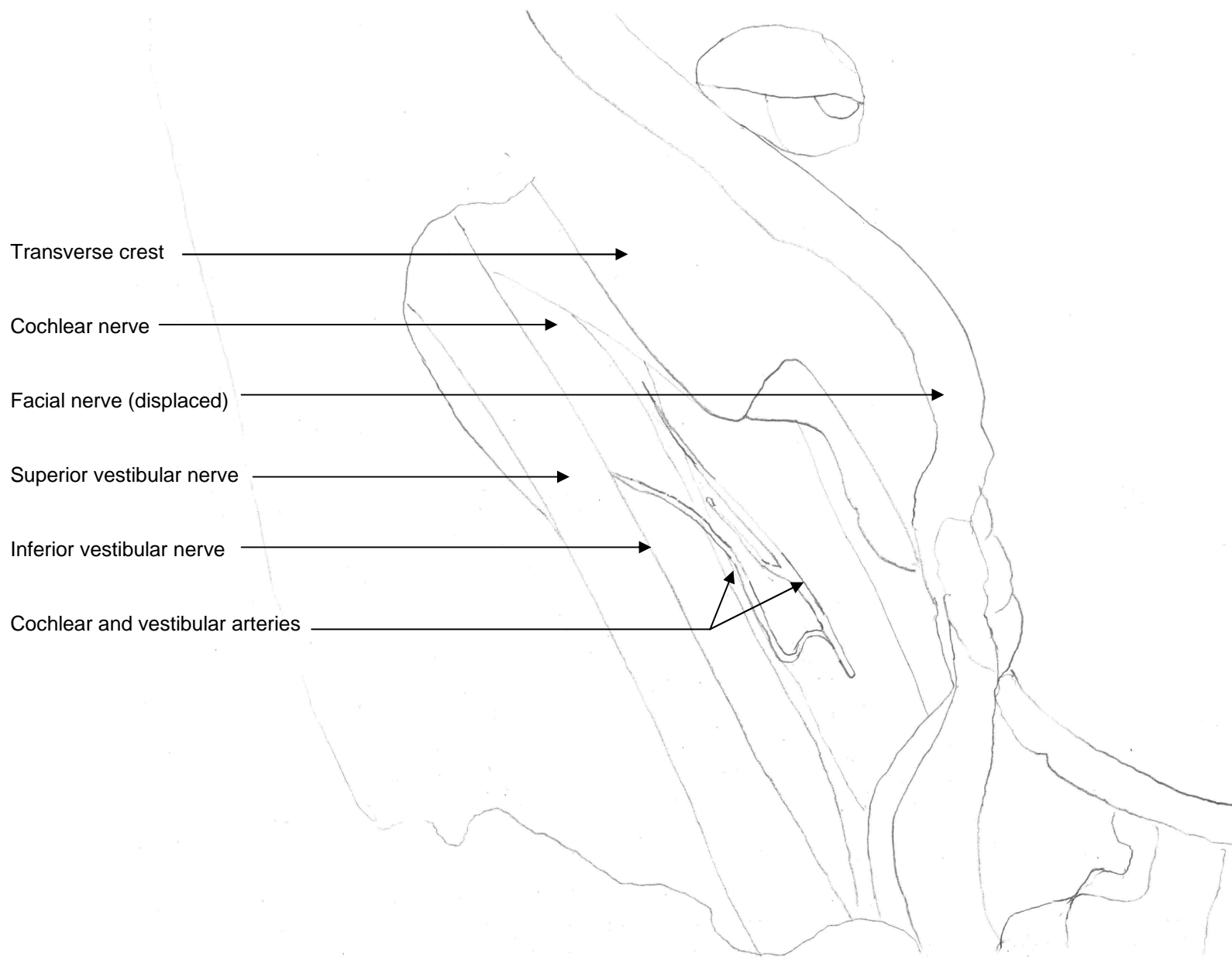


Figure 163 Diagram of left internal acoustic meatus de-roofed and facial nerve retracted

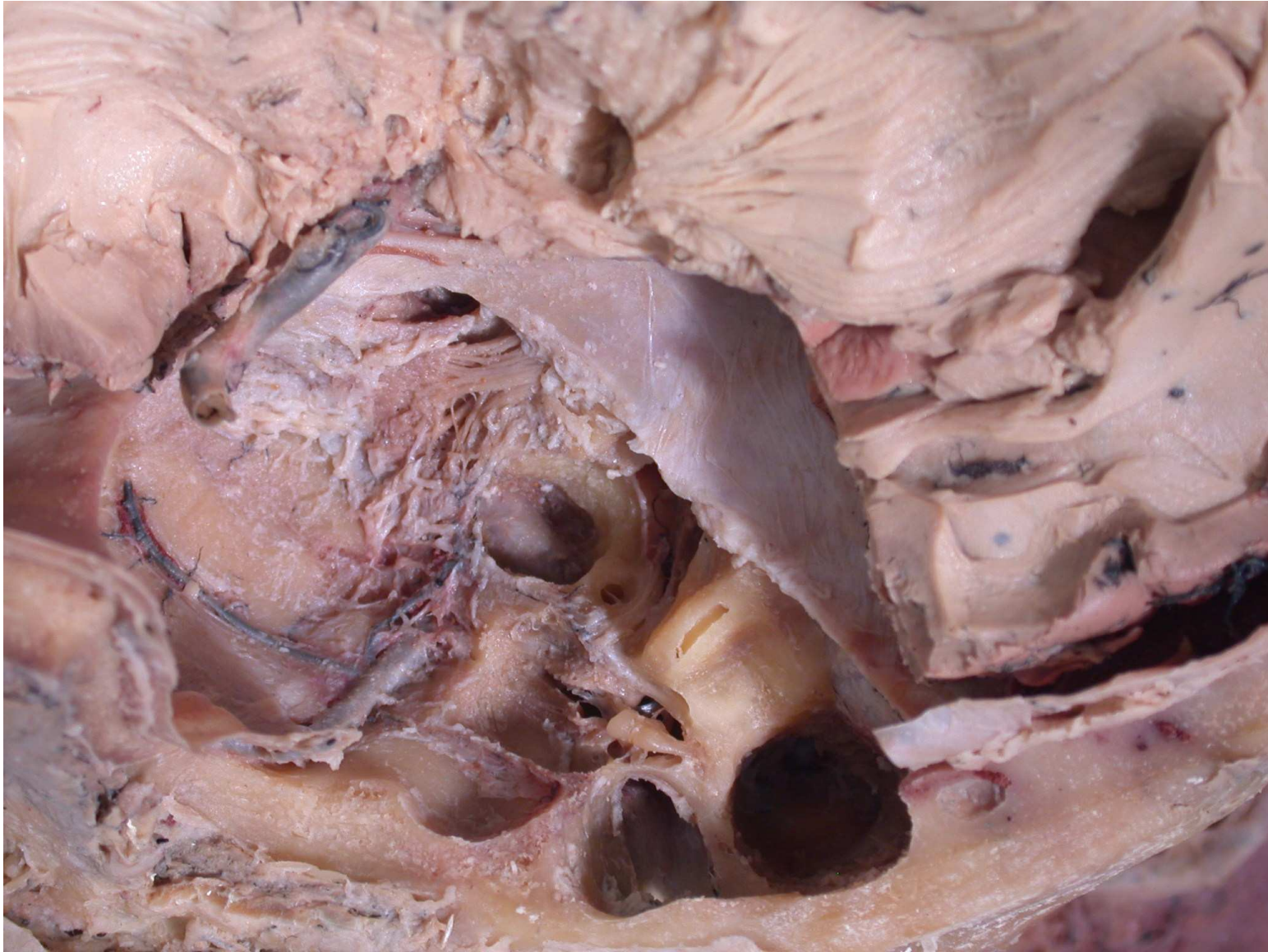


Figure 164 Photograph of superior view of dissected left middle cranial fossa floor

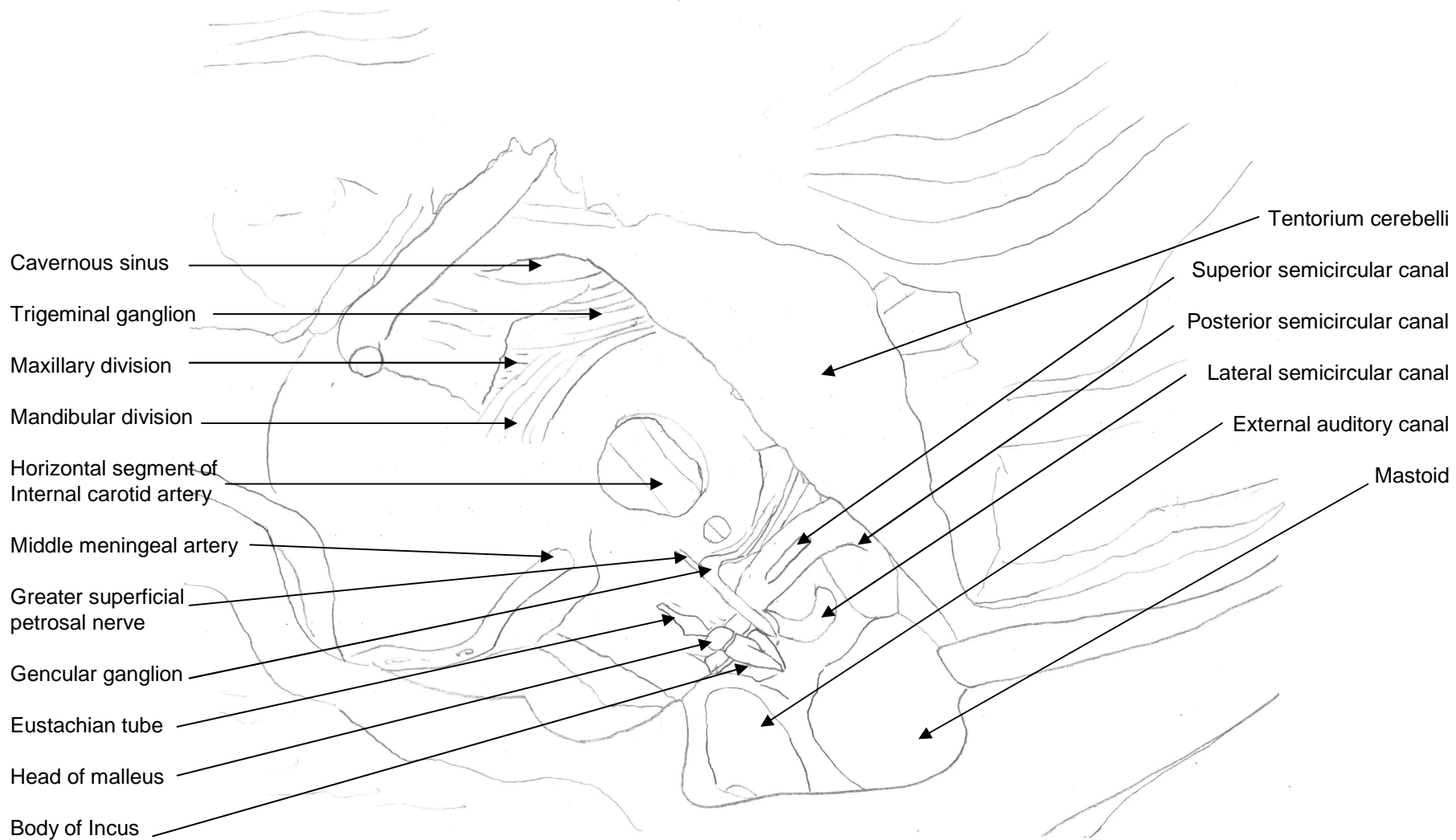


Figure 165 Diagram of superior view of dissected left middle cranial fossa floor

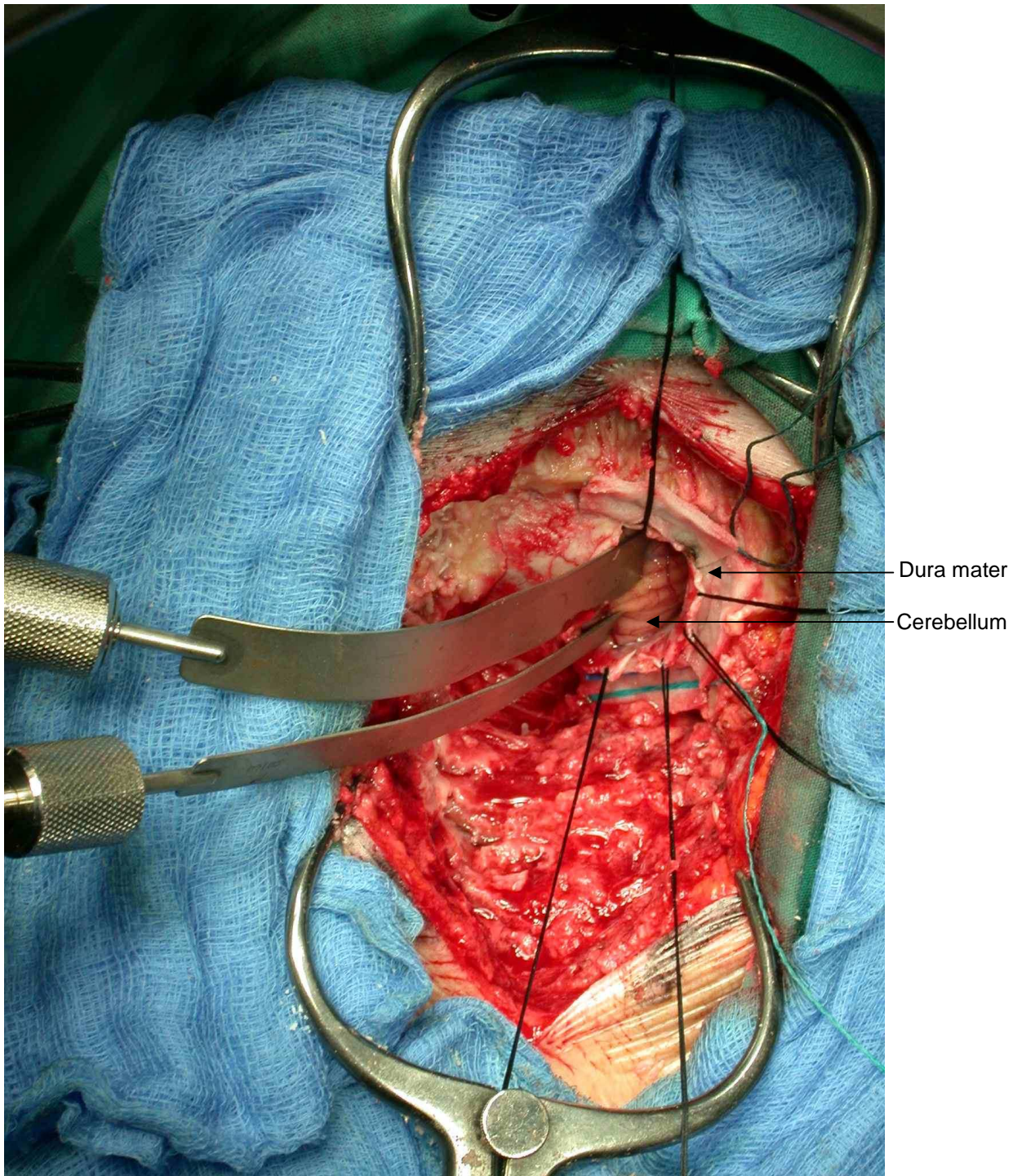


Figure 166 Intraoperative photograph of acoustic neuroma resection showing cerebellum being retracted through an occipital craniotomy

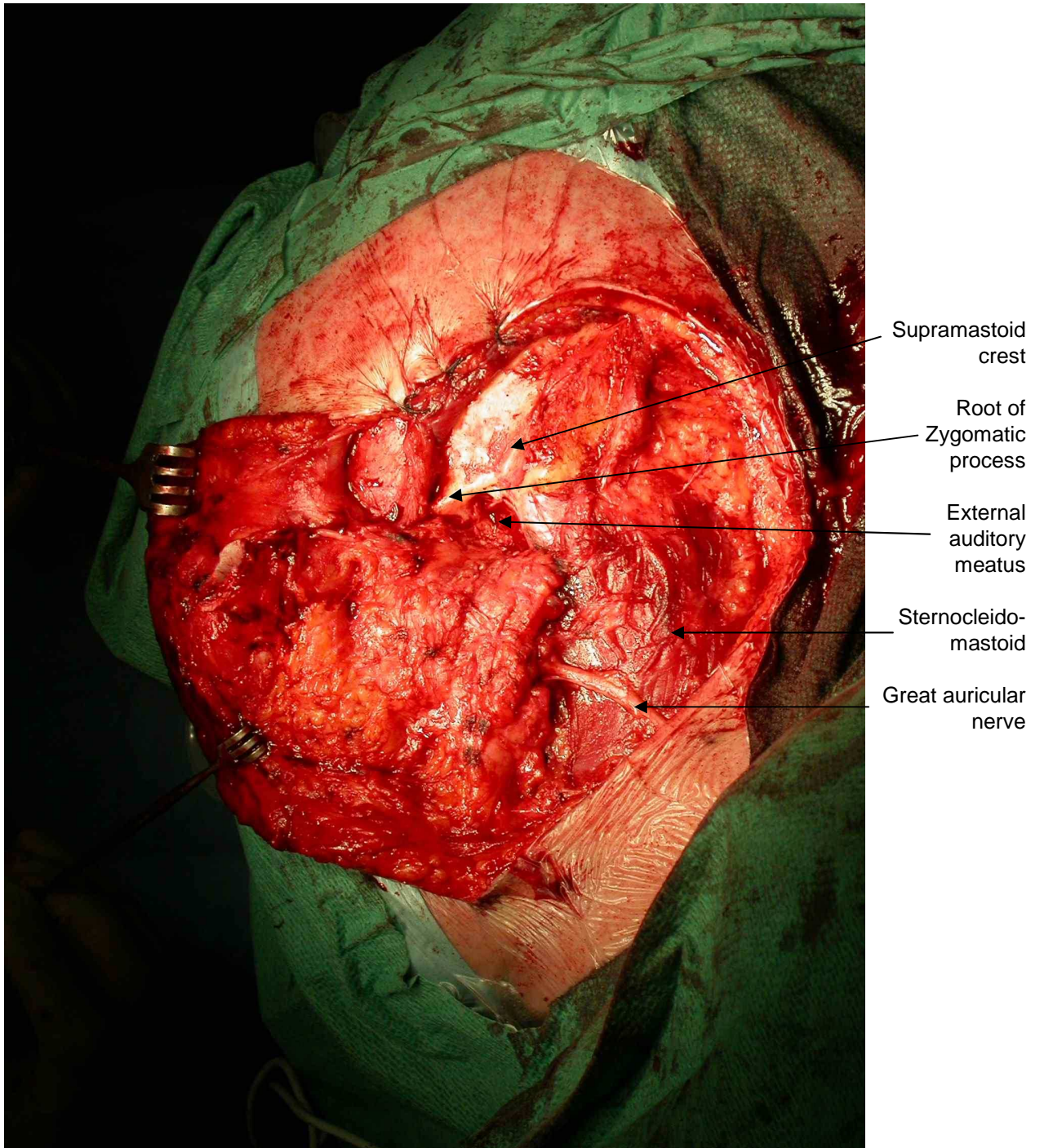


Figure 167 Intraoperative photograph of glomus jugularae resection showing skin flap being retracted to reveal mastoid process

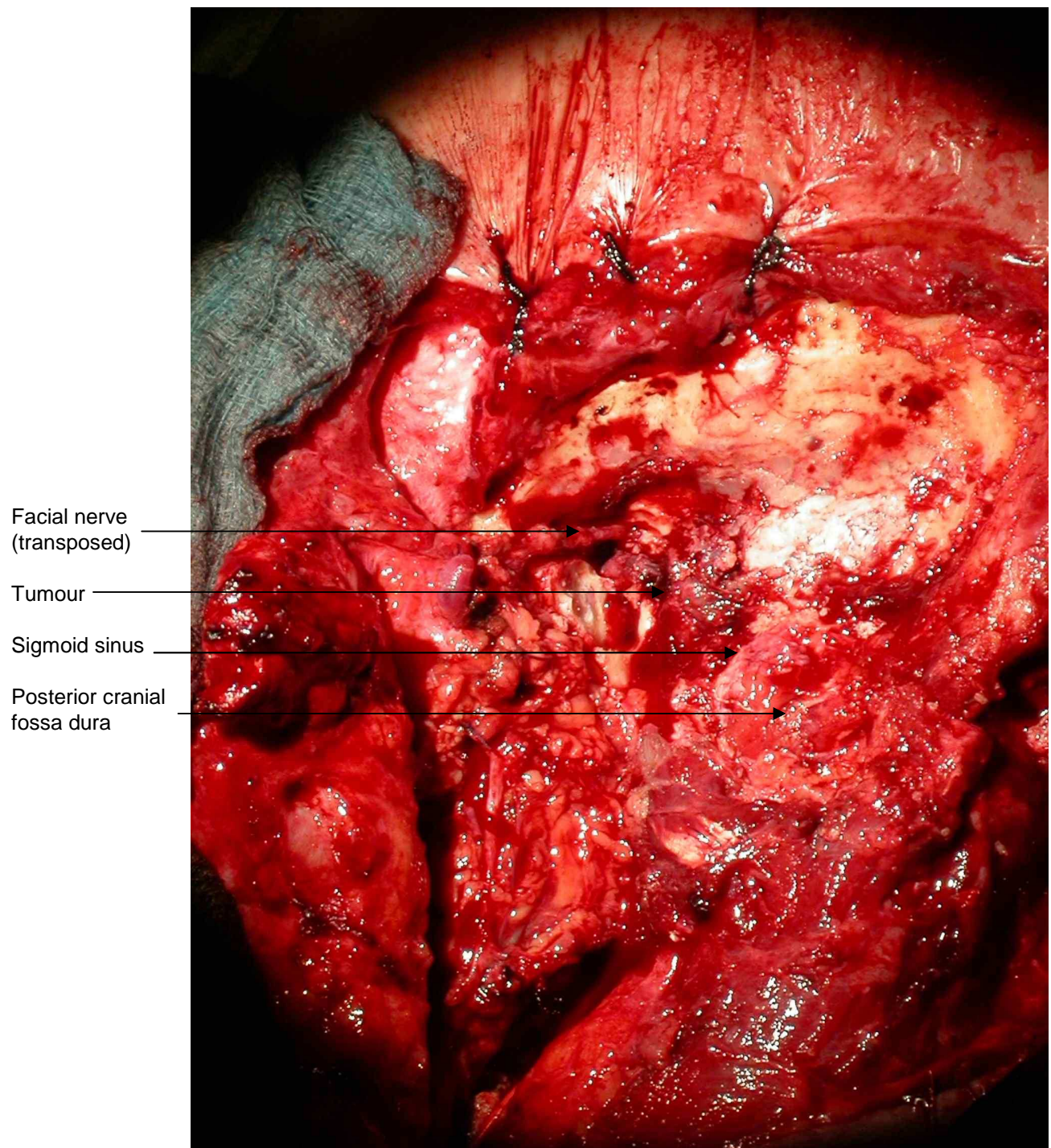


Figure 168 Intraoperative photograph of glomus jugularae resection following superficial parotidectomy and transposition of the vertical segment of the facial nerve

Section 4

Discussion

STATEMENT OF FINDINGS

The endolymphatic sac is a complex structure which is part of the membranous labyrinth. It arises from within the petrous part of the temporal bone and extends into the dura of the posterior cranial fossa.

The endolymphatic sac has a readily identifiable lumen, but there is great variability in the size of the sac. The endolymphatic sac does not always extend into the dura of the posterior cranial fossa. There is always a thickening of the dura where the intra-dural component of the endolymphatic sac would be located.

The transmastoid approach has many hazards including the vertical segment of the facial nerve, the sigmoid sinus, posterior cranial fossa dura and the lateral and posterior semicircular canals.

The endolymphatic sac can be approached by surgical routes other than the transmastoid. The transmastoid approach however provides the most unrestricted view of the dura covering the posterior cranial fossa and the underlying bone.

STRENGTHS AND WEAKNESSES

All of this research was conducted solely on human material. This removes the inherent problems of applying the results of animal studies to humans. It allows for easier comparisons between studies.

The availability of cadaveric material at the University of Glasgow allowed for repeated attempts at endolymphatic decompression for auditing purposes.

The mastoidectomy procedures were performed using a high speed drill and with an operating microscope, allowing dissections as close as possible to the actual operation being audited.

All cadaveric material used in this research was embalmed by perfusion fixation. Although this provides good preservation of the material it unfortunately also exposes the delicate structures of the inner ear to abnormal pressures. This may result in damage which is difficult to interpret. As other studies (Schuknecht, 1983) have used material which is not perfusion fixed then there are possible artifactual differences. This has been minimised by avoiding comparisons between specimens which have been processed using different techniques.

When processing temporal bones for histological examination, a hot wax technique was employed. This unfortunately resulted in hardening of the tissues with possible disruption, again making interpretation of the fine structures of the inner ear difficult. For the histological examination of the intraosseous portion of the endolymphatic sac this was minimised by removal of the dura from the bone and processing in isolation. It is of course possible that the very act of removing the dura from the bone is going to have a detrimental effect on the fine structure.

The material used in this research was obtained from an elderly population. The medical history and in particular the presence or absence of any ear disease is unknown. The group examined may not represent the population to which the research is being applied.

As the dried skulls and dried temporal bones used for study have come from Indian skeletons, there may be racial differences. The use of local cadavers and examination of the temporal bones however should overcome this.

SUMMARY OF FINDINGS

Embryology

This work has shown that the endolymphatic sac develops with the inner ear as an extension of the membranous labyrinth.

In the 55mm embryo the close relationship between the relatively large and simple endolymphatic sac and the sigmoid sinus can be seen. It can be seen that the

endolymphatic sac consists of a single lumen and not multiple tubules at this stage in this particular embryo. The sac is clearly visible within the dura mater overlying the sigmoid sinus, and it can be seen that the sac does not communicate with the sigmoid sinus. Other studies have shown that the endolymphatic sac develops initially as a simple sac like structure and then later grows into the adult form with multiple tubules (Matthew and Linthicum, 1998, Bagger-Sjoback et al, 1990). The first of these studies suggested that the adult form could be attained as early as 26 weeks gestation. The second study suggested that there are three phases in the development of the endolymphatic sac: the first phase terminating at week 10 with a single lumen, the second phase between 11 and 16 weeks with more mature crypts and folds and the third phase lasting to week 20 where the sac divides into many tubules (Bagger-Sjoback, 1993). Another study by Matthew (2000) concluded that in some people the endolymphatic sac does not reach maturity until well after birth, although most reach maturity by 1 year of age and both sides tend to mature together. All the adult endolymphatic sacs examined in this present study by histological means, had an adult form, i.e. a complex tubular structure in the intradural part. This study therefore supports the theory that the sac develops initially as a simple outgrowth of the membranous labyrinth which later develops a more complex structure.

The inner ear develops along with the rest of the head and neck. The endolymphatic sac is joined to the utricle by the endolymphatic duct. These structures develop in close proximity and with linear alignment initially. The endolymphatic sac is in connection with the dura of the posterior cranial fossa, and as the fossa extends, the sac is pulled downwards with the sigmoid sinus and the endolymphatic sac develops a J shaped form. After birth therefore when there is pneumatization of the temporal bone the sigmoid sinus and endolymphatic sac will move relative to the labyrinth as the mastoid increases in size. This mechanism could explain the possible relationship between the distance from the operculum to the sigmoid sinus and the length of the sac as measured. It may also explain why the fibrous thickening of the dura around the sac extends from the operculum all the way to the sigmoid sinus, as it is pulled with the dura as the temporal bone develops.

The degree of pneumatization of the temporal bone has been studied (Lindsay, 1941, Schuknecht, 1968) and has been shown to be greatly variable. This impacts on both the eventual arrangement of the mastoid and the position of the sigmoid sinus and endolymphatic sac.

Structure

The endolymphatic sac as demonstrated is part of the membranous labyrinth and is connected to the membranous labyrinth by the endolymphatic duct. The endolymphatic duct is connected to both the utricle and the saccule. The utricle is joined by the utricular duct and the saccule by the saccular duct. At the junction of the utricle and the utricular duct in man a thickening of the membrane separating the structures at the mouth of the duct was found. This structure is described by Schuknecht and Belal (1975) as the utriculo-endolymphatic valve. This structure may have a role in pressure regulation in the inner ear.

It was found that the endolymphatic sac changes in structure as it passes from the terminal part of the vestibular aqueduct and out under the operculum into the dura mater of the posterior cranial fossa. The proximal part consisted of what appears to be a single tubular structure with an irregular convoluted border, although it is very difficult to distinguish it from the endolymphatic duct within the vestibular aqueduct. The epithelium appears squamous. Here the sac is surrounded by a loose connective tissue with blood vessels present. As the sac passes under the operculum there are multiple lumens present and the epithelium is cuboidal in shape. As the sac moves distally towards the sigmoid sinus there are multiple tubules present which appear to form independent clusters at the terminal part of the sac. This description matches the work previously published (Bagger-Sjoberg et al 1990, Friberg et al 1988,). In these papers where post mortem human endolymphatic sacs were studied with cross-sectional histology the sac is described as having three parts, a proximal, intermediate and distal part which correspond well with the areas located in this study. The proximal part is the intraosseous part with a single lumen, the intermediate part is the section where multiple tubules begin to appear. The lining becomes cuboidal and it has an intraosseous and

extraosseous component. The distal part lies within the layers of the dura mater and consists of many tubules. The three dimensional structure of the intermediate and distal sac has been described as a series of interconnecting tubules and sacs and not just a convoluted tubule cut on cross-section. The tubules do not unite distally and do not drain into the sigmoid sinus (Bagger-Sjoback et al, 1990). Two particular features that are not well described in previous work are the dura surrounding the endolymphatic sac and the longitudinal vessels lying deep to the intermediate and distal part of the sac.

Dura

From histological and gross analysis it is evident that the dura mater of the posterior cranial fossa is thicker in the area where the endolymphatic sac lies, the foveate fossa, inferior to the operculum and lateral to the internal acoustic meatus.

The dura mater within the cranial cavity is frequently considered as two layers, an outer endosteal and an inner meningeal layer. The outer layer is described as being adherent to the underlying bone and that the layers separate to enclose the dural venous sinuses (Standring et al, 2006).

The dura appears to split in the same way to envelop the endolymphatic sac and the perisaccular connective tissue lying on the foveate fossa. The superficial layer of dura appears to be arranged in sheets at about 90 degrees to the orientation of the tubules of the sac. Cell nuclei are sparse in this area. Then there appears to be a layer of looser connective tissue first running again at about 90 degrees to the sac, but in a deeper plane the loose connective tissue is parallel to the sac. The tubules of the sac are encountered with blood vessels surrounding them separated from the surrounding tissue. Deep to the sac there is a thicker layer of loose connective tissue running parallel to the sac before finally a layer of more dense tissue running at about 90 degrees and lying on the surface of the underlying bone. This thickening of the dura appears larger than the actual endolymphatic sac, filling the foveate fossa and running from the level of the operculum laterally and inferiorly over the sigmoid sinus.

In the specimens where no extraosseous portion of the sac could be identified by gross analysis, the thickening of the dura was still evident, extending from the operculum to the sigmoid sinus.

When the endolymphatic sac was decompressed by the removal of the bone of the posterior cranial fossa the trapezoid projection in the dura of the dura was clearly visible in every case projecting laterally and inferiorly from deep to the posterior semicircular canal towards the sigmoid sinus. Identification and removal of the bone covering this section of dura is central to the transmastoid endolymphatic sac decompression. What this research shows is that the presence of this trapezoid thickening of dura does not uniformly signify the presence or location of the endolymphatic sac. As demonstrated there may be no identifiable extraosseous portion to the sac.

There have been many studies on the location and variation in structure and size of the extraosseous portion of the endolymphatic sac. Shea et al (1978) used a combination of gross and histological methods to demonstrate the sac. He injected dye into the endolymphatic space to fill the endolymphatic sac and then measured the distances from the incus and the dome of the horizontal canal to the most inferior point of the otic capsule and the endolymphatic sac in 15 specimens. Marked variation in the sac is apparent and Shea suggested a more conservative dissection for operating surgeons to decompress the sac. However they do not comment on the presence of a dural thickening. Bagger-Sjoberg (1993) and Friberg et al (1988) also describe variation in the size of the sac but do not comment on the surrounding dura. Without the benefit of dye within the endolymphatic compartment, the surgeon may find that the presence of this trapezoid thickening of dura may be easily mistaken for and labeled as the endolymphatic sac itself.

Vascular

On histological examination of the endolymphatic sac the perisaccular tissue with a rich vascular network was identified. This has been widely described (Friberg et al, 1988, Schuknecht, 1986). However, in 2 specimens, a series of about 4 and 5 comparatively

large vascular structures were identified running parallel to the endolymphatic sac on its deep surface. These vessels, often a large distended vein with a smaller adjacent arteriole lay in the endosteal layer of the dura, between the endolymphatic sac and the underlying petrous temporal bone. The veins had a diameter between 2 and 4 times the depth of the sac at that level. These veins are of larger diameter than the depth of the sac alone, but the diameter is comparable to the depth of the sac when combined with the surrounding perisaccular connective tissue. The veins were traced inferiorly and laterally but the structures they drain into could not be identified. Vessels of this size have surgical implications in decompression of the sac and possibly during insertion of an endolymphatic shunt. They may be liable to bleed when decompressing the distal portion of the sac, bleeding which could be difficult to control as the surgeon would not want to damage the dura mater overlying the posterior cranial fossa. The close proximity of these vessels may lead a surgeon to mistake them and the surrounding dura for the endolymphatic sac. Damaging or affecting these vessels could affect the tissues they drain, potentially including the endolymphatic sac itself. Friberg suggested a link between occlusion of the vein of the vestibular aqueduct with perisaccular fibrosis and Ménière's disease. From examination of post mortem temporal bones, they proposed that altered haemodynamics may contribute to the pathogenesis of endolymphatic hydrops and Ménière's disease (Friberg, 2002).

There is a great deal of literature which describes the perisaccular connective tissue and vasculature for the proximal part of the endolymphatic sac (Schuknecht, 1986). There are fewer descriptions of the distal endolymphatic sac and the surrounding vasculature. Secretan (1944) for example studied sections of the sac by histological means from the operculum to the sigmoid sinus. He found numerous perisaccular vascular channels around the distal endolymphatic sac which drained into the transverse sinus.

Histology / Scanning electron microscopy

The scanning electron micrographs of the saccule and the endolymphatic sac show a similar epithelium. They both show flattened epithelial cells with regular borders and a prominent bulge in the middle corresponding to the nucleus of the cell. This is further

evidence to show that the endolymphatic sac is part of the membranous labyrinth. A section of the deep wall of the extraosseous part analysed shows the epithelium of the sac with the fibrous structure of the dura on either side. Amongst the flattened epithelial cells, domed cells are found. Yasuo Harada in his scanning electron microscopy atlas of the ear also found dome-like dark cells in human endolymphatic sacs. The rest of the cells were flattened epithelial cells with a few polyp-shaped microvilli. The proportion of the flattened cells and the domed cells alters through the sac (Harada 1983). Under the epithelial cells large irregular macrophage like cells were seen which could suggest an immunological role or a role removing debris.

Electron microscopy confirmed that the sac was identified in the cases as stated, as the medial wall of the sac was analysed to confirm the presence of an epithelial lining. This confirms that the sac can be identified and opened by means of gross dissection.

Function

Guild (1927) first proposed the theory of longitudinal flow of endolymph within the membranous labyrinth. It was proposed that endolymph was produced by the dark cells of the stria vascularis and circulated around the cochlea into the saccule and through the saccular duct to the endolymphatic duct and then into the endolymphatic sac where it was resorbed. Endolymph is also produced by the dark cells of the ampulla of the semicircular canals and then flows into the utricle and through the utricular duct to the endolymphatic duct.

Studies have suggested 3 mechanisms for pressure regulation of endolymph within the membranous labyrinth. The first is based on pressure regulation by endolymph resorption. The second is based on pressure regulation by mechanical factors and the third is based on pressure regulation by secretory activity (Wackym et al, 1987). As the endolymphatic sac is the only part of the membranous labyrinth not contained within bone, it may act like a pressure release valve to maintain endolymphatic pressure. Proximally the convoluted structure and distally the tubular structure provides the lumen

with a larger surface area. This could be for resorption of fluid, secretion of products, or could allow expansion of the sac to accommodate rises in volume.

Three processes were suggested by which endolymph could be resorbed (Wackym et al, 1987). Firstly there could be a passive transcellular movement of water across the epithelium. The second involves an active transcellular ion exchange with passive transepithelial outflow of water. The third is an active transcellular vacuolar bulk endolymph outflow. This last theory would require a highly vascular tissue to perform such an energy demanding task. The proximal endolymphatic sac was seen to have surrounding it a very rich vascular plexus. The epithelium of the sac is formed by cuboidal and columnar cells with a large darkly stained nucleus.

At the junction of the endolymphatic duct and the proximal endolymphatic sac there is a sharp change in direction. The J shaped endolymphatic duct is almost horizontal but the endolymphatic sac runs inferiorly and laterally. It is possible that this sharp angle has pressure regulatory role. The tubules of the sac could expand to accommodate an increase of pressure, or fluid may be resorbed through the sac epithelium into the surrounding vasculature, but the sharp angle may reduce the back flow of pressure from the sac into the rest of the membranous labyrinth. This would protect the delicate inner ear structures from sudden changes in intracranial pressure. The position of the extraosseous portion of the sac in the dura of the posterior cranial could make it vulnerable to changes in cerebrospinal fluid pressure. The angle has been found to be 90 – 135 degrees in humans (Wilbrand et al, 1974). Salt and DeMott (1998) suggested that endolymph is insensitive to cerebrospinal fluid pressure changes as the endocochlear potential is affected by injections of perilymph into the scala vestibule but not into the scala tympani which is connected to the subarachnoid space by the cochlear, perilymphatic, duct. In another study analysing patients with unilateral Ménière's disease, they found a significantly larger tympanic membrane displacement in the diseased ear due to raised perilymphatic pressure as a result of postural changes. This suggests a more effective route of pressure transfer between the cochlea and intracranial fluid compartments (Konradsson, 2000).

Hosseinzadeh et al (1998) presented a case of a man who underwent a labyrinthectomy for Ménière's disease in an ear with no serviceable hearing. At surgery a large anomalous vein (4 to 5 times the normal size) was encountered close to the endolymphatic duct and endolymphatic sac which seemed to cause an obvious mechanical compression of the duct and sac. This would support the theory that mechanical factors and the level of the duct and proximal sac may affect endolymphatic pressure.

A second possible mechanical pressure regulatory mechanism can be seen at the opening of the utricular duct. The proximal wall of the duct has a thickened lip which if pressed against the wall of the utricle could prevent movement of endolymph into the utricular duct. Schuknecht and Belal (1976) described this as the utriculo-endolymphatic valve.

Within the lumen of the tubules of the endolymphatic sac in this and other studies can be seen a colloid like substance, homogenous in nature. This has been reported in other papers (Wackym et al, 1987). It has been suggested that this substance may be a proteoglycan with a high affinity for water which is produced by the sac so as to control water balance. Rask-Andersen found that after injecting artificial endolymph into the second turn of the cochlear in guinea pigs there was an almost total absence of the normal intraluminal homogenous substance on the injected side and after withdrawal of endolymph there was found to be increased amounts of homogenous substance. These observations suggested that the disappearance of the homogenous substance occurs by both enzymatic and macrophagic activity (Rask-Andersen et al, 1999). In another animal study where colchicine was given to interfere with carbohydrate secretion, the secretion in the endolymphatic sac was effectively disturbed (Takumida et al, 1991). Given the complexity of the structure it is possible that the actual mechanisms by which the endolymphatic sac affects the endolymph are a combination of the above theories.

Pathology

In each case of Ménière's disease, the affected ears were found to have distension of the membranous labyrinth, referred to as endolymphatic hydrops (fig 128). This distension is clearly evident when an ear with Ménière's disease is compared to a normal ear (fig 100). Endolymphatic hydrops has been well described. Hallpike and Cairns published their first paper describing the pathological changes, endolymphatic hydrops, associated with Ménière's Disease in 1938 (Hallpike and Cairns, 1938).

In this study of post mortem temporal bones from the Massachusetts Eye and Ear infirmary temporal bone collection some part of the membranous labyrinth was distended in both cases with Ménière's disease. Previous studies have classified this distension of the membranous labyrinth as either generalised, as in endolymphatic hydrops, localised to the cochlea or the cochlea and saccule in cochlear hydrops, or to the semicircular canals or the canals and the utricle in vestibular hydrops (Schuknecht and Gulya, 1983). These subdivisions of hydrops follow the anatomical division of the membranous labyrinth into the pars superior and pars inferior. In some cases the saccular wall was adherent to the footplate of the stapes on the lateral wall of the vestibule.

A clinical review has shown that although all patients with Ménière's disease may have endolymphatic hydrops, when viewed post-mortem on temporal bone examination, not all patients with endolymphatic hydrops showed the symptoms of Ménière's disease (Merchant, 1995). This could represent a group of people who have asymptomatic hydrops. Ménière's disease might be the expression of symptomatic hydrops or there may be another pathology linked to Ménière's disease which separates it from those with simple hydrops.

Ruptures of the membranous labyrinth were evident in certain ears affected by Ménière's disease. It has been proposed that the pressure in the membranous labyrinth which results in the distension of the delicate membranous wall can also result in ruptures occurring in parts of the membranous labyrinth. It has been suggested that it is this process that lies behind the classical symptoms of Ménière's disease where, as the pressure rises within the membranous labyrinth, there is a sensation of fullness in the ear.

When the membrane ruptures the perilymph and endolymph mix which acutely disturbs the electrolyte balance resulting in acute vertigo (Schuknecht et al, 1962). Repeated ruptures over time were proposed to account for the progressive sensorineural hearing loss. However one of the surgical treatments for Ménière's disease, the 'pick' procedure, involves creating a fistula between the saccule and the vestibule by means of a pick introduced through the round window. This conversely relieves the symptoms of Ménière's disease without producing the debilitating vertigo that is thought to occur when the endolymph and perilymph mix. It is worth noting however that in many patients with advanced Ménière's disease, the saccule has become so distended that the wall becomes adherent to the round window. In these circumstances the pick procedure would not theoretically produce an endolymph to perilymph fistula but instead would join the middle ear tympanic cavity to the saccule. It is also worth noting that in the theory of the symptoms of Ménière's, these natural fistulae occur at different parts of the membranous labyrinth wall. They are spontaneous and do not communicate with the low pressure middle ear cavity as the pick procedure does.

Identification of the endolymphatic sac

Endolymphatic sac decompression is thought to allow the endolymphatic sac to expand in volume to compensate for the changes in volume of the endolymphatic compartment in endolymphatic hydrops. Portmann first described a technique for decompressing the endolymphatic sac (Portmann, 1927). When decompressing the endolymphatic sac, the sac is approached from the mastoid and therefore there is much literature in landmarks used to locate the sac (Shea et al, 1978). When auditing the transmastoid endolymphatic sac decompression, the thickening of the dura which contains the sac was located in the dura of the posterior cranial fossa with the superior border positioned on an imaginary line drawn from the lateral semicircular canal at the same angle as the axis of the semicircular canal. The sac emerged from deep to the posterior semicircular canal and extended towards the sigmoid sinus and the jugular bulb.

Of the 14 temporal bones examined to measure the dimensions of the extratemporal portion of the endolymphatic sac, 2 had no identifiable sac within the dura. The tissue

immediately inferior to the operculum was examined in these cases and no lumen could be found. The dura was thickened in this area as in all cases. The endolymphatic sac in the remaining 12 cases was readily identifiable within the dura immediately inferior and lateral to the operculum. Removal of the dura covering the operculum allowed identification of this bony structure and the underlying endolymphatic sac.

The mean width of the operculum was 4.5mm (range of 1.7 to 6.9mm), the distance of the internal acoustic meatus was 9.6mm (range 8.5 to 10.8mm) to the medial limit and 12.6mm (range 10.8 to 15.1mm) to the lateral limit of the operculum. The mean distance from the lateral limit of the operculum to the superior petrosal sinus was 9.6mm (range 6 to 12.6mm) and 10.7mm (range 6.1 to 13.7mm) from the medial end. These figures show that there is variation in the width of the operculum and slight variation in the distance from the superior petrosal sinus and the sigmoid sinus; however the relative positions are constant. These figures may be of use when attempting to identify the general location of the endolymphatic sac in the posterior cranial fossa. They correlate with the figures used in Harold Schuknecht's book on the anatomy of the temporal bone in which he describes the operculum as lying 10mm inferior to the superior petrosal sinus and 10mm lateral to the internal acoustic meatus (Schuknecht and Gulya, 1986).

Previous studies have found a correlation between the distance from the operculum, external aperture of the vestibular aqueduct, and the sigmoid sinus (Friberg, 1988). This study revealed the temporal bone with the shortest endolymphatic sac (3.5mm) also had the shortest distance from the operculum to the sigmoid sinus (7.9mm) and the bone with the longest sac (17.3mm) had the second longest distance from the operculum to the sinus (14.7mm). So it would appear also that sac length may depend on the distance from the operculum to the sigmoid sinus. In 5 cases the endolymphatic sac overlies the sigmoid sinus to varying degrees. This represents about 1/3 of cases which is the same as in previous work (Friberg et al, 1988).

In the series of fourteen temporal bones dissected to assess the position and size of the endolymphatic sac, no extraosseous portion of the sac was identified in 2 cases. Friberg

et al (1984, 1988) using a histological technique to assess the size did not find any sac epithelium in two cases out of 29. Of the remaining 12 in this study, the mean width of the sac was 11.9mm (range 7.0 to 16.0mm). The mean length of the sac along the medial limit was 11.0mm (range 8.4mm to 14.7mm), extending to the sigmoid sinus and jugular bulb. The mean length of the lateral limit was 10.6mm (range 6.6mm to 16.6mm), extending towards the sigmoid sinus. In half of the cases the sac was seen to overly the sigmoid sinus distally. In all cases the endolymphatic sac was located within a thickening of dura, and this was confirmed with histological analysis. The thickening of the dura was seen to extend from the level of the operculum to the sigmoid sinus. In the two cases where no extraosseous portion of the sac was identified, this thickening of the dura was present.

Shea et al(1979) used a method of injecting the endolymphatic compartment, to highlight the endolymphatic sac and then identify by means of a transmastoid dissection. This method could possibly exaggerate the size of the sac by causing artificial distension of it. They identified an edolymphatic sac in every specimen. I was unable to reproduce their work. In this study 2 in 14 specimens had no identifiable extraosseous endolymphatic sac. Shea also suggested that you could decompress the sac and not drill close to the posterior canal. This study does not confirm this, to succesfully decompress the sac the one has to be removed adjacent to the posterior semicircular canal. The other studies principally examining the endolymphatic sac (Bagger- Sjöbäck, 1993; Friberg et al, 1988) are all from the same unit. They utilise a method of processing the specimens of sac histologically and then creating a 3D reconstruction. By using a third method in this present study, I was unable to produce result similar to Shea et al (1979).

This research has shown that there is considerable variation in the size of the extraosseous portion of the endolymphatic sac. A study examining the surface area of endolymphatic sacs found that there is great variation from 2mm² to 35mm² with a mean of 15mm² (Bagger- Sjöbäck, 1993). On average the sacs dissected in this study were larger. The nature of this study may over estimate the size of the sac as it may be artificially enlarged as the sac is dissected from the dura, the embalming process may

artificially enlarge the sac and distort the membranous labyrinth. As it is based on gross dissection it also makes identification of small endolymphatic sacs difficult.

Surgery on the temporal bone

Temporal bone anatomy is notoriously complex and difficult to understand. Part of the problem is that there are so many structures packed so close together. To complicate the picture further the facial nerve passes through the temporal bone extremely close to other important structures. The facial nerve has been described as the “sword of Damocles” hanging over all head and neck and temporal bone surgeons, as they may be the cause of the nerve’s severance’ (Curtin et al 1990).

Transmastoid approach to decompress the endolymphatic sac

The transmastoid approach to the endolymphatic sac is well described (Portmann 1927, Paparella 1975). When auditing the transmastoid approach to decompress the endolymphatic sac, my initial dissections proved difficult. As a newcomer to the high speed drill, combined with the complexities of dissecting the temporal bone, led me to numerous ‘accidents’. Therefore the conclusions I drew about the relative safety and hazards of this procedure were greatly affected by the level of operator experience. It is difficult to quantify the hazards associated with a surgical procedure. What I have attempted to do is place emphasis on structures that when damaged will potentially result in significant morbidity.

The transmastoid approach utilises a post-auricular incision, placing the lesser occipital nerve and posterior auricular artery at risk. This may result in anaesthesia or paraesthesia in the area of distribution post operatively. Bleeding can be controlled intraoperatively. The mastoid emissary foramen and vessels are also encountered when drilling the cortex of the mastoid. This creates a risk of air embolus if the patient’s head is raised to the point where venous pressure falls below atmospheric pressure (Bithal et al, 2004).

Once drilling is undertaken within the mastoid the structures which are principally at risk of damage are the sigmoid sinus and jugular bulb, the vertical segment of the facial

nerve, the lateral and posterior semicircular canals and the dura of the posterior and middle cranial fossae. Damage to the facial nerve could result in possible temporary or permanent damage and that could be partial or complete ipsilateral facial palsy. Damage to the semicircular canals may result in complete ipsilateral sensorineural hearing loss, this risk is worse if the bone around the canal is thinned until the canal is visible as in blue-lining (Shea et al, 1979). Damage to the sigmoid sinus or the jugular bulb will result in haemorrhage which may be difficult to control. Damage to the dura may result in a cerebrospinal fluid leak which again may be difficult to control and there is the potential for the introduction of infection and development of bacterial meningitis.

In this procedure, the bone is removed from the tissue deep to the endolymphatic sac. At this point the sac itself may be damaged, by direct trauma or by affecting the arterial supply and venous drainage of the sac.

Care was taken when removing the bone from the dura of the posterior cranial fossa and the part of the dura containing the sac. However damage to the dura was inevitable and this was especially evident when examining the endolymphatic sac histologically. The specimens for histological analysis were harvested by dividing the sac proximally at the operculum and then peeling the sac with the surrounding dura from the underlying bone. The bone was removed in a similar manner to how it is removed in theatre when decompressing the sac. The sac on histological examination shows clear disruption of the fine tubular structure especially in the plane through the depth of the sac. There was also separation of the surrounding perisaccular connective tissue. If the dura and especially the sac with the highly vascular surrounding connective tissue were to be damaged in such a way intra-operatively then fibrosis of the sac and the surrounding tissue could occur. This could account for the patients who describe initial resolution of their symptoms, possibly due to the decompression and then recurrence, possibly due to formation of scar tissue affecting the function of the sac. The literature is not clear on the disruption of the sac secondary to decompression but the occurrence of fibrosis after the insertion of silastic stents has previously been discussed (Pulec, 1998). However the

effects were not confirmed by a study of post mortem specimens from patients who have had endolymphatic sac decompression and stent insertion.

The transmastoid approach therefore presents many hazards and is not without risk of serious complication. The figures for the Massachusetts Eye and ear infirmary put the risk of sensorineural hearing loss at less than that for intratympanic gentamycin injection i.e. less than 10% (Nadol, 2005).

Identification of the endolymphatic sac by transmastoid approach

The endolymphatic sac was found to lie in a trapezoid shaped thickened area of the dura of the posterior cranial fossa. The superior limit of the thickening of the dura, which was presumed to contain the sac, was found in every dissection to lie on or slightly below a line projected on the same axis as the lateral semicircular canal. This corresponds with previous work where the endolymphatic sac is said to lie on or below Donaldson's line (House, 1964), a line projected from the lateral semicircular canal. This thickening of the dura in the posterior cranial fossa dura, extends from behind the posterior semicircular canal and towards the sigmoid sinus. In the dissections of the endolymphatic performed in this study, it was seen that in every cadaver a thickening of the dura of the posterior cranial fossa in the region of the endolymphatic sac was present. The superior border of the thickening was located clearly, but the inferior border posed more difficulties due to the proximity of the sigmoid sinus and the jugular bulb. In this study it was seen that the distal segment of the endolymphatic sac overlapped the sigmoid sinus in 6 of the 20 cases. The great variability of the size of the endolymphatic sac is evident, the width ranges from 7.0mm to 14.1mm and the length from 7.6mm to 16.2mm. This study also showed the variability between the two sides of the same head, one cadaver had an identifiable sac on one side and not on the other.

This study also clearly showed the proximity of the distal part of the endolymphatic sac and the jugular bulb. Shea et al (1979) say that other papers do not report the extent of the inferior projection of the sac and the proximity to the jugular bulb. They suggested an alteration to the technique to decompress the sac which would involve removing the

bone inferior to the posterior canal without the need to ‘blue line’ the posterior and lateral canals. This would reduce the incidence of post operative sensorineural hearing loss. As this approach involves drilling the air cells from around the sigmoid sinus and the jugular bulb initially and then removing the bone from the posterior cranial fossa dura working up to the posterior canal, there is a risk of damaging the posterior canal from below as it has not been located as it would be in the standard method. Shea and his colleagues do not state their post operative sensorineural hearing loss figures.

Among the temporal bones held at the Massachusetts Eye and Ear Infirmary, there is a temporal bone from a patient who suffered from bilateral Ménière’s disease. He had had a left sided cortical mastoidectomy, sac decompression and silastic stent insertion at the age of 74. The operative note states that the operation was successful with the sac visualised, decompressed and a silastic stent inserted. Clear fluid was noted to drain from the sac. The patient recovered and reported resolution of his symptoms for 1 year. He died from a myocardial infarction at the age of 81. Histological studies showed bilateral severe endolymphatic hydrops and diminished neuronal populations in both the cochlear and vestibular systems. The membranous labyrinth showed ruptures and outpouchings. My examination of the specimen confirmed hypoplastic endolymphatic sacs, with minimal extraosseous component. The endolymphatic sac shunt was also visualised passing through the dura into the subarachnoid space. The implant has penetrated the dura mater, and fails by 4.5mm to reach the hypo-plastic endolymphatic sac. This confirms what this study suggests that in cases with a small extraosseous endolymphatic sac, there is still a thickening of dura which may be misleading to the surgeon as in this case.

Thomsen et al (1981) conducted a study comparing endolymphatic sac decompression via the standard mastoid approach with a placebo procedure, consisting of a simple cortical mastoidectomy in which the bone from the posterior cranial fossa dura was left in place thus not decompressing the sac. Thomsen’s study concluded that both procedures produce the same results with similar numbers of patients reporting improvement in their symptoms. The study however is not comparing endolymphatic sac decompression with a true placebo as a procedure has been performed. It is possible that in drilling the

mastoid and approaching the labyrinth, the blood supply through the temporal bone is being altered with resultant disruption of function of parts of the inner ear. Another study looking at cortical mastoidectomy and endolymphatic sac surgery was not able to give conclusive results as the number of patients involved was too small (Kerr et al, 1989)

Kerr et al (1989) discussed how the thickening of the dura which may contain the sac can be reached by a transmastoid approach. This however is complicated by the fact that the sac may be small, or hypoplastic and can not then be decompressed in this way. The sac may be large and overlay the sigmoid sinus so that this approach would only decompress a section of the sac. In all cases the operator may believe the sac has been decompressed as the thickening of the dura which may contain the sac has been visualised.

Alternative approaches

Given the potential difficulties in decompressing the endolymphatic sac by a transmastoid approach, 3 alternatives based on recognised approaches to the temporal bone were examined. These are standard temporal bone approaches and are well described in the literature (Rhoton, 2000, Nadol, 2005). The lateral approach was examined in a glomus jugulare resection and the suboccipital approach was examined in an acoustic neuroma resection. Anatomical dissections were used to analyse an infratemporal approach, a middle cranial fossa approach and a posterior cranial fossa approach. In all of the clinical operations, facial nerve monitoring was employed so that the nerve could be identified and accidental damage to the nerve minimised.

Middle cranial fossa approach

In the middle cranial fossa approach, the temporal lobe is retracted giving rise to increased morbidity and risk of epilepsy (Nadol, 2005). The mastoid is drilled from above, but there is still significant risk to the semicircular canals and the horizontal and vertical segments of the facial nerve. Drilling the mastoid from above allows the distal endolymphatic sac to be decompressed, proving more difficult with the more inferior part towards the jugular bulb. Drilling above the operculum and medial to the posterior and superior canal would allow the proximal sac to be decompressed, however this would put

the superior and posterior canals at significant risk. This approach has increased morbidity and restricts exposure of the endolymphatic sac making it non viable for a standard endolymphatic sac decompression.

Posterior cranial fossa approach

In this study, the endolymphatic sac was also identified and examined from the posterior cranial fossa. In surgical practice the endolymphatic sac may be approached from the posterior cranial fossa in a retrosigmoid posterior cranial fossa approach, acoustic neuroma resection. Here the posterior wall of the internal acoustic meatus may be drilled, after removal of the overlying dura. This brings the operator into close proximity with the sac (Malis, 2001). The landmarks used to identify the sac were the superior petrosal sinus, internal acoustic meatus and the ridge of the operculum.

The posterior cranial fossa approach involves opening the dura of posterior cranial fossa with a significant increase in morbidity associated. This approach however gives a view of the operculum and overlying dura. Drilling in this region would allow decompression of the proximal segment of the endolymphatic sac, deep to the operculum. There would be significant risk of possible damage to posterior semicircular canal. This approach does not provide exposure of the bone deep to the extraosseous portion of the sac to facilitate decompression. Reflecting the dura containing the sac would allow the bone deep to the dura to be drilled, but this would greatly increase the possibility of damage to the sac.

Combined transmastoid and suboccipital approach

If a transmastoid and retrosigmoid suboccipital approach were combined then both the proximal and distal parts of the endolymphatic sac may be decompressed. There would be an increase in resultant morbidity. It would allow for decompression of the endolymphatic sac in patients who have a small or no extra osseous component to the sac as the more constant proximal segment would be decompressed. The posterior cranial fossa approach would allow exposure of the operculum by removal of the dura over the operculum and temporal bone superior to this. Careful drilling would then allow for the

proximal sac to be visualised and traced towards the endolymphatic duct within the vestibular aqueduct. Care has to be taken in this region due to the proximity of the crus commune formed by the superior and posterior semicircular canals.

Section 5

Conclusion

The endolymphatic sac is the terminal expansion of the endolymphatic duct. This in turn is the terminal part of the membranous labyrinth and contains endolymph. The endolymphatic sac is a complex structure with proximal, intermediate and distal parts. The proximal and intermediate parts are contained within the petrous temporal bone. The distal part extends onto the posterior surface of the temporal bone within the thickness of the dura mater of the posterior cranial fossa, but one in seven cases examined, this extraosseous component was not present.

The proximal part of the endolymphatic sac is a simple tubular, saccular structure, but as it expands it becomes more complex with the appearance of multiple longitudinal tubules. The sac is lined by a simple epithelium which resembles that of the other parts of the membranous labyrinth with an underlying connective tissue and surrounding vasculature. At the distal end, larger, multiple vascular structures resembling veins can be identified parallel to the long axis of the sac and lying deep to it.

Great variation was identified in the length and width of the sac, between cadavers and between sides in individual cadavers. The sac was also identified in cases overlapping the sigmoid sinus. Some specimens do not have an identifiable extraosseous part to the endolymphatic sac. The sac was encased within a thickening of the dura mater of the posterior cranial fossa. This thickening was identified in every specimen extending from the operculum to the sigmoid sinus and jugular bulb.

The transtemporal approach is the standard approach to decompress the endolymphatic sac. The vertical segment of the facial nerve, the sigmoid sinus and the lateral and posterior semicircular canals are at risk. To provide maximal decompression of the sac, the maximum amount of surrounding bone should be excised. This may include the bone adjacent and posterior to the posterior semicircular canal. Further thinning of the bone around the posterior, and if required lateral, semicircular canal, often called 'blue lining', increases the risk of perforating the canals and resultant sensorineural hearing loss.

I have confirmed that it is possible by the transmastoid approach to remove the bone forming the posterior wall of the petrous temporal bone deep to the dura of the posterior cranial fossa where the expansion that may contain the endolymphatic sac is positioned. The bone can be removed from the region of the posterior border of the posterior canal to the upper limit of the sigmoid sinus and from the superior petrosal sinus to the jugular bulb. This is also subject to anatomical variation of the surrounding structures.

However, this study has shown that although the dural thickening can be decompressed, this does not always mean that the endolymphatic sac has been decompressed because the sac may be small with little or no extrasosseous component.

If it was known pre-operatively that there was an extrasosseous component to the sac then the operator could be more precise in patient selection for surgery. With more precise selection, perhaps with the use of high resolution magnetic resonance imaging of the temporal bone, there may be an improvement in long term outcome from endolymphatic sac decompression.

The transmastoid approach does not allow decompression of the proximal endolymphatic sac and may provide inadequate decompression of the distal endolymphatic sac. The posterior cranial fossa approach however allows decompression of the proximal endolymphatic sac. A combined transmastoid and retrosigmoid posterior cranial fossa approach was explored. This in theory would allow decompression of both the proximal and distal endolymphatic sac. The distal sac would be decompressed through the mastoid and the proximal sac would be decompressed via the suboccipital approach with removal of the bone operculum and overlying the proximal endolymphatic sac, but probably at the expense of far greater morbidity.

Section 6

Appendices

APPENDIX 1

EMBALMING PROTOCOL

Cadavers are initially embalmed using arterial injection and completed by subcutaneous spot injection.

An incision is made above the clavicle and the carotid artery is raised and opened to accept a large bore cannula. Initially 3 litres of Industrial Methylated Spirits is injected. 14-16 litres of embalming fluid are then injected using a Pierce Royal Bond pump at 9psi. Once initial arterial injection is complete, the cadaver is left over night to allow fixative to settle and any areas of poor fixation remaining is subcutaneously spot injected using an open ended cannula connected to the embalming pump. The carotid incision is closed and the body is bagged in a clear plastic body bag, tagged and placed in a fridge at 4 degrees centigrade for 6 weeks minimum.

Cambridge formulation embalming fluid is used, from Vickers Laboratories, Pudsey, West Yorkshire, LS28 6QW

One litre of embalming fluid contains:	Industrial Methylated Spirits	625ml
	Phenol	125ml
	Formaldehyde 37%	75ml
	Glycerol	175ml

5ml of Phenoxetol, mould growth inhibitor is added.

APPENDIX 2

Arterial latex injection

Once the initial arterial injection (embalming) is complete, 1 litre of 20% ammonia in warm water is injected through the carotid artery. Immediately 500ml of latex solution is then injected.

Latex solution consists of 50ml of white latex, 450ml of cold water and black Indian ink.

100ml of Glacial acetic acid is injected to accelerate the curing of the latex.

APPENDIX 3

Tissue processing and embedding for paraffin wax sectioning

Fixed material was stored in 10% formal saline, 9g NaCl in 1000ml of 10% formalin, prior to processing. Small blocks, 5 – 6mm were processed using the automated Histokinette.

Histokinette tissue processing schedule for small blocks

70% methyl alcohol	2 – 4 hours	agitating occasionally
90% methyl alcohol	2 – 4 hours	agitating occasionally
2 % celloidin in absolute ethyl alcohol	2 – 4 hours	agitating occasionally
2 % celloidin in absolute ethyl alcohol	2 – 4 hours	agitating occasionally
2 % celloidin in absolute ethyl alcohol	2 – 4 hours	agitating occasionally
1 st amyl acetate	2 – 4 hours	agitating occasionally
2 nd amyl acetate	2 – 4 hours	agitating occasionally
3 rd amyl acetate	2 – 4 hours	agitating occasionally
1 st wax	4 – 6 hours	agitating occasionally
2 nd wax	4 – 6 hours	agitating occasionally

Large blocks were processed manually

70% methyl alcohol	1 week	agitating occasionally
90% methyl alcohol	1 week	agitating occasionally
2 % celloidin in absolute ethyl alcohol	1 week	agitating occasionally
2 % celloidin in absolute ethyl alcohol	1 week	agitating occasionally
2 % celloidin in absolute ethyl alcohol	1 week	agitating occasionally
1 st amyl acetate	1 week	agitating occasionally
2 nd amyl acetate	1 week	agitating occasionally
3 rd amyl acetate	1 week	agitating occasionally
1 st wax	1 week	agitating occasionally
2 nd wax	48 hours	agitating occasionally

The tissue was then placed in an appropriately sized container which was filled with wax and then allowed to cool. The specimen was not allowed to contact the bottom of the container so as to ensure an adequate margin of wax around the entire specimen.

The container was placed on a cold plate to cool the wax rapidly.

The block was attached to an appropriately sized chuck by heating the block with a metal plate and then placing the block on the chuck and allowing to cool. Once cool, excess wax was removed with a knife.

APPENDIX 4

Paraffin sectioning cutting

Tissues were cut using a microtome. Small blocks were cut on a standard microtome and large blocks were cut on a sledge microtome.

The metal chuck with the sample attached is placed in the microtome and orientated so that the face of the block is parallel with the cutting knife.

The knife is aligned correctly.

The desired cutting thickness is then selected, normally 8 micrometers.

All clamps are secured

Sections are then removed forming a ribbon. Care is taken to ensure that the ribbon does not come into contact with skin. The sections are placed on a cutting board.

Sections to be examined are then selected.

The sections are trimmed with a scalpel.

A slide is taken and a drop of albumin smeared on the surface and then a few drops of water are placed on the slide.

The sections are placed on the slide and transferred into a water bath, set at 40 degrees centigrade.

The sections are allowed to float of the slide onto the surface of the water.

The sections are then, after 1 minute, collected back onto the slide and removed.

The slides are then placed in an oven set at 37 degrees centigrade and left overnight.

The sections are then ready for staining.

APPENDIX 5

Haematoxylin and Eosin staining

Slides are placed in HistoClear to dewax	10 minutes
Hydration: 1 st Absolute alcohol	1 minute
2 nd Absolute alcohol	1 minute
90% alcohol	1 minute
70% alcohol	1 minute
Wash in water	
Wash in water	
Haematoxylin (Mayers)	5 minutes
Wash in water	
Wash in water	
Blue in Scotts	
The specimen is then checked with a microscope. If the Haematoxylin is too dark, further differentiation is required in acid alcohol.	
Wash in water	
Wash in water	
Eosin	3 minutes
Wash in water	
Wash in water	
Dehydrate: 70% alcohol	1 minute
90% alcohol	1 minute
1 st Absolute alcohol	1 minute
2 nd Absolute alcohol	2 minute
Clear in HistoClear	10 minutes

Mount on slide with cover slip using hystomount

Three drops of hystomount is placed on the cover slip and then the slide is placed onto the cover slip, sections facing the slip. Pressure is applied evenly so that no air bubbles are trapped between the slide and the cover.

APPENDIX 6

DECALCIFICATION WITH NITRIC ACID PROTOCOL

As described in Lord Zuckerman's "A new system of anatomy (1981).

Immerse temporal bone in a 10% solution of concentrated nitric acid for 7 to 14 days.

The solution is changed twice weekly.

To test for decalcification a needle was inserted into the specime. When decalcified the needle sinks with pressure.

When decalcification is complete the specimen is washed in running water for 24 hours.

The specimen is stored in a 50% alcohol solution.

APPENDIX 7

DECALCIFICATION WITH EDTA PROTOCOL

Ethylenediaminetetracetic acid in phosphate buffer was used.

Temporal bone blocks were emmersed in EDTA solution and placed on an agitation table.

Solution was changed once per week.

After 6 months, the specimen was checked for decalcification once weekly.

APPENDIX 8

PROCESSING OF TISSUE FOR SCANNING ELECTRON MICROSCOPY

Fixation and Dehydration

Fixed material is placed in pH 7.4 Buffer	1 hour
Impregnate or post fix with buffered 1% Osmic Acid	30 mins
Transfer to pH 7.4 Buffer	60 mins
Dehydrate through the following series:	
50% Acetone	1 hour
Absolute Acetone	1 hour
Absolute Acetone	1 hour
Absolute Acetone	1 hour
Hexamethyl Disilalane	1 hour
Hexamethyl Disilalane	1 hour

Sputter Coating

Specimens were then coated with gold to protect them from the electron beam in the microscope using a Polaron SEM Coating Unit E5000.

APPENDIX 9

Patient "A"
Tray # R-1594, L-1595

Age: 12

DOB September 11, 1982

Date of Death: April 15, 1995
Ethnic origin: Caucasian
FIXATIVE: 10% formalin (118 days)

CAUSE OF DEATH: Crushing force trauma

- OTOLOGIC DIAGNOSES:
1. Ménière's disease, right
 2. Endolymphatic hydrops, cochlear and vestibular labyrinths, severe, right
 3. Microdehiscence, facial canal, oval window region, bilateral
 4. Dehiscence, genicular ganglion, right
 5. Artifact, removal, external auditory canal and mastoid, left

OTOLOGIC HISTORY:

This 13-year-old girl had problems with episodic vertigo and right sided hearing loss since at least 3 years of age. The vertigo would come in spells, usually in conjunction with a "flu-like" illness. Often, the illness would start with fever and aching joints. All her joints would ache including the wrists, elbows, shoulders and knees. The joints would not become red or inflamed. She would then develop spinning-type vertigo with nausea and vomiting. The spinning would last a minute or so. The spells would be repeated frequently over the course of 3 to 5 days. These spells were quite incapacitating in that she would miss school. She reported a ringing-type tinnitus which would get louder during the vertiginous spells. She did not report change in her hearing or distortion of hearing during the periods of vertigo. Antivert helped her dizziness. The episodes of vertigo were similar each time and would happen as often as once per month.

Otolaryngologic evaluation two months prior to death revealed mild retraction of the left tympanic membrane and mild nasal congestion. The rest of her ENT examination was unremarkable. There was no spontaneous or positional vertigo. Cranial nerve and cerebellar testing was normal. Audiometric evaluation revealed a severe sensorineural loss on the left. Discrimination was 84% on the right and 100% on the left. The hearing thresholds were felt to be reliable. Vestibular testing showed no spontaneous gaze nystagmus. Smooth pursuit and optokinetic tests were normal. Warm caloric irrigation

gave good responses bilaterally which were symmetric. The caloric testing simulated the patient's subjective sense of vertigo. Additional testing included a normal CBC with differential, normal ESR, normal urinalysis, and a normal CT scan of the temporal bones. Differential diagnosis entertained included an autoimmune inner ear disorder and perilymphatic fistula.

She was participating in a fund-raising project, picking up debris from a field and putting it into a front-end loader. She ran up to the left side of the tractor with some sticks in her hand and suddenly collapsed, falling in front of the rear wheel. The tractor ran over her. This resulted in severe crushing injury to the chest and upper abdomen with a fatal outcome. At autopsy, the brain on gross examination was oedematous but otherwise appeared normal. Both temporal bones were removed for histologic study. They were preserved in 10% formalin for 118 days followed by EDTA decalcification for 230 days.

HISTOPATHOLOGY

RIGHT EAR

The temporal bone specimen includes the external auditory canal, middle ear and mastoid and inner ear. Preservation of neurosensory structures of the inner ear is fair. However, considering the long post-mortem time, it is rather remarkable that there is not more autolysis. The preparation is excellent.

There is subepithelial haemorrhage within the external auditory canal and the tympanic membrane. The tympanic cavity, ossicles and mastoid appear normal. The annular ligament and round window membrane are normal with no evidence of perilymphatic fistula. Similarly, there is no fistula the fistula ante fenestrum or fossula post fenestrum.

The major abnormality is within the inner ear and consists of diffuse, extensive and severe endolymphatic hydrops within both the cochlear and vestibular labyrinths. Hydrops affects all turns of the cochlea with greater hydrops towards the apex. Reissner's membrane has herniated through the helicotrema into the middle turn (#201). There are no ruptures of Reissner's or basilar membranes. In spite of the post-mortem change, both inner and outer hair cells can be identified and appear to be in normal numbers throughout the cochlea. There is mild patchy atrophy of the stria vascularis. The spiral ligament appears unremarkable. There is advanced autolytic change of the cochlear neurones and their outlines are rather faint. However, it appears that there is a good population of neurones plus their central and peripheral processes.

The saccule shows massive hydrops with ballooning of its membranous wall in all directions. The saccular wall touches the footplate, herniates into the nonampullated end of the lateral canal, extends superiorly to surround parts of the utricle, and extends inferiorly to lie adjacent to the ductus reunions. There are no ruptures of the saccular walls. The saccular vestibular epithelium shows good numbers of hair cells and nerve fibres in the stroma. The utricle is also hydropic. There are ruptures of its membranous walls in the superior aspect (#81). One such rupture appears to have caused a medial displacement of a part of the utricular macula (#91). Again, there appear to be good

numbers of vestibular hair cells within the utricular macula as well as nerve fibres within its stroma.

All three ampullae show dilatation as well as ruptures. Hair cells are preserved in all three cristae. The superior crista shows cystic change within its stroma (#21, 31). The nonampullated part of the superior duct shows hydrops and a rupture (#51). The utriculoendolymphatic valve is open (#201). The endolymphatic sac shows a homogenous intraluminal material in many sections (example #160), a finding which is also seen in the opposite ear. There are also scattered pigmented cells and macrophages within the sac lumen (#141), a finding which is also present on the opposite side. None of the inner ear structures show any evidence for vasculitis or formation of new bone. The cochlear and vestibular aqueducts are unremarkable.

The otic capsule is normal. The internal auditory canal has the cochlear, vestibular and facial nerves. Scarpa's ganglion is unremarkable. The facial nerve shows dehiscence of the geniculate ganglion in the floor of the middle cranial fossa (#31) and a microdehiscence of its canal wall near the oval window (#171). The carotid artery has been avulsed from its canal. Similarly, the dura has been avulsed from the posterior fossa surface of the temporal bone. The petrous apex is filled with bone marrow. The promontory shows a nice example of a glomus body along the inferior tympanic nerve (#371, 381); also, the nerve courses in a tunnel on the promontory.

LEFT EAR

There is an artifact of removal in that the saw cut has transacted the external canal at the level of the tympanic membrane and most of the mastoid is missing from the specimen. The preservation of neurosensory elements of the inner ear is fair, similar to the opposite side. The preparation is good.

The tympanic cavity, ossicles and the few remaining mastoid air cells appear normal. The posterior crus of the stapes is less curved than average, which is probably an anatomical variant (#231). The oval and round windows appear normal. The petrous apex shows bone marrow and the otic capsule is normal. The internal auditory canal contains the cochlear, vestibular and facial nerves.

The cochlea shows apical hydrops (#181). Hair cells can be identified throughout the cochlea and appear to be in normal numbers. The stria vascularis and spiral ligament appear normal. The cochlear neurons show autolytic change, but the staining is somewhat more intense than the other ear. The neurons appear to be present in normal numbers. The saccule shows a questionable degree of dilatation of hydrops (#171, 181). The utricle shows an artifactual tear of its membranous wall within its inferior recess (#191). The semicircular canals appear normal. Hair cells are present in all maculae and cristae, probably in normal numbers. The endolymphatic sac has a dense staining intraluminal material in many sections with intraluminal pigmented cells, similar to the opposite ear (#221,331). The cochlear and vestibular aqueducts are normal. The saw cut has transacted the distal part of the vestibular aqueduct and the latter is therefore filled

with bone dust (#250). The promontory shows the inferior tympanic nerve coursing in bony tunnel and there is also a small glomus body, similar to the opposite ear (#210).

The geniculate ganglion of the facial nerve is not dehiscent. Some cells within the ganglion are pyknotic whereas others show a pericytoplasmic halo (#11). The facial canal a microdehiscence near the oval window, similar to the opposite ear (#181). The carotid artery is within the specimen but has been partially avulsed from its canal. The dura is avulsed from the posterior fossa surface of the temporal bone.

SUMMARY AND COMMENT

This 13-year-old girl suffered from recurring bouts of vertigo and severe, right-sided sensorineural hearing loss and tinnitus from age three years. The vertiginous spells would consist of spinning-type sensations lasting a minute or so, and these would occur repeatedly over the course of 3 to 5 days. There was usually associated nausea and vomiting. The bouts would often be preceded by a “flu-like” syndrome consisting of fever and joint pains. Audiometric evaluation two months prior to death revealed a severe, right sensorineural hearing loss with greater loss for the low frequencies. Vestibular testing was normal.

The principal pathologic finding is diffuse endolymphatic hydrops involving the cochlea, otolith organs and semicircular canals in the right ear. There are multiple ruptures within the membranous walls of the utricle and ampullae. The neurosensory elements within the auditory and vestibular systems appear to be intact.

The clinical features along with the histopathologic findings are consistent within Ménière’s disease affecting the right ear. There is no evidence for perilymphatic fistula. The association of fever and joint pains with vestibular symptoms is not typical for Ménière’s disease and suggests that an additional unknown systemic factor or factors influencing the course of events. There are no overt features within the temporal bone to suggest autoimmune disease such as leukocytic infiltration, vasculitis, or new bone formation.

The light microscopic findings of preservation of hair cells, neurons, stria vascularis and the spiral ligament within the cochlea is typical for Ménière’s disease. By itself, it cannot account for the severe sensorineural hearing loss that was observed in this patient. There remains the possibility of degeneration at a sub-light microscopic level of the hair cells and/or the afferent synapses, as has been demonstrated in Ménière’s disease (Nadol & Thornton, 1987). The preservation of vestibular hair cells and Scarpa’s ganglion cells is consistent with normal vestibular function as demonstrated by her normal ENG two months prior to death.

The unfortunate and terrible accident that led to her demise could conceivably been a Ménière attack. While the exact mechanism of drop attacks remain unknown, it has been felt to be a sudden, paroxysmal but momentary alteration of otolith function, perhaps induced by physical phenomena such as shifting membranes within the inner ear. There is displacement of the superior part of the utricular macula that appears to have resulted

from a rupture and ballooning of the adjacent wall of the utricle. One could speculate that this rupture may possibly have triggered a drop attack in this patient.

APPENDIX 10

Patient "B"

Age at death: 81 years

OCCUPATION: Retired produce buyer

CAUSE OF DEATH: Cardiogenic shock due to acute myocardial infarction

- OTOLOGIC DIAGNOSES:
1. Ménière's disease, severe, bilateral
 2. Endolymphatic hydrops, Ménière's, severe, bilateral
 3. Endolymphatic system, Ménière's, ruptures, bilateral
 4. Endolymphatic sac, hypoplasia, Ménière's, bilateral
 5. Cristae, loss of hair cells, secondary to streptomycin ablation, bilateral
 6. Saccule, loss of hair cells, moderate, secondary to streptomycin ablation, bilateral
 7. Presbycusis, mixed, stria and neuronal
 8. Neuronal atrophy, cochlear, primary, bilateral
 9. Stria vascularis, atrophy, severe, bilateral
 10. Neuronal atrophy, vestibular, primary, bilateral

OTOLOGIC HISTORY

This 81-year-old male died in March of 1987 following an acute myocardial infarction. The past medical history revealed that he had hypertension for which he received medication. He had a non insulin-dependant diabetes mellitus, a successfully treated squamous cell carcinoma of the lip, and a resection of the prostate gland for benign hypertrophy.

His otologic history dates back to 1960 when at the age of 55 he developed episodic vertiginous symptoms associated with nausea, vomiting, palpitations and sweating. About this time he noted tinnitus and a hearing loss in the left ear. The vertiginous episodes were characterised as a sensation of spinning and occurred several times per week, lasting for several hours. After some years, the vertiginous episodes were associated with nausea but not vomiting. He then developed sudden episodes in which he had a sense of fainting and would fall to the ground. None of these sudden crises were associated with cardiac problems, drug intake, diplopia, vertigo, bowel or bladder incontinence, or any neurologic deficits. He never sustained injuries during the falls. He experienced five to seven falling attacks per year.

Two years later in 1962 at age 57 he noted tinnitus in his right ear. At that time he experienced increased frequency of vertiginous episodes and the falling attacks continued. While the tinnitus was now constant in the left ear, it was intermittent in the right ear. In the ensuing years his hearing deteriorated in both ears but was always worse on the left side. He was hospitalised nine times for diagnostic evaluation and attempts to

bring his attacks of vertigo under control. Treatment consisted of low-sodium diet, diuretics, nicotinic acid, sublingual and intravenous histamine, vitamin-B complex, and Dilantin.

In 1965 at age 60 attempts were made to ablate the vestibular system with the intramuscular administration of streptomycin sulphate. He was given a total of 55g over a period of two courses which was not successful in totally ablating caloric response. Because of continuing vertiginous episodes a third course of streptomycin sulphate was given in a total of 22.5g which was successful in ablating ice-water caloric response in both ears. The streptomycin was administered in equally divided doses of one gram twice per day. The hearing remained unchanged during these periods of streptomycin treatment and the vertigo and falling attacks decreased markedly; however, he developed severe ataxia which was worse when attempting to walk in the dark. His hearing during the subsequent 15 years gradually deteriorated in both ears, and during the latter years of life he could not walk without support. In 1979 at his age of 74 a left endolymphatic sac to mastoid shunt procedure was performed. Via a transmastoid approach, the dura was exposed in the region between the posterior semicircular canal and the sigmoid sinus. A strip of silastic was presumably introduced into the endolymphatic sac. It is recorded in the operative note that perilymph oozed from the silastic strip. For one year his dizziness was said to be improved but then it recurred in 1980 at his age 75. He was then confined to a wheelchair because of disabling ataxia which persisted until the time of his death. He had been wearing hearing aids in both ears for the last 20 years of his life. He died at age 81 and both temporal bones were removed for histologic study.

HISTOPATHOLOGY

Both ears. Both temporal bones are in an excellent state of histologic preservation and preparation. The findings are almost identical and can be described together. The external auditory canals, tympanic membranes, ossicles, tympanic cavities, mastoids, petrous apices and bony labyrinths show no significant pathology.

Both membranous labyrinths show enormous dilation of the endolymphatic spaces characteristic of the endolymphatic hydrops of Ménière's disease. Reissner's membranes have been displaced into the scala vestibule. In the apical turns Reissner's membranes are herniated through the helicotrema and extend into the scala tympani as far as the mid-portion of the second turn. In the extreme apical regions of both cochleae the limbi, organs of Corti, and basilar membranes have been displaced posteriorly and lie on the interscalar septa. The organs of Corti are present in all turns and are represented by intact pillar cells, Hensen's cells, Deiters' cells, inner phalangeal cells, inner hair cells, and 80 to 90% of outer hair cells. The limbi and tectorial membranes appear normal. There is about 80% loss of the stria vascularis in all three turns of the cochleae.

There is a loss of about 50% of the cochlear neurons in all three turns. The dendritic and axonal fibre populations appear about equal, thus the neural loss appears to be a primary neuronal degeneration rather than a retrograde neuronal degeneration.

Both saccules are enormously dilated with the saccular walls in contact with the walls of the vestibules including the stapedial footplates and herniations into the nonampullated ends of the lateral semicircular canals and superiorly into the area medial to the utricle. There is a loss of about 50% of the hair cells in the right saccular macula and a less severe loss in the left saccular macula. Both utricles are dilated and the inferior utricular recesses are compressed by encroachment of the enlarged saccules. There is a large rupture and outpouching of the left utricular wall. The utricular maculae show normal hair cell populations.

The ampullary walls of the semicircular canals are dilated with several outpouchings which are interpreted to represent ruptures with healing. There are also several ruptures present in the walls of the semicircular ducts. There is a loss of about 90% of hair cells in all three cristae of both temporal bones. The vestibular neuronal population is diminished to an extent that is consistent with age.

The dark cell areas and the underlying melanin-bearing cells in the ampullae of the cristae of both temporal bones are atrophied. Both endolymphatic sacs are hypoplastic, and the foveate fossae are small.

The sinuses of the endolymphatic ducts appear to be blocked by distension of the walls of the saccules and utricles. The endolymphatic ducts, while patent, contain eosinophilic fluid.

In addition, the left ear shows a surgical exenteration of the mastoid air cell system with exposure of the dura mater in the region between the posterior semicircular canal and the sigmoid sinus. Lying within the dura mater is the silhouette of the Silastic implant which is embedded in multi-layered fibrous tissue capsule. The silastic implant extends from the sigmoid sinus to the anterior margin of the exposed dura. Here it is folded on itself and penetrates the dura mater. In the subarachnoid space it is covered by a single layer of fibrocytes. The silastic implant measures 0.3mm in thickness and 8mm in anteroposterior length and fails by 4.5mm to make contact with the hypoplastic endolymphatic sac.

SUMMARY

This man developed vertiginous episodes at age 55 associated with a progressive left hearing loss. At age 57 he developed hearing loss in his right ear and an increase in the severity of the episodes of vertigo. Over a period of years, he had nine hospital admissions in attempts to control his disequilibrium. He had streptomycin ablation therapy performed at age 60 which rendered him ataxic but improved his episodic vertigo. He had an endolymphatic sac shunt procedure performed on the left ear at age 64. During the last several years of life he was confined to a wheelchair because of ataxia.

Histologic studies show bilateral severe endolymphatic hydrops and diminished neuronal populations in both the cochlear and vestibular systems. There is a severe loss of hair cells in the cristae and a moderate loss in the saccular maculae but no loss in the utricles. The membranous labyrinths show ruptures and outpouchings. The endolymphatic sacs

are markedly hypoplastic. The silastic implant in the left ear which was intended to shunt the endolymphatic fluid into the mastoid is imbedded in fibrous tissue, has penetrated the dura mater, and fails by 4.5mm to reach the hypoplastic endolymphatic sac.

APPENDIX 11

Cadaver No. (Code)	Sex	Age	Cause of death
1 (00/01 14)	F	80	Cerebrovascular Accident
2 (01/02 3)	F	88	Cerebrovascular Accident
3 (01/02 11)	F	75	Cerebrovascular Accident
4 (01/02 31)	F	81	Arteriosclerosis
5 (01/02 38)	M	92	Cerebrovascular Accident
6 (01/02 18)	F	96	Cerebrovascular Accident
7 (01/02 29)	F	88	Myocardial Infarction
8 (01/02 36)	M	90	Myocardial Infarction
9 (01/02 14)	F	83	Myocardial Infarction
10 (01/02 33)	M	82	Cardiac Failure
11 (00/01 34)	F	78	Myocardial Infarction
12 (02/03 29)	F	65	Emphysema
13 (01/02 30)	F	88	Cerebrovascular Accident
14	F	84	Myocardial Infarction

Table 4 Age, sex and cause of death of cadavers

APPENDIX 12

Endolymphatic sac decompression dissection

To begin, proceed with cortical mastoidectomy and then the endolymphatic sac decompression. With the largest cutting burr drill a large vertical opening over the region of the sigmoid sinus and identify the sigmoid sinus plate. Uncover the sigmoid sinus plate from the mastoid tip up to the level of the middle cranial fossa dura observing the normal curvature. Remove the bone posterior and lateral to the sigmoid sinus, identifying the mastoid emissary vein and the dura of the posterior cranial fossa, posterior to the sigmoid sinus. Continue removing this bone inferiorly until you identify the apex of the digastric groove and digastric muscle posterior to the sigmoid sinus. Follow this digastric apex towards the mastoid tip.

Identify the middle cranial fossa dural plate by removing the superior bone which is immediately below the suprameatal line. Open up the sino-dural gutter to the point where the sigmoid sinus and middle fossa dura meet.

Identify the antrum by removing the bony cortex between the middle fossa plate and the roof of the external auditory canal. Continue removing the cortex until the fundamental anatomical landmark is identified which is the lateral semicircular canal.

Remove bone inferiorly until the superior surface of the short process of the incus and the body of the incus are identified. Remove further bone anteriorly from the lateral wall of the attic until the head of the malleus is identified. Continue removing bone anteriorly in order to identify the attic anterior to the head of the malleus and the Eustachian tube orifice.

Remove the cellular bone from the posterior fossa plate anterior to the sigmoid sinus. Identify the smooth bone of the posterior semicircular canal by removing the air cells posterior to the posterior end of the lateral canal.

Having identified the digastric groove, confirm the anatomy by removing the apex of the groove to expose the digastric muscle. Remove the air cells from the mastoid tip following the digastric apex inferiorly and medially to the most inferior point and then continue to follow it superiorly and medially to the stylomastoid foramen.

Having opened up the apex of the digastric groove as far as the stylomastoid foramen then identify the vertical segment of the facial nerve following this from the stylomastoid foramen directly superior in a line which goes just anterior to the inferior limb of the posterior canal.

Remove the bone from the sigmoid sinus and retract the sinus posteriorly. Identify the bony posterior canal. Remove the bone of the posterior fossa plate from the bony posterior semicircular canal to the junction between the sigmoid sinus and the posterior fossa dura. Remove the bone from the posterior fossa plate from the superior petrosal sinus superiorly to the jugular bulb inferiorly.

Appendix 13 Dissections

Dissection 1: Floor of cranial cavity

An incision was made around the circumference of the head, 2 cm above the superior orbital margin anteriorly to the level of the external occipital protuberance posteriorly. All the tissues down to the level of the bone were divided. Using an oscillating saw the bone of the vault was cut along the incision already made and the cap removed. Care was taken to separate the dura from the vault using the blunt handle of a scalpel.

The dura was then divided along the same line as the saw cut. The falx cerebri was divided anteriorly 2 cm above the crista galli and posteriorly 2 cm above the insertion into the tentorium cerebelli.

The cerebral hemispheres were carefully raised off the floor of the cranial cavity. Using a scalpel, the olfactory nerves were separated from the under surface of the frontal lobes adjacent to the optic chiasm. The optic tracts were divided 5 mm posterior to the optic chiasm. The hemispheres were then dissected bluntly by peeling the hemisphere until the cortex separated from the diencephalon revealing the fibres of the internal capsule and the corona radiata with the lateral ventricles placed deeply. The great cerebral vein was divided as it enters the straight sinus. The cortex along the midline was removed by separating the remaining parts of the two hemispheres bluntly until the corpus callosum and anterior cerebral arteries were visible. The cortex was then pulled laterally to separate it from the underlying structures. All of the cortex was removed on both sides. The branches of the anterior and middle cerebral arteries were divided to allow removal of the cortex. The middle cerebral artery was divided 3cm lateral to the circle of Willis.

On the left the thalamus and putamen were removed along with the corona radiata to leave only the fibres of the internal capsule attached to the cerebral peduncle by using the blunt handle of a scalpel and stripping the tissue off. On the right the corona radiata was removed and the thalamus was left with the fibres of the internal capsule running over the surface.

The mid brain was transected immediately below the superior colliculus. The optic tracts were separated from the surface of the cerebral peduncles. The pituitary gland, pituitary stalk and inferior aspect of the hypothalamus were left in place but all other remaining mid brain and forebrain above this level was removed.

An incision was made through the tentorium cerebelli along the superior edge of the petrous temporal bone and along the line of insertion into the lateral venous sinuses. Care was taken anteriorly when dividing the dura so as not to damage the trochlea nerves as they enter the cavernous sinus. The straight sinus was divided posteriorly and the tentorium cerebelli was removed.

To aid removal of the cerebellum, the posterior third of the cerebellum was removed by dividing the cerebellum with a coronal incision and then carefully removing the cut piece. Care was taken not to put excessive traction on the brainstem and the cranial nerves. The

superior middle and inferior cerebellar peduncles were divided. Gentle traction was put on the cerebellum to facilitate this. Care was taken not to damage the trochlear nerves as they leave the brainstem and loop around to the front. The cerebellar arteries were divided close to the brainstem. Blood within the subarachnoid space was washed out using a syringe of water and then using suction to remove the excess fluid.

To view the oculomotor, trigeminal and abducens nerves fully the midbrain was gently retracted posteriorly.

Dissection 2: Eustachian tube

This dissection was performed on a temporal bone block. The periosteum and dura mater were stripped from the superior surface of the petrous part of the temporal bone. The greater superficial petrosal nerve was located as it emerges from the anterior surface and was separated from the surrounding dura mater.

The trigeminal ganglion was located by probing Meckels cave and removing the dura superiorly so that the fibres of the ganglion could be seen. The petrosal nerve was traced anteromedially, inferior to the trigeminal ganglion.

The tegmen tympani was removed, along with the roof of the mastoid antrum and cavity. The internal acoustic meatus was opened by removing the roof immediately superior to the meatus. The facial nerve and the genicular ganglion were identified along with the greater petrosal nerve.

The pinna was removed entirely while the bony and cartilaginous parts of the external auditory canal were left intact. The remains of the parotid gland were removed and the branches of the facial nerve were traced back to the main trunk, which was then traced to the stylomastoid foramen. A vertical cut was made through the petrous temporal bone parallel to the long axis, immediately lateral to the tympanic membrane. The cut only went to level with the base of the tympanic membrane. A horizontal cut was then made perpendicular to the previous one through the external auditory meatus and temporal bone until the two cuts connected. The upper lateral portion of the dissection was then removed.

The styloid muscles, styloglossus, stylohyoid and stylopharyngeus were located and cleaned while still attached to the styloid process. The internal carotid artery and the internal jugular vein were identified and stripped of surrounding fascia. The belly of tensor tympani was located lying in a canal on the vertical cut surface, parallel to the cut. Tensor veli palatini was located attached to the remains of the upper part of the pharynx.

The vagus nerve, the glossopharyngeal nerve, and the accessory nerve were located and traced superiorly to the jugular fossa. The internal jugular vein was removed the nerves were identified in the jugular fossa.

The Eustachian tube was located by making thin horizontal slices, parallel to the long axis of the temporal bone, superior to the belly of tensor tympani where it is found. The Eustachian tube was traced to the pharynx and opened distally. A thin probe was introduced into the Eustachian tube and gently pushed into the tympanic cavity to demonstrate the continuity.

Dissection 3: Temporal bone with jugular nerves

In the soft tissues of a temporal bone block the hypoglossal nerve was located with the branch to the ansa cervicalis. The hypoglossal nerve was then traced superiorly towards the jugular fossa. The vagus nerve was located in the carotid sheath and then traced superiorly towards the jugular fossa. The accessory nerve was located as it entered the sternocleidomastoid muscle by dissecting on the anterior edge of the muscle. The accessory nerve was divided at this point and then traced superiorly. The sternocleidomastoid muscle was removed along with the posterior belly of digastric. The external carotid artery and its branches were removed. The temporalis muscle was completely removed with the deep temporal nerves and vessels. The styloid muscles were removed from the styloid process. Care was taken when removing stylopharyngeus so as not to damage the glossopharyngeal nerve. The internal jugular vein was divided 2 cm inferior to the jugular fossa and the internal carotid artery was divided 2 cm inferior to the carotid canal opening. The head of the mandible was disarticulated and removed along with the joint disc. The muscles attached to the squamous part of the occipital bone were separated from the bone. The vertebral column and paravertebral muscles were removed by separating the atlas from the occipital condyles and dividing all the connecting tissue. The zygomatic arch was divided close to the temporal bone and the masseter muscle was removed.

Using the drill and a large sized burr the temporal bone was separated from the parietal and occipital bone by following the line of the sutures. On the floor of the cranial cavity the dura was stripped off the sphenoid and the occipital bone. The temporal bone was then separated from the occipital bone and the greater wing of the sphenoid.

The temporal bone was freed by dividing the surrounding tissues. The hypoglossal nerve along with the branch to the ansa cervicalis and the vagus nerve were divided distally and separated from surrounding tissue. The glossopharyngeal nerve was divided 5cm inferior to the jugular fossa. All soft tissue attached to the temporal bone on the lateral and inferior aspect was removed with the exception of the internal carotid artery, the internal jugular vein and the cranial nerves already dissected.

Dissection 4: Deep neck and temporal, infratemporal fossa dissection

The cadaver used in this dissection had previously been dissected by medical students. The vault had been removed by dividing the soft tissues circumferentially on a line 1cm superior to the superior orbital margin anteriorly, and 2cm superior to the external occipital protuberance posteriorly. The bone was then cut along this line with an oscillating saw and separated from the underlying dura. The dura was divided along this line. The tentorium cerebelli was cut on both sides, anteriorly along a line 0.5cm posterior and medial to the superior petrosal sinus and posteriorly along the transverse sinuses. The olfactory and optic nerves were divided anteriorly and the remaining cranial nerves were divided close to the brainstem. The internal carotid artery and pituitary stalk were divided. The medulla oblongata was then cut distally and the vertebral arteries divided, to allow the brain to be removed along with the tentorium cerebelli and the falx cerebri. The head and neck were separated from the cadaver by dividing the neck at the level of the clavicle. The neck, face and the infratemporal fossae had been dissected superficially. The mandible had been completely removed but the temporal bones had not been dissected. The soft tissues along the midline were divided and the head and neck were bisected using a band saw

On the left the lingual nerve with the submandibular ganglion were exposed. The fibres from the ganglion entering the deep part of the submandibular gland were identified. The lingual nerve was then traced superiorly towards the foramen ovale. The cut end of the inferior alveolar nerve was identified and traced to the union with the lingual nerve. The remaining fat and venous plexus in the infratemporal fossa was removed. The external carotid artery was divided superior to the posterior auricular branch and the maxillary artery was divided in the infratemporal fossa to allow removal of the superficial temporal artery and the first part of the maxillary artery. The remaining fibres of temporalis were removed whilst care was taken not to damage the deep temporal nerves. The deep temporal nerves were located and traced back to the mandibular nerve.

The hypoglossal nerve was located in the neck as it hooks around the occipital artery. The branch to the ansa cervicalis was located and traced inferiorly. The digastric muscle was divided through the intermediate tendon and the posterior belly was removed by detaching it from the digastric groove. The stylomastoid foramen with the main trunk of the facial nerve was located at the anterior limit of the digastric groove. The nerve to digastric was divided to allow removal of the posterior belly of digastric. The main trunk of the facial nerve was divided 1cm distal to the stylomastoid foramen and any remaining pieces of the parotid gland was removed along with the retromandibular vein.

The common carotid artery, internal jugular vein and the vagus nerve were identified in the carotid sheath. The common carotid was traced superiorly to the bifurcation. The internal carotid artery and internal jugular vein were traced superiorly to the inferior aspect of the styloid process by removing the tissue of the carotid sheath. The vagus was traced superiorly along with the hypoglossal nerve.

The remaining fibres of sternocleidomastoid were removed from their attachment onto the mastoid process. The spinal accessory nerve was located and divided proximal to sternocleidomastoid.

The remaining part of the epicranial aponeurosis was removed along with the belly of occipitalis and the overlying greater occipital nerve and the occipital artery. The remaining parts of trapezius, levator scapulae and splenius capitis were removed.

Stylohyoid, styloglossus and stylopharyngeus were divided 1cm inferior to the styloid process. Stylopharyngeus was divided with care so as not to damage the glossopharyngeal nerve. The styloid process was separated from the base of the skull using a drill and a medium sized burr. The glossopharyngeal nerve was located after removal of the styloid process.

The infraorbital nerve was located as it emerged from the infraorbital foramen and traced outwards along with the accompanying infraorbital artery. The zygomaticofacial nerve was located. The supraorbital nerve was located in the soft tissues above the orbit. The circumferential fibres of orbicularis oculi were removed along with the remaining fibres of frontalis. The soft tissues over the nose and maxilla were removed to the level of the bone while care was taken to leave buccinator and the previously identified structures.

The greater occipital nerve was located piercing semispinalis capitis. The nerve was located on the back of the head close to the occipital artery and then traced inferiorly. The nerve was traced deep to the muscle by dividing the muscle and then semispinalis capitis was removed. The nerve was traced to the inferior border of obliquus capitis inferior. Obliquus capitis superior and rectus capitis posterior major were identified. The fascia in the suboccipital triangle was removed along with the venous plexus so that the vertebral artery could be seen. The occipital artery was traced around longissimus capitis towards the external carotid artery. Longissimus capitis was removed along with obliquus capitis inferior and superior and rectus capitis posterior major and minor. Semispinalis cervicis was removed. Splenius cervicis and all other muscles attached to the spinous processes and posterior aspect of the transverse processes of the vertebrae were removed. Care was taken not to damage the vertebral artery. Rectus capitis lateralis was removed.

Dissection 5: External auditory canal and tympanic membrane dissection

The anterior half of the cartilaginous portion of the external auditory canal was removed along with the tragus. The tympanic plate was removed to the depth of the tympanic ring using a drill and medium sized burr. Care was taken not to damage the tympanic ring. The tympanic ring and membrane were identified.

The internal carotid and internal jugular vein were traced superiorly to the skull base. The glossopharyngeal nerve was traced over the lateral aspect of the internal carotid artery to the jugular foramen. The vagus and hypoglossal nerves along with the accessory nerve were traced superiorly. The internal jugular vein was divided as it emerges from the jugular fossa whilst care was taken not to damage the cranial nerves or the jugular bulb. The internal jugular vein was removed.

Dissection 6: Jugular fossa dissection

The internal jugular vein was stripped on its lateral side from the wall of the jugular fossa. The glossopharyngeal nerve was traced to the superior notch in the jugular foramen by separating from the overlying part of the internal jugular vein. The vagus and accessory nerves were then freed towards the inferior notch in the jugular fossa. The hypoglossal nerve was traced superiorly and then medially to the hypoglossal canal. The remaining parts of the internal jugular vein were then removed. Care was taken not to damage the dura at the jugular foramen and the hypoglossal canal.

Dissection 7: Neck, temporal fossa, infratemporal fossa and sphenoid dissection

This dissection began in the same way as dissection 6 so that the glossopharyngeal, vagus, accessory and hypoglossal nerves were traced up to the jugular fossa with the remaining upper part of the internal jugular vein. The vertebral artery was traced through the foramen transversarium of C1 and C2 and towards the foramen magnum. The mandibular division of the trigeminal nerve was traced superiorly to the foramen ovale.

The anterior wall of the cartilaginous portion of the external auditory meatus and the tragus were removed. Using the drill and a medium sized burr the tympanic plate was removed.

All soft tissue was removed from the lateral aspect of the sphenoid, temporal and parietal bone along with the tissue on the posterior and inferior aspect of the squamous part of the occipital bone. The remaining part of the zygomatic arch was removed. Vertical lines were then drilled using a large burr in the bone through the greater wing of the sphenoid anteriorly and in line with the posterior wall of the external auditory meatus posteriorly. These lines were continued onto the floor of the middle cranial fossa, meeting at the foramen ovale, and producing a wedge of bone which was then able to be removed. Care was taken not to damage the tympanic membrane or the tympanic cavity. Using a small burr the bone around the superior, lateral and inferior aspect of the tympanic membrane was thinned to reveal the tympanic ring.

The portion of the internal jugular vein inferior to the jugular fossa was removed whilst care was taken not to damage the glossopharyngeal, vagus, accessory or hypoglossal nerves.

Dissection 8: Right tympanic ring and cavity dissection

This dissection was performed on the right side. The tympanic membrane was carefully removed by separating from the surrounding bone using a scalpel. The membrane was then carefully separated from the handle of the malleus. The chorda tympani was noted along with the contents of the tympanic cavity.

Dissection 9: Right jugular fossa dissection

This dissection was performed on the right side. The superior jugular bulb was carefully removed from the jugular fossa. The anterior wall was stripped first and then the glossopharyngeal, vagus and accessory nerves were separated from the posterior wall before it was removed. The hypoglossal nerve was traced superiorly adjacent to the

vagus and the wall of the internal jugular vein and then towards the hypoglossal canal below the jugular fossa. The bone inferior to the tympanic membrane and lateral to the jugular bulb was thinned and carefully removed to increase the exposure of the jugular fossa.

Dissection 10: Left tympanic cavity dissection

The anterior half of the tympanic ring and tympanic membrane was removed by dividing the tympanic membrane vertically immediately anterior to the handle of the malleus and then using the drill with a small burr to divide the bone at top and bottom. The promontory with the overlying tympanic plexus was visualised.

The posterior part of the tympanic membrane was then removed by dividing the handle of the malleus at the mid point and cutting around the peripheral attachment of the tympanic membrane. The ossicles along with the round window were then visualised.

Using the drill and a small sized burr the bone over the promontory was progressively thinned and then removed to reveal the basal turn of the cochlea from the anterior limit of the tympanic cavity to 1mm anterior to the oval window.

Dissection 11: Left decalcified petrous temporal bone

This dissection was performed on a left temporal bone. The block was prepared by firstly removing the soft tissues attached inferiorly and laterally to the block. The skin, temporalis fascia and temporalis muscle were removed from the side of the block along with the pinna and the cartilaginous portion of the external auditory meatus. The muscles were stripped from the styloid and mastoid processes.

The greater superficial petrosal nerve was identified and then separated from the surrounding dura. The dura and periosteum were stripped from what would be the floor of the middle cranial fossa. The superior petrosal sinus was removed along with the dura. The tegmen tympani was removed to open the tympanic cavity and the malleus and incus were identified. The mastoid antrum was opened by removing the bony roof. The loose bone of the mastoid cavity was removed to identify the dense bone of the otic capsule forming the semicircular canals.

The bone was removed from over the genicular ganglion. The bone forming the roof of the internal acoustic meatus was removed along with the bone of the floor and medial wall to reveal the turns of the cochlea as in the previous dissection. The semicircular canals were opened to reveal their lumen using the same technique as detailed in the previous dissection.

On the posterior surface of the temporal bone, the operculum was identified along with the endolymphatic fossa. The dura superior to the operculum was then stripped, with care not to damage the endolymphatic sac. The dura on, lateral and medial to the operculum was then elevated and pulled inferiorly so that the endolymphatic sac could be identified on the under surface of the dura and traced deep to the operculum. The lumen

of the endolymphatic sac was opened using a scalpel and a probe was passed into the lumen to identify the medial, lateral and inferior limits of the sac. A rectangular hole was then cut out of the posterior wall of the sac. The operculum was removed and the vestibular aqueduct, containing the proximal endolymphatic sac and endolymphatic duct was traced superiorly, medially and anteriorly towards the vestibule. The bone over the aqueduct was removed to open the lumen. Care was taken not to damage the semicircular canals.

Dissection 12: Right decalcified petrous temporal bone dissection

This dissection was performed on a decalcified right temporal bone block. The greater superficial petrosal nerve was located and then traced laterally and posteriorly towards the genicular ganglion. The bone superficial to the ganglion was removed. The superior petrosal sinus was identified and opened by progressively trimming the remaining attached part of the tentorium cerebelli, parallel to the petrous apex.

The bone forming the roof of the internal acoustic meatus was removed by making vertical incisions along the axis of the medial and lateral walls of the internal acoustic meatus. The part of the superior petrosal sinus that is attached to the petrous apex immediately superior to the meatus was removed with the block of bone. The facial nerve was followed through the meatus to the genicular ganglion.

The bone forming the floor and medial wall of the meatus, medial to the facial nerve, was carefully removed to reveal the turns of the cochlea. Care was taken when opening the cochlea not to damage the modiolus or the bone between the turns of the cochlea. The cochlear nerve was identified and traced through the meatus to the cochlea. The inferior and superior vestibular nerves were identified.

A vertical cut was made parallel to the long axis of the petrous temporal bone, immediately anterior and lateral to the genicular ganglion. The cut went through the tympanic and mastoid cavities. The cut separated the external auditory canal and lateral part of the tympanic and mastoid cavities from the remainder of the block. The promontory was noted within the tympanic cavity with the tympanic plexus lying on the surface.

The block was then cut on a vertical line perpendicular to the previous cut and running through the middle of the mastoid cavity. This separated the block from the remaining section of the squamous part of the temporal bone.

The roof of the mastoid cavity was removed, so that the mastoid antrum and the mastoid cavity could be visualised. Using forceps the loose cellular bone of the mastoid cavity was removed, superior and lateral to the semicircular canals. The dense cortical bone of

the otic capsule was located, forming the superior, posterior and lateral semicircular canals. The semicircular canals were then opened, starting with the superior canal.

The arcuate eminence was identified. Using a scalpel, the bone lateral to the superior canal and superior to the posterior canal was removed. Slices of bone were removed parallel to the arcuate eminence, about 5 millimeters deep, progressively working towards the arcuate eminence. Care was taken so that the blocks were not so deep as to damage the posterior or lateral semicircular canals. The blocks were also narrowed, about 2 millimeters at a time so that the superior canal was not removed with a slice. A slice was made parallel to the axis of the posterior canal through the middle of the lumen so that the medial aspect was left in the block. After the superior aspect of the superior canal was identified, horizontal slices were made perpendicular to the previous, from the lateral edge of the block to the superior canal. The slices were 2 millimeters thick and were progressively cut until the superior aspect of the posterior canal was opened. The crus commune was identified and opened by removing any excess bone remaining between the posterior limb of the superior canal and the superior limb of the posterior canal. A curved cut was made around the superior and medial aspect of the periphery of the posterior canal so that the lumen was opened. Care was taken when cutting inferiorly so as not to damage the lateral canal. Removing the superior wall opened the lateral canal. The anterior limb of the lateral canal was identified by removing, 2 millimeter, horizontal slices of bone, progressively working inferiorly. The axis of the superior canal was the medial limit and the anterior wall of the posterior canal was the posterior limit of the slices. The posterior limb of the lateral canal was identified by removing the bone forming the roof of the canal.

A cut was made parallel to the long axis of the petrous apex, posterior to the bony wall of the posterior canal through the bone posterior to the semicircular canals and lateral to the internal acoustic meatus down to the level of the lateral semicircular canal. The air cells posterior to the otic capsule were noted.

Dissection 13: Left petrous temporal bone dissection

Using a drill and a large burr a vertical hole was drilled in the temporal bone starting at the suprameatal triangle and drilling superiorly. A vertical hole was drilled in the greater wing of the sphenoid immediately posterior to the zygomatico-sphenoidal suture and continuing through the lateral aspect of the frontal bone. These vertical tunnels were continued as horizontal tunnels through the cranial base meeting at the foramen ovale to remove a wedge of bone. The posterior tunnel was made parallel to the superior ridge of the temporal bone from the tympanic ring to the foramen ovale.

The remaining dura was removed from the floor of the middle cranial fossa to reveal the greater superficial petrosal nerve and the trigeminal ganglion. The mandibular division of the trigeminal nerve was identified leaving the ganglion and was traced through the foramen ovale. By reflecting the mandibular division anteriorly the otic ganglion was identified. The cavernous sinus was opened by removing the dura forming the lateral

wall. The oculomotor, trochlear, abducens and ophthalmic division of trigeminal nerves were identified and defined within the sinus along with the carotid siphon.

The anterior wall of the tympanic cavity was removed with the drill and medium sized burr. The canal of tensor tympani was identified and then the bony part of the Eustachian tube was identified and opened by progressively thinning and then removing the lateral bony wall. The Eustachian tube was traced deep to the mandibular nerve. A long thin probe was inserted into the Eustachian tube and gentle pressure was applied until it passed through into the pharynx through the opening into the Eustachian tube.

The tegmen tympani was thinned and removed using a medium sized burr. Malleus and incus were identified within the tympanic cavity. The roof of the mastoid was removed using a medium sized burr to visualise the mastoid antrum. The aditus ad antrum was de-roofed.

The greater superficial petrosal nerve was traced posteriorly and laterally to the genicular ganglion by removing the bone over the ganglion. Bills bar (separating the facial and superior vestibular nerves) was identified and then the meatal segment of the facial nerve was followed posteriorly and medially by de-roofing the internal acoustic meatus and removing the dura forming the roof of the canal. Care was taken not to damage the posterior or superior semi-circular canal or the vestibule. The superior canal was identified by progressively thinning the bone from the superior surface of the temporal bone and working inferiorly until the line formed by the lumen of the canal was visualised. The canal was traced posteriorly towards the crus-commune and anteriorly towards the ampulla of the superior canal close to the horizontal segment of the facial nerve. The lateral canal was identified bulging into the mastoid antrum and the bone forming the lateral and anterior wall of the canal was thinned until the lumen was visible. The horizontal segment of the facial nerve was followed through the tympanic cavity towards the vertical segment by carefully removing the bone forming the antero-lateral wall of the canal.

Dissection 14: Right petrous temporal bone dissection

The endolymphatic sac and petrous temporal bone dissection was then performed on the right side. The temporal bone was then divided vertically, perpendicular to the long axis and 1cm medial to the cochlea to enable the bony and membranous labyrinth to be visualised from an anteromedial direction.

Dissection 15: Posterior surface of petrous temporal bone dissection

The dura on the posterior surface of the temporal bone (left side) was removed from the superior petrosal sinus down to the level of the operculum laterally and down to the level of the jugular fossa medially. The bone of the posterior cranial fossa posterior to the posterior semicircular canal was progressively thinned down to the level of the operculum to reveal the superior part of the posterior canal and the crus commune. The bone over the intraosseous part of the endolymphatic sac was thinned until the sac was visible through a thin layer of bone.

The bone between the posterior canal and the junction of the petrous temporal bone and the squamous part was removed to reveal the superior aspect of the mastoid antrum.

The bone inferior and medial to the internal acoustic meatus was progressively thinned to reveal the first and basal turn of the cochlea along with the carotid in the carotid canal.

Dissection 16: Genicular ganglion dissection

This was performed on an isolated decalcified temporal bone block. The periosteum and dura mater were stripped from the superior surface of the petrous part of the temporal bone. The greater superficial petrosal nerve was located as it emerged from the anterior surface and was separated from the dura mater. The petrosal nerve was traced anteromedially inferior to the trigeminal ganglion. The bone from which the petrosal nerve emerges was removed and the nerve was traced laterally towards the genicular ganglion. Using a scalpel the roof of the tympanic cavity, tegmen tympani, was removed. Care was taken when removing the roof so as not to damage the contents of the tympanic cavity. The internal acoustic meatus was opened by removing the roof immediately superior to the meatus; the facial nerve was then followed into the genicular ganglion. The superior part of the cochlea was opened when the roof was removed from the internal acoustic meatus.

The malleus and incus were noted in the tympanic cavity and the synovial joint between them was identified. The horizontal segment of the facial nerve was noted running posteriorly and laterally from the genicular ganglion.

Removing the bone forming the roof immediately posterior to the tympanic cavity opened the mastoid antrum. The mastoid cavity was noted with the air cells contained within.

Dissection 17: Left cortical mastoidectomy dissection

Using a large burr the mastoid cortex was progressively thinned using a sweeping motion but remaining inferior to the level of the supramastoid crest. The sigmoid sinus plate was located and the bone over the sinus thinned. The curvature of the sigmoid sinus was followed, to thin the bone over the middle cranial fossa superiorly and to the mastoid tip inferiorly. The apex of the digastric groove and insertion of the posterior belly of digastric is located inferiorly. The bone lining the middle cranial fossa had already been dissected. The bone posterior to the sigmoid sinus is thinned to identify the dura of the posterior cranial fossa. Removing the cortex lying between the supramastoid crest and the suprameatal spine allowed the identification of the mastoid antrum. The bone was thinned posterior to the external auditory meatus to reveal a triangle with the sigmoid sinus inferiorly, the middle cranial fossa superiorly and the external auditory canal anteriorly. The cortex was removed to identify the dense bone surrounding the lateral semicircular canal. The bone of the lateral wall of the lateral semicircular canal was thinned until the canal was opened and the membranous canal was identified.

The bone around the digastric groove was removed to reveal the digastric muscle and the apex was followed medially and inferiorly and then superiorly and medially to the

stylomastoid foramen. The bone forming the facial nerve canal was removed to reveal the vertical segment of the facial nerve, which was followed superiorly on a line, anterior to the inferior segment of the posterior semicircular canal. The chorda tympani branch of the facial nerve was identified.

The dense bone surrounding the posterior semicircular canal was then identified and thinned. The bone overlying the posterior cranial fossa dura between the posterior semicircular canal and the sigmoid sinus was then removed. Next the bone overlying the posterior fossa dura from the superior petrosal sinus superiorly to the jugular bulb inferiorly was removed. The sigmoid sinus required to be retracted posteriorly to visualise and remove the bone directly posterior to it.

The superior semicircular canal was identified and opened along with the posterior in a similar manner to that in which the lateral canal was opened.

Dissection 18: Lateral wall of pharynx dissection

This dissection was performed on the right side of the hemisected head from the medial aspect. The nasal septum was intact on the right side.

The mucosa was stripped from the left side of the nasal septum. Care was taken not to damage the anterior ethmoidal nerve and artery and the olfactory nerves. The vomer bone and perpendicular plate of the ethmoid were carefully removed. The sphenopalatine artery and nasopalatine nerve were identified on the deep surface of the mucosa forming the right side of the nasal septum. The mucosa of the septum was completely stripped leaving the anterior ethmoidal artery and nerve, olfactory nerves and nasopalatine nerve and sphenopalatine artery intact.

The mucosa was stripped from the lateral wall of the nasopharynx from the level of the soft palate to the Eustachian tube orifice. The anterior and posterior borders of levator veli palatini were defined. The mucosa was stripped from the upper surface of the soft palate and from the lateral and posterior wall of the nasopharynx. Salpingopharyngeus and palatopharyngeus were identified and cleared of overlying tissue. Longus coli and longissimus capitis were identified.

The mucosa was stripped from the lateral nasal wall. Using coarse forceps the inferior, middle and superior turbinals were removed. The ethmoid bulla and ethmoid cells were opened by removing all the bony partitions. The lamina papyracea was left in place. The medial wall of the maxillary sinus was then partially removed to allow a view of the interior of the sinus. Care was taken when removing the bone of the posterior part of the medial wall so as not to damage the palatine nerves. The mucosa from the walls of the maxillary sinus was stripped away.

The greater and lesser palatine nerves were identified by using forceps to de-roof their canals. The greater palatine nerve was traced from the greater palatine foramen superiorly towards the pterygopalatine ganglion

The infraorbital nerve was located in the roof of the maxillary sinus. The infraorbital nerve was traced anteriorly towards the infraorbital foramen and posteriorly towards the foramen rotundum and the adjacent pterygopalatine ganglion by removing the thin layer of bone covering the nerve.

The mucosa was stripped from the lateral and posterior wall of the oropharynx and the laryngopharynx. The mucosa anterior to the palatoglossal fold was left intact. Care was taken to avoid damaging the glossopharyngeal nerve.

The internal carotid artery was located and traced superiorly. The external carotid artery was located at the level of the epiglottis and again was traced superiorly to identify the superior thyroid and lingual branches. Care was taken when opening the carotid sheath from the medial aspect so as not to damage the vagus nerve or the adjacent sympathetic trunk. The superior cervical ganglion was located and the sympathetic trunk traced inferiorly.

The superior thyroid nerve was identified at the superior border of the thyroid cartilage and then traced back to the vagus nerve.

Dissection 19: Carotid canal and siphon dissection

Next the internal carotid artery was followed through the temporal bone and along the sphenoid bone. Firstly to increase access the cartilaginous prominence superior to the Eustachian tube orifice was removed whilst care was taken not to damage the Eustachian tube. Levator veli palatini was traced superiorly to the sphenoid bone and then this muscle was removed completely. Salpingopharyngeus was removed. Tensor veli palatini was cleared of overlying tissue and traced from the pterygoid hamulus to the Eustachian tube and inferior aspect of the temporal bone.

The sphenoidal sinus septum was then removed to allow access to the right sphenoidal air sinus. The anterior wall of the sinus was removed using the drill and a medium sized burr. In the wall of the sinus the bulges formed by the internal carotid artery and the optic nerve were located. The parts of longus coli and longissimus capitis superior to the body of C2 were removed by stripping them from their attachments and dividing the muscles at the level of C2.

The internal carotid artery was traced superiorly to where the artery enters into the carotid canal. The carotid sheath was carefully divided so as not to damage the sympathetic plexus on the surface of the artery or the nerves crossing from the superior cervical ganglion to the artery. Using the drill and medium and small sized burrs the carotid canal was opened through its entire length. Care was taken when tracing the carotid not to damage the vessel or the plexus lying on the surface. Firstly the bone was removed medial and anterior to the artery in the vertical portion. Then the bone was removed inferior, medial and lateral to the artery in the horizontal portion.

The carotid siphon was visualised by following the internal carotid artery out of the carotid canal and onto the surface of the sphenoid bone and into the cavernous sinus. The cartilage block in the foramen lacerum, where the carotid makes a 90 degree turn

superiorly, was removed using a scalpel and forceps as the drill was unsuitable for removing cartilage. Care was taken when removing the cartilage so as not to damage the greater superficial petrosal nerve, the deep petrosal nerve or the start of the nerve of the pterygopalatine canal. The bone of the posterior aspect of the sphenoid bone and the anterior part of the occipital bone forming the clivus along with the bone forming the pituitary fossa and roof of the sphenoidal sinus was progressively thinned until only a dural plate remained.

The bone forming the posterior wall of the maxillary sinus was removed so that the infraorbital nerve could be traced into the sphenopalatine ganglion. To visualise the ganglion the maxillary artery and branches around the ganglion were removed. The maxillary nerve was traced from the pterygopalatine ganglion posteriorly through the foramen rotundum to the trigeminal ganglion. The foramen rotundum was opened by removing the medial wall. To locate the trigeminal ganglion the internal carotid artery was retracted medially. The ophthalmic division of the trigeminal nerve was located at the trigeminal ganglion and traced anteriorly towards the superior orbital fissure. The bone forming the medial wall of the superior orbital fissure was not removed. In the cavernous sinus the oculomotor, trochlear and abducens nerves were identified.

The inferior aspect of the sphenoidal sinus was drilled. The vidian nerve, nerve of the pterygopalatine canal, was located by removing the thin layer of bone over the nerve forming a ridge in the floor of the sinus. The remainder of the inferior and medial aspect of the sphenoid bone was removed to the level of the medial pterygoid plate. The greater palatine nerve was traced superiorly into the sphenopalatine ganglion.

The bone of the medial wall and the floor of the orbit were removed. The periorbital fat was removed to reveal the lateral, inferior and superior rectus muscles. Lacrimal branches from the maxillary nerve were traced into the orbit. The optic nerve was located in the globe and traced posteriorly to the optic canal by removing the surrounding fat. The optic canal was left intact. The optic nerve was then followed posteriorly to the optic chiasm.

Dissection 20: Endolymphatic sac and petrous temporal bone dissection

The dura was stripped from the floor of the middle and posterior cranial fossa. When removing the dura from the posterior part of the petrous temporal bone, care was taken not to remove the extraosseous portion of the endolymphatic sac. The transverse and sigmoid sinus were removed from the grooves formed in the posterior cranial fossa to where the sigmoid sinus enters the jugular foramen. The greater superficial petrosal nerve was located in the floor of the middle cranial fossa and traced posteriorly and laterally to where it leaves the petrous part of the temporal bone. The middle meningeal artery was located and then traced to the foramen spinosum. The trigeminal nerve was located as it enters into Meckel's cave. Meckel's cave and the trigeminal ganglion were de-roofed by removing the overlying dura. Care was taken not to damage the trigeminal nerve or the divisions of the nerve.

Using the drill and a medium sized burr the bone forming the arcuate eminence was carefully thinned following the course of the superior semicircular canal. The bone of the

posterior aspect of the petrous part of the temporal bone was thinned over the crus commune and posterior semicircular canal. The bone superior to and forming the operculum was thinned so that the intra-osseous part of the endolymphatic sac could be visualised. When thinning the bone over the inferior limb of the posterior semicircular canal the canal was traced to where it runs deep to the endolymphatic sac.

The bone forming the roof of the internal acoustic meatus was removed to reveal the dura forming the roof of the canal. The bone was removed medial to the superior semicircular canal until the lumen of the canal was opened from the ampulla anteriorly to the crus-commune posteriorly. The dura was then removed from the roof of the canal. The facial nerve was traced towards the genicular ganglion. The thin layer of bone over the ganglion was removed so that the ganglion and the start of the greater superficial petrosal nerve could be visualised. The bone lateral to the superior semicircular canal was thinned and the mastoid antrum was opened. The tegmen tympani was removed to reveal the malleus and the incus in the tympanic cavity.

The superior vestibular nerve was traced anteriorly and laterally towards the vestibule. Using the drill and a small sized burr the bone forming the roof of the vestibule medial to the superior semicircular canal was removed to reveal the utricle. The bone was then drilled medial to the facial nerve in the internal auditory meatus to reveal the first and basal turn of the cochlea. The cochlear nerve was traced into the modiolus.

Dissection 21: Otic capsule dissection

Otic capsules were isolated from temporal bones using a high power drill and varying sizes of burrs. Six temporal bones were removed from cadaver heads as detailed earlier (isolated decalcified temporal bone dissections) but were not decalcified. Of the six otic capsules obtained, two were processed for histological analysis, two were processed and cleared to visualise the internal structures and two were retained for display.

To prepare an otic capsule, firstly the soft tissues were removed from over the lateral aspect of the temporal bone. The mastoid process was stripped of overlying periosteum. Using a large burr the bone of the mastoid cortex overlying the sigmoid sinus was thinned progressively making sweeps in the direction of the sinus. The bone was removed and the sigmoid sinus was followed superiorly and posteriorly until the dura of the middle cranial fossa was visualised. The bone was then removed working anteriorly towards Macewan's triangle. The bone posterior to the posterior bony wall of the external auditory meatus was progressively thinned and removed. The aditus ad antrum was located by drilling deep in Macewan's triangle. The lateral canal bulging into the antrum was then located. Next the posterior canal was located and then the bone was removed from the posterior cranial fossa plate from the greater petrosal sinus superiorly down to the jugular bulb inferiorly. The digastric apex was located inferiorly and then followed anteriorly towards the stylomastoid foramen. The vertical segment of the facial nerve was located and carefully traced from the stylomastoid foramen up to the genu at the lateral and posterior semicircular canals.

The bone forming the mastoid process and air cells was then completely removed until the lateral canal was reached. The bony external auditory meatus was left in place and care was taken not to damage the facial nerve or the chorda tympani. Next the squamous part of the temporal bone was removed along with the zygomatic process. The bone anterior to the tympanic cavity was removed along with the styloid process and bone inferior to the tympanic cavity.

The dura over the superior and posterior surfaces of the petrous temporal bone were removed along with the sigmoid and superior petrosal sinus. When removing the dura from the posterior surface, care was taken to leave the endolymphatic sac in place. Next the bone around the internal auditory meatus was progressively thinned and the air cells present were removed, however care was taken to leave a plate of bone around the meatus.

The superior canal was then defined by progressively removing the bone superior, anteromedial and posterolateral to the canal. The posterior canal was defined along with the crus commune, whilst care was taken not to damage the endolymphatic duct and endolymphatic sac. The remaining bone forming the posterior wall of the petrous temporal bone was removed. The three semicircular canals were defined along with the internal auditory meatus and then the cochlea.

The carotid canal was opened and the internal carotid artery was removed. The internal jugular vein and jugular bulb were removed. The bone inferior and anterior to the vestibule was progressively thinned whilst care was taken not to open the vestibule.

Dissection 22: Superficial Head and neck

This dissection was performed on a right hemisected head and neck. The skin and subcutaneous fat was firstly removed from the neck to reveal the platysma. The external jugular vein was identified on sternocleidomastoid and cleared of surrounding tissue. The transverse cervical and greater auricular nerves were identified as they emerge from behind sternocleidomastoid. The transverse cervical nerve was traced anteriorly. The greater auricular nerve was traced superiorly and the branching pattern was noted. The anterior branches were traced onto the surface of the parotid gland.

The skin of the face and back of head was removed; however the skin was left on the pinna. The lesser occipital nerve was traced along the posterior border of sternocleidomastoid.

The muscles around the pinna were identified, auricularis posterior, superior and anterior. The posterior auricular nerve was identified and a branch of the posterior division of the greater auricular nerve was traced to the posterior auricular nerve.

The greater occipital nerve was identified lying on the surface of occipitalis, adjacent to the occipital artery. Occipitalis was cleared of overlying fascia whilst care was taken not to damage the nerves or vessels.

Anterior to the pinna the superficial temporal artery and the auriculotemporal nerve were identified and traced superiorly onto the scalp. Temporoparietalis was identified.

The muscles of facial expression were identified and cleared of overlying tissue and subcutaneous fat. Frontalis was identified with the supraorbital and supratrochlear nerves and vessels.

Dissection 23: Back of neck and head dissection

The cadaver used for this dissection had previously had an anterior full thickness temporalis muscle, fascia and skin flap raised along with a supranasal full thickness flap and a bilateral full thickness neck flap, containing skin, subcutaneous tissue, investing fascia, sternocleidomastoid and the strap muscles.

This dissection was performed on both sides.

A vertical incision was made in the skin from the vertex down the midline onto the back to the level of the seventh cervical vertebrae. A horizontal incision was then made across to the acromion. The skin was then reflected laterally.

The greater occipital nerve and the occipital artery were identified 2 to 3 cm lateral to the external occipital protuberance where they perforate the deep fascia. The greater occipital nerve was traced back to where it perforates the trapezius muscle. The occipital artery was located lateral to the greater occipital nerve and was traced by stripping the overlying fascia.

The occipitalis muscle was identified lying deep to the greater auricular nerve and the occipital artery. The fascia was then removed to reveal the entire muscle belly. On the lateral aspect of occipitalis, the fascia overlying the muscle was removed to identify the auricularis posterior and auricularis superior muscles. By carefully removing the skin and fascia which covers the auricularis posterior muscle the posterior auricular nerve was identified. The epicranial aponeurosis attached to occipitalis was identified and then the overlying fascia was cleared working anteriorly towards the superficial temporal artery. The posterior auricular artery, between auricularis anterior and superior was defined and traced over the epicranial aponeurosis.

Dissection 24: Dissection of face

This dissection was performed on both sides. The skin was removed from the face and the muscles of facial expression were identified and cleared of overlying fascia. Frontalis, orbicularis oculi, zygomaticus major, orbicularis oris, depressor anguli oris, depressor labii inferioris and auricularis anterior were all identified. The deep fascia was stripped of the surfaces of these muscles and then the edges were separated from surrounding tissue.

The parotid gland was identified. The parotid duct was identified and traced from the gland towards buccinator. Branches of the facial nerve were located arising from the

edge of the parotid gland, these were traced distally. The superficial temporal artery was traced inferiorly towards the parotid and superiorly over the lateral aspect of the head. The branches of the auriculotemporal nerve were located lying adjacent to the anterior division of the superficial temporal artery and traced inferiorly towards the main trunk of the nerve. The posterior and anterior branches of the great auricular nerve were traced, the posterior lying posterior to the parotid and the anterior lying on the surface of the parotid.

The external jugular vein was identified and followed superiorly to the posterior division of the retromandibular vein. The supraorbital nerve and artery were traced from the superior orbital notch over the surface of frontalis. The supratrochlear nerve was identified.

The branches of the facial nerve were followed back into the parotid gland towards the pes anserinus, posterior to the retromandibular vein, separating the nerve from the surrounding tissue. The retromandibular vein was then followed through the gland along with the superficial temporal artery. The parotid gland was then removed. Care was taken not to damage the branches of the facial nerve including the branch to the posterior belly of digastric and stylohyoid. The auriculotemporal nerve was followed inferiorly, posterior to the temporomandibular joint. The posterior and anterior branches of the great auricular nerve were preserved.

The facial artery and facial vein were followed over the mandible and traced across the face. The muscles of facial expression previously identified were all removed on the right, with the exception of orbicularis oculi. Frontalis and the attached remaining section of the epicranial aponeurosis were removed together whilst preserving the supraorbital nerve and the supratrochlear nerve. The muscles of facial expression identified on the left with the exception of occipitalis, frontalis and orbicularis oculi were removed. Whilst removing the muscles, the branches of the facial nerve attached were divided, close to the muscle.

Levator labii superioris was then identified and removed to reveal the infraorbital nerve deep to it. The infraorbital nerve was then separated from the surrounding fascia. The superior and inferior labial branches of the facial artery were followed to the midline.

The masseter muscle was identified and cleaned of fascia whilst preserving the branches of the facial nerve. The buccinator muscle was cleared of overlying fascia and fat.

The periosteum of the mandible anterior to the attachment of masseter and lateral to the attachment of buccinator was removed. The mental foramen and nerve were identified. The periosteum of the zygomatic arch was stripped from posterior to anterior to uncover the zygomatic foramen. The zygomaticofacial nerve was then identified. On the right hand side the fat and tissue over the temporalis fascia was removed.

Dissection 25: Pinna dissection

This dissection was performed on the left side. The skin was removed from the pinna. An incision was made in the skin of the anterior and posterior external auditory canal walls. The skin was slowly dissected with care not to damage the underlying vessels and nerves. The branches of the great auricular nerve were identified along with the auricular branches of the vagus nerve.

The pinna and the cartilaginous part of the external auditory canal were then removed in one piece. Whilst retracting the pinna anteriorly auricularis posterior was cut through the middle. The fascia was resected until the periosteum of the mastoid process posterior to the canal was reached. The auricular branches of the posterior auricular artery were cut. The pinna was then retracted inferiorly as auricularis superior and auricularis anterior were cut in the middle of their bellies. The fascia was resected until the periosteum of the bone superior to the external canal was reached. A scalpel was used to separate the cartilaginous and bony parts of the external auditory canal. The remaining parts of the auricular muscles were removed. The periosteum was stripped from the tympanic plate and from the visible mastoid process.

The superficial temporal fascia was removed inferior to the superior temporal line. An incision was made in the dense connective tissue of the scalp, along the edge of the aponeurosis of occipitofrontalis. The incision was curved, lying lateral to the frontalis muscle anteriorly and lateral to the occipitalis muscle posteriorly. The incision followed the curve of the superior temporal line. Anteriorly the fascia was separated from the temporal crest of the frontal bone. The temporal fascia was then stripped whilst care was taken not to damage temporalis. Those fibres of temporalis which gain origin from the temporal fascia superiorly and posteriorly were cut whilst the fascia was retracted towards the zygomatic arch. The superficial fascia was separated from the zygomatic arch and the fat deep to the fascia above the zygomatic arch was removed whilst care was taken not to damage the middle temporal vessels. The deep part of the temporalis fascia overlying temporalis was removed and separated from the fascia overlying masseter with which it is continuous.

The supramastoid crest was cleared of fascia and periosteum whilst care was taken not to damage the temporalis muscle or the branches of the superficial temporal artery and the posterior auricular artery.

Dissection 26: Mastoidectomy (Cadaver 14)

This dissection was performed according to the standard text (O'Reilly 2002).

Dissection 27: Back of neck dissection

The trapezius muscle was cleared of the overlying fascia, taking care to identify the great occipital and the third occipital nerves. The edge of the muscle was identified and

cleaned. Sternocleidomastoid was then identified. The great auricular nerve was traced inferiorly to where it turns around the posterior border of sternocleidomastoid. The transverse cervical nerve was then located and traced back to the posterior edge of sternocleidomastoid. Lying parallel to sternocleidomastoid in the posterior triangle of the neck the lesser occipital nerve was located and then traced from where it emerges inferiorly, deep to sternocleidomastoid, to its branching superiorly. After identifying these nerves as they passed around the edge of sternocleidomastoid, the deep fascia was cleared off the muscle and the edge was stripped of fascia.

The accessory nerve was located in the posterior triangle lying in the deep fascia. It was separated from the surrounding tissue and traced from the edge of sternocleidomastoid to where it enters the trapezius muscle. The external jugular vein was identified in the posterior triangle and traced over the sternocleidomastoid muscle. The suprascapular nerves were located in the posterior triangle and traced from below sternocleidomastoid onto the chest wall anterior to the clavicle.

Between the anterior edge of trapezius and the posterior edge of sternocleidomastoid, splenius muscle was identified and the overlying deep fascia was removed. Inferior to splenius, levator scapulae was noted and cleared of fascia.

On the right hand side, the insertion of sternocleidomastoid and trapezius muscles onto the occipital bone was revealed by removing auricularis posterior and occipitalis muscles. The right side of the epicranial aponeurosis, which was attached to occipitalis, was removed.

Trapezius was then separated from the superior nuchal line on the occipital bone whilst ensuring that the greater occipital nerve and the occipital artery were not divided. Trapezius, bilaterally, was then reflected inferiorly and separated from the ligamentum nuchae.

The splenius capitis muscle was cleaned of the overlying fascia and the superior and inferior borders were identified and cleaned from their origin to their insertion.

Dissection 28: Suboccipital dissection

The reflected upper part of trapezius was divided down the midline. Trapezius was then divided vertically with an incision 1 cm lateral to the spinous processes of the vertebrae. Trapezius was then reflected laterally with the superficial branch of the transverse cervical artery on the deep surface.

Rhomboid major and rhomboid minor were divided medially and reflected laterally. The scapula was moved laterally to reveal more of the thoracolumbar fascia and serratus posterior superior. Serratus posterior superior was then divided medially and reflected laterally. The upper part of the thoracolumbar fascia was removed to reveal erector spinae and the inferior part of splenius capitis. The margins of splenius were defined and then the muscle was removed, first dividing the attachment to the spinous processes and

then the attachment to the mastoid process and occipital bone. Care was taken not to damage the structures deep to the muscle or the perforating nerves medially.

Semispinalis capitis and longissimus capitis muscles were identified with the occipital artery winding superficially around longissimus capitis inferior to its attachment onto the mastoid process. The fascia was removed from around these muscles, whilst care was taken not to damage the venous plexus, the occipital artery and its branches and the greater occipital nerve.

Longissimus capitis was divided along with fibres of longissimus cervicis to reveal the length of semispinalis capitis. Semispinalis capitis was detached from the temporal bone and reflected inferiorly. The superior part of the muscle was split with a vertical incision to free the greater occipital nerve, which perforates it. Tension was applied to the muscle and the attachments to the spinous processes were then divided, whilst preserving the nerves that perforate the muscle medially. Semispinalis cervicis was then identified and cleared of the overlying fascia whilst preserving the venous plexus, arteries and dorsal rami running over the surface of the muscle. The deep cervical artery was identified on the muscle and followed superiorly to where it anastomoses with the occipital artery.

The greater occipital nerve is followed inferiorly to the inferior border of obliquus capitis inferior. The inferior border was followed medially to the spinous process of the second cervical vertebrae. The inferior part of rectus capitis posterior major was then located and followed from the spine of the axis to the occipital bone. The edges of this muscle were then defined whilst taking care not to damage rectus capitis posterior minor, which lies deep and medially. Rectus capitis posterior minor was then located and the edges defined. Longissimus capitis was then dissected off the mastoid process and reflected laterally. Now the muscles deep to longissimus capitis could be located. Obliquus capitis inferior was followed laterally to the transverse process of the first cervical vertebra. Obliquus capitis superior was followed from the transverse process to the occipital bone. The edges of these muscles were defined. Care was taken not to damage the venous plexus or branches of the occipital and deep cervical arteries.

Dissection 29: Deep Suboccipital and neck dissection

This dissection was performed on the left side. The suboccipital venous plexus was removed whilst preserving the branches of the occipital artery. The attachments of the muscle onto the cervical vertebrae were then cut and the muscle was removed, whilst care was taken not to damage the occipital artery. The fascia was stripped from the muscles of the suboccipital triangle so that the boundaries of the triangle could be well defined. The dense fascia within the triangle was carefully removed so as to locate the branches of the dorsal ramus of the first cervical spinal nerve. The branches of this nerve were traced back to the main trunk and followed deep into the triangle, whilst care was taken not to damage the vertebral artery deep in the triangle. The triangle was cleared of fascia and the remains of the venous plexus were removed so that the vertebral artery could be

defined, superior to the dorsal ramus of the first cervical nerve and lying on the first cervical vertebra.

The internal carotid artery was located anterior and lateral to the superior aspect of levator scapulae. The visible carotid sheath was opened and stripped whilst care was taken not to damage the internal jugular vein and the vagus nerve. The spinal accessory nerve was traced superiorly to where it is deep to digastric.

The posterior belly of digastric was removed. The muscle was detached from the digastric groove, and then the posterior belly was cut transversely, level with the anterior aspect of the internal jugular vein. The fascia around the occipital artery was removed and the branches including the branches to the mastoid process were defined.

Levator scapulae was defined and then detached from the transverse process of the first cervical vertebra. The muscle belly was cut close to the insertion onto the scapula. Splenius cervicis was detached from the upper cervical vertebrae and the muscle belly was divided at the level of the scapula.

Obliquus capitis inferior was removed by detaching the muscle from the spinous process of the axis and the transverse process of the atlas. Obliquus capitis superior was removed by detaching the muscle from the transverse process of the atlas and the occipital bone. The posterior tubercle of the transverse process of the atlas was defined and then periosteum was stripped from the transverse process whilst care was taken not to damage the vertebral artery. Rectus capitis posterior major was removed by detaching the muscle from the spinous process of the axis and from the occipital bone. The periosteum was stripped from the posterior arch of the first cervical vertebra and from the posterior aspect of the second cervical vertebra.

The joint capsule covering the articulation of the inferior facet of the atlas and the superior facet of the axis was located and then the visible portion of the capsule was removed. The inferior articular facet of the atlas and the superior articular facet of the axis were located and the surrounding fascia was removed to demonstrate the articulation. Care was taken to avoid damaging the vertebral artery and the first and second cervical nerves. The fascia was removed from between the first and second vertebra so that the dura could be defined. The atlanto-occipital membrane was located between the occipital bone and the first vertebrae, lateral to rectus capitis posterior minor and then defined. Rectus capitis lateralis was located between the transverse process of the atlas and the occipital bone, and the muscle was then defined. The capsule of the atlas and occipital articulation was located and defined.

The greater occipital nerve was traced deeply until the dorsal root ganglion of the second cervical nerve was located. The ganglion was then defined and the ventral ramus located on the surface of the vertebral artery.

The spinal accessory nerve was traced superiorly towards the jugular foramen whilst the surrounding fascia was cleared. The vagus nerve was located, deep to the internal carotid and traced superiorly, separating the nerve from the surrounding fascia. The internal carotid was then retracted laterally and forwards so that the superior ganglion of the sympathetic trunk could be located more deeply. The glossopharyngeal nerve was located winding around the lateral surface of stylopharyngeus and then traced superiorly between the internal jugular vein and the internal carotid artery.

Dissection 30: Posterior and middle cranial fossa dissection

This dissection was performed on the right side. Using the drill with a large diameter burr the posterior and middle cranial fossa dura was exposed. A vertical cut was made in the posterior part of the temporal bone, in the same direction as the sigmoid sinus. With vertical sweeping movements, the bone was continually thinned until the sigmoid sinus was revealed. A cut was made along the supramastoid crest to join with the cut over the sigmoid sinus. The drilling was made to the depth of the underlying periosteum and dura. This was continued anteriorly until the pterion was reached. A cut was made horizontally running from the bottom of the sigmoid sinus running across the occipital bone, just superior to the attachments of the suboccipital muscles onto the occipital bone. This cut continued posteriorly until the occipital artery was reached. Now a large curved cut running through the parietal bone, 2 cm above the temporoparietal suture, was made to join the line at the pterion with the line on the occipital bone. When complete dura was visible around the entire circumference of the bone, which was to be removed.

Using the handle of a scalpel, the bone was prised from the underlying dura. Care was taken not to damage the dura or vessels on the dura. When complete the middle meningeal artery was noted, along with the posterior aspect of the sigmoid sinus and the anterior aspect of the transverse sinus.

The posterior cranial fossa was opened by dividing the visible dura along the inferior bony margin and then dividing the dura from the sigmoid sinus with a vertical incision. The dura was firstly reflected superiorly and then divided from its attachment to the transverse sinus. The cerebellum and the vessels on the surface were noted. Using a curved retractor the cerebellum was carefully retracted in a posterior direction. A dissecting microscope was then used to visualise the posterior cranial fossa anterior to the cerebellum and a syringe containing water was used to clear debris off the structures to be visualised. The seventh and eighth cranial nerves were first noted. Further retraction was then performed to visualise the third, fourth, fifth and sixth cranial nerves. The anterior inferior cerebellar artery was also noted. The retractor was then placed more inferiorly and traction applied again, so that the ninth, tenth, eleventh and twelfth cranial nerves came into view along with the basilar artery.

On the posterior part of the petrous apex, the internal acoustic meatus was noted, and then looking more laterally Irv's ridge was found with a depression inferiorly, which would contain the endolymphatic sac.

The dura of the middle cranial fossa was opened with an incision, which was made diagonally from the superior aspect posteriorly to the inferior aspect anteriorly. As the dura was retracted, cerebral veins were noted crossing the subarachnoid space and entering the transverse sinus. Using the dissecting microscope the arcuate eminence was visualised.

Dissection 31: Suboccipital and brainstem dissection

On cadaver 1, the skin was removed from the right hand side of the head and neck whilst preserving the underlying tissue. Platysma was identified and then the overlying fascia was removed over the extent of the muscle. The superficial temporal artery was identified and traced to the anterior edge of the external auditory canal. Posterior to the edge of trapezius, the great auricular nerve was identified and separated from surrounding fascia. The nerve was traced from the edge of sternocleidomastoid to the inferior border of the parotid gland. The external jugular vein was identified at the posterior edge of the platysma muscle and followed superiorly to the inferior edge of the parotid.

After the cadaver was rotated onto the front, the skin over the posterior aspect of the head, neck and back, to the inferior level of the scapula and to the shoulder tips, was removed. In the underlying subcutaneous tissue the great occipital nerve and accompanying occipital artery were identified. The nerve was located 3 cm inferolateral to the inion as it pierces the trapezius muscle. The lesser occipital nerves were identified lying in the posterior triangle, anterior to trapezius and posterior to sternocleidomastoid. The accessory nerves were then identified in the posterior triangle. After identification of these nerves, the surrounding fascia and fat was removed to reveal the musculature: trapezius, sternocleidomastoid, splenius and levator scapulae.

Trapezius was divided superiorly below its attachment onto the superior nuchal line, and then the muscle was split down the middle to separate the two halves which were then held apart using a retractor. The superior aspect of semispinalis capitis was then identified. Splenius capitis was separated from the surrounding fascia and from the ligamentum nuchae and then reflected laterally and held in place with a retractor. The greater occipital nerve was identified piercing the semispinalis capitis muscle inferior to its attachment onto the occipital bone. The nerve is followed through the muscle. Semispinalis capitis was then divided superior to the greater auricular nerve and reflected inferiorly and laterally. The greater occipital nerve was then traced inferiorly to locate the inferior border of obliquus capitis inferior (inferior oblique). The surrounding fascia and venous plexus were removed to enable identification of semispinalis cervicis, inferior oblique, superior oblique, rectus capitis superior major and rectus capitis superior minor. These muscles were then cleaned whilst preserving the greater occipital nerve and the occipital artery. The muscles of the suboccipital triangle were then removed. The posterior arch of atlas was identified and cleaned using a fixed blade scalpel and then the atlanto-occipital membrane was identified. The dorsal root ganglion of C2 was identified.

The vertebral artery was identified passing through the foramina transversaria of axis and atlas. The vertebral artery was traced around the superior articular process of the atlas

and in its groove on the arch of the atlas and through a hiatus in the posterior atlanto-occipital membrane.

The bone of the inferior and posterior aspect of the occipital bone was removed using a large diameter drill bit and high-speed drill with irrigation. The bone was removed as far as the transverse sinus superiorly, the foramen magnum inferiorly and the sigmoid sinus laterally.

The dura was then incised along the same margin as the removed bone. The cerebellum was identified. The cerebellum was then removed by cutting the inferior, middle and superior cerebellar peduncles.

The hind and mid brain were identified along with the fourth ventricle. The seventh and eighth cranial nerves were followed from the internal acoustic meatus back to the pontomedullary junction. The jugular nerves were traced back from the jugular foramen. Irv's ridge was identified with the endolymphatic sac lying inferior to this and extending laterally towards the sigmoid sinus.

Dissection 32: Deep back of neck dissection

This dissection was performed on left side. Trapezius and splenius capitis were removed completely on both sides. On the right side semispinalis capitis was divided at the level of the spinous process of the third cervical vertebra and the superior portion was removed. Semispinalis was reflected laterally to view the branches of the cervical nerves innervating the muscle. The remainder of the dissection is concerned with the left side.

Inferior oblique, semispinalis capitis, semispinalis cervicis and levator scapulae were all identified and then removed. Laterally sternocleidomastoid, the occipital artery and longissimus capitis were identified. Longissimus capitis was removed whilst care was taken not to damage the surrounding structures.

The cervical plexus and the brachial plexus were identified and the primary dorsal rami of the cervical nerves were traced deeply towards the cervical spinal nerves. The posterior and middle scalene muscles were identified and removed. Care was taken not to damage the cervical plexus or the brachial plexus and the accompanying branches. Care was taken not to damage the carotid sheath and vessels and the sympathetic trunk. The carotid sheath was opened and the carotid vessels and internal jugular vein and vagus nerve were identified. The accessory nerve was located crossing anterior to the internal jugular vein. The phrenic nerve was identified.

The posterior arch of C1 and the lamina of C2, C3, C4, C5 and C6 were identified and the periosteum was removed. Using a medium sized burr, the laminae of C2, C3, C4, C5 and C6 were progressively thinned and then removed to reveal the underlying dura surrounding the spinal cord. The transverse processes were also removed whilst care was taken not to damage the spinal nerves, dorsal root ganglia and the vertebral artery.

Dissection 33: Deep back of head dissection

This dissection was performed on the left side. A coronal incision was made through the remaining tissues of the scalp and periosteum 3 cm anterior to the tragus from the midpoint of the vertex to the suture line between the parietal and temporal bones. The incision was then continued posteriorly along the suture line. A mid-sagittal incision was also made joining with the previous incision and extending posteriorly along the vertex to the posterior limit of the dissection. The superficial tissues were then removed to reveal the parietal and remaining occipital bone. Using the incision as a guide the visible bone was removed. The drill was used along the perimeter and the bone was gradually thinned and removed until the dura was visible. Then with a blunt scalpel handle the remaining bone was elevated without damage to the dura. The posterior branches of the middle meningeal artery were identified.

The dura was then excised following the outline already in place. Care was taken not to open the superior sagittal or the transverse venous sinuses. The left cerebral hemisphere was removed. The lateral 4cm of the left hemisphere was removed by making a sagittal incision through the hemisphere down to the level of the cranial base. The lateral segment was removed and the cerebral veins were divided. The corpus callosum was then divided along the midline. The remaining parts of the left hemisphere were removed by peeling the hemisphere superiorly and posteriorly away from the cerebral peduncle to leave the internal capsule and the thalamus in place.

The lateral geniculate body was identified along with the optic tract. The optic radiation was separated from the lateral geniculate body by making a coronal cut through the posterior border of the lateral geniculate body. The right anterior cerebral artery was identified along with the great cerebral vein.

Dissection 34: Extra-temporal portion of the facial nerve (Cadaver 13)

As with the right side the skin was removed from the face and neck. The muscles of facial expression were identified and cleared of fascia. Platysma was identified and all overlying tissue was removed.

The transverse cervical nerve and the greater auricular nerve were identified at the posterior border of sternocleidomastoid. The transverse cervical nerve was traced to the posterior border of the platysma. The greater auricular nerve was traced superiorly and the divisions were traced over the surface of the parotid gland. The posterior division of the greater auricular nerve was traced posteriorly behind the auricle.

The anterior border of sternocleidomastoid was separated from the parotid gland. At this stage the posterior division of the great auricular nerve was divided. The posterior auricular nerve was identified piercing the fascia and curving posteriorly and superiorly inferior to the external auditory meatus.

The branches of the facial nerve leaving the parotid gland were identified with the exception of the marginal mandibular and cervical which lay deep to platysma.

Retractors were used to separate the parotid gland and the anterior border of sternocleidomastoid to allow identification of the posterior belly of digastric. The digastric muscle was traced towards the digastric groove on the mastoid tip. The stylomastoid artery was identified and divided to allow greater access and visualisation of the facial nerve. The main trunk of the facial nerve was then identified by using the digastric muscle and digastric groove as landmarks. The posterior auricular nerve was traced to the main trunk of the facial nerve and the nerve to digastric was identified.

Dissection 35: Left cortical mastoidectomy and endolymphatic sac decompression

This performed as in standard textx (O'Reilly, 2002)

Dissection 36: Middle cranial fossa petrous temporal bone dissection

The pharynx and larynx had been removed from the specimen along with the left parotid gland by other dissectors. The head and neck was separated from the rest of the body by dividing with a saw at the level of the first thoracic vertebrae.

The skin was removed from the face and the head. The supraorbital and the supratrochlear nerves were identified and separated from the surrounding tissue. The maxillary nerve, the zygomaticofacial and the mental nerves were identified and separated from the surrounding tissue. The temporalis muscles were identified and cleared of overlying tissue. The masseter muscles were identified and cleared of overlying tissue. The remaining tissues of the face and the muscles of facial expression were all removed. The visible periosteum was stripped from the mandible, the maxilla, the frontal bones and the temporal bones. The cartilaginous portion of the external auditory meatus was removed on both sides.

The subcutaneous tissue was removed from the back of the head along with the visible vasculature. Trapezius was removed bilaterally and the right splenius capitis was removed. Longissimus capitis and the posterior belly of digastric were removed on both sides. Obliquus capitis inferior, obliquus capitis superior, rectus capitis posterior major and rectus capitis posterior minor were identified on the left side. The visible periosteum on the back of the head was then removed.

On the left a horizontal cut was made through the belly of the temporalis muscle. The cut was on a line, which lay 2cm above the orbit anteriorly and projected to the external occipital protuberance posteriorly. The fibres of temporalis above the cut were removed and the periosteum deep was stripped from the bone. Using a large burr, the bone was thinned down to the dura in a straight line parallel and level with the cut edge of temporalis. A cut was then made in the vault from anterior to posterior, joining with the cut already made. Care was taken not to damage the dura or the vessels in the dura with the drill. Using a blunt scalpel handle inserted under the edge of the bone, the dura and periosteum was stripped from the left side of the vault. The left side of the vault was then removed to reveal the underlying dura and periosteum. The middle meningeal artery was noted.

A triangular shaped section of bone was then removed from the left temporal area. A vertical incision was made in the temporalis muscle through the entire thickness from the cut edge superiorly to the junction of the zygomatic arch and the supramastoid crest inferiorly. The remaining part of temporalis, posterior to the incision was then removed entirely and the underlying periosteum was stripped from the temporal bone. Using the drill with large diameter burr, a vertical cut was made in the squamous part of the temporal bone, immediately posterior to the cut edge of temporalis. A horizontal cut was then made in the squamous part of the temporal bone immediately superior to the supramastoid crest from the inferior edge of the vertical incision anteriorly to the cut edge posteriorly. The triangular shaped segment of bone was then removed by peeling off the underlying periosteum and dura using the blunt handle of a scalpel. Care was taken not to damage the middle meningeal artery.

Working inferiorly and using the blunt handle of a scalpel, the dura was stripped from the remaining part of the squamous portion of the temporal bone and onto the base of the middle cranial fossa. The dura and periosteum were then stripped from the base of the middle cranial fossa, working from lateral to medial. The periosteum was stripped off progressively until the superficial petrosal nerves were located emerging from the petrous part of the temporal bone through the hiatus. Further dura was then stripped medially whilst taking care not to damage these nerves. The middle meningeal artery was traced posteriorly and medially towards the foramen spinosum. The dura was stripped from the petrous apex so that the arcuate eminence could be identified.

To ensure that the brain was sufficiently preserved prior to dissection, small holes were made through the dura mater and then the head and neck was submerged overnight in a bath of 10% embalming fluid and 90% water mix. The head and neck was then submerged, overnight, in a bath of 40% ethanol and 60% water to ensure that the brain was solid enough to dissect. The tissue was rinsed with a 10% embalming fluid and 90% water mix to prevent dehydration of the soft tissues.

A sagittal incision was made along the vertex, one centimeter lateral to the midline on the left side, lateral to the superior sagittal sinus, through the full thickness of the dura mater. The incision went from the cut surface of the frontal bone anteriorly to the cut edge of the occipital bone posteriorly. The incision was noted to run through the lacuna lateralis and the arachnoid villi were also noted. The dura was then incised along the line of the cut bone edges laterally so that the dura covering the left cerebral hemisphere could be removed. The dura, which had been elevated from the middle cranial base, was not removed. The left cerebral hemisphere was noted with the pia mater lying on the surface with the cerebral arteries and veins present. The thin walled cerebral veins were noted on the surface of the brain traversing the subarachnoid space and draining into the superior sagittal sinus and the transverse sinus.

The superficial arteries and veins were then stripped from the visible surface of the hemisphere along with the pia matter. Care was taken when stripping the pia matter and the vessels from the surface, so as not to damage the substance of the brain.

The insula was exposed by making a large C shaped incision with the centre located at the junction of the central sulcus and the lateral sulcus. The upper limb of the C is from the inferior frontal sulcus anteriorly and lies parallel to the lateral sulcus. The vertical limb is level with the posterior ramus of the lateral sulcus and the lower limb is a horizontal line through and parallel to the middle gyri on the temporal lobe. The frontoparietal operculum, superior cut surface, was then lifted and pulled superiorly and posteriorly, tearing the underlying tissue so as to expose the remaining part of the insula and the posterior part of the superior longitudinal bundle. The frontal operculum was torn anteriorly to expose the anterior part of the insula and the anterior part of the superior longitudinal bundle.

The pia mater and the blood vessels lying on the surface of the insula were carefully stripped away whilst preserving the brain matter. The middle cerebral artery was cut where it lies on the limen insulae, where it turns laterally to lie on the surface of the insula.

Using the blunt handle of a scalpel the insula was raised from the lower border towards the superior longitudinal bundle. The insula was removed to expose the claustrum lying deeply and then this was removed to reveal the external capsule inferiorly and the fan shaped fibres of the corona radiata superiorly. The uncinat fasciculus was located superior to the stem of the lateral sulcus, deep to the limen insulae. The fasciculus uncinatus was released from the underlying part of the external capsule by passing the blunt handle of a scalpel downwards between the two structures. The posterior part of the superior longitudinal bundle was visualised by tearing the occipitotemporal part posteriorly. This was accomplished by inserting the blunt handle immediately superficial to where the superior longitudinal fibres meet it and levering the tissue off the fibres.

Removing the external capsule revealed the lentiform nucleus. The fibres of the external capsule were removed in vertical strips with the blunt handle of a scalpel and then they were torn in the direction of the corona radiata.

To expose the internal capsule, the lentiform nucleus was removed by making horizontal sweeps with the blunt handle of a scalpel, tearing the connections with the internal capsule. The darker outer part, the putamen, and the lighter inner part, the globus pallidus were both removed. The internal capsule is traced inferiorly to the optic tract. The fibres of the superior longitudinal bundle were removed by separating them from the fibres of the corona radiata with the blunt handle of a scalpel. The uncinat fasciculus was divided anteriorly and the remainder of the temporal lobe was removed by separating it from the occipital lobe posteriorly. The cerebral veins were cut inferior to the temporal lobe to allow it to be removed. The internal capsule was traced under the optic tract to the crus cerebri.

The optic tract was traced to the optic chiasm and then the optic nerves were visualised. The left olfactory nerve was traced to the olfactory bulb. The arcuate eminence with overlying dura was noted.

Dissection 37: Petrous temporal bone dissection

This dissection was performed on the left side. Cerebral veins were noted in the visible area of the middle cranial fossa floor, attached to the dura overlying the transverse and the sigmoid venous sinuses. The middle cerebral artery was noted and traced back to the internal carotid artery.

A stitch was placed in the free edge of the dura so that it could be retracted medially to allow dissection of the petrous part of the temporal bone. The greater superficial petrosal nerve was located and then traced posteriorly to where it emerges from the temporal bone. Using a small diameter burr the bone overlying the greater superficial petrosal nerve was removed and the nerve was followed posteriorly and laterally to the genicular ganglion.

The tegmen tympani was removed from the roof of the tympanic cavity whilst care was taken not to damage the malleus and incus. Laterally the bone overlying the mastoid antrum was removed to expose the opening and inferiorly, the dense bone of the otic capsule forming the superior aspect of the most lateral part of the lateral semicircular canal. The horizontal segment of the facial nerve was traced from the genicular ganglion to the genu adjacent to the lateral semicircular canal by removing the bone from the roof of the canal. Medially the ampulla of the lateral semicircular canal was opened so as to expose the facial nerve, which is deeply placed.

Drilling posterior and medial to the genicular canal, the facial nerve was traced into the fundus of the internal auditory canal. Drilling medial to the facial nerve in the fundus of the canal exposed the roof of the cochlea. The roof was then opened to reveal the modiolus of the cochlea. The dense bone forming the roof of the internal auditory canal was removed from the fundus to the meatus and from the petrous apex to the dura lining the roof of the canal. Care was taken when drilling laterally and posteriorly so as not to damage the superior semicircular canal and the vestibule.

To allow greater room for photography the dura of the middle cranial fossa floor was removed. A cut was made parallel to the axis of the petrous apex, immediately anterior to the superior petrosal sinus. The dura was then stripped from the floor to the lesser wing of the sphenoid anteriorly and to the roof of the cavernous sinus medially. The lateral wall of the pituitary fossa was left intact. The middle meningeal artery was traced back to the foramen spinosum and the branching pattern was noted.

The roof of the trigeminal cave was removed, and the trigeminal nerve was traced into the trigeminal ganglion. The ganglion and then the ophthalmic, maxillary and mandibular branches were defined. The internal carotid artery was located in the cavernous sinus; the blood within the sinus was flushed out using a syringe filled with water.

After removing the bone forming the roof of the internal acoustic meatus the underlying lining of dura was removed to reveal the contents. The facial nerve was reflected medially, removing the labyrinthine segment from the canal. The superior vestibular nerve was noted laterally with the inferior vestibular nerve lying deep to the superior vestibular nerve. The cochlear nerve was located deep to the facial nerve and the singular nerve was located.

Using a small diameter burr the bone overlying the superior semicircular canal was progressively thinned until the lumen of the canal was visible. The curve of the canal was followed with the drill. The bone lateral to the posterior segment of the superior canal was then progressively thinned to locate the posterior semicircular canal. The lateral semicircular canal was then located by progressively thinning the bone between the posterior and the superior canal. The subarcuate artery was located.

The bone lateral to the semicircular canals was then removed, opening the mastoid cavity. The mastoid cavity was drilled out leaving the posterior cranial fossa dura posteriorly and the mastoid aditus anteriorly. The bone was then drilled down to the jugular bulb inferiorly. The endolymphatic sac was located lying on Donaldson's line, an imaginary line projected from the lateral semicircular canal onto the posterior cranial fossa dura on the same axis as the canal. The bone forming the medial wall of the mastoid cavity, deep to the semicircular canals, was progressively thinned to locate the vertical segment of the facial nerve. Care was taken when drilling anteriorly, on the posterior wall of the external auditory canal, so as not to damage the chorda tympani or remove the bone of the posterior wall.

The bone posterior to the greater superficial petrosal nerve and between the cochlea, which was previously identified, and the trigeminal ganglion was removed to identify the internal carotid artery in the bony part of the carotid canal.

The bone anterior to the mastoid cavity and lateral to the tympanic cavity was thinned to reveal the lining of the external auditory canal. The skin forming the roof of the canal was removed to identify the lumen. The bone was removed medially to identify the tympanic membrane and the tympanic ring.

The bone anterior to the greater superficial petrosal nerve was removed in a line parallel to the nerve from the tympanic cavity laterally to the middle meningeal artery medially and anteriorly to identify the tensor tympani muscle and the bony part of the Eustachian tube. The superior part of the lining of the Eustachian tube was removed to identify the lumen.

The glossopharyngeal nerve, the vagus nerve and the accessory nerve were traced superiorly into the jugular fossa.

Section 7

References

Alleman A, Dornhoffer J., Arenberg K. Walker P. 1997
Demonstration of Auto antibodies to the Endolymphatic Sac in Ménière's disease
Laryngoscope: 107(2), 211-215

Atkinson M., 1961
Ménière's Original Papers reprinted with an English translation with commentaries and
biographical sketch
Acta Oto-Laryngologica: Sup 162:14

Axleson A., 1968
The vascular anatomy of the cochlea in guinea pig and man
Acta Otolaryngologica: Suppl 243

Bagger-Sjöbäck D., Birgitta J., Friberg U., Rask-Andersen H., 1990
Three-dimensional Anatomy of the Human Endolymphatic Sac
Archives of Otolaryngology, Head and Neck Surgery: 116, 345-349

Bagger-Sjöbäck D., 1993
Surgical anatomy of the endolymphatic sac
The American Journal of Otology: 14(6), 576-579

Baloh R.: 2001,
Prosper Ménière and His Disease
Archives of Neurology: 58(7), 1151-1156

Birgitta L., Boström M., Gerdin B., Rask-Andersen H., 2001
In Vitro growth of Human Endolymphatic Sac Cells: A Transmission Electron
Microscopic and Immunohistochemical Study in Patients with Vestibular Schwannoma
and Ménière's Disease
Otology & Neurotology: 22(6), 938-943

Bithal PK, Pandia MP, Dash HH, Chohan RS, Mohanty B, Padhy N, 2004
Comparative incidence of venous air embolism and associated hypotension in adults and
children operated for neurosurgery in the sitting position
European Journal of Anaesthesiology: 21, 517-522

Blakley B., 2000
Update on Intratympanic Gentamycin for Ménière's Disease
Laryngoscope: 110(2 part1), 236-241

Boulassel M., Tomasi J., Deggouj N., Gersdorff M., 2001
COCH5B2 is a target antigen of anti-inner ear antibodies in autoimmune inner ear
diseases.
Otology & Neurotology: 22(5), 614-618

Bradley WD., Clarkson MW., Miles BA., Schmalbrock P., Williams PM., Chakeres DW., Oehler MC., 1996
Submillimeter Magnetic Resonance Imaging of the Temporal Bone in Ménière's Disease
Laryngoscope: 106(11), 1359-1364

Brookes G., 1996
The pharmacological treatment of Ménière's disease
Clinical Otolaryngology and Allied Sciences: 21(1), 3-11

Bui HT., Linthicum FH., Hofman FM., Bowman CA., House WF., 1989
An Immunohistochemical Study of the Endolymphatic Sac in Patients with Acoustic Tumours
Laryngoscope: 99, 775-778

Cairns H., Hallpike CS., 1938
Observations on the pathology of Ménière's syndrome
Proc Society Medicine 31:1317-1321

Calenoff E., Zhao J., Derlacki E., Harrison W., Selmeczi K. Dutra J., Olson I., Hanson D., 1995
Patients with Ménière's disease possess IgE reacting with herpes family viruses
Archives of Otolaryngology - Head & Neck Surgery: 121(8), 861-864

Camilleri A., Howarth K., 2001
Prognostic value of electrocochleography in patients with unilateral Ménière's disease undergoing saccus surgery
Clinical Otolaryngology and Allied Sciences: 26(3), 257-260

Curtin, H. Arriaga M, Takahashi, H. Hirsch, B E. Kamerer, D B.
Staging proposal for external auditory meatus carcinoma based on preoperative clinical examination and computed tomography findings.
Annals of Otolaryngology, Rhinology & Laryngology. 99(9 Pt 1):714-21

Danckwardt-Lillieström N., Friberg U., Kinnefors A., Rask-Andersen H., 2000
Ultrastructural analysis of 20 intraosseous endolymphatic sacs from patients with cerebello-pontine angle tumours
Auris Nasus Larynx: 27(4), 311-321

Devaiah AK., Ator GA., 2000
Clinical indicators useful in predicting response to medical management
Laryngoscope: 110(11), 1861-1865

Dhillon RS., East CA., 1999
Ear, Nose and Throat, and Head and Neck Surgery: An illustrated Colour Text
2nd Edition
Chrchill Livingston

- Dornhoffer J., Danner C., Li S., 2002
Natriuretic Peptide Receptors in the Human Endolymphatic Sac
Archives of Otolaryngology- Head & Neck Surgery: 128(4), 379-383
- Filipo R., De Seta E., Bertoli GA., 2000
Intraoperative Videomonitoring of the Facial Nerve
American Journal of Otology 21(1), 119-122
- Fletcher H., Munson WA., 1933
Loudness of a complex Tone, Its Definition, measurement and Calculation
The Journal of the Acoustical Society of America: 5, 82-108
- Fletcher H., 1938
The mechanism of hearing as revealed through experiment on the masking effect of thermal noise
Journal of Acoustical Society of America: 24, 265-274
- Friberg U., Birgitta J., Rask-Andersen H., Bagger-Sjöbäck D., 1988
Variations in Surgical Anatomy of the Endolymphatic Sac
Archives of Otolaryngology, Head and Neck Surgery: 114, 389-394
- Friberg Ulla, Rark-Anderson H., 2002
Vascular occlusion in the endolymphatic sac in Ménière's disease
Annals of Otology, Rhinology and Laryngology: 111, 237-245
- Fritsch B., Beisel KW., 2001
Evolution and development of the vertebrate ear
Evolution of the Nervous System: 55(6) 711-721
- Gacek RR., Gacek MR., 1996
Comparison of labyrinthectomy and vestibular neurectomy in control of vertigo
Laryngoscope: 106(2), 225-230
- Gloddek B., Wolfgang A., 1998
The Endolymphatic Sac Receives Antigenic Information from the Organs of the Mucosa-Associated Lymphatic System
Acta Otolaryngologica: 118, 333-336
- Guild S., 1927
Observations upon the structure and normal contents of the ductus and saccus endolymphaticus in the guinea-pig (*cavia cobaya*)
The American Journal of Anatomy: 39(1), 1-56
- Hall-Craggs, 1993

Anatomy as a basis for clinical medicine, 2nd edition
Lippincott Williams & Wilkins

House, 1964

Subarachnoid shunt for drainage of Endolymphatic Hydrops: A report of 63 cases
Archives Otolaryngology: 79, 338-354

Hessen Södermann AC., Ahlner K., Bagger-Sjöbäck D., Bergenius J., 1996
Surgical treatment of vertigo - the Karolinska Hospital Policy
The American Journal of Otology: 17(1), 93-98

Hosseinzadeh M., Hilinski J., Turner W, Harris J., 1998
Ménière's disease caused by an anomalous vein of the vestibular aqueduct
Archives of Otolaryngology – head and neck surgery: 124(6), 695-698

Ishiyama G., Ishiyama A., Jacobson K., Baloh R., 2001
Drop attacks in older patients secondary to an otologic cause
Neurology: 57(6), 1103-1106

James AL., Burton MJ., 2001
Betahistine for Ménière's disease or syndrome (Cochrane review)
The Cochrane Library: Database Systematic reviews 2001(1)

Kerr AG., Toner GJ., Mckee GJ., Smyth GD., 1989
Role and results of cortical mastoidectomy and endolymphatic sac surgery in Ménière's disease
Journal of Laryngology and Otology: 103, 1161-1166

Kobayashi M., Fukaya T., Noda M., 2000
The Endolymphatic Sac in Patients with Ménière's Disease: Correlation between MRI and the surgical findings
Acta Otolaryngologica: 120, 955-959

Konradsson, KS., Nielsen, Lars H., Carlborg, BI, Borgkvist B., 2000
Pressure transfer between intracranial and cochlear fluids in patients with Ménière's Disease
Laryngoscope: 110(1), 264-268

Larsen W, 2001
Human Embryology, 2nd edition
Churchill Livingston

Lohuis P., Klis SF., Klop WM., 1999
Signs of endolymphatic hydrops after perilymphatic perfusion of the guinea pig cochlea with cholera toxin; a pharmacological model of acute endolymphatic hydrops
Hearing Research: 137, 103-113

Lysakowski, 1993
Otolaryngology – Head and Neck Surgery 4.Cranial Base, 2nd Edition
Mosby

Malis LI, 2001
Nuances in Acoustic Neuroma Surgery
Neurosurgery: 49, 337-341

Mateijssen D., Van Hengel P., Van Huffelen W., Wit H., Albers F., 2001
Pure-tone and speech audiometry in patients with Ménière's disease
Clinical Otolaryngology and Allied Sciences: 26(5), 370-387

Matthew NG., Linthicum FH., 1998
Morphology of the Developing Human Endolymphatic Sac
Laryngoscope: 108(2), 190-194

Matthew NG., 2000
Postnatal Maturation of the Human Endolymphatic Sac
Laryngoscope: 110(9), 1452-1456

Megerian CA., Hanekamp JS., Cosenza MJ, Litofsky NS., 2002
Selective retrosigmoid vestibular neurectomy without internal auditory canal drill-out: an anatomic study
Otology & Neurotology: 23(2), 218-223

Merchant S.N. 1995
Ménière's disease
European Archives of Otorhinolaryngology: 252, 63-75

Meyerhoff W., Paparella M., Shea D., 1978
Ménière's disease in children
The Laryngoscope: 88, 1504-1511

Morrison A., 1981
Ménière's disease
Journal of the Royal Society of Medicine: 74, 183-189

Morrison A., 1997
Prosper Ménière (1799-1862) A synopsis of His Life and Times
ENT: Ear, Nose & Throat Journal: 76(9), 626-631

Nadol, JB. Mckenna, MJ., 2005
Surgery of the Ear and Temporal Bone
Lippincott Williams & Wilkins

Niyazov DM., Andrews JC., Strelloff D., Sinha S., Lufkin R., 2001
Diagnosis of Endolymphatic Hydrops in Vivo with Magnetic Resonance Imaging
Otolaryngology & Neurotology: 2296, 813-817

Odabasi O., Hodges A., Balkany T., 2000
Electrocochleography: validity and utility
Current opinion in Otolaryngology & Head and Neck Surgery: 8, 375-379

Ogura Y., 1971
A study of the gross anatomy of the human vestibular aqueduct
Annals of Otolaryngology, Rhinology and Laryngology: 80, 813-825

O'Reilly B., 2002
Temporal bone surgery, essential anatomy for trainee surgeons
University of Glasgow

Paparella, 1975
Endolymphatic Sac Drainage for intractable vertigo
Laryngoscope: 86, 697-703

Parada, Carlos
Greek Mythology Link
Online Resource

Pasha R., 1993
Otolaryngology: Head and Neck Surgery: A Clinical & Reference Guide
Plural Publishing

Pfaltz, CR. 1986
Controversial aspects of Ménière's Disease
Georg Thieme Verlag Stuttgart – New York

Portmann G., 1927
The saccus endolymphaticus and an operation for draining the same for the relief of
vertigo
The Journal of Laryngology and Otolaryngology: 1927, XLII. 809-817
Reproduced: The Journal of Laryngology and Otolaryngology: 105, 1109-1113

Pulec J., 1995
Permanent restoration of hearing and vestibular function by the endolymphatic
subarachnoid shunt operation
ENT: Ear, Nose & Throat Journal: 74(8), 544-546

Pulec 1998
Endolymphatic Subarachnoid shunt failure caused by silastic allergy

Ear, Nose & Throat journal: 77(8) 614-616

Quaranta A., Onofri M., Sallustio V., Iurato S., 1997
Comparison of long-term hearing results after vestibular neurectomy, endolymphatic mastoid shunt and medical therapy
The American Journal of Otology: 18, 444-448

Qvortrup K., Rostgaard J., Holstein-Rathlou N., 1996
The inner ear produces a natriuretic hormone.
American Journal of Physiology: 270, 1073-1077

Qvortrup, K. 1999
The Endolymphatic Sac, a Potential Endocrine Gland?
Acta Otolaryngologica: 119, 194-199

Raphael 2003
Structure and innervation of the cochlea
Brain Research Bulletin: 60, 397-422

Rask-Andersen H., J.E.DeMott,D.Bagger-Sjoback and A.N. Salt, 1999
Morphological changes of the endolymphatic sac induced by microinjection of artificial endolymph into the cochlea
Hearing research: 138, 81-90

Rauch, SD., Merchant, SN., Thedinger, BA., 1989
Ménière's syndrome and endolymphatic hydrops double blind temporal bone study
Annals of otology, Rhinology & Laryngology: 98(11), 873-883

Rhoton A., 2000
The temporal bone and transtemporal approaches
Neurosurgery 47(3), 211-316

Rhoton A., 2002
The anterior and middle cranial base
Neurosurgery 51, 273-302

Romanes GJ., 1986
Cunningham's manual of practical anatomy: volume 3. Head and neck and brain
g.j. roman, 15th edition
Oxford university press

Saeed S., 1998
Diagnosis and treatment of Ménière's disease
British Medical Journal: 316, 368-372

Salt A., 1995

Endolymph volume changes during osmotic dehydration measured by two marker techniques
Hearing Research: 90, 12-23

Salt A., 1997
Longitudinal endolymph flow associated with acute volume increase in the guinea pig cochlea
Hearing research: 107, 29-40

Salt A. and DeMott JE., 1998
Longitudinal endolymph movements induced by perilymphatic injections
Hearing Research: 123, 137-147

Schindler RA., 1980
The ultrastructure of the endolymphatic sac in man
Laryngoscope: 19(6), 1-39

Schuknecht HF, Benitez Hf., Beekhuis J., 1962
Further observations on the pathology of Ménière's disease
Annals of Otolaryngology and Rhinology: 71, 1039-1053

Schuknecht H, 1974
Pathology of the Ear
Harvard University Press

Schuknecht HF, Belal AA., 1975
The utriculo-endolymphatic valve: its functional significance
Journal of Laryngology and Otolaryngology: 89, 985-996

Schuknecht HF., 1978
A critical evaluation of treatments of Ménière Disease
J Cont Ed ORL 40: 15-30

Schuknecht HF., 1982
Cochleosacculotomy for Ménière's disease: theory, technique and results.
Laryngoscope: 92, 853-858

Schuknecht HF., Gulya AJ., 1983
Endolymphatic hydrops – an overview and classification
Annals of Otolaryngology and Rhinology: 92 (Suppl 106), 1-20

Schuknecht HF., Gulya AJ., 1986
Anatomy of the temporal bone with surgical implications, 2nd edition
Informa Health Care

Secretan Davos, 1944

De l'histologie normale du sac endolymphatique chez l'homme
Acta Otolaryngologica: 32(2), 119-163

Shambaugh GE., 1966
Surgery on the Endolymphatic Sac
Archives of Otolaryngology: 83(4), 305-315

Shea DA., Chole RA., Paparella MM., 1979
The endolymphatic sac: anatomical considerations
Laryngoscope: 89(1), 88-94

Shea J., Ge X., Warner R., Orchik D., 2000
External aperture of the vestibular aqueduct in Ménière's disease
The American Journal of Otology: 21(3), 351-355

Silverstein H., Rosenberg S., 1991
Intraoperative facial nerve monitoring
Otolaryngologic clinics of North America 24(3), 709-725

Smith, 1999
The case for structuring the discussion of scientific papers
BMJ: 318, 1224-1225

Smith PF., 2000
Pharmacology of the vestibular system
Current Opinion in Neurology 13(1), 31-37

Stahle J., Wilbrand H., 1974
The vestibular aqueduct in patients with Ménière's disease. A tomographic and clinical investigation.
Acta Otolaryngologica: 78, 36-48

Storper I., Spitzer J., Scanlan M., 1998
Use of Glycopyrrolate in the Treatment of Ménière's Disease
Laryngoscope: 108(10), 1442-1445

Standring, Healy, Johnson, Williams, Ellis, 2004
Gray's Anatomy: The Anatomical Basis of Clinical Practice, 39th edition
Elsevier, Churchill Livingstone

Takumida M, Harada Y, Rask-Andersen H, Bagger-Sjöbäck D, 1988
Modulation of the endolymphatic sac function
Acta Otolaryngologica 481:129-34

Taylor GD., 1969
Evolution of the ear

Laryngoscope 79(4) 638-651

Thomsen J., Bretlau P., Tos M., Johnsen N., 1981
Placebo effect in surgery for Ménière's disease
Archives of Otolaryngology: 107, 271-277

Tsun-Sheng H., Ching-Chen L., 2001
Delayed endolymphatic hydrops: Study and review of clinical implications and surgical treatment
ENT Ear, Nose & Throat Journal: 80(2), 76-91

Wackym PA., Friberg U., Bagger-Sjöbäck D., Linthicum FH., Friedmann I., Rask-Andersen H., 1987
Human endolymphatic sac: possible mechanisms of pressure regulation
The Journal of Laryngology and Otology 101(8): 768-779

Wangemann P., 2002
K⁺ cycling and the endocochlear potential
Hearing research: 165, 1-9

Wangemann P., 2002
Adrenergic and muscarinic control of cochlear endolymph production
Advances in Oto-Rhino-Laryngology: 59, 42-50

Widmaier EP., Raff H., Strang K., 1994
Vander, Human Physiology, 6th edition
McGraw Hill

Wilbrand HF, Rask-Andersen H, Gilstring D., 1974
The vestibular aqueduct and the paravestibular canal: an anatomic and radiologic investigation.
Acta Radiologica 15:337-355

Zuckerman, Darlington D., Lisowski P., 1981
A new system of anatomy
Oxford University press

